Pharmaceutical Tablet Compaction: Product and Process Design

Mridula Pore

B.A. Chemical Engineering

Sidney Sussex College

University of Cambridge, 2003

M.Eng. Chemical Engineering

Sidney Sussex College

University of Cambridge, 2003

SUBMITTED TO THE DEPARTMENT OF CHEMICAL ENGINEERING

IN PARTIAL FULFILLMENT OF THE REQUIREMENTS FOR THE DEGREE OF

DOCTOR OF PHILOSOPHY IN CHEMICAL ENGINEERING PRACTICE

AT THE

MASSACHUSETTS INSTITUTE OF TECHNOLOGY

June, 2009

ARCHIVES

Author:......................   ....

Mridula Pore

Department of Chemical Engineering

May 27, 2009

Certified by:......................   ....

Charles L. Cooney

Robert T. Haslam Professor of Chemical Engineering

Thesis supervisor

Accepted by:...........................   ....

William M. Deen

Carbon P. Dubbs Professor of Chemical and Biological Engineering

Chairman, Committee for Graduate Students
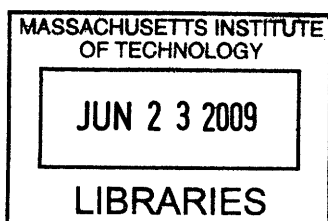
Pharmaceutical Tablet Compaction: Product and Process Design

Mridula Pore

B.A & M.Eng Sidney Sussex College, University of Cambridge, 2003

ABSTRACT

This thesis explores how tablet performance is affected by microstructure, and how microstructure can be controlled by selection of excipients and compaction parameters. A systematic strategy for formulation and process design of pharmaceutical tablets is proposed.

A modified nanoindenter method was used to test the mechanical behavior of diametrally compressed excipient granules. X ray micro computed tomography and Terahertz pulsed spectroscopy (TPS) and imaging (TPI) were used to analyze the microstructure of the tablet core and detect internal defects.

Granule failure mechanisms are found to be consistent with tablet microstructure. MCC granules deform plastically when tested and X ray images show individual granules undergoing increasing deformation in tablets as higher compaction forces are used. A highly interconnected pore-structure limited tablet hardness and led to bursting behavior during dissolution. No effect of compaction force or speed was observed in dissolution profiles. Lactose granules fracture at strains less than 5%, forming monolithic structures with no evidence of initial granule shape or size. Pore size decreases as compaction force is increased for DCL 11 tablets. A decreasing pore size corresponds to increasing THz refractive index, tablet hardness and dissolution time. DCL 11 and DCL 14 tablets compacted under the same conditions have the same pore size distributions and hardness, although DCL 14 granules are weaker than DCL 11, and DCL 14 tablets dissolve up to four times slower than DCL 11 tablets.

No difference was observed between the THz spectra of tablets made from the two grades of lactose. Further work is needed to understand the physical significance of the THz measurements. TPI can detect laminated tablets and is faster than X ray micro CT.

In order to develop a rational design methodology, two key areas for future research are building a process model for compaction and developing quality testing methods that can be analyzed mechanistically.

The capstone project explores strategic decision making for innovator firms and generic drug manufacturers in the period surrounding patent expiry. Statin products were used as an illustrative case of a pharmaceutical technology experiencing commoditization. A system dynamics model was used to simulate historic results and explore options for products still under patent protection. Current models of technology market dynamics apply to statins, but regulation and legislation play a large role in controlling market entry, leading to strong sequencing effects.

Thesis Supervisor: Charles L. Cooney
Title: Robert T. Haslam Professor of Chemical Engineering

To my teachers, past and present, with gratitude.

To my family, with love.

Acknowledgements

Over the course of working on this thesis, I have been fortunate to meet and learn from numerous people, at MIT and beyond.

Firstly, I would like to thank my advisor, Prof Charles L. Cooney for his guidance. Not only did I benefit from his technical expertise, but he has been an inspiration and taught me by example how to lead, communicate, teach and mentor. I am grateful for the varied opportunities he has provided to expand my horizons.

Dr Henry Weil supervised my capstone paper research. He has been instrumental in guiding my thinking and helping me to consolidate material learnt in various Sloan classes. I am grateful for his encouragement and enthusiastic support. I would also like to thank my thesis committee, Professors George Stephanopoulos, Alan Hatton, Christine Ortiz and Steve Eppinger, for their valuable suggestions and advice.

I am grateful to the Consortium for the Advancement of Manufacturing of Pharmaceuticals (CAMP) for financial support and to its members for their input.

My thanks to the Cooney group: Yu Pu, Samuel Ngai, Lakshman Pernenkil, Matthew Abel, Brian Mickus, Erin Bell, Claudia Fabian, Daniel Weber, Farzad Jalali-Yazdi and Ben Lin for their friendship and support. Rosangela dos Santos has been an invaluable support and a caring and friendly presence. It has been a pleasure working with them all. I benefited greatly from interactions with the undergraduate students in the UROP program and in classes 10.29: Cathleen Allard, Moira Kessler, Shannon Nees, Sidra Khan, Kyle Yazzie, Deepika Singh, Jamira Cotton, Joe Roy-Mayhew and Mary Machado. Also, thanks to Margo Servison. I am grateful to Dr Bill Dalzell for offering me a position as teaching assistant with the class of 10.32, Spring 2008. I believe I learnt at least as much from them, as they (maybe) did from me.

Many people have been kind enough to train and assist me in the different experimental techniques described in this research. They are too numerous to list here and are acknowledged in the appropriate chapters.

On a personal note, I would like to thank my beloved husband, Raj, for his unwavering patience, good humor and affection. Finally, I could not have attempted this endeavor without the boundless love, support and encouragement of Aai, Baba and Meenal. They are always at the heart of my success.

Table of Contents

List of Figures

List of Tables

Introduction

Current state of tablet product development and manufacturing

Tablets are the most common form of drug delivery as they are a robust, inexpensive and effective method of delivering drug substance to a patient; 46% of drug products approved by the FDA are in tablet form (Figure 1). Although pharmaceutical tablets have been around for several decades, little has changed in the way they are designed and manufactured. Product and process development teams rely heavily on past experiences with similar materials and equipment, and design improvements tend to be incremental rather than radical.
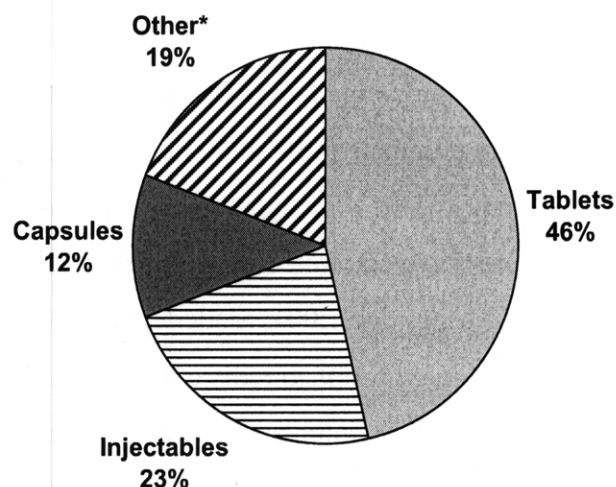
Figure 1: Dosage Form of FDA-approved Drug Products (*includes inhalation and topical products, Source: Drugs@FDA, 2005)

The current drug product development process has much iteration as the drug progresses through pre-clinical and clinical trials. Currently, the development of the formulation and process design is governed by the need to meet tight deadlines so that the drug can be the first to market. Due to the high failure rate of drugs in the early stages of clinical trials, the emphasis is on speed, rather than optimizing the dosage form. Only small samples of the drug substance are available at early stages, so the extent of experimentation is limited by materials as well as time. Different dosage forms and strengths may be required for the purposes of 'blinding' during clinical trials, so the initial formulation and dosage form is different from the final market version. Process scale-up is performed

only at the later stages of clinical development, so potential manufacturing problems cannot be identified until the formulation and dosage form specifications have been fixed by regulatory documentation. Hence processes that are sub-optimal in terms of cost-efficiency or raw material usage are often implemented.

Direct compression is a tablet-making process whereby active pharmaceutical ingredients (API's) are simply blended with other ingredients (excipients) and the resulting powder mixture is compacted. This is the simplest and most cost-effective process for manufacturing tablets. However, the impact of material properties and process attributes on product quality is not well understood. As a result, there is a high perceived risk associated with the process and only a small fraction of manufacturing processes are direct compression (McCormick, 2005). Most manufacturing processes involve additional operations, such as wet granulation or roller compaction. More complex processes result in additional capital, energy and material requirements and introduce sources of variation. It is desirable to eliminate these increased costs and uncertainties by increasing the fundamental knowledge of the direct compression process.

It has been proposed in the literature that a combined product design and process systems engineering approach (Cussler and Moggridge, 2001, Sieder et al., 2004) could be applied to the development of solid dosage forms to reduce the time and effort required for the launch of a new solid dosage product (Fung and Ng, 2003, Hardy and Cook, 2003). There is also a strong regulatory driver for a rational design approach. For example, the ICH Q8 guidelines (FDA, 2004) advocate 'designing and developing formulations and manufacturing processes to ensure predefined product quality'. For this to be a realistic goal, the materials and process must be thoroughly understood and there should be capacity to predict their effects on the product quality. Better understanding of the process and the sources of variability allows a control strategy to be implemented, which would lead to more robust manufacturing processes.

The 'Structured Chemical Product' Design paradigm

There is a growing body of chemical engineering literature that discusses approaches for designing products whose structure is a key part of their functionality. A pharmaceutical tablet falls in this category. Hill (2004) describes structured products as complex,

multiphase materials, with microstructures on the scale of 0.1-100µm. Some familiar examples include consumer products such as ice-cream and chocolate: solids whose crystal structure affects their taste, or skin creams and margarine, whose 'spreadability' depends on the structure of the emulsion. Their structure, more than the chemical composition, determines the functional properties of these materials.

The design approach suggested for such products is presented in Figure 2. The starting point (read right to left) for design is identifying consumer needs, the definition of quality and the key product performance criteria. These must then be translated into engineering specifications for the microstructure. The next step is to achieve the desired structure through a combination of formulation and process design.

Raw material Inputs (Formula) ⬌ **Process** ⬌ **Structure** ⬌ **Performance**
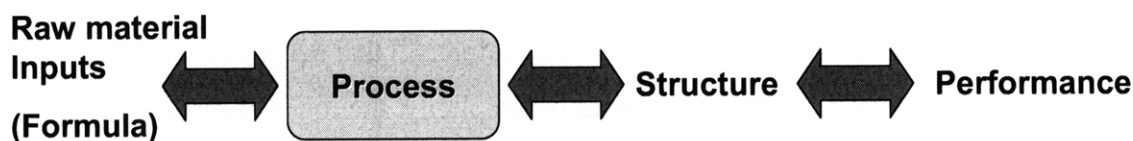
Figure 2: Design approach for structured products (adapted from Hill, 2005)

For a totally rational approach to design, one needs to work from right to left on this diagram. However, in order for this to be possible, a thorough understanding is needed of how the raw materials and the process parameters affect the microstructure and in turn, how microstructure affects performance (i.e. left to right). The aim of this thesis is to develop this understanding for pharmaceutical tablets.

A pharmaceutical tablet falls in this category of structured products. The important functional properties for the purposes of this study were the tablet hardness (see Part IIA) and tablet dissolution (see Part IIB); two common, in-vitro tests which are used in development and quality control and are important for regulatory purposes. Hardness and dissolution properties are a function of both the chemical composition and physical structure of the tablet. The physical structure of the tablet will, in turn, depend on both the formulation and the manufacturing process.

Effect of tablet structure on dissolution and hardness

There has been some work done on relating tablet hardness and dissolution to tablet porosity (e.g. Cruard et al, 1980, Olsson and Nystrom, 2001), or tablet surface

morphology (e.g.Narayan and Hancock, 2003). However, these are usually correlative relationships and there are limitations to the structural information obtained. Porosity has typically been measured by permeametry in these studies and an average value for the tablet is obtained. Therefore qualitative morphological data is not available.

Surface imaging, by ESEM for example, can give us high resolution information about the tablet. However, the surface of a tablet or a broken fragment typically does not represent the internal structure due to wall effects during compaction or smearing effects during breakage. Until recently it was not possible to obtain high resolution images (on the order of microns) of the internal structure of tablets.

Effect of formulation and compaction process on tablet structure

Most commercially-produced tablets consist of a coating around a core containing the active ingredient plus other materials (known as excipients) that act as fillers, binders, lubricants, disintegrants etc. For the purposes of simplicity, the focus of this study is on uncoated tablets.

At the manufacturing scale, tablets are produced by rotary presses at high speed (Fette, 2007, Natoli, 2007), although at the development stages, a single station press is often used. A schematic of the tablet compaction cycle is presented in Figure 3. Powder compaction to form tablets has two phases; compression and densification. During the initial, compression phase the powder is filled into the die and pressure is applied. The apparent density of the powder increases due to particle movement. The change in apparent density will depend on particle size, shape, cohesion and friction; the same characteristics that govern powder flow. It is believed that the contacts formed during this phase determine the interaction of particles during the densification stage. In manufacturing processes there may be a pre-compaction step that is performed at lower pressure than the main compaction. The reasons for this step are to allow displacement of air and allow the material to relax and form greater solid bonds (Schwartz, 2002). As greater pressure is applied, the powder particles deform elastically and then undergo irreversible plastic deformation and / or brittle fracture.

Die Filling   Compression   Pre-compaction   Compaction   Ejection
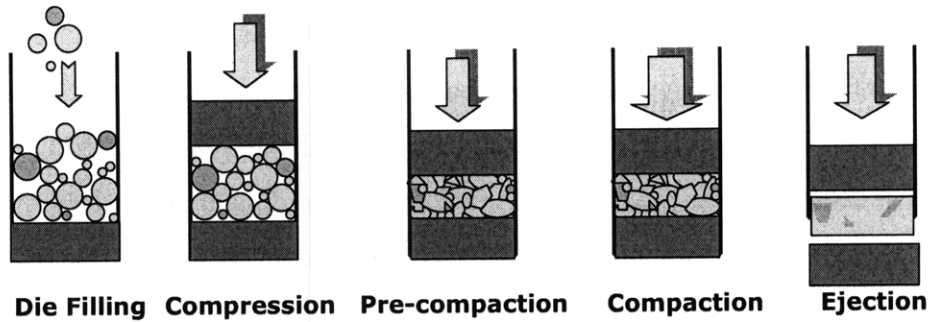
Figure 3: Tablet compaction cycle

Pharmaceutical excipients are known to exhibit a range of deformation behavior under uniaxial compression (Figure 4) and hence the deformation mechanics and kinetics cannot be described by a single parameter.

Therefore, the physical structure of the tablet is determined both by physical properties of the materials and the nature of the compaction process, e.g. die-filling, compaction cycle (compaction speed and maximum compaction force) and tooling geometry.

E (GPa)	σ_y (MPa)	H (MPa)	SRS (%)	Description		Consolidation behavior	Material examples
>40	>300	>1000	0-10	Hard	Brittle	Fragmentation	Inorganics
					Ductile	Plastic flow at contact points	Metals
12-30	80-200	250-600	5-40	Moderately hard	Brittle	Fragmentation some flow at contact points	Paracetamol
					Brittle/ ductile		Lactose
					Ductile	Less fracture more plastic flow	Sucrose
4-12	40-80	150-250	40-80	Soft	Ductile	Plastic flow	Microcrystalline cellulose
					Ductile/ elastic	Elastic and plastic deformation	Starch
<4	<40	<120	>60	Very soft	Highly visco-elastic	Total plastic flow	PTFE

Figure 4: Relationship between material properties and compaction behavior (Rowe and Roberts, 1996)

Market dynamics of patent expiry

In addition to the FDA regulatory initiatives that seek to promote better process understanding, pharmaceutical firms also face commercial pressures that should encourage them to invest in this type of research. The time and cost pressures on all

aspects of these firms, including product development and manufacturing, have been increasing due to the product pipeline concerns currently facing most companies. The shortage of products in the pipeline can be explained on one hand by lower R&D productivity that leads to fewer products making it to the market, and on the other hand by increasing generic competition at the other end of the product's lifecycle that erodes profitability for innovator firms. Understanding these market dynamics in the context of the current theories of technology market dynamics can provide insights into how formulation and process development can be critical to the commercial success of a product.

Objectives

The objectives of this thesis were to

- o Identify and investigate tools for characterization of powder mechanical properties

- o Identify and investigate analytical tools to probe tablet microstructure

- o Investigate the links between raw materials, process, tablet structure and tablet performance

- o Evaluate the potential of a rational design methodology based on tablet microstructure

- o Explore the market dynamics around patent expiry that contribute to time and cost pressures on pharmaceutical products

Approach

The design of tablet microstructure has two main degrees of freedom: formulation and process parameters. The rationale behind the experimental design is presented below with an outline of the investigation of tablet microstructure.

Formulation Design

Lactose and microcrystalline cellulose are two commonly used excipients. Both can be used as binder/fillers for tablets made by direct compression, which is the simplest tablet

manufacturing process. A direct compression process was used in this research to eliminate sources of variation from blending and other preliminary steps. The potency of new drugs is increasing and hence dosages are lower. In this case, excipients will form a large part of the tablet and the characteristics of the excipient will play a dominant role in determining tablet physico-chemical properties. Therefore, this study focuses on tablets made only of direct-compression excipients. The only exception is the dissolution study, where small amounts of caffeine were added to the tablet to act as a tracer.

As shown in Figure 4, lactose and MCC are believed to have very different mechanical characteristics. Therefore they were chosen as materials to investigate the effects of granule mechanical properties on tablet structure and performance.

MCC Celphere CP102 lot no. 15J1 (Asahi Kasei, Japan) and Lactose DCL 11 lot number 10218008 (DMV International, The Netherlands) were used to compare the effects of different granule failure mechanisms. Lactose DCL 14 lot number 10185935 (DMV International) was used for a quantitative comparison with DCL11.

The physical and mechanical characteristics of these powders were obtained experimentally and are presented in Part I. The effects of material on tablet performance and physical structure are presented in Parts II and III respectively.

Process Design

In this study, the effects of compaction speed and maximum compaction force were investigated. The tooling geometry was kept constant and a uniaxial, constant-speed compaction cycle was used for making the tablets.

The effects of speed and force on tablet hardness and dissolution are presented in Part II and the effects on tablet structural features are presented in Part III.

Tablet structural analysis

Terahertz spectroscopy and imaging, and X ray microCT are tools that are relatively new in the area of pharmaceutical solids analysis. Their potential for characterizing the structure of the tablet was investigated. The tools were used to obtain information about the microstructure of the tablet (length scale of 1-100 microns) and also to detect large structural features (on the order of millimeters). This investigation is presented in Part III of this thesis.

In Part IV, the implications of the experimental findings on product and process design are considered.

Market dynamics of patent expiry

Statin drug products were selected for this investigation, as there are several indicators showing that they are illustrative of a pharmaceutical market undergoing the process of commoditization . As this is a high-profile market, pricing and market data is available in the public domain for analysis.

The following frameworks for the strategic analysis of technology markets were applied: S-curve industry dynamics frameworks (Foster, 1986) and the value capture framework by Teece (1986).

A system dynamics model was created in Vensim® and used to replicate and explain the dynamics of products that have already seen generic entry and to explore options for those products that still have patent protection. This work is described in Part V.

References

Cruaud O.; Duchene D.; Puisieux F.; Carstensen J. T. *J. Pharm. Sci.* **1980**, *69 (5)*, 607-608

Cussler E.L.; Moggridge G.D. *Chemical Product Design*, Cambridge University Press, Cambridge (UK), **2001**

Drugs@FDA Database, *www.fda.gov/CDER*, Accessed **19th September 2005**

FDA *International Conference on Harmonization (ICH) Guidelines, Q8: Pharmaceutical Development,* Food and Drug Administration, **2004**

Fette GmBH, *www.fette.com*, accessed **July 2007**

Foster R. '*The S-curve: A new forecasting tool' Chapter 4 in Innovation: The attacker's advantage'* Simon and Schuster, New York (NY), **1986**, 88-111

Fung K.Y.; Ng K.M *AIChE J.* **2003**, *49 (5)*, 1193

Hardy I.J.; Cook W.G. *J. Pharm.Pharmacol.* **2003**, *55 (3)*

Hill M. *AIChE J.*, **2004**, *50 (8)*

Hill M. *Presentation at Process Systems and Engineering Consortium Meeting, Amherst, MA,* **October 14, 2005**

McCormick D. *Pharm. Tech.* **2005**, *29c(4)* 52

Narayan P.; Hancock B.C.,*Mat. Sci. Eng.* **2003**, *A355*, 24-36

Natoli, *www.natoli.com*, accessed **July 2007**, Natoli Inc.

Olsson H.; Nystrom C. *Pharm. Res.* **2001**, *18 (2)*, 203-210

Rowe R.C.; Roberts R.J. *Pharmaceutical Powder Compaction Technology*, Marcel Dekker, **1996**

Schwartz J.B. *Pharmaceutical Process Scale-Up*, Marcel Dekker, Ed. Levin M. **2002**

Seider W.D.; Seader J.D.; Lewin D.R. *Product and Process Design Principles; Synthesis, Analysis and Evaluation, 2nd Ed.*, Wiley **2004**

Teece D.J. *Research Policy, 15*, 285-305, **1986**

Part I: Physical and Mechanical Characterization of Excipient Powders

Microcrystalline cellulose (Celphere® CP102) and spray-dried lactose (DCL 11 and DCL 14) powders were characterized by their physical and mechanical properties. The aim was to identify differences in granule properties to account for differences in tablet structure and performance (as described in Part II).

DCL 11 and 14 were found to have similar particle size distribution, density, shape and surface morphology. MCC granules are of similar density and shape, but slightly larger in size and have a much smoother, less porous surface than spray-dried lactose.

A modified nanoindenter method was used to test the mechanical behavior of diametrally compressed single granules. The results confirm that MCC granules undergo plastic deformation and lactose granules fail predominantly by fracture, as hypothesized in the literature. MCC granules were found to be tough and withstood loads and displacements up to the equipment limits, whereas lactose granules failed at strains of less than 5%. The heterogeneous nature of spray-dried lactose agglomerates must be considered to explain the experimental results. Spray dried lactose granules exhibit a force-displacement profile that is initially linear. A range of behaviors was observed (fracture, fracture with local damage, and disintegration). Fracture was found to occur at higher frequency for higher loading rates. The parameters associated with fracture- the slope of the profile (indicative of granule stiffness) and the fracture load - were used to characterize DCL 11 and DCL 14 grades of spray dried lactose. DCL 14 granules were found to be weaker than DCL 11 and have a wider range of granule strength. DCL 14 granules also have a greater tendency to disintegrate than DCL 11.

As the granules in this study have similar physical properties, differences in tablet structure and performance must be due to differences in mechanical properties. These, in turn, are a result of chemical and polymorph composition, and internal structure of the granules.

I.A: Physical Characterization of Powders

Introduction

The size, shape and density of excipient powders used in this study were characterized using standard methods. The purpose was to detect any differences between the raw materials (other than their mechanical properties under loading) that might be the source of variation in tablet structure. For example, smaller particles (Yang et al, 2000) or wider particle size distributions (Nolan and Kavanagh, 1993) lead to denser packing structure in a powder bed, which increases the number of particle-particle contacts and determines force transmission pathways during compaction.

Reviews and comparisons of methods to measure and describe powder size distribution have been presented by Rhodes (1998), Naito et al (1998), Etzler and Sanderson (1995) and Domike (2003) and will not be covered here.

Excipient powders were prepared by a standard procedure, as described below. Only the sieve fraction 106-212 microns was used for all experiments in this thesis. Granule size distribution was measured using laser light diffraction (Wedd, 2003, Plantz, 2005) and density was measured using helium pycnometry (USP 2005, ASTM, 2005, Webb, 2001 Keith, 2006, Micromeritics, 1996) . Powder granules were imaged using ESEM to study surface morphology and optical microscopy was used to measure sphericity.

<u>Material preparation</u>

MCC Celphere ® CP102 lot no. 15J1 (Asahi Kasei, Japan), Lactose Pharmatose® DCL 11 lot number 10218008 (DMV International) and DCL 14 lot number 10185935 (DMV International) were analyzed. The powders were sieved using a standard sieve tester SS-15 (Gilson Company Inc.) and ASTM E11 standard sieves.

50g of powder was sieved for five minutes on top of a stack of sieves (ASTM number 140 and 70) to obtain the sieve fraction 106-212 microns. The sieving time was kept to a minimum to prevent damage to the powder granules (Pernenkil, 2006).

Once sieved, the powder was stored over saturated magnesium nitrate solution in a dessicator (at 55% relative humidity) for at least 24 hours prior to testing.

Experimental Methods

Granule Size

A Microtrac ASVR / X100 system was used to obtain the granule size distribution by laser light diffraction. The data was analyzed with Microtrac v9.1.15 software. 200 proof USP grade ethyl alcohol was used as the dispersion medium, as lactose and cellulose are both insoluble in ethanol.

Three batches of each material were sieved. One spatula of each sieve fraction was analyzed. Each analysis consisted of three consecutive readings.

The equipment was rinsed twice with ethanol between samples to remove any powder residue. If a bimodal distribution was observed for MCC samples, ultrasonication was used to disperse the granules and the measurement was repeated. Ultrasonication was not used for lactose powders to prevent damage to the granules.

Pycnometric Density

A 1cc AccuPyc 1330 Helium Pycnometer (Micromeritics Inc.) was used to measure the true volume of the powder samples (Keith, 2006). Pycnometric volume can be considered the 'apparent particle volume' as it includes the solid volume and the volume of closed pores, but excludes interstitial and open pore volume.

Powder was weighed into the sample cup to an accuracy of 0.1mg. The analysis consisted of five purge runs to remove water vapor and contaminants, followed by five measurement runs. Four samples of powder were measured for each material.

The temperature range during calibration and measurement was 25.8 – 26.1°C, which is within the 2°C variation permitted by the USP standard <699> (USP, 2005a).

Environmental Scanning Electron Microscopy

A FEI/Philips XL30 FEG ESEM apparatus was used in low-vacuum mode to image MCC and DCL11 granules before and after washing with ethanol. This was to ensure that ethanol did not affect the morphology of the granules during particle size analysis and sample preparation for nanoindenter experiments (see part I.B).

Optical Microscopy

An in-line 4X zoom optical microscope was used to image granules before mechanical testing with a MicroMaterials Ltd Nanotest device (see Part I.B). The length scale of images was calibrated using glass spheres of known diameter. The ratio of the Feret diameter in two perpendicular directions (see Figure 5) was calculated as a measure of sphericity of the granules.

$$Asphericity = Max\left(\frac{d_x}{d_y}, \frac{d_y}{d_x}\right) \qquad\qquad (I.A-1)$$
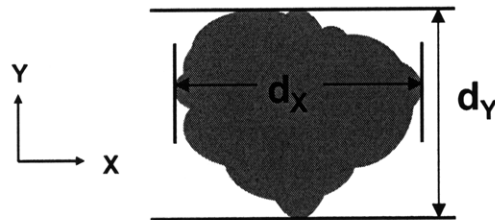
Figure 5: Feret diameter measurement

Results

Particle Size Distribution

A lognormal distribution was found to fit the granule size distributions well. The number distribution with 95% confidence intervals are presented in Figure 6. The lognormal distribution parameters are presented in Table 1.

Table 1: Lognormal parameters of particle size number distribution

	MCC	DCL 11	DCL 14
X_{50} (microns)	159.7	114.6	126.6
Standard deviation $(X_{84}/X_{16})^{1/2}$	1.20	1.32	1.27

The distributions fall largely in the 106-212 micron range, as expected after sieving. MCC has a larger average particle size and a narrower distribution than the lactose powders. DCL 11 and DCL 14 have similar distributions, but DCL 14 granules appear to be slightly bigger and DCL 11 has a wider distribution.
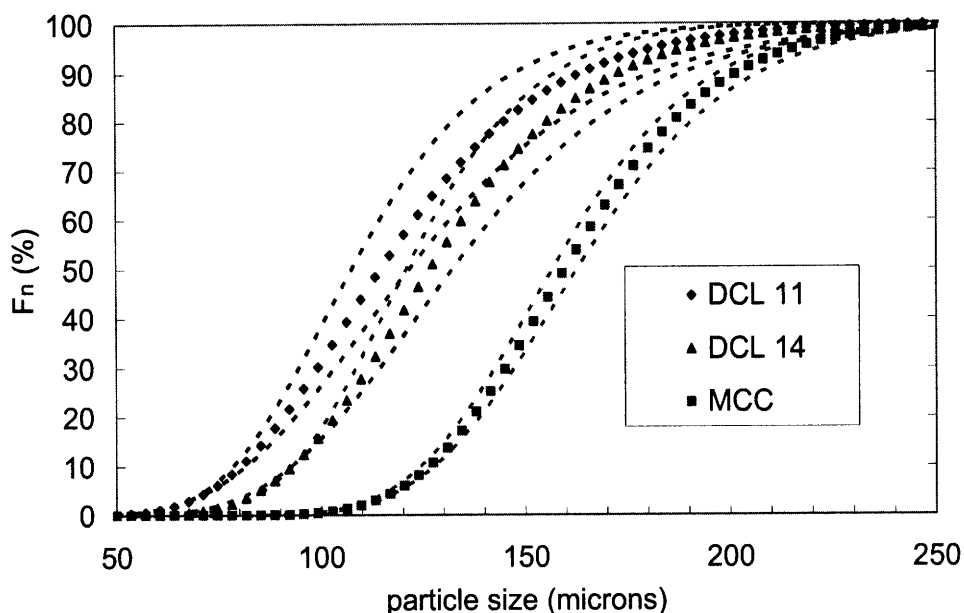
Figure 6: Lognormal number distribution of particle size (dotted lines represent upper and lower 95% confidence intervals)

Pycnometric Density

MCC was found to have a slightly lower pycnometric density than both lactose grades (Table 2). DCL 11 and DCL 14 do not have significantly different densities.

Table 2: Pycnometric density of excipient powders

Material (sieve fraction 106-212μm)	Pycnometric density (g/cm^3)
MCC Celphere® CP 102	1.516 ± 0.004
Pharmatose® Lactose DCL 11	1.529 ± 0.004
Pharmatose® Lactose DCL 14	1.535 ± 0.003

Shape and Morphology

ESEM images of DCL 11 and MCC Celphere® granules before and after washing in ethanol are presented in Figure 7. From 2 (a) and (b) we can see that the surface morphology of the two materials are quite different. MCC has a relatively smooth, continuous surface, whereas lactose is rough and looks porous. DCL 11 is a grade of spray-dried lactose (DMV International, 2005), and the individual crystals that make up the granule are visible at the surface.

No change in morphology is observed after washing in 200 proof (USP grade) ethanol, which indicates that ethanol is a suitable medium for particle size measurement.

(a) Pharmatose® DCL 11 - as received

(b) MCC Celphere® - as received

(c) Pharmatose® DCL 11 – washed in ethanol

(d) MCC Celphere® – washed in ethanol
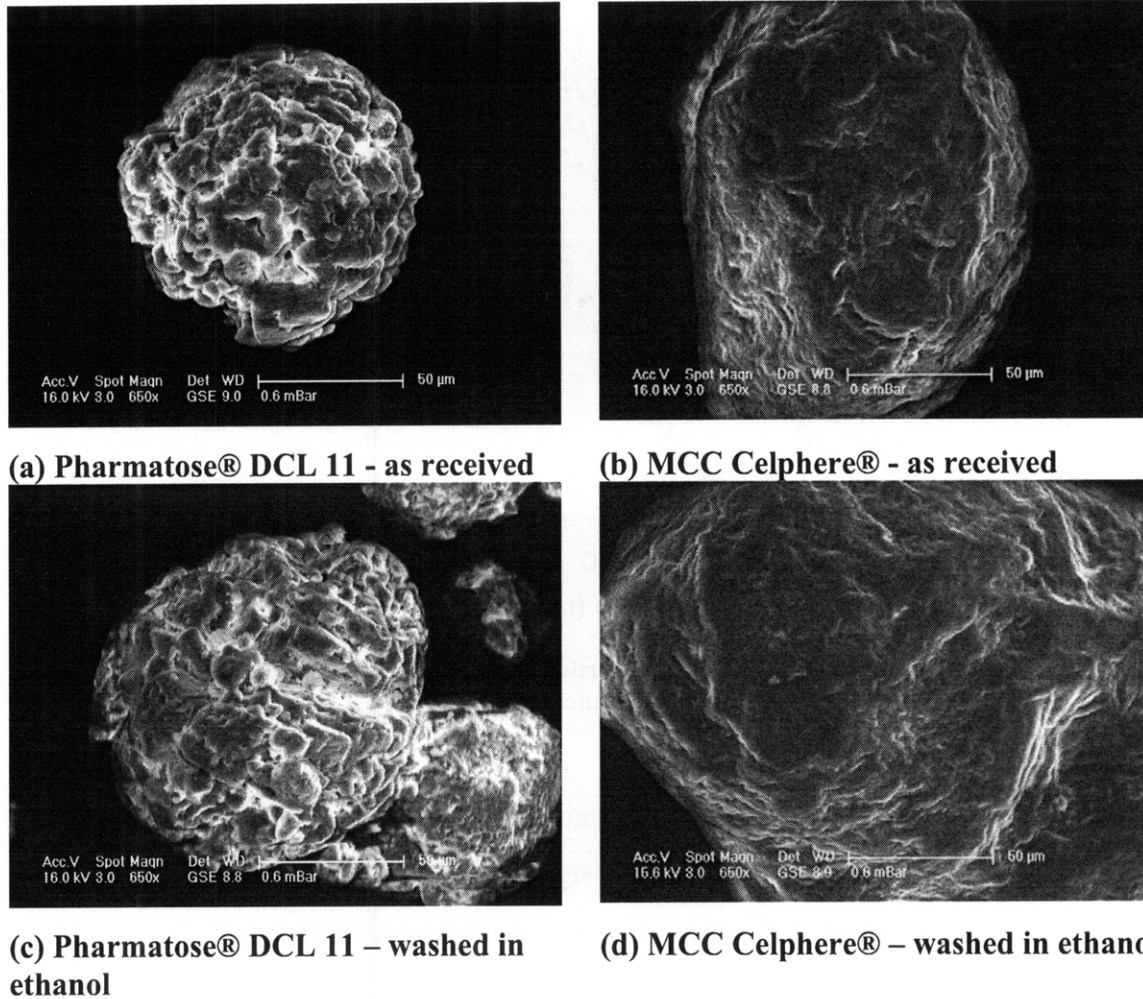
Figure 7: ESEM images of granule morphology before and after ethanol wash. No change is observed.

ESEM images of DCL 11 and DCL 14 (supplied by vendor) are presented in Figure 8. No difference in surface morphology is seen.
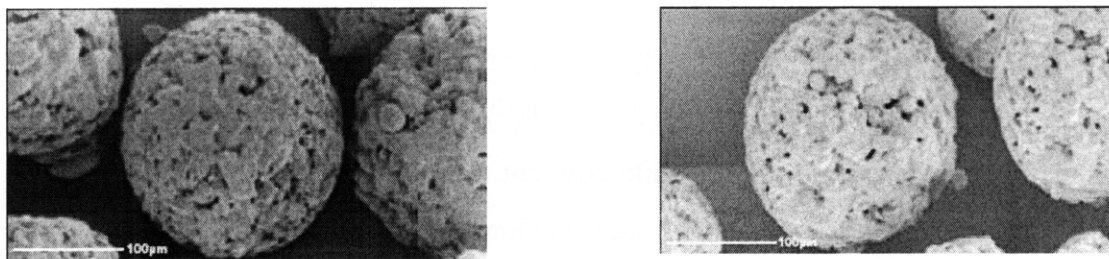
Figure 8: Environmental scanning electron microscope images of DCL 11 (left) and DCL 14 (right) granules (DMV International, 2005)

The ratio of granule lengths was used as an indicator of asphericity for DCL 11 and DCL 14. The average and standard deviation of 25-30 samples is presented in Table 3. There is

no significant difference in sphericity of the granules. Both are close to a value of one, indicating that the granules are almost spherical in shape.

Table 3: Asphericity of DCL 11 and DCL 14 granules

	DCL 11	DCL 14
Average asphericity (-)	1.080	1.067
Standard deviation (-)	0.078	0.064

Discussion

Particle size distribution is known to vary with the analytical method used (Naito et al, 1998, Etzler and Sanderson, 1995). Therefore, a widely used method, laser diffraction, was selected to analyze the powders that had already been sieved. MCC powders have a distribution within the sieve fraction range. DCL 11 and DCL 14 contain some fines (about 25% of particles are less than 100microns), which may be the result of attrition during handling, as they are known to be fragile. The creation of fines leads to a wider particle size distribution. Wider distributions are known to create denser packings of the initial powder bed. However, the subsequent effect on the tablet structure will also depend on the granule failure mechanism and the evolution of the powder bed structure during the compaction process.

For the density measurement, variation in volume is within the 0.2% variation permitted by the USP standard (USP, 2005). Pycnometric volume measurements are more accurate if the sample is previously dried to prevent water vapor from contributing to pressure measurements. However, in this case, the density at a given humidity was required, so the samples were not previously dried. The density of the three powders analyzed did not differ by more than 1%, therefore, density differences are unlikely to affect the powder flow behavior during die filling (Ngai, 2005, Pu, 2007).

Physical characterization of MCC, DCL 11 and DCL 14 indicate that the sieved powders have similar particle size distributions and densities. The surface morphology of the granules varies with material, but the granules are near-spherical in shape. Therefore although surface, and hence powder flow, properties are likely to be different, the initial packing of the powder bed should be similar. Therefore differences in tablet structure and

performance must be due to differences in chemical composition and the mechanical response of the powder bed during compaction.

Conclusions

Physical characterization of MCC, DCL 11 and DCL 14 granules indicates that they have similar particle size distributions, densities and shape. This indicates that the pre-compaction packing of the powders is similar and differences in tablet structure and performance must be due to differences in chemical and mechanical properties of the powders.

References

ASTM *D5550 Test Method for Specific Gravity of Soil Solids by Gas Pycnometer* American Society for Testing Materials **2005**

DMV International *Product Group Overview, Pharmatose ® DC Lactose* **February 2005**

USP Test <699> Density of Solids *United States Pharmacopeia* **2005**, 2670

Keith, A. *Micromeritics Instrument Corporation, Personal Communication* **2006**

Webb, P.A. *Volume and Density Determinations for Particle Technologists* www.micromeritics.com **2001**

Micromeritics, *AccuPyc 1330 1-cm3 Samples Operation Manual*, Micromeritics Instrument Corporation **1996**

Pernenkil L. *Continuous Blending of Pharmaceutical Powders* PhD Thesis, MIT **2006**

Domike R.R. *Pharmaceutical Powders in Experiment and Simulation* PhD Thesis, MIT **2003**

Etzler F.M.; Sanderson M.S. *Part. Part. Syst. Char.* **1995**, *12 (5)*, 217-224

Naito M.; Hayakawa O.; Nakahira K.; Mori H., Tsubaki J. *Powder Technol.* **1998**, *100*, 52-60

Nolan G.T.; Kavanagh P.E. *Powder Technol.* **1993**, *76(3)*, 309-316

Ngai S.S.H. *Multiscale Analysis and Simulation of Powder Blending in Pharmaceutical Manufacturing,* PhD Thesis, MIT **2005**

Plantz, P.E. *Explanation of Data Reported by Microtrac Instruments, Microtrac Inc. Application Note* **2005**

Pu Y. *Theoretical and Experimental Investigation of Particle Interactions in Pharmaceutical Blending* PhD Thesis, MIT **2007**

Rhodes M. *Introduction to Particle Technology* John Wiley and Sons **1998**

Wedd, M.W. *Determination of Particle Size using Laser Diffraction, Educational Resources for Particle Technologists (www.erpt.org)* AIChE **2003**

Yang R.Y.; Zou R.P.; Yu A-B. *Phys. Rev. E.* **2000**, *62(3) B*, 3900-3908

I.B Mechanical Characterization of Powders

Introduction

The behavior of a powder bed subjected to uniaxial compaction will depend on both the properties of the powder granules and the parameters of the compaction process. Important material properties include the mode of deformation or failure and the granule strength. This chapter presents work done on characterizing the failure mode of powder particles, and qualitative and quantitative comparisons of common excipients.

Materials

The mechanical properties of microcrystalline cellulose (Celphere® CP102 Lot 15J1, Asahi Kasei, Japan), and two grades of spray-dried lactose (DCL11 Lot 10218008 and DCL 14 Lot 10185935, DMV International, Netherlands) were investigated experimentally.

Literature Search

A literature search was undertaken to identify a suitable method to test the mechanical properties of powders. The single-granule diametral test was selected. The literature on experimental and computational work on this test method was reviewed.

Methods to characterize mechanical properties of powders

Current methods to characterize materials used in pharmaceutical tablet compaction either test the final compact e.g., beam bending (Bassam et al, 1991), Vickers indentation (Ridgeway et al., 1969) or mimic the tablet compaction process e.g. Heckel analysis (Heckel, 1961, Hassanpour and Ghadiri, 2004, Roberts and Rowe, 1987). These testing methods give a single parameter value that describes the 'macroscopic' behavior of the powder bed or compact. Therefore the values are not purely properties of the particulate material, but include the influence of the compact preparation method. The numerical values of the parameters depend on the testing equipment (one exception is Hiestand indices, which use a standard testing configuration (Hiestand, 1996)) and modeling methods indicate that values extrapolated from bulk testing are not representative of single granule properties (Hassanpour and Ghadiri, 2004). These tests do not give insight

into the mechanisms of tablet compaction or enable prediction of process problems such as tablet lamination or capping. Therefore, methods for probing the behavior of individual granules are required.

In this study an attempt was made to characterize the mechanical properties of individual powder granules and investigate whether these properties are predictive of tablet structure and product performance.

Reviews of mechanical testing of powders have been published by Bemrose and Bridgwater (1987) and Couroyer et al. (2000). There are two classes of single-granule testing methods to predict the behavior under compression; indentation and single-granule diametral compression tests. Impact testing was not considered for this study because the short time-frame limits data collection.

Indentation

Indentation is a means of assessing the mechanical properties of a material (typically hardness) by probing the surface with a sharp tip and observing the response. Indentation of pharmaceutical materials has been performed at the micro- and the nano-scale. Indentation hardness has been used to obtain an estimate for stiffness and yield stress of crystals and observation of cracks has been used to obtain the fracture toughness. This method only probes the surface of the material, therefore these values may not be representative of the entire granule. Microindentation is performed with a Vickers indenter (also used for standardized testing of catalysts or metals) which requires hard particles in the size range of millimeters (Duncan-Hewitt, 1993). Hence it is unsuitable for pharmaceutical excipients, which are small (10-100s of microns), porous and relatively soft. Nanoindentation using a sharp tip has been used to compare the mechanical properties of API crystals and sucrose and shown to give rank order agreement with literature values of stiffness (Liao and Wiedmann, 2005). A brittleness index calculated from nanoindentation methods has also been demonstrated to be predictive of milling behavior of pharmaceutical crystals (Taylor et al., 2004). Nanoindentation requires a flat, homogeneous surface and the technique can be highly sensitive to the substrate that the granule is placed on. Therefore, it may better suited for analysis of crystalline materials, such as API's, rather than soft, irregular and porous excipient materials.

Single granule diametral compression test

The single-granule diametral compression test is a standard method for testing catalyst beads and other granular materials in the size range of millimeters (ASTM, 1982). It is also known as the Brazilian or single-granule crushing test. The test consists of placing a single granule between two flat, parallel plates, applying force on the upper plate (Figure 9) and measuring the resulting force-displacement profile. The profile can be analyzed to extract various data, typically the Young's modulus, yield stress or crushing strength, depending on the nature of the material. However, this method has rarely been used for particles less than 1 mm in diameter. In the recent literature, attempts have been made to extend this technique to particles as small as 5 microns (Koopman et al., 2005, Carlisle et al, 2006). This project attempted to use this technique to characterize single pharmaceutical excipient granules.
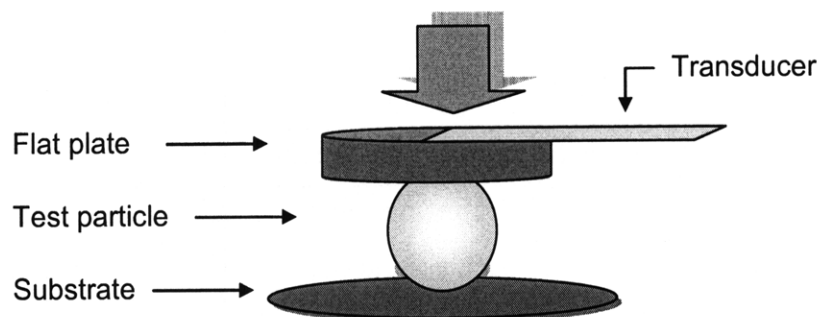
Figure 9: Equipment geometry for single granule compression test

A group at Imperial College, London has built an apparatus based on an inverted optical microscope to observe the behavior of alumina agglomerates of a size range 180-200 microns under compression (Sheng et al., 2004a). There are references in the literature to a 'nanocrusher' built by a group led by M. Ghadiri in the University of Leeds, UK, although, no data from this has been found in the published literature. Most recently, a nanoindenter has been used with a flat punch to study glass microballoons at the University of Alabama (Koopman et al., 2005, Carlisle et al, 2006). It is believed that nanoindenters are being used with a flat punch for powder analysis for confidential applications, but this data is not available in the public domain (Vodnick, 2005). The principle of the test is the same in each apparatus. It is necessary to have good alignment of the granule with the plates. Spherical granules are desirable because the

geometry lends itself to analytical equations for data analysis and granule orientation is not an issue. For non-spherical granules, measurements for different orientations of the granules relative to the punch will be required. The granule size, temperature and relative humidity may determine the nature of the material failure mode.

In compaction of bulk powder, a granule will typically be subjected to forces from multiple adjoining granules or surfaces, hence the mechanical response does not correlate directly to that observed in a diametral test. However, this testing configuration most closely represents the loading experienced during the compaction process.

Modeling the single granule crushing test

Various models have been developed to explain the mechanical behavior of single powder granules. Some models treat the granule as a homogeneous continuum, whereas some models attempt to incorporate information on internal structure to explain the mechanisms behind the deformation of the granule. For smaller powder granules, it is not possible to experimentally capture parameters relating to internal structure. However, the structural models give considerable insight into the failure mechanisms and how internal parameters affect the mechanical behavior. Both types of models and information about the internal structure of the tested materials are presented below.

Materials structure

One pharmaceutical grade of microcrystalline cellulose (Celphere® CP102 Lot 15J1, Asahi Kasei, Japan), and two grades of spray-dried lactose (Pharmatose® DCL11 Lot 10218008 and DCL 14 Lot 10185935, DMV International, Netherlands) were investigated for their mechanical properties. The materials were selected because MCC and lactose are commonly used direct-compression excipients. The specific grades were chosen for their spherical morphology, which eliminates the issue of granule orientation during testing and allows for more direct comparison with published theoretical and experimental results.

Celphere® is produced by granulation of MCC around a core (Asahi Kasei, 2007). The manufacturer-supplied images indicate that this forms a spherical, smooth, non-porous particle (see Figure 10). It is sold for the manufacture of larger granules for encapsulation.
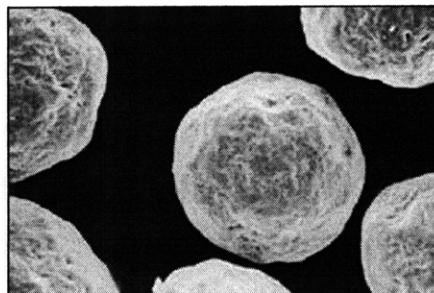
Figure 10: Environmental scanning electron microscope image of MCC Celphere® granules (Asahi Kasei, 2007)

DCL 11 and DCL 14 are both spray-dried grades of lactose sold for direct-compression tablets, capsules and sachet formulations. A slurry of small α-monohydrate lactose crystals is spray dried to form spherical, porous agglomerates with an amorphous lactose binder (DMV, 2005). DCL 11 is made of primary particles (lactose crystals) approximately 35 microns in size, whereas DCL 14 is made of primary particles of approximately 23 microns (DMV, 2007a and 2007b).
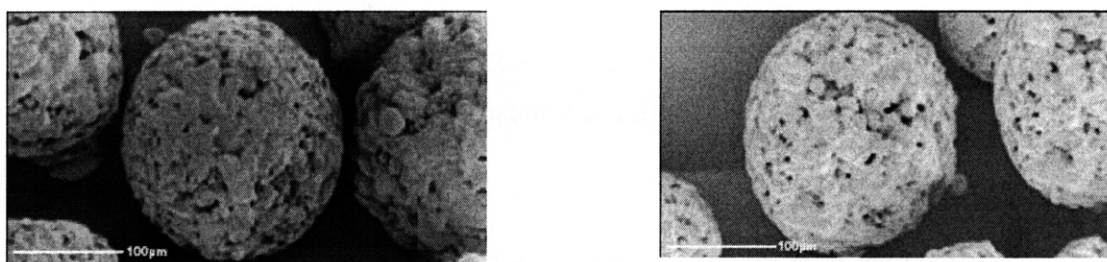
Figure 11: Environmental scanning electron microscope images of DCL 11 (left) and DCL 14 (right) granules (DMV International, 2005)

Bolhuis et al (2004) found that DCL 14 forms harder tablets than DCL 11 under the same conditions and proposed that smaller primary particle size is responsible for this as there is increased surface area for inter-particle bonding.

Continuum models

First order Hertz theory gives an analytical solution for small deformations of homogeneous, perfectly elastic spheres against a flat plate. The following expression is obtained for the force-displacement profile obtained using a diametral compression test if we use Johnson's method (1973) as outlined by Sheng et al. (2004b).

$$F = \left[\frac{4R^{1/2}}{3.2^{3/2}} E_r \right] h^{3/2}$$ (I.B-1)

F is the force, R is the diameter of the granule and h is the displacement. The value, E_r, is not exactly the Young's modulus because it depends not only on the fundamental properties of the material, but also on the structure of the granule. However, this is the desired contribution if we want to understand the granule's behavior under stress.

The derivation of this expression assumes perfectly elastic deformation at frictionless contacts. It also assumes that the deformation is localized to the contact and zones of deformation that form at different contact points do not impinge on one another.

If the granule undergoes more severe deformation, including plastic deformation, an analytical solution is not possible. A finite element method (FEM) model is required to model a single granule. These can incorporate elasto-plastic behavior, but not fracture. The parameters of constitutive equations for the model can be obtained by fitting from experiment data and these values will characterize the material. A combined FEM/DEM model can be used to simulate the compaction of a powder bed (e.g. Gethin et al, 2006).

DEM models for agglomerate damage

Many powders exist in the form of agglomerates. Agglomerates are clusters of primary particles that may be formed by granulation or spray drying. Agglomerates are common in process industries, as they have better flow properties than the primary particles alone. Spray-dried lactose is a commonly-used material for pharmaceutical tablet direct-compression processes and is investigated in this study.

The heterogeneous nature of agglomerates can be modeled using discrete element method (DEM). This technique explicitly defines each single primary particle and models its progress through a process by satisfying force and momentum equilibria at discrete time steps. A single agglomerate can be assembled from primary particles that are assumed to be non-breakable and non-deformable, and have a defined inter-particle bond strength (see Figure 12).
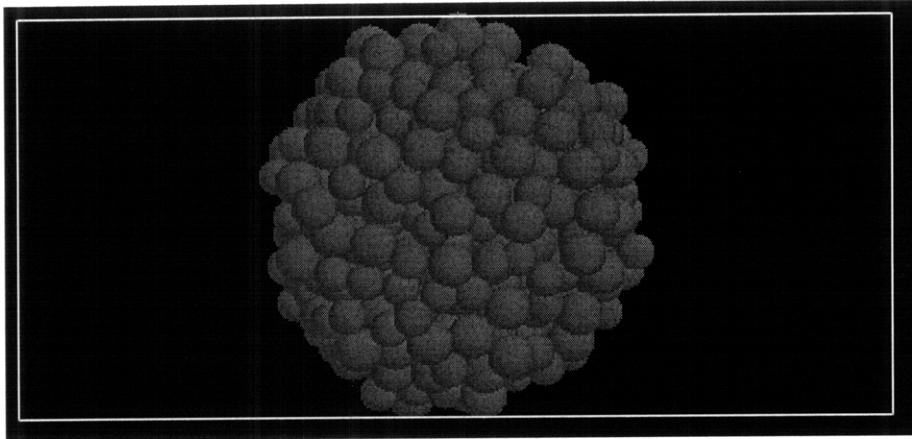
Figure 12: DEM simulation of agglomerate (Martin, 2007)

Single agglomerates can be subjected to stresses imitating those used in testing techniques such as diametral compression and impact testing (Thornton and Liu, 2004, Thornton et al, 2004, Thornton et al, 1999, Kafui and Thornton, 2000, Martin et al, 2006) and the intra-granular force evolution and failure can be observed. An assembly of agglomerates can be subjected to processes such as closed die compaction, however there are currently computational limitations on the size of the assembly that can be simulated, so it is not possible to simulate at the process-scale (Martin et al, 2006).

Hence, DEM can be used to relate intragranular bonding and geometry of agglomerates to their mechanical properties, which can be experimentally observed. It accounts for the effects of heterogeneity within in the agglomerate and enhances understanding of granule failure behavior. The source of heterogeneity is the random structure of the assembly of primary particles in the agglomerate. This leads to non-uniform force transmission and intra-granular microstructural changes when the agglomerate is subjected to applied stresses. These force transmission pathways and microstructural changes determine the observed mechanical response.

These simulations require input parameters describing intra-granule structure, such as primary particle packing or bond strength. However, theoretical simulations with assumed parameters can give considerable qualitative insight into failure mechanisms and can aid in the interpretation of single-granule testing results.

In simulations of diametral compression testing of 3D spherical, random-structured agglomerates, two modes of agglomerate failure have been identified; fracture and disintegration (Thornton et al, 2004 and Martin et al, 2006).

(a) Dense agglomerate visualization	(b) Force-strain for dense agglomerate
(c) Loose agglomerate visualization	(d) Force-strain for loose agglomerate
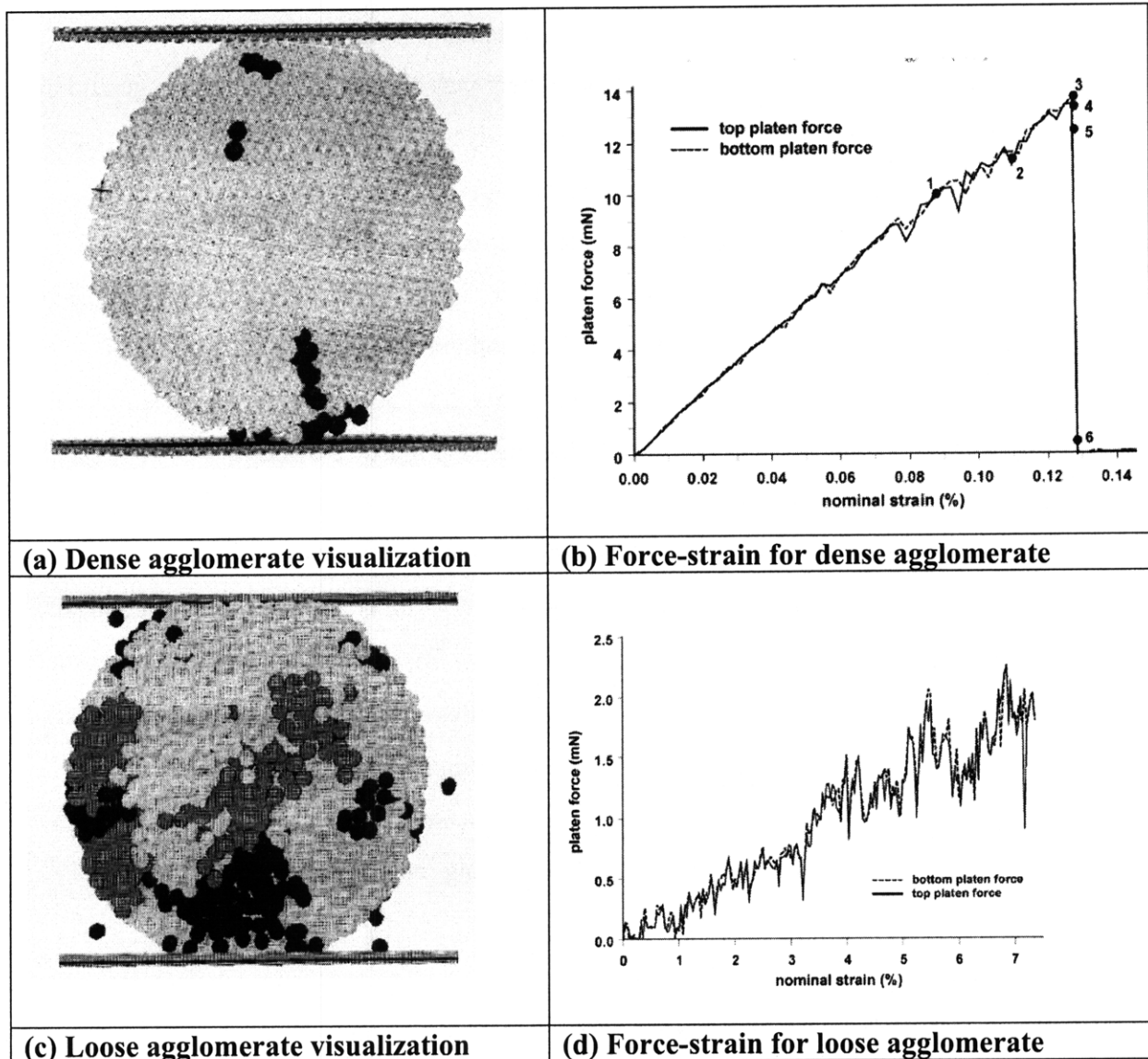
Figure 13: Comparison of DEM simulations for single granule compression testing of dense and loose packed agglomerates, resulting in fracture (a,b) and disintegration (c,d) respectively (Thornton et al, 2004)

Fracture is characterized by the presence of clear fracture planes (Thornton et al, 2004, Martin et al, 2006). Two or more large daughter particles are produced, with fines produced at platen-granule contacts. During loading, stresses build at the upper and lower platen contacts and bond rupture is concentrated at these points, leading to flattening of the contacts. The force transmission pathways propagate in planes parallel to the direction of loading. Bond breakage occurs in a random order at a steady rate with no

clear evidence of a propagating front. Hence a linear force-strain profile of the plates is observed. As compression proceeds, there are fluctuations in the profile due to small jumps in bond breakage (see Figure 13b). This is followed by instantaneous fracture along a plane slightly inclined to the direction of loading. Thornton et al (2004) also observed other weakened radial planes where there was significant bond breakage and the secondary fracture of one of the hemispherical daughter fragments.

Disintegration is the gradual attrition of the entire granule into small fragments. The force-strain profile of a diametral compression test is linear with small fluctuations as internal cracks form and fragments break off. There is no significant build up of forces at the platen contacts as the energy is dissipated in bond breakage and microstructural rearrangement. Hence forces do not propagate throughout the agglomerate. Eventually the agglomerate collapses into many small fragments (Figure 13 c and d).

Thornton et al (2004) noted that the failure modes and fracture patterns for diametral compression were the same as those observed in simulations of impact testing. For both fracture and disintegration, the break-up of the agglomerate is a progressive process and is shear-induced. The planes of weakness observed in fracture are believed to be a subset of the fracture planes that occur in granules that shatter on impact. Therefore, pre-existing flaws do not have a significant effect on granule strength or failure mode (Kafui and Thornton, 2000).

The factors determining failure mode in impact testing include (Thornton et al, 2004):

1. Impact speed

2. Porosity or solid fraction of agglomerate

3. Bond strength between primary particles

Thornton et al (1999) demonstrated that as the impact velocity is increased, the granule first rebounds, then undergoes fracture and at high velocities, it shatters into small fragments.

Mishra and Thornton (2001) demonstrated that dense agglomerates tend to undergo fracture, whereas loose agglomerates disintegrate in an impact test. Thornton et al (2004) demonstrated that the same trend is seen in a diametral compression test (Figure 13). For fracture to occur, strong force transmission pathways must exist. This is possible in a dense structure as the primary particles are constrained. In the loose structure, energy is

dissipated in rearrangement, leading to disintegration. For granules with intermediate density, the failure mode will depend either on the contact density or on other factors, such as the location of the impact site, speed or bond strength. Wikberg and Alderborn (1992) demonstrated experimentally that lactose granules exhibit a linear force-displacement profile, followed by fracture. They found that the stiffness and fracture force of lactose granules increased for decreased granule porosity. They concluded that granule porosity is one of the most critical physical properties of granules for their volume reduction behavior and hence the pore structure of the final compacts (Alderborn and Wikberg, 1996).

The presence of disintegration and fracture behaviors, and their dependence on granule density and impact velocity have been confirmed experimentally by Subero and Ghadiri, (2001). A high speed camera was used to observe the impact testing of agglomerates of glass ballotini. They identified four regimes of agglomerate failure (Figure 14) and noted that the frequency of fragmentation (fracture) increases with increasing impact velocity and void number and size.
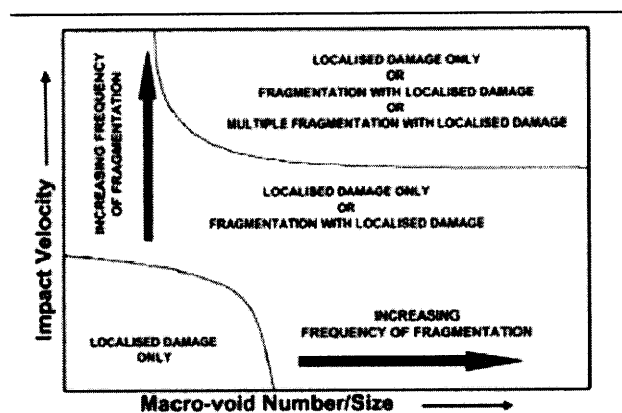
Figure 14: Map showing the dependence of granule breakage regime on impact velocity and solid fraction (Subero and Ghadiri, 2001)

Kafui and Thornton (2000) showed that for a given bond strength between the primary particles, there is a given impact velocity which produces a complete set of fracture planes. A subset of these fracture planes occur at lower velocities. Martin et al (2006) show that increased area of bonding between primary particles relative to the particle size leads to stronger agglomerates. This suggests that granules with a smaller primary particle size should be stiffer and more resistant to fracture, as they will have better packing and lower porosity, and hence a greater primary particle bonding area.

Experimental Investigation

Objectives

The objectives of this study were:

1. To determine whether failure modes can be identified for commercially available pharmaceutical excipient powders using a modified nanoindenter apparatus to conduct single granule diametral compression

2. To quantitatively compare differences in granule properties using this method

Method

Two machines were used to perform the diametral compression tests. The first was a MTS Nanotester, which has a vertical punch configuration (see Figure 9). This apparatus was used to test the feasibility of using a nanoindenter for the selected pharmaceutical materials. The second rig was a Micro Materials Ltd. Nanotest, which has a pendulum configuration (see Figure 15). This was used for the remainder of the experiments.

Preliminary test

An MTS Nanotester XP was used to test 3 granules each of lactose DCL 11 and MCC Celphere® with sapphire flat cylindrical tip of diameter 89 micron. The calibration and testing method is described in Koopman et al (2005). No sample preparation was necessary. The powder sample was scattered on a horizontal plate. Individual granules were subjected to a constant strain rate of 0.05 s^{-1}. The force-displacement profile of the upper punch was recorded. Top-view images of the granules were captured with an optical microscope before and after testing.

Micro Materials Ltd. Nanotest: Equipment configuration

A Micro Materials Ltd. Nanotest instrument was used to conduct tests on lactose DCL 11, DCL 14 and MCC Celphere®. The Micro Materials Ltd. Nanotest Materials Testing platform v 3.14 software was used to control the indenter and record data. The inbuilt 4x Zoom Microscope with Biokinetics Digital Display software was used for particle imaging (see also Part I.A). The apparatus has a pendulum configuration (Figure 15).

An aluminum sample stub and a brass tip of 2mm diameter were covered with a glass slides using an epoxy adhesive. This created two parallel, smooth surfaces for uniaxial compression (see Figure 15 inset).
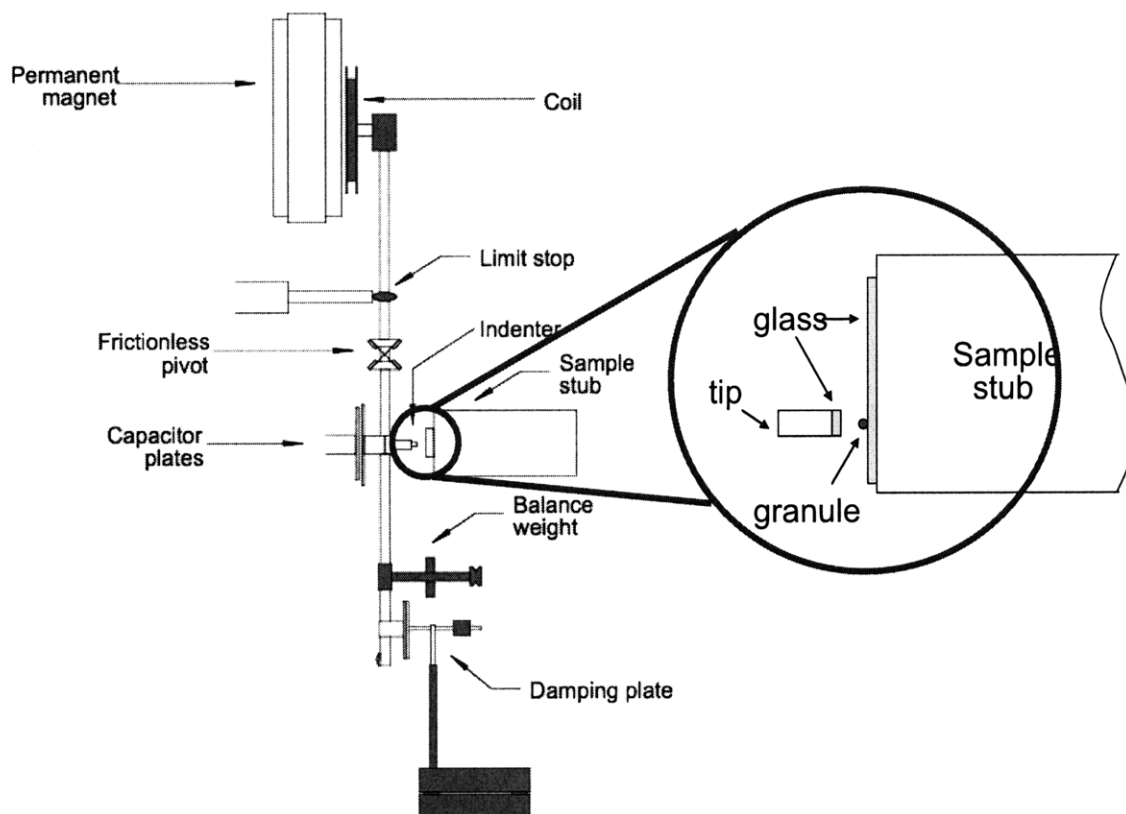
Figure 15: Schematic of Micro Materials Ltd Nanotest apparatus with detail of stub and tip

The granules were mounted onto the sample stub, as described below. During testing, the stub is static and the pendulum is swung back into a vertical position, compressing individual granules at a specified loading rate. Contact was made at a speed of 0.5 μm/s. As lactose and MCC fail in different force ranges, different pendula were used for testing the two materials. Lactose is tested with the NT2 pendulum (load range 30-200 mN) and MCC is tested with the MT pendulum (load range up to 20N).

Sample preparation

In order to test the granules in the pendulum configuration, it was necessary to mount them onto the sample stub. Granules were spread on a microscope slide. Individual

particles were selected and transferred onto a sample stub covered with a film of 200 proof USP grade ethanol. The granules were spaced at least 2 mm apart on the sample stub to prevent impingement on surrounding granules during testing. The stub surface was allowed to dry under ambient conditions for at least 2 hours and then stored overnight in a dessicator over saturated magnesium nitrate solution (at 55% relative humidity) prior to testing. The capillary force due to ethanol residues was sufficient to keep granules on the slide and prevent slipping during testing. MCC and lactose are both insoluble in ethanol. In order to check that coating the granules in ethanol did not cause changes to the morphology, environmental scanning electron microscope (ESEM) images were taken of DCL 11 and Celphere® granules before and after washing with 200 proof ethanol. No morphological changes were observed.
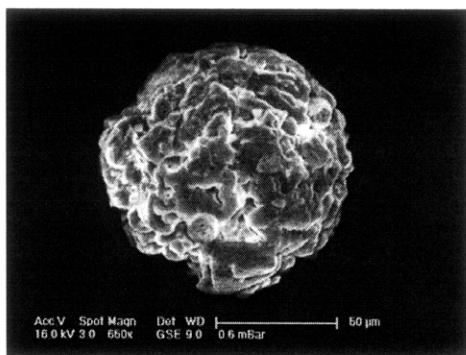
(a) Pharmatose® DCL 11 - as received
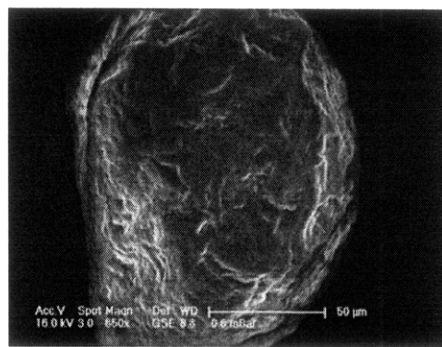
(b) MCC Celphere®- as received
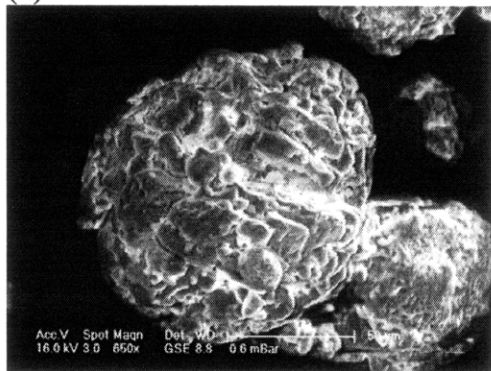
(c) Pharmatose® DCL 11 – washed in ethanol
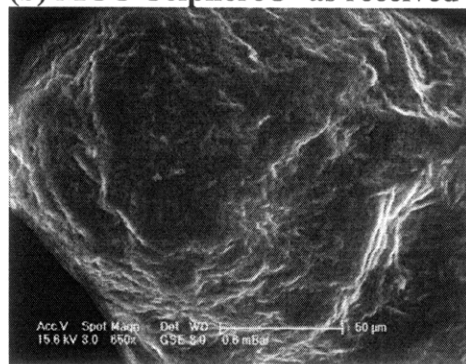
(d) MCC Celphere® – washed in ethanol

Figure 16: ESEM images of granule morphology before and after ethanol wash. No change is observed.

Testing

Depth calibration was performed prior to each round of testing using a fused silica sample and Berkovitch tip for the NT pendulum and a spherical tip for the MT. Frame

compliance, optical calibration and thermal drift correction were found to be negligible. The gain was set to 25% to maximize the displacement range.

Granule images were captured before and after testing using an in-built 4x microscope. The optical microscope is mounted parallel to the tip. A glass bead of known dimensions was used to calibrate the optics so that the size of the granules could be determined. The chamber temperature was maintained at 27° C. Humidity could not be controlled tightly because of the need to open and close chamber doors frequently for tip cleaning. Testing humidity was in the range of 25-45%. The granule size is estimated by taking the mean of the Feret diameters in the X and Y directions, d_X and d_Y, as illustrated in Figure 17.
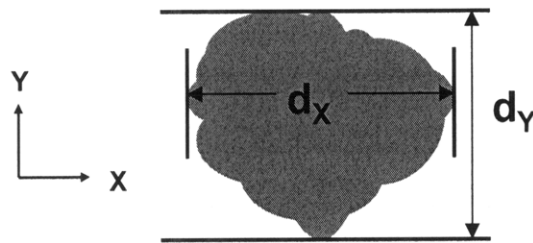
Figure 17: Feret diameter measurement

i) Polystyrene microspheres

Polystyrene microspheres (Polystyrene DVB, Duke Scientific Corp., Cat# 434, Lot # 23218) of diameter 290-330 microns were subjected to loading and unloading (with NT1 electronics settings) to maximum loads between 5 and 30mN. The purpose of testing with polystyrene spheres was to check if the equipment was aligned correctly and whether the required force-displacement profile was being measured. In particular, it was necessary to confirm that the instantaneous fracture observed for lactose granules was actually due to breakage and not slip. Polystyrene beads were selected because they have smooth surfaces, are spherical and behave elastically at low loads.

ii) Comparison of MTS and Nanotest indenters

Due to the horizontal geometry of the Nanotest and the sample preparation required, the results were compared for consistency between the MTS and the Nanotest systems. Pharmatose® DCL11 and MCC Celphere® granules were tested at $0.05s^{-1}$ with the MTS indenter and at 2mN/s on the Nanotest.

iii) Effect of loading rate

The effect of loading rate on lactose DCL 11 granules was investigated. Granules were compressed at 0.2mN/s, 2mN/s and 10mN/s. At loading rates higher than 10mN/s, there were insufficient data points to characterize the profile. 25-30 granules from a sieve fraction of 106-212 microns were investigated for each loading rate.

iv) Comparison of DCL 11 and DCL 14

The behavior of DCL11 and DCL 14 was compared for a loading rate of 10mN/s. Between 25 and 30 granules from a sieve fraction of 106-212 microns were investigated for each loading rate.

v) Cyclic loading

DCL 11 and DCL 14 granules were subjected to cyclic loading to increasing loads. The purpose of this test was to determine whether the granules exhibit elastic recovery prior during loading. Granules were selected from a sieve fraction of 106-212 microns. DCL 14 granules were loaded to an initial load of 10mN, followed by complete unloading and then loading to 20mN. DCL11 granules were subjected to an initial load of 20mN and then 40mN.

Results

Polystyrene microspheres

The polystyrene beads were observed to remain in the same position before and after testing, confirming that there is little or no slip. The force-displacements profiles were plotted on a log-log scale and the slope (the 'Hertz factor' as defined by Sheng et al, 2003) was calculated. Based on equation (I.B-1), if the conditions for Hertz theory are true, the slope will be 1.5. The experimental results gave a value of 1.46 ± 0.22, so a Hertzian relationship can be considered to be valid.

The reduced modulus of polystyrene was calculated from the data and compared to literature values (Table 4). The Poisson's ratio and modulus of polystyrene will vary depending on the chain length distribution. Therefore order-of-magnitude agreement of the modulus was considered to be sufficient to demonstrate that the data fit the Hertzian model. The variance could be attributed to the onset of plastic deformation and friction at the contact due to the ethanol residues used to mount the beads on the sample stub. In addition, in any mechanical test, an arbitrary load threshold is set to determine the point

of contact between the substrate and the tip. The Hertz factor was found to be very
sensitive to the threshold load.

Table 4: Literature and experimental values for mechanical properties of polystyrene

	Value	Reference	Experimental data
Poisson's ratio	0.325	Boundy and Boyer, 1952	Assumed to be
	0.33	Nielsen, 1962	0.33
Tensile modulus (MPa)	3200	Rudd and Gurnee, 1957	
	3400	Dow, 1965	
Compressive modulus (MPa)	3000	Dow, 1965	4850 ± 2400

Comparison of force-displacement profiles of MCC and lactose

Lactose and MCC granules exhibited distinctly different behaviors when subjected to a
uniaxial compression test. A Hertzian relationship was not valid for either material.

For MCC, initial stiffening of the granules was observed, followed by the onset of yield,
observed at loads greater than 1N (Figure 18). This suggests that there is initial flattening
of the granule-platen contacts followed by plastic deformation. The granules did not fail
within the load limits of the MTS indenter (limits: 500mN load, several mm
displacement), or within the displacement limits of the Nanotest (limits: 20N load,
approximately 15 micron displacement).

Lactose granules had a linear force-displacement profile, consistent with experimental
and numerical results for single granule compression of agglomerates (Figure 19). The
granules failed at low strain (typically less than 5%), by instantaneous fracture. With the
MTS indenter data, compression of the daughter particles and debris was observed. This
was not seen in the Nanotest data due to the limited displacement range.
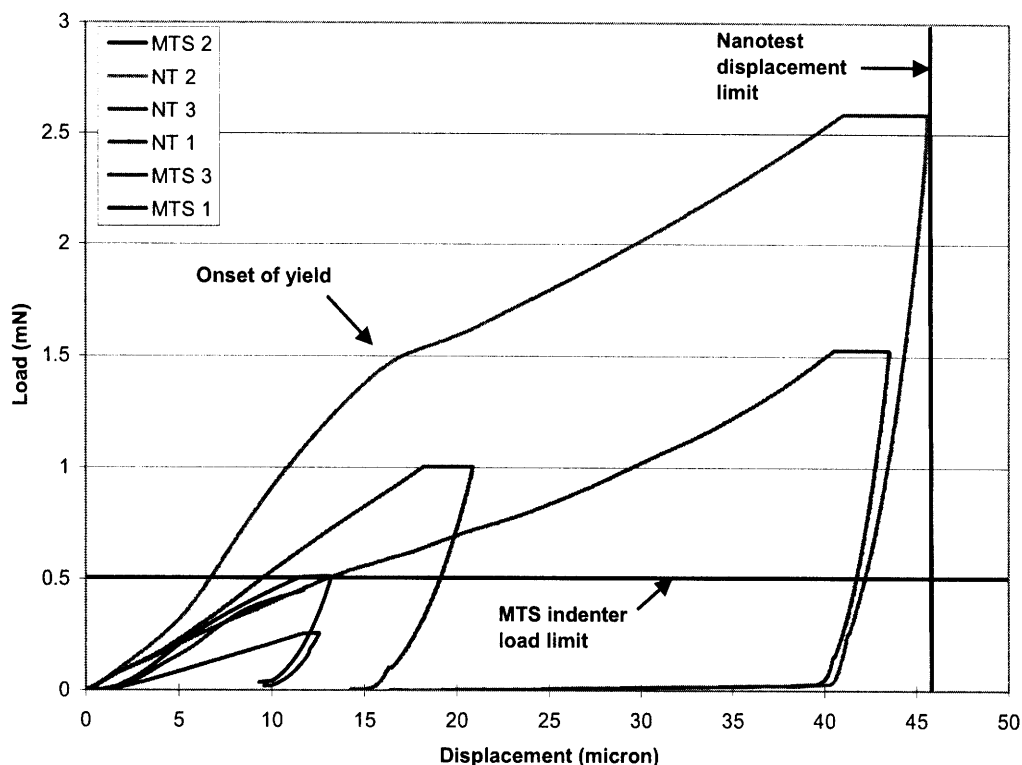
Figure 18: Comparison of force-displacement profiles obtained for MCC Celphere® granules tested with a MTS Nanoindenter and a Micromaterials Ltd. Nanotest.

MCC granules are much stiffer than lactose granules. This suggests compaction to a specified force would result in MCC tablets being weaker than lactose tablets as the granules will be less deformed.

For both the MCC and lactose granules, the data from the MTS and the Nanotest indenters had the same qualitative features, suggesting that the equipment configuration and sample preparation method does not affect the results. There is insufficient data from the MTS indenter to make a quantitative comparison.
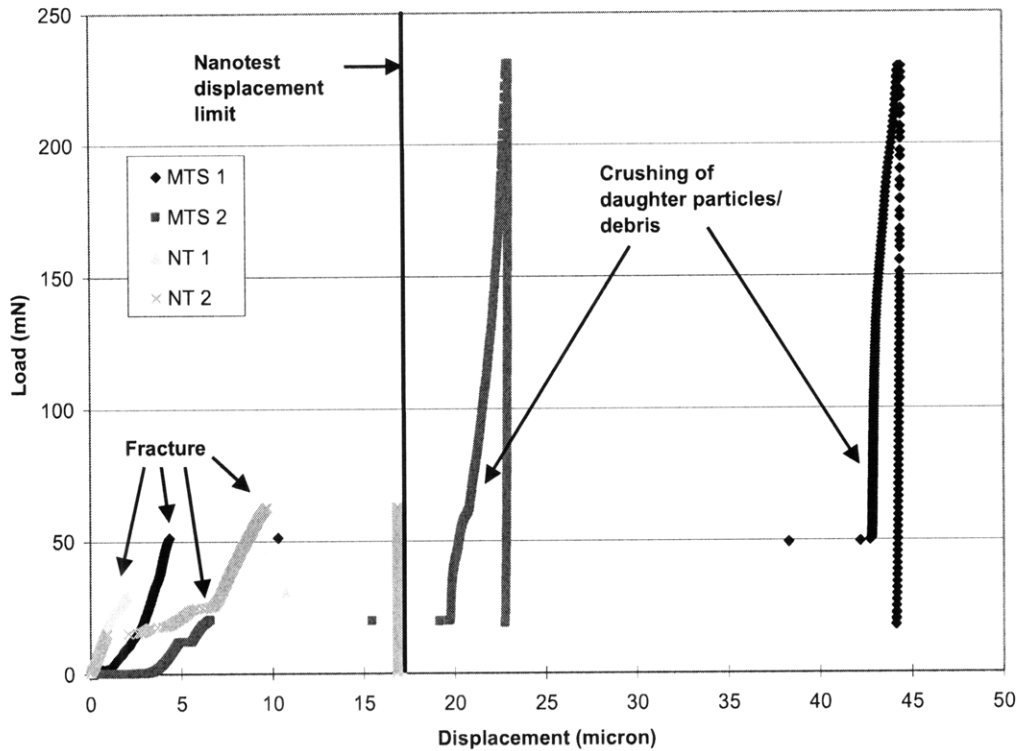
Figure 19: Comparison of force-displacement profiles obtained for DCL 11 granules tested with a MTS Nanoindenter and a Micromaterials Ltd. Nanotest.

Data analysis of lactose test results

Three major modes of failure were identified for lactose DCL 11 and DCL 14 granules using the Nanotest indenter: fracture, fracture with local damage and disintegration. These were classified by qualitative features of the force-displacement profile and images of the granules after loading (Figure 20). Fracture alone is characterized by linear, unbroken profile with a distinct threshold load at which the granule cracks into two or more large fragments. Fracture accompanied by local damage is characterized by a more irregular profile. Fracture was found to occur at strains in the range of 1-5%. Disintegration is characterized by a profile with multiple steps in it and many small daughter fragments.

Fracture

Fracture with local damage

Local damage/disintegration

Force-displacement profiles.
Source: experimental results

Damage zones/ fracture planes
Adapted from: Subero J. and
Ghadiri M., (2001)

Resulting fragments
Source: experimental
results
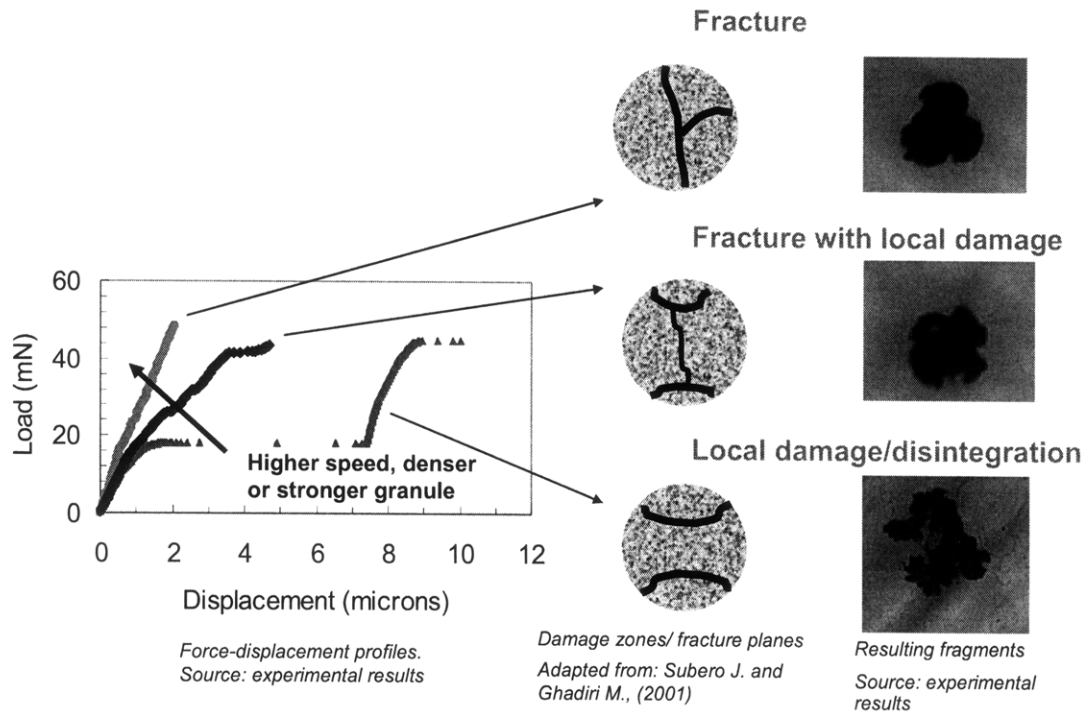
Figure 20: Failure modes of lactose agglomerates, characterized by force-displacement profile,
fracture planes and daughter fragment size

No effect of particle size on fracture load or 'stiffness' was observed for the size range investigated (for example, see Figure 21). However, it should be noted that only the sieve fraction between 106-212 microns was tested. Granules smaller and larger than this size range tended to be highly irregular in shape and so tended to show disintegration behavior as the surface protrusions were subjected to loading.
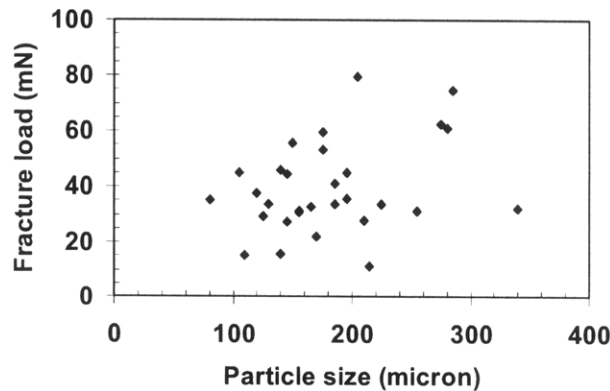
Figure 21: DCL 11 granules tested at 2mN/s show no correlation
n between particle size and fracture load

The force-displacement data could not be converted to a stress-strain plot, as the contact area between the platen and the granule is unknown. The linear force-displacement profile suggests that there is considerable flattening of the contact (this is also observed in DEM simulations, eg. Martin et al, 2006, Thornton et al, 2004).

Therefore, the slope of the profile ('stiffness') and the load at which fracture occurs were selected as mechanical parameters to characterize the material behavior. 25-30 data points were collected for each sample and loading conditions. A lognormal distribution was found to give a good fit of the cumulative frequency profile for each dataset.

Effect of loading rate on DCL 11

Fracture is the dominant mechanism of granule failure for DCL 11 (Table 5). There is a higher tendency for fracture to be accompanied by local damage at lower loading rates. It is not possible to collect the fractured samples after testing to analyze the resulting fragments. It was observed that the resulting fragments often stuck to the indenter tip, and so could not always be observed with the microscope.

Table 5: Effect of loading rate on failure mode of DCL11 granule

DCL 11 granule failure mode	Frequency of occurrence		
	0.2 mN/s	2 mN/s	10 mN/s
Fracture only	0.15	0.29	0.74
Fracture with local damage	0.73	0.71	0.19
Local damage/disintegration only	0.12	0.00	0.07

The median fracture load increases with loading rate (Table 6). The higher loading rate will allow less time for rearrangement of primary particles within the granule. Therefore there will be propagation of forces chains throughout the granule, released by instantaneous fracture. There is also less variation at higher loading rates. This is likely because as the loading rate is increased, shear forces have a larger effect on the creation of fracture planes than pre-existing intra-granule flaws, so variability due to granule structure is reduced. There is no discernable effect of loading rate on granule stiffness.

Table 6: Effect of loading rate on mechanical properties of DCL 11 granules

Loading rate		0.2 mN/s	2 mN/s	10mN/s
Slope of load-displacement profile	Median (X_{50})	14.9 kN/m	19.0 kN/m	15.9 kN/m
	Standard deviation $(X_{84}/X_{16})^{1/2}$	1.48	1.49	1.34
Fracture load	Median (X_{50})	33.00mN	33.67 mN	48.88 mN
	Standard deviation $(X_{84}/X_{16})^{1/2}$	1.70	1.46	1.32

Comparison of DCL 11 and DCL 14

DCL 14 has lower frequency of fracture than DCL 11for same testing conditions (Table 7). Based on the literature (Subero and Ghadiri, 2001, and Thornton et al.2004, Martin et al, 2006), this implies that DCL 14 allows for more intra-granular re-arrangement of primary particles during loading. This could be due to weaker primary particle bonding or a less dense structure.

Table 7: Granule failure modes for DCL 11 and DCL 14 tested at 10mN/s

Granule Failure Mode	Frequency of occurrence at 10mN/s loading	
	DCL 11	DCL 14
Fracture only	0.74	0.34
Fracture with local damage	0.19	0.52
Local damage/ disintegration only	0.07	0.14

The mechanical properties are best described by lognormal distributions, as shown in Figure 22 and summarized in Table 8.

DCL 11 granules are distinctly stronger than DCL 14, as they undergo fracture at higher loads. DCL 14 has wider distribution than DCL 11. DCL 11 appears to have a bimodal distribution of fracture load and granule stiffness, although this may be an artifact of a limited data set.
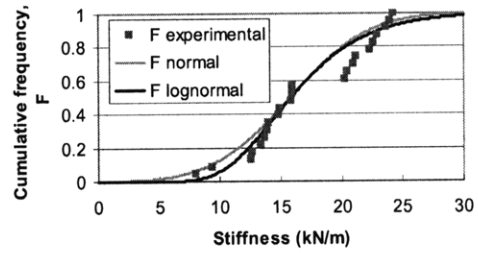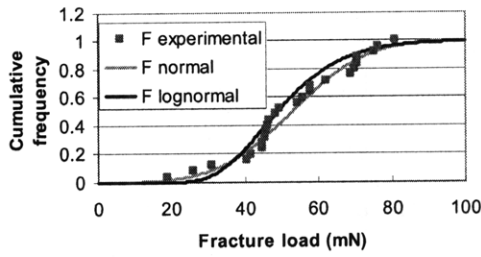
(a) Fracture load distribution for DCL 11 **(b) Stiffness distribution for DCL 11**
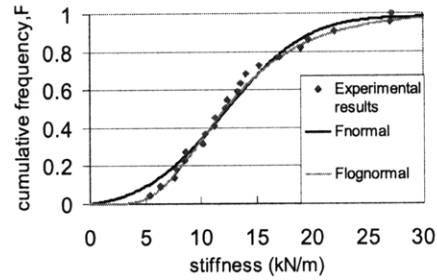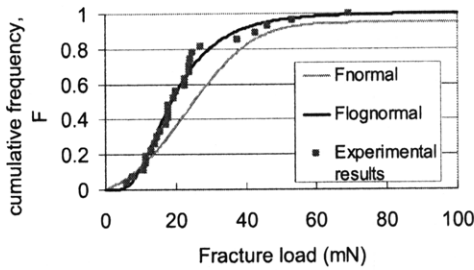
(c) Fracture load distribution for DCL 14 **(d) Stiffness distribution for DCL 14**

Figure 22: Distributions of mechanical properties for DCL 11 and 14 tested at 10mN/s

DCL 11 granules are distinctly stronger than DCL 14, as they undergo fracture at higher loads. DCL 14 has wider distribution than DCL 11. DCL 11 appears to have a bimodal distribution of fracture load and granule stiffness, although this may be an artifact of a limited data set.

Table 8: Comparison of mechanical properties of DCL 11 and DCL 14 tested at 10mN/s

		DCL 11	DCL 14
Slope of load-displacement profile	Median (X_{50})	15.85 kN/m	12.2 kN/m
	Standard deviation $(X_{84}/X_{16})^{1/2}$	1.34	1.58
Fracture load	Median (X_{50})	48.88 mN	18.71 mN
	Standard deviation $(X_{84}/X_{16})^{1/2}$	1.32	1.72

DCL 11 is slightly stiffer than DCL 14, but the standard deviation of DCL 14 values is larger. Again, this suggests that DCL 14 has weaker primary particle bonding or a less

dense structure, allowing more primary particle rearrangement during compression and hence there is a larger influence of the granule structure.

Cyclic loading

DCL 11 and DCL 14 granules both demonstrated some recovery of the granule during unloading (Table 9). However, in each case, there was considerable stiffening, with the unloading slope being 20-500% greater than during loading. This is consistent with damage occurring at the granule-platen contact, resulting in local densification. DCL14 shows more variability in stiffness increase than DCL 11, which implies that local structure is having a significant effect. This could be because the granule is less dense, or because the initial loading is lower for DCL 14 than for DCL 11, therefore there is less flattening of the granule.

Table 9: Stiffening effects are observed during cyclic loading of DCL 11 and DCL 14 granules

		DCL 11	DCL 14
First loading limit		20mN	10mN
Second loading limit		40mN	20mN
% increase in profile slope (granule 'stiffness') between consecutive loading	Average	106%	124%
	Standard Deviation	68%	161%

These results indicate that there is densification and deformation at the granule-platen contact prior to fracture. Therefore the linear portion of the profile does not represent elastic behavior.

Discussion

The results demonstrate that single compression testing can be used to determine qualitative and quantitative differences between mechanical properties of pharmaceutical powder.

The method of using a nanoindenter to perform single-granule diametral compression tests shows agreement with the theoretical model for polystyrene microspheres. The data is qualitatively consistent for two indenters in both the vertical and pendulum configurations. This suggests that the test can be performed in any apparatus with a

parallel plate geometry and the capability to control and record small loads and displacements. It also suggests that our sample preparation method had little or no effect on mechanical properties of the granules.

The compression test demonstrated that MCC granules undergo plastic deformation, whereas lactose agglomerates tend to undergo fracture. Multiple modes of granule failure were observed for lactose agglomerates; fracture only, fracture with local damage and local damage/disintegration only. The relative prevalence of each mode depends on both the loading speed and the grade of material (i.e. on the nature of the primary particles, binder and manufacturing method).

The strain rates used for granule testing are much lower than those used in tablet manufacturing processes. However, the purpose of the test is to detect relative differences between the materials by subjecting the granules to loading conditions similar, but not identical, to those in compaction. Due to the random structure of the loose powder bed, loading conditions will vary significantly from granule to granule and as the compaction proceeds. It is not possible, nor necessarily desirable, to replicate such multi-point loading in a characterization technique. Fracture was found to be the dominant mode of granule failure for the lactose grades studied. Given the constrained positions of granules in a closed die, it is most likely that they will undergo a combination of fracture and disintegration and unlikely that they will undergo shattering or other failure pattern. Therefore, parameters associated with fracture have been used to characterize the materials.

Quantitative differences between different grades (DCL 11 and DCL 14) can be measured. DCL 14 is less stiff than DCL 11 and undergoes fracture at lower loads. This suggests that it will undergo greater volume reduction than DCL 11 during compaction to a given load. The product literature (DMV, 2007 (a) and (b)) suggests that DCL 14 has smaller primary particles (23 microns) than DCL 11 (35 microns). This would suggest that DCL 14 granules are more dense than DCL 11 and also that there is a greater contact area between the primary particles, hence they are stronger. However, the experimental findings do not support this. Based on the literature on DEM modeling of agglomerates, DCL 14 should be less dense and/or have weaker inter-primary particle bonding than DCL 11, as it more prone to disintegration and fails at lower loads. One possible

explanation is that there is another, non-geometric contribution to intra-granular bond strengths. It is possible that a different manufacturing process gives rise to different proportions of lactose crystalline forms between DCL 11 and DCL 14, which affects the bond strength between primary particles.

Potential applications of this analytical technique are to enable specifications for vendor-supplied materials, such as those studied here, or to determine the necessary process settings in a granulation process that precedes compaction. The parameters can also be used in a model to predict the behavior of the powder during uniaxial compaction.

To fully capture the multi-mode behavior of lactose granules during compaction, data is needed on primary particle size distribution, intra-granular structure and intra-granular bonding strength. However, information at this scale cannot be obtained for off-the shelf excipients such as spray dried lactose. Fracture parameters, such as pre-fracture stiffness and fracture load, may be sufficient to characterize the differences in materials and predict their relative performance during compaction. Suitable process models are presented in part IV.

Conclusions

A nanoindenter with a flat tip can be used in either a vertical or pendulum configuration to measure the mechanical response of pharmaceutical powder granules to uniaxial compression.

Pharmaceutical excipient granules are unlikely to fit the Hertzian model for elastic deformation. Numerical methods to simulate plastic deformation or agglomerate compression can provide insight into the intra-granule structure and bonding. The quantitative measurements could be used as inputs for powder compaction models.

References

Alderborn G.; Wikberg M., *Pharmaceutical Powder Compaction Technology, Ed. Alderborn G. and Nystrom C.* Marcel Dekker **1996**

Asahi Kasei *http://www.ceolus.com/eng/product/celphere/index.html*, accessed **January 15, 2007**

ASTM, *Test D4179: Single pellet crush strength of formed catalyst shapes,* American Society for Testing Materials **1982**

Bassam F.; York P.; Rowe R.C.; Roberts R.J. *Powder Technol.* **1991**, *65*, 103

Bemrose C.R.; Bridgwater J. *Powder Technol.* **1987**, *49 (2)*, 97-126

Bolhuis G.; Kusendrager K.; Langridge *Pharm. Technol. Suppl. Excipients and Solid Dosage Forms* **2004**, 26-31

Boundy R. H.; Boyer R. F. (Eds.) *Styrene, Its Polymers,Copolymers and Derivatives* Reinhold, New York **1952**

Carlisle K.; Chawla K.K.; Gladysz G.; Koopman M,, *J. Mater. Sci.* **2006**, *41*, 3961-3972

Couroyer, C.; Ghadiri, M.; Laval, P.; Brunard, N.; Kolenda, F. *R. I. Fr. Petrol* **2000**, *55 (1)*, 67-85

Dow '*Strength and Stiffness*' in *Plastics Design Data, Dow Technical Chemical Publication* **1965**

DMV International, *Product Group Overview, Pharmatose ® DC Lactose* **2005**

DMV International, *Directly compressible lactose: high speed compaction, DMV excipient guide 3.2.2,* **2007(a)**

DMV International, *Directly compressible lactose: general considerations, DMV excipient guide 3.2.1,* **2007(b)**

Duncan-Hewitt W.C. *Drug Dev. Ind. Pharm.* **1993**, *19*, 2197-2240

Gethin D.T.; Yang X.S.; Lewis R.W. *Comput. Methods Appl., Mech Engrg* **2006**, *195* 5552-5565

Hassanpour A.; Ghadiri M. *Powder Technol.* **2004**, *141*, 251-261

Heckel R.W., *Trans Metal Soc*, AIME, **1961**, *221,* 671

Hiestand E.V., *Pharmaceutical Powder Compaction Technology, Ed. Alderborn G. and Nystrom C.* Marcel Dekker, **1996**

Kafui K.D.; Thornton C. *Powder Technol.* **2000**, *109*, 113–132

Koopman M.; Gouadec G.; Carlisle K.; Chawla K.K.; Gladysz G., *Scripta Mater.* **2004**, *50*, 593-596

Laio X.; Wiedmann T.S., *J. Pharm. Sci.* **2005**, 94, 79-92

Martin C.L. http://www.gpm2.inpg.fr/perso/doc_cm/crushing_aggregate.html, accessed **Jan 2007**

Martin C.L.; Bouvard D.; Delette G. *J. Am. Ceram. Soc* **2006**, *89 (11)*, 3379-3387

Mishra B.K.; Thornton C. *Int. J. Miner. Process.* **2001**, *61 (4)*, 225-239

Nielsen L. E. *Mechanical Properties of Polymers*, Reinhold, New York **1962**

Ridgway K.; Glasby J.; Rosser P.H. *J. Pharm. Pharmacol.* **1969**, *21:24S*

Roberts R.J.; Rowe R.C. *Chem Eng. Sci.* **1987**, *42*, 903

Rudd J. F.; Gurnee, *J. Appl. Phys.* **1957**, *28*, 1096

Sheng Y.; Briscoe B.J.; Maung R.; Rovea C. *Powder Technol.* **2004 (a)** , *140*, 228-239

Sheng Y.; Lawrence C.J.; Briscoe B.J.; Thornton C. *Eng. Computation*, **2004b,** *21*, 304-317

Subero J.; Ghadiri M. *Powder Technol.* **2001**, *120* , 232–243

Snowden M.J. *Org Proces Res Dev.* **2004,** *8*, 674-679

Taylor L.J.; Papadopoulos D.G.; Dunn P.J.; Bentham A.C.; Dawson N.J.; Mitchell J.C.;

Thornton C.; Ciomocos M.T.; Adams M.J. *Powder Technol.* **1999**, *105*, 74–82

Thornton C., Ciomocos M.T., Adams M.J., *Powder Technol.* **2004 (a)**, 140, 258– 267

Thornton C.; Liu L. *Powder Technol.* **2004 (b)**, *143-144*, 110-116

Vodnick, D. Hysitron Inc. *Personal Communication,* 18th November **2005**

Wikberg M.; Alderborn G. *STP Pharma Sci*, **1992**, *2*, 313

Part II: Tablet Performance

Standard industry tests were used to assess tablet performance; the tablet hardness (diametral compression test) and the US pharmacopeial dissolution test. The effect of compaction force and speed on hardness and dissolution was investigated for tablets made of microcrystalline cellulose (Celphere® CP102) and spray-dried lactose (Pharmatose® DCL 11 and DCL 14). Caffeine was used as a model drug substance for the dissolution studies.

Compaction speed was found to have no effect on tablet hardness or dissolution for any of the materials within the speed range investigated.

For MCC tablets, hardness increased slightly with compaction force up to loads of 20kN. Loading to higher forces had no effect on hardness. MCC tablets exhibited bursting behavior during dissolution and released their API load rapidly. No effect of compaction force was observed in the dissolution profiles.

DCL 11 and 14 tablet hardness and dissolution time increased with compaction force. There was no difference in hardness for tablets made of the two grades of lactose compacted under the same conditions. However, DCL 14 tablets dissolved up to four times slower than DCL 11 tablets. Variability in tablet hardness and dissolution increased at higher loads, indicating that tablet lamination may have occurred during compaction. There is some evidence that models to describe surface-erosion limited drug release could be used to describe the dissolution of lactose tablets, but further studies are needed to test this hypothesis.

II.A: Tablet Hardness

Introduction

Tablets are typically tested for mechanical strength (commonly termed 'hardness') by diametral compression testing. Tablet hardness is not a pharmacopeial standard test, but one that is a commonly used tool for development and quality control.

The standard testing procedure involves compression between two platens (one stationary and one moving) until tablet failure is observed. Loading may be either displacement- or load-controlled. The load at which failure occurs is used to measure tablet strength. The case of point-loading of a homogeneous disk at diametrically opposite points (Figure 23) can be solved analytically using continuum mechanics equations. These indicate that tension is induced in the direction perpendicular to loading (Den Hartog, 1952). For test results to be comparable, failure must occur by tension induced by the loading, rather than by shear. Shear failure is characterized by crushing at the contacts and the progression of failure zones until the tablet collapses (Figure 23 (c)). Tensile failure is characterized by a clean, instantaneous break along the loaded diameter (parallel to the direction of loading) or by a triple cleft failure (Figure 23 (a) and (b)). In either case, there should be little crushing at the loading points.
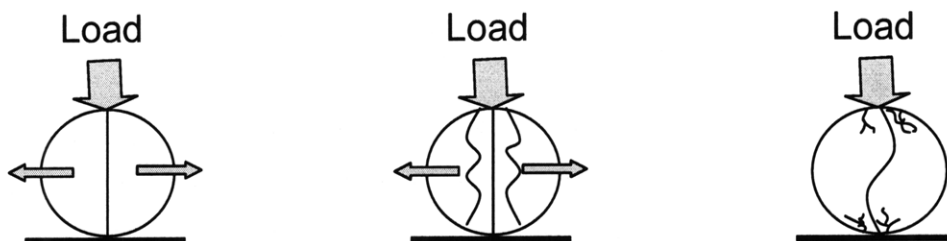
Figure 23: Tablet failures modes (left to right): (a) simple tensile failure, (b) triple cleft (tensile failure) (c) shear-induced failure (adapted from Davies and Newton, 1996).

The tensile strength of the tablet, often inaccurately described in the pharmaceutical literature as hardness, is calculated by the following equation (Mohammed et al, 2005):

$$\sigma_t = \frac{2P}{\pi D t} \qquad\qquad \text{(II.A-1)}$$

Where σ_t is the tensile strength, P is the failure load, D is the tablet diameter and t is the tablet thickness.

Factors affecting tablet hardness

Tablet hardness is an indicator of the tablet structure; a combined result of the powder mechanical properties and the compaction process. Some attempts have been made to relate hardness directly to structural characteristics of the tablet.

Tablet hardness is known to increase with increased solid volume fraction, as decreased porosity is believed to reduce sources of crack propagation. Mohammed et al. (2005) note that the extent of volume reduction can be related to the amount of energy that goes into plastic deformation during compaction for a range of materials.

Olsson and Nystrom (2001) found that the specific surface area of the tablet (measured by permeametry) is also a factor in determining tablet tensile strength. They attribute this effect to greater inter-particle bonding surface area creating greater bond strength.

De Boer et al (1986) found that for different types of fragmenting lactose, tablet strength is simply a function of specific surface area (measured by mercury porosimetry) and does not depend on the crystalline form. They investigated α-lactose monohydrate, anhydrous α-lactose, roller-dried β lactose and crystalline β lactose. This suggests that the same binding mechanism applies to all forms of crystalline lactose. However, for materials that deform plastically, tablet strength was not found to be related to surface area. For example, increasing fractions of amorphous lactose in spray-dried lactose was found to increase tablet strength but did not increase surface area of the tablets (Vromans et al, 1986).

Narayan and Hancock (2003) related tablet surface morphology to the consolidation mechanism of direct compression powders, and hence to tablet strength. They found that brittle materials produced smooth and brittle compacts, whereas plastic materials produced rough and ductile compacts.

Various models have been proposed to predict tablet hardness. Of these, the most commonly cited were proposed by Rumpf (1962), Hiestand (1991) and Leunberger (1982). These models assume that the tensile strength of the tablet is equal to the sum of the bonding strength along the failure plane and all bonds are separated instantaneously.

Therefore, tablet tensile strength is dependent on bonding surface area and the inter-particulate bond strength.

Objectives

The objective of this study was to study the effect of compaction speed and force on the mechanical strength of tablets made of microcrystalline cellulose (Celphere CP102), and two grades of spray-dried lactose (DCL 11 and DCL 14).

Method

MCC Celphere, DCL 11 and DCL 14 powders were sieved to obtain the sieve fraction 106-212 microns. The powders were stored over saturated magnesium nitrate solution (at 55% relative humidity) for a minimum of 10 hours before compaction.

Powder beds of depth 4mm were compacted at constant upper punch speed (0.5, 5 or 50 mm/min) and to a range of final compaction forces (5-75kN). This corresponded to 430±10 mg MCC and 350±10 mg lactose. Flat-faced punches were used with a 12.7mm diameter punch. An Instron 4260 mechanical tester was used to compact the tablets. Tablets were then stored at 55% relative humidity for a minimum of 72 hours before testing.

Tablets were tested between two flat, stainless steel plates with a 2kN load cell in an Instron 8848 MicroTester. Loading was performed at a constant upper plate speed of 5mm/min until tablet failure. The lower plate was stationary. The resulting fragments were inspected to identify the failure mode. Data was collected only from tablets that failed in tension.

Results

A comparison of lactose (DCL11) and MCC tablets is presented below. For both materials tensile strength varied with compaction force (Figure 24). Compaction speed had no detectable effect in the range studied. The tensile strength of MCC tablets was lower than that of lactose tablets for the same compaction conditions. Tensile strength increases with compaction force between 5-20kN, but is not increased by applying forces greater than 20kN.

Lactose, on the other hand, does not form tablets at forces less than 20kN. Tablet strength
increases in a linear fashion between 20-60kN. At forces greater than 60kN, tablets
tended to split or flake, rather than fail instantaneously. When they failed in tension, the
tablet strength was lower than that predicted by the linear relationship seen at lower
loads.
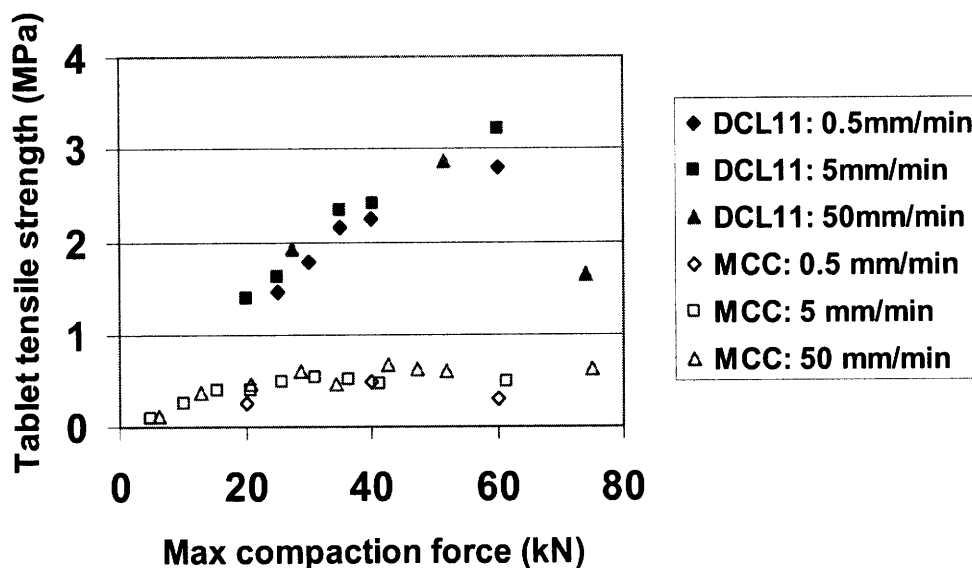
Figure 24: Tensile strength of MCC and DCL 11 tablets

The tensile strength of lactose DCL 11 and DCL 14 tablets was compared (Figure 25).
There was no significant difference between the two materials for the range of
compaction speeds and forces tested. Variability of tensile strength increased with
increasing force.
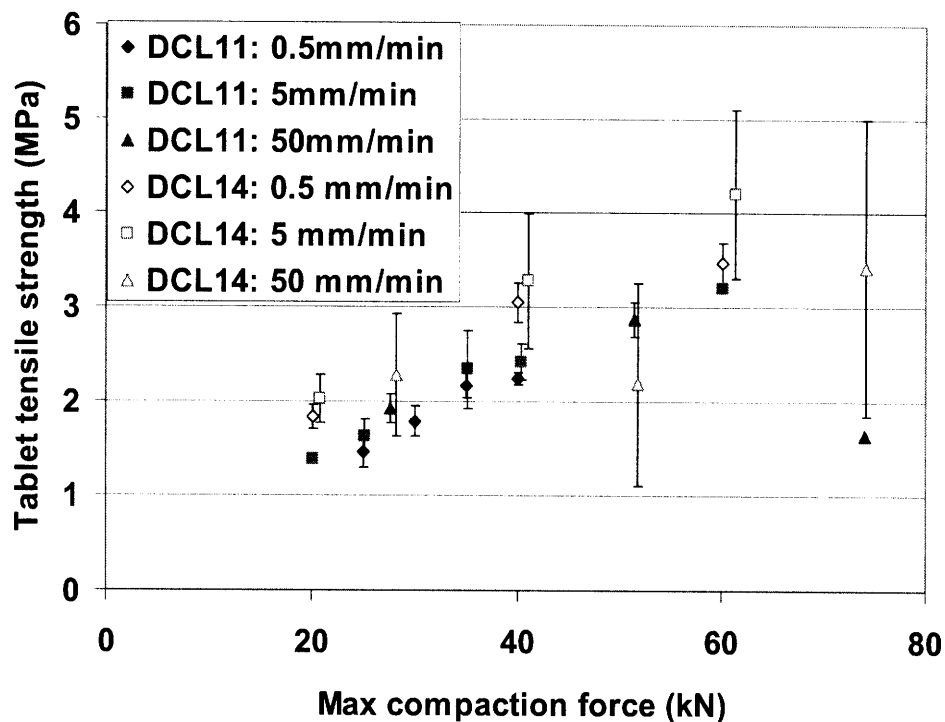
Figure 25: Comparison of tensile strength for DCL11 and DCL14 tablets

Discussion

The results do not agree with findings by Bolhuis et al. (2004), who found that for tablets of 250mg mass, 9mm diameter, made from powders stored at 30% humidity, DCL 14 tablets are 30-50% stronger than those of DCL 11 in the force range 5-20kN. This suggests that humidity, tablet dimensions or additives (they used magnesium stearate as a lubricant) may have different effects on the different materials.

The decrease in tensile strength for lactose tablets at high loads arose from a combination of lower failure loads and thicker tablets (see Equation II.A-1). This suggests that lamination during compaction, rather than microstructure, was affecting tablet properties at the higher forces.

This is also suggested by the increase in variance at higher loads. If there are existing cracks in the tablet, failure will tend to occur along these defects. Therefore, failure will depend on the pattern of the pre-existing cracks, which introduce variation. However, in a defect-free tablet, cracks must be initiated due to the stress field induced by testing. Compaction speed was found to have no effect on tablet strength. The speed range of the experimental equipment is at least an order of magnitude lower than that of

manufacturing equipment, so this observation may be a result of a narrow experimental range.

Conclusions

Pharmaceutical materials show different trends in tablet hardness when subjected to a range of compaction forces. This indicates that an understanding of the compaction mechanism is necessary to predict tablet hardness. Compaction speed had no effect on tablet strength for any of the materials studied.

References

Bolhuis G.; Kusendrager K.; Langridge *Pharm. Technol. Suppl. Excipients and Solid Dosage Forms* **2004**, 26-31

Davies P.N.; Newton J.M in *Pharmaceutical Powder Compaction Technology Eds. Alderborn G.; Nystrom C.* Marcel Dekker, New York, **1996**, 165

De Boer A.H.; Vromans H.; Lerk C.F.; Bolhuis G.K.; Kussendrager K.D.; Bosch H. *Pharm Weekbl. Sci. Ed.* **1986**, *8*, 145

Den Hartog J.P. *Advanced Strength of Materials*, McGraw-Hill, New York, **1952**

Hiestand H. Int. J. Pharm. **1991a**, *67*, 217-229

Hiestand H. Int. J. Pharm. **1991b**, *67*, 231-246

Leuenberger H. *Int. J. Pharm.* **1982**, *12*, 41-55

Olsson H.; Nystrom C. *Pharmaceutical Research*, 2001, *18 (2)*, 203-210

Mohammed H.; Briscoe B.J.; Pitt K.G. *Chem. Eng. Sci.* **2005**, *60*, 3941-3947

Narayan P.; Hancock B. *Mater. Sci. Eng.*, **2003**, *A355*, 24-36

Rumpf H. *Agglomeration Ed. Knepper W.A.*, Interscience, New York, **1962**, 379

Vromans H.; Bolhuis G.K.; Lerk C.F.; Kussendrager K.D.; Bosch H. *Acta. Pharma. Suec.* **1986**, *23*, 231

II.B: Dissolution

Introduction

From a regulatory perspective, tablet dissolution characteristics are important at many stages in product development, manufacturing and post-marketing activities (Dressman and Kramer, 2005). In many cases, the dissolution properties of a tablet are used as an indicator of bioavailability. In R&D, dissolution testing is used to guide formulation and process development. In manufacturing, dissolution is a quality control test to check for batch-to-batch variability and can also be a criterion for releasing a product into the market. Once a product has been approved and gone into full-scale production, dissolution profiles can be used to check for product similarity following changes in the formulation or manufacturing process. When an ANDA (abbreviated new drug application) is filed for approval of a generic product, dissolution studies form part of the studies to establish bioequivalence of the generic and the original products (FDA, 2007).

Testing equipment and protocol

Standards for the test equipment and protocol are outlined by the United States, European and Japanese Pharmacopeias. The USP describes four types of apparatus (paddle, basket, reciprocating cylinder and flow-through cell (USP, 2007)) of which the paddle apparatus is the most commonly used (Kramer et al, 2005). It consists of a vessel of specified geometry agitated at constant speed by a flat paddle. The dissolution properties are measured by inserting the tablet into a fixed volume of medium and sampling the solution periodically to generate a time-profile of concentration.

Analysis of dissolution data

There are multiple ways of characterizing the dissolution profile, depending on the requirements. In some cases it is necessary to simply compare multiple profiles for reproducibility or to a reference profile. This can be performed by calculating a characteristic index, such as the difference (f_1), the similarity (f_2) or the Rescigno indices. A description of the different indices and their suitability under different conditions is

given by Vertzoni et al (2005). Another common indicator is the time for a given fraction of the drug to be released, e.g. t_{50} for 50%, or t_{90} for 90% of drug released.

Other analyses focus on capturing the shape of the cumulative time-concentration profile. These models fall into two categories (Nicolaides et al, 2001, Costa and Lobo, 2001): the empirical formulae, such as zero or first-order equations, or a Weibull model (Langenbucher, 1976), that allow us to fit and compare parameters, and the mechanistic models, which attempt to identify the key steps in tablet dissolution. Empirical models do not give us insight into the physics of dissolution; therefore for the purposes of this study, mechanistic models are of more interest. These models have been applied mainly to the study of sustained-release formulations with polymeric matrices. Much of the literature concerns diffusion-limited drug release from an insoluble polymer matrix, using a stagnant film model (Higuchi, 1961 and 1963, Desai et al 1966a and b, Korsmeyer et al, 1983, Peppas, 1985). However, this is not relevant to the materials in this study, as the MCC matrix disintegrates and the lactose matrices dissolve.

The solubility of caffeine is 21g/liter and of lactose is 170g/liter (Dean, 1999). Therefore, it is unlikely that there is any leaching of caffeine from the lactose matrix. It is more likely that the erosion (dissolution) of the lactose matrix is the rate determining step for drug release.

Cooney (1972), Hopfenberg (1976) and Katzenhendler (1997) developed models where surface erosion of the tablet is the rate-limiting step for drug release.

It should be noted that none of the models described above explicitly account for the hydrodynamics of the testing apparatus, or how changes in testing parameters, such as agitation speed, might affect dissolution.

Surface-erosion limited drug release

Katzenhendler et al (1997) developed a model for erosion of a disk shaped tablet of radius, a, thickness, b (Figure 26).
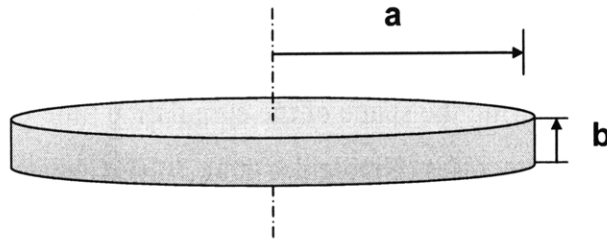
Figure 26: Tablet erosion model (Katzenhendler et al., 1997)

Erosion in the linear dimensions was assumed to be zero order:

$$a = a_0 - \frac{k_a t}{C_0} \qquad \text{(II.B-1)}$$

$$b = b_0 - \frac{2k_b t}{C_0} \qquad \text{(II.B-2)}$$

Where k_a and k_b are the rate constants in the radial and the vertical directions and C_0 is the concentration of active ingredient (API).

Assuming that the drug is uniformly distributed throughout the matrix, the fractional amount of drug released from the tablet at time t, M_t/M_∞ will be

$$M_t / M_\infty = 1 - \pi a^2 b / \pi a_0^2 b_0^2 \qquad \text{(II.B-3)}$$

Substituting the rate equations gives

$$M_t / M_\infty = 1 - \left(1 - \frac{k_a t}{C_0 a_0}\right)^2 \left(1 - \frac{2k_b t}{C_0 b_0}\right) \qquad \text{(II.B-4)}$$

Katzenhendler et al. present several limiting cases of this equation based on geometric and kinetic extremes. For the experiments described here, the initial dimensions of the tablet, a_0 and b_0, were not varied (except for small differences in b_0 due to different extents of compression. The thickness and the diameter are of the same order of magnitude, but not equal ($2a_0/b_0 \sim 6$), so it is not reasonable to reduce dimensionality and model the tablet as a slab, an infinite cylinder or a sphere. However, it is possible that the anisotropic compaction could lead to significantly different rates of erosion in the radial and the vertical directions. Three possible cases are presented below.

(1) $k_b >> k_a$ Tablet thickness decreases much faster than tablet radius
Equation II.B-4 reduces to a linear relationship between M_t/M_∞ and time.

$$M_t / M_\infty = \frac{2k_b t}{C_0 b_0} \qquad \text{(II.B-5)}$$

(2) $k_a >> k_b$ Tablet radius decreases much faster than tablet thickness

$$M_t / M_\infty = 1 - \left(1 - \frac{k_a t}{C_0 a_0}\right)^2 \qquad \text{(II.B-6)}$$

In this case a function of M_t/M_∞ will be proportional to time.

$$1 - \exp\left[\frac{1}{2}\ln\left(1 - \frac{M_t}{M_\infty}\right)\right] = \frac{k_a}{C_0 a_0} t \qquad \text{(II.B-7)}$$

(3) $k_a \approx kb = k_0$

In this case, the rate of drug release can be described by a single rate constant and M_t/M_∞ is a cubic function of time.

$$M_t / M_\infty = 1 - \left(1 - \frac{k_0 t}{C_0 a_0}\right)^2 \left(1 - \frac{2k_0 t}{C_0 b_0}\right) \qquad \text{(II.B-8)}$$

Method

Caffeine (Sigma Aldrich C0750, Lot no: 014K0036) was sieved through a 212 micron sieve.

Three powder blends were made, consisting of 0.5g caffeine and 9.5g of either MCC, DCL 11 or DCL 14. The powders were blended using a 42ml capacity V-shaped blender rotated at 10rpm for 15 minutes. The powders were stored over saturated magnesium nitrate solution in a dessicator overnight (at 55% relative humidity) before blending and again before compaction.

Powder beds of depth 4mm were compacted at constant upper punch speed (0.5, 5 or 50 mm/min) and to a range of final compaction forces (5-75kN). This corresponded to 430 ±10 mg MCC and 350 ±10 mg lactose. Flat-faced punches were used with a 12.7mm diameter punch. An Instron 4260 mechanical tester was used to compact the tablets. Tablets were then stored at 55% relative humidity for a minimum of 72 hours before testing.

A paddle apparatus (Distek Dissolution system 2100B) was used to perform the dissolution testing. 1 liter of Millipore-filtered water was placed in the vessel and the paddles rotated at 225 rpm. The tablet was inserted into the vessel and 1ml samples of the solution were extracted from the top of the vessel at fixed intervals. The caffeine concentration in the samples was measured using UV spectrophotometry (Hewlett-Packard 8452A) at 274nm wavelength. The water temperature was not controlled but was

in the range of 19-23°C. Physical limitations restricted sampling intervals to a minimum of 10s.

Results

MCC is water-insoluble and the tablets disintegrated during testing. All the tablets released their caffeine load in less than 100 seconds. Compaction force and speed had no detectable effect on the profile. 'Bursting' effects were observed in some cases (Figure 27); at some time points prior to complete drug release, the measured concentration of the sample is higher than the final concentration. This suggests that there are fragments of the tablet breaking off and suddenly releasing their drug load near the surface, causing localized regions of high caffeine concentration. As the profiles were not smooth and there were few data points in the transient portion, no quantitative analysis could be performed on the cellulose tablet dissolution profiles.
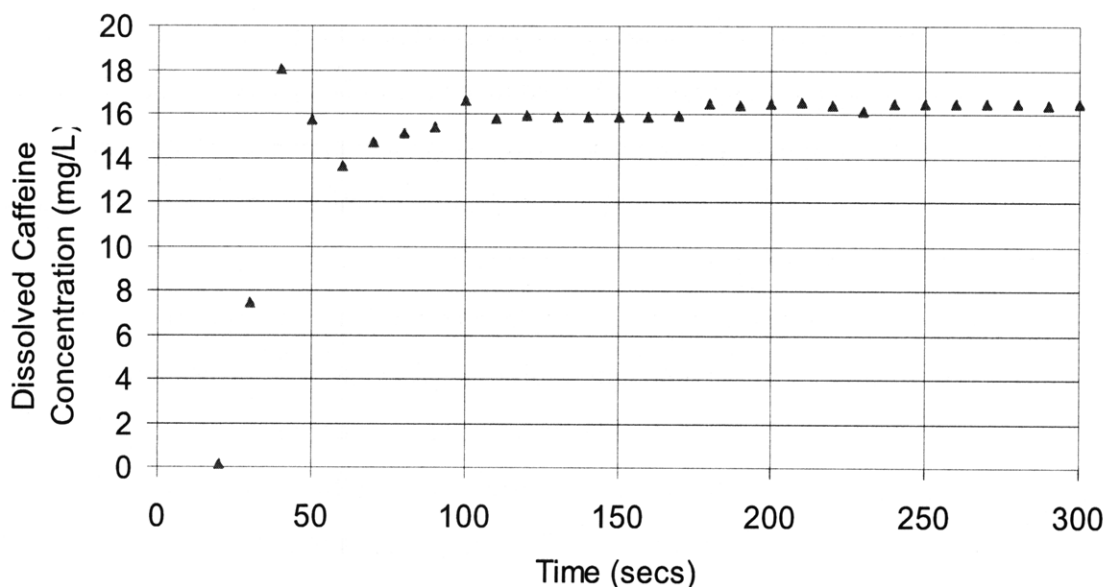
Figure 27: Dissolution profile for 5% caffeine, 95% MCC tablet compacted to 60kN at 50mm/min
The lactose DCL 11 and DCL 14 tablets dissolved completely. Both lactose grades exhibited longer dissolution times with increasing force of compaction (Figure 28), but no effect of compaction speed was observed. DCL 14 tablets have up to fourfold longer dissolution times than DCL 11, when compacted under the same conditions. Variance in

t_{90} increases with compaction force. Although the variance in t_{90} is greater, individual profiles are smooth curves.
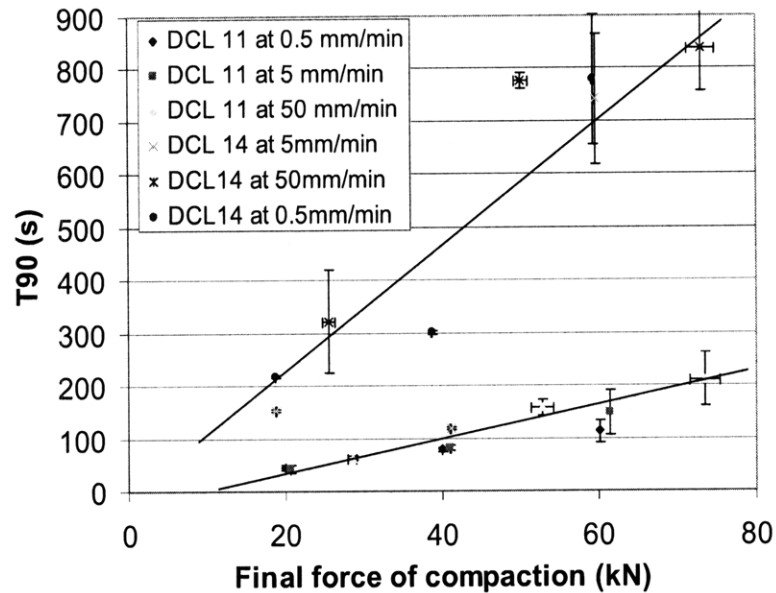
Figure 28: T_{90} for lactose DCL11 and DCL 14 tablets compacted at a range of speeds and forces

An attempt was made to fit the data to Katzenhendler's models. Only the data up to 90% dissolution was considered. A cubic relationship was found to fit all the profiles of M_t/M_∞ versus time (R^2 values were greater than 0.96), suggesting that the rates of surface erosion in the radial and vertical directions are comparable ($k_a \sim k_b$, or $k_a \approx kb = k_0$). The fit parameters are not presented as values for b_0 are not available; therefore it is not possible to calculate values of k_0. Also, there is no data to indicate whether a single rate constant is sufficient to describe erosion.

DCL 11 profiles all have a similar shape (Figure 29) and this is similar to DCL 14 tablets compacted to forces less than 41kN (Figure 30). A transition was observed in DCL 14 tablets between 41kN and 50kN. The profile shape changes from a concave to a convex form. At forces greater than 50kN, the profile fits Equation II.B-6 well, indicating that radial erosion may dominate drug release at higher compaction loads for DCL 14.
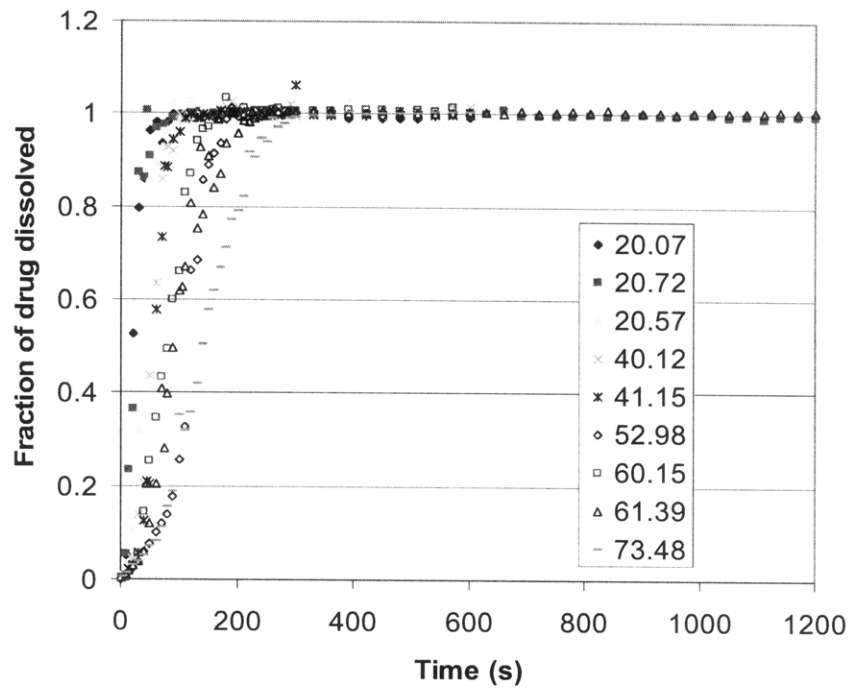
Figure 29: Normalized dissolution profiles for 5% caffeine, 95% DCL 11 tablets compacted to different forces (shown, in kN)
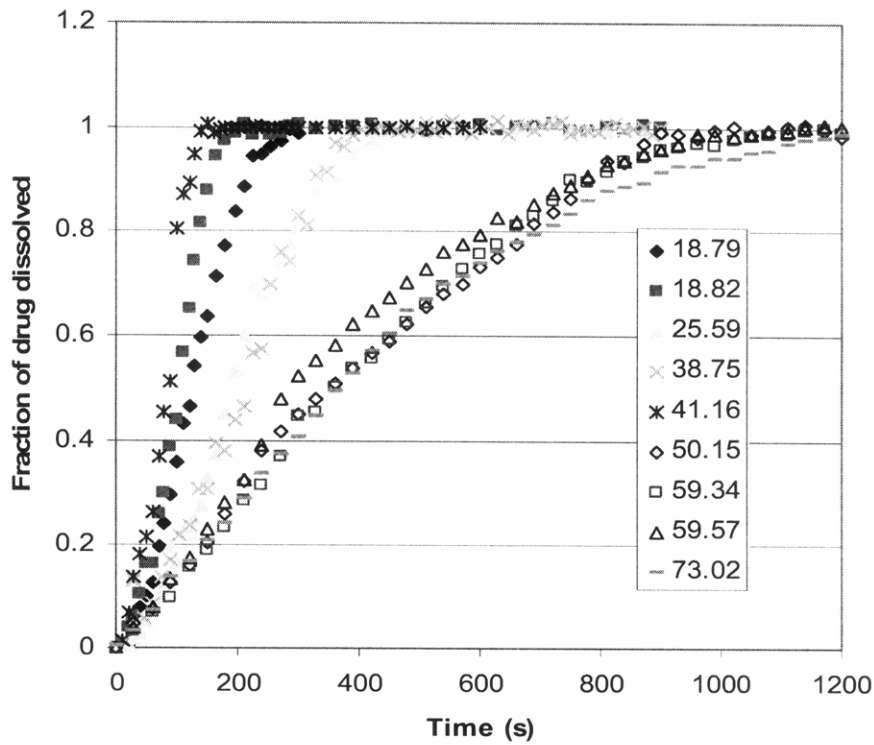
Figure 30: Normalized dissolution profiles for 5% caffeine, 95% DCL 14 tablets compacted to different forces (shown, in kN)

Discussion

The increasing variance in t_{90} as compaction force increases may be attributed to the increased probability of lamination during compaction, leading to cracks in the tablets. If cracks are present, the data is unlikely to fit the surface erosion model. However, the profiles are quite smooth, which suggests that there was not much fragmentation or bursting of tablets during dissolution. It is possible that the cracks allow more penetration in the radial direction, and hence increase the rate of radial erosion, leading to the DCL 14 data fitting Equation II.B-6. This could be confirmed by calculating the erosion rate constant(s) by fitting the curves to a cubic equation and measuring the dimensions of tablets withdrawn from the apparatus at different times. The geometry of the tablets (a_0/b_0) can be varied to investigate its effect on dissolution. However, it is possible that different geometry will lead to different stresses during compaction and hence it may not be possible to vary geometry independently of matrix solubility.

DCL 11 has shorter dissolution times, which limits the number of data points, as the solution was sampled manually. Automatic sampling and analysis would lead to better quality of data.

The standard paddle apparatus was used for this study as it is the most relevant to the pharmaceutical industry. However, it is not well-suited for developing understanding about how tablet microstructure affects dissolution. Firstly, the hydrodynamics of the apparatus are complicated and poorly-understood, therefore mass transfer within the medium volume cannot be modeled easily. Secondly, the tablet geometry can complicate the analysis, as seen above. It may be possible to eliminate the effect of tablet geometry by, for example, encasing part of the tablet in a wax, so that drug release can be considered to be from a flat surface. A non-standard testing configuration will likely be necessary to develop an understanding of the relationship between tablet microstructure and dissolution behavior.

Conclusions

The USP dissolution test is not well-suited for modeling of tablet dissolution, due to complex hydrodynamic and geometric factors. Excipient choice determines whether compaction parameters can be used to modify dissolution behavior.

Increasing compaction force was found to increase dissolution times for DCL 11 and 14, but no effect of speed was observed for the range investigated.

There is some evidence that the rate-limiting step for drug release is surface erosion of the tablet, but disintegration studies are needed to confirm this hypothesis.

References

Cooney D.O., *AIChE J*, **1972**, *18*, 446-449

Costa, P.; Lobo J.M.S. *Eur. J. Pharm. Sci.* **2001**, *13*, 123-133

Dean, J.A. *Lange's Handbook of Chemistry* (15th Edition). McGraw-Hill. **1999**

Desai S.J.; Singh P.; Simonelli A.P.; Higuchi W.I. *J. Pharm Sci.*, **1966a**, *55*, 1230-1234

Desai S.J.; Singh P.; Simonelli A.P.; Higuchi W.I. *J. Pharm Sci.*, **1966b**, *55*, 1235-1239

Dressman J.; Kramer J. (Eds), Pharmaceutical Dissolution Testing, Taylor and Francis Group, LLC **2005**

FDA, *ANDA Checklist for CTD or eCTD format for completeness and acceptability of an application for filing, Office of Generic Drugs, Center for Drug Evaluation and Research*, U.S. Food and Drug Administration, **2007**

Hopfenberger H.B. In *Controlled Release Polymeric Formulations Eds. Paul D.R., Haris F.W.* ACS Symposium Series 33: American Chemical Society, Washington DC, **1976**, 26-31

Higuchi T. *J. Pharm Sci.* **1961**, *50*, 874-875

Higuchi T. *J. Pharm Sci.* **1963**, *52*, 1145-1149

Katzenhendler I.; Hofman A.; Goldberger A.; Friedman M. *J. Pharm. Sci*, **1997**, *86*, 110-115

Korsmeyer R.W., Gurny R., Doelker E.M., Buri P., Peppas N.A., *Int. J. Pharm.* **1983**, *15*, 25-35

Kramer J.; Grady, L.T.; Gajendran J. 'Historical Development of Dissolution Testing' in *Pharmaceutical Dissolution Testing, Ed. Dressman J., Kramer J.*, Taylor and Francis Group, LLC **2005**

Langenbucher F. 'Interpretation of in vitro-in vivo time profiles in terms of extent, rate, and shape' in *Pharmaceutical Dissolution Testing, Ed. Dressman J., Kramer J.*, Taylor and Francis Group, LLC **2005**

Nicolaides E.; Symillides M.; Dressman J.B.; Reppas C. *Pharmaceut. Res.***2001**, *18 (3)*, 380-388

Peppas N.A. *Pharm. Act. Helv.* **1985**, *60*, 110-111

Vertzoni M.; Nicolaides E.; Symillides M.; Reppas C.; Iliadis A. 'Orally administered drug products: Dissolution data analysis with a view to in vitro-in vivo correlation' in *Pharmaceutical Dissolution Testing, Ed. Dressman J., Kramer J.*, Taylor and Francis Group, LLC **2005**

USP, Chapter <711> Dissolution, *United States Pharmacopeia National Formulary*, Volume 1, **2007**

Part III: Imaging and Spectroscopic Analysis of Tablet Structure

X ray micro computed tomography and Terahertz pulsed spectroscopy (TPS) and imaging (TPI) were used to analyze the microstructure of the tablet core (III.A and III.B) and to detect internal defects (III.C) in MCC Celphere®, and Pharmatose® DCL 11 and DCL 14 tablets.

Using TPS, changes in refractive index spectra caused by different compaction conditions were observed for MCC and DCL 11 tablets. No changes in spectral features were found, but the profile is translated along the axis of refractive index. The average refractive index was found to correlate well to tablet hardness for DCL 11, but not for MCC tablets. DCL 11 and DCL 14 tablets compacted at the same conditions were analyzed by TPS. No difference between the spectra of the two grades of lactose was observed.

The X ray images showed that MCC tablets formed by plastic deformation of the granules, whereas lactose tablets were monolithic structures, that showed no evidence of initial granule shape or size. Pore size, rather than average porosity was found to be a better indicator of structural changes. The average 2D pore area and the volume-average pore diameter decreased with increasing compaction force for DCL 11 tablets (and increasing average THz refractive index). However, at higher forces, scanning resolution may have been a limiting factor. No effect of compaction speed was observed. DCL 11 and DCL 14 tablets compacted under the same conditions had the same pore size distributions.

TPI was found to detect internal defects in tablets. The presence or absence of defects was confirmed by X ray micro CT.

A comparison of commercially-available imaging techniques used for analysis of pharmaceutical tablets is presented in chapter III.D. TPS has some advantages over near infra-red spectroscopy (the current non-destructive technique for assessing tablet hardness). However, further work is needed to understand the physical significance of the THz measurements. TPI is a more rapid method of tablet defect detection than X ray micro CT. A quantitative assessment of the resolution and limit of detection of the TPI technique will be required before it can be a reliable quality assessment tool.

III.A: Terahertz Pulsed Transmission Spectroscopy

An introduction to Terahertz technology

Terahertz radiation is a term used for the portion of the electromagnetic spectrum between microwave and mid-infrared (0.1-10THz, or 3-333cm^{-1}). Unlike Raman and mid-IR wavelengths which excite *intra*molecular covalent bonds, the THz range causes vibration and translation of *inter*molecular non-covalent bonds, and hence is sensitive to changes in crystalline structure (Day et al, 2006). A description of the technology for generation and detection of THz pulses is presented by Ho et al (2006).

Commercial terahertz pulsed spectroscopy (TPS) devices have been on the market for less than 10 years, and the technique has shown promise for pharmaceutical applications, as outlined by Zeitler et al (2007). TPS has been shown to detect polymorphic differences in solids (Upadhya et al, 2004, Taday et al, 2003) and to quantify the composition of a mixture of polymorphs (Strachan et al., 2005).
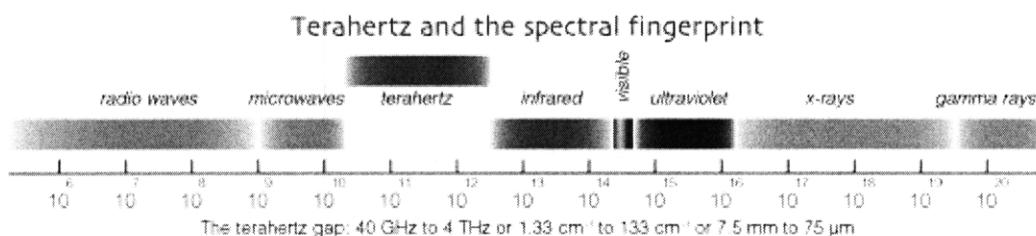
Figure 31: The position of terahertz radiation in the electromagnetic spectrum (Source: TeraView, 2007)

Objective

This study investigated the potential of THz spectroscopy to evaluate tablet hardness and dissolution.

Method

Sample preparation

The samples tested are single-component wafers of MCC Celphere®, lactose Pharmatose® DCL 11 or lactose DCL 14.

MCC, DCL 11 and DCL 14 powders were sieved to obtain the sieve fraction 106-212 microns. The powders were stored over saturated magnesium nitrate solution (at 55% relative humidity) for a minimum of 10 hours before compaction.

Powder beds of depth 4mm were compacted at constant upper punch speed (0.5, 5 or 50 mm/min) and to a range of final compaction forces (5-75kN). This corresponded to 430±10 mg MCC and 350±10 mg lactose. Flat-faced punches were used with a 12.7mm diameter punch. An Instron 4260 mechanical tester was used to compact the tablets. Tablets were made in triplicate for each set of compaction parameters and stored in air-tight containers for approximately 3 weeks before testing.

TPS Measurement

Samples were analyzed using a TPS Spectra 1000 transmission spectrometer (TeraView Ltd., Cambridge, UK). No sample preparation was necessary. The sample was inserted in a holder in the chamber. The chamber was then purged with nitrogen for 4 minutes to remove water vapor before scanning. Each sample was measured in triplicate, each measurement being an average of 1800 scans.

The spectrometer samples the entire thickness of the tablet at a central point, but the spot size varies with wavenumber. A spectrum of refractive index (RI) in the THz range as a function of wavenumber is obtained.

The sample thickness is required to calculate the refractive index and was measured with a vernier scale (Mitutoyo Absolute Digimatic) to an accuracy of 0.01m.

Results

Spectral changes as a function of compaction conditions for MCC and DCL 11

The spectra are reproducible for each set of compaction conditions. The mean values (of three tablets per curve) are plotted in Figure 32 and Figure 33.

For MCC tablets, the refractive index increases with increasing compaction force. However, there is overlap between the spectra in the force range 41-62kN. As it was not possible to ensure that tablets were compacted to the same force at different speeds, the effect of speed is inconclusive from this plot.
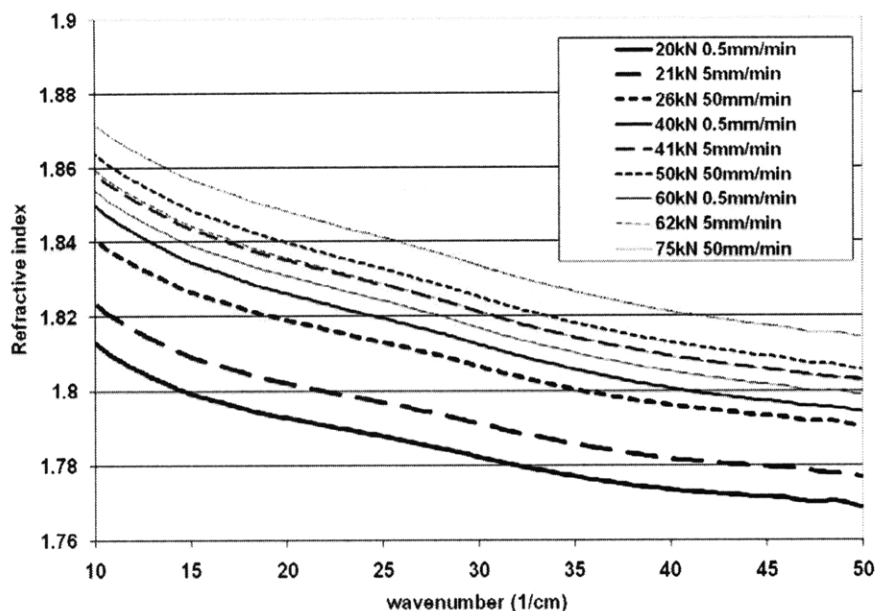
Figure 32: Mean refractive index data for MCC tablets prepared under different compaction conditions

For the lactose DCL 11 tablets, a distinct spectral form is apparent (Figure 33). Again, this profile is shifted along the vertical axis, with average RI increasing with compaction force. However, the RI decreases for tablets compacted to 73kN at 50 mm/min. This could be due to structural defects e.g. internal cracks, or differences in microstructure due to rapid compaction. The data in the range 46 cm^{-1} is not plotted because of the presence of artefacts resulting from data smoothing algorithms in this range.
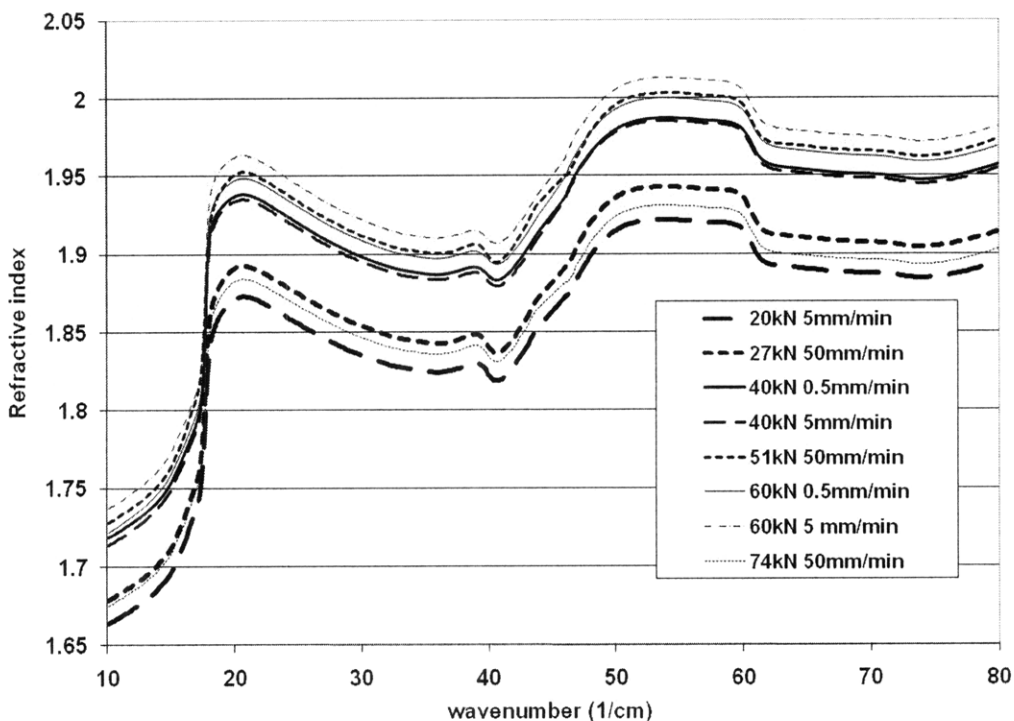
Figure 33: Mean refractive index data for lactose compacts prepared under different compaction conditions

Correlation between tablet hardness and THz refractive index

Tablet hardness was measured for a set of identical tablets, as described in chapter IIA and hardness was plotted against refractive index (Figure 34). A poor correlation is observed for MCC tablets. However, the range of tablet hardness achievable was narrow. For the lactose DCL 11 tablet data (Figure 34), an outlying data point is observed that corresponds to tablets compacted to 73kN at 50mm/min. If this data point is excluded, a good correlation is observed between tablet hardness and refractive index. The refractive indices for lactose tablets were higher than for MCC tablets
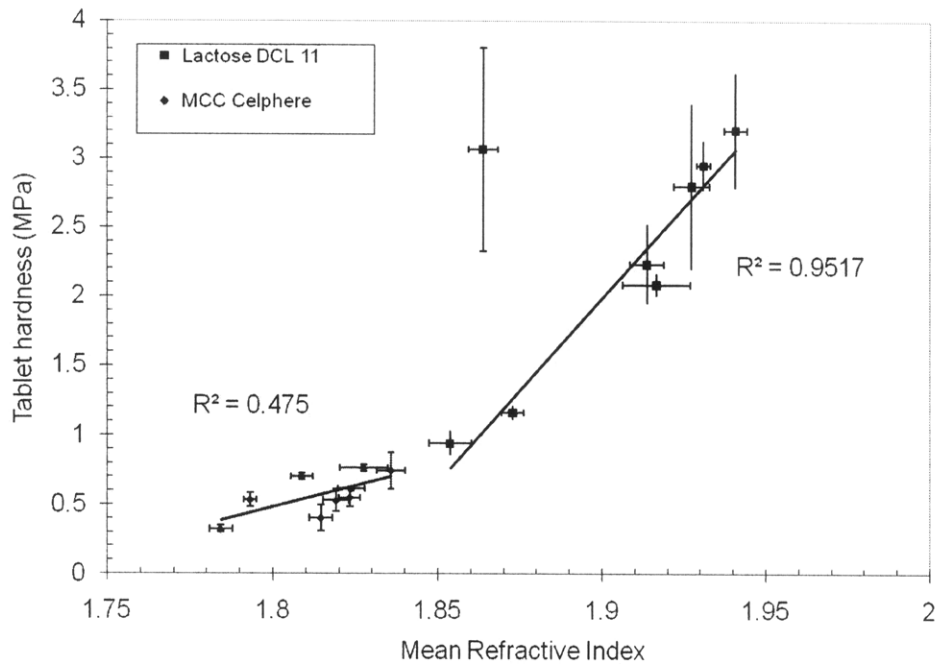
Figure 34: Correlation between tablet hardness and THz mean refractive index (averaged over 10-50 cm^{-1} for MCC tablets and 10-80 cm^{-1} for MCC tablets

Comparison of DCL 14 and DCL 11
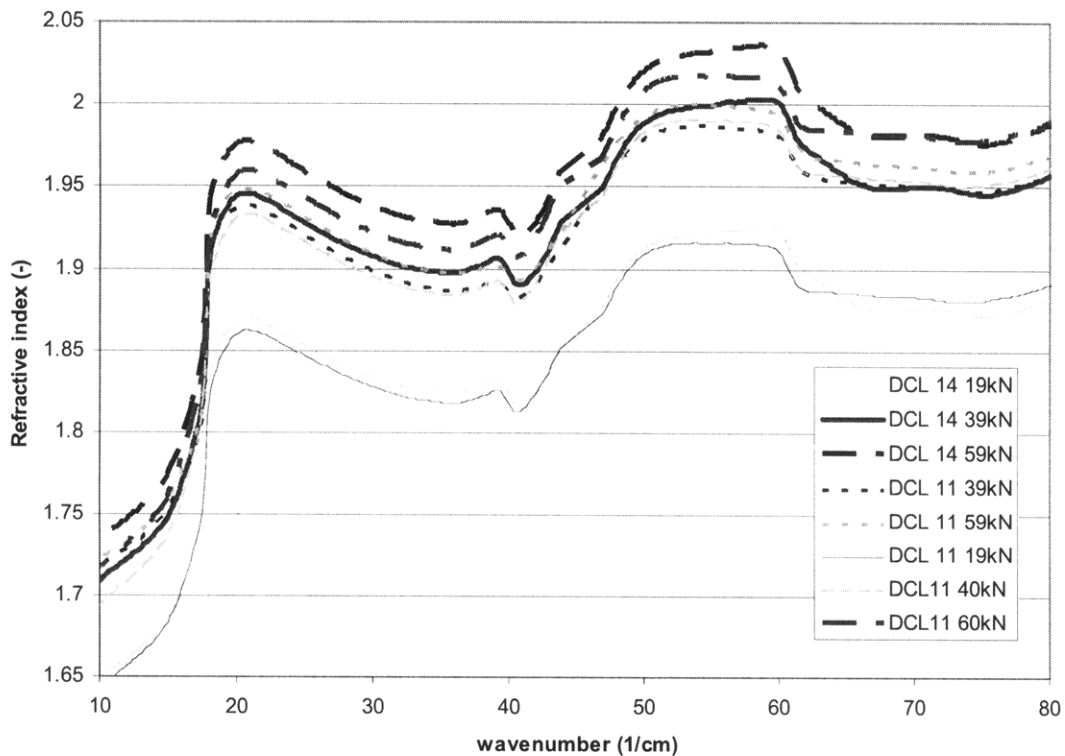
Figure 35: Spectra of DCL11 and DCL 14 tablets compacted at 0.5mm/min to different final forces

The RI spectra of DCL 11 and DCL14 tablets compacted at 0.5mm/min are plotted in Figure 35. The range 44 - 46 cm^{-1} is omitted, because of the presence of numerical artefacts. No difference is observed in the spectra for DCL 11 and DCL 14 tablets compacted under the same conditions.

Discussion

Effect of compaction conditions

The lack of peaks in the MCC profile is consistent with an unstructured molecular organization, as observed for amorphous materials by Strachan et al (2004) and Walther et al. (2003). DCL 11 and DCL 14 consist of a mixture of amorphous and α-monohydrate lactose, which accounts for the more distinct features observed in the spectra.

The outlier in Figure 34 is possibly due to the presence of cracks in the tablets. Lamination was detected by THz pulsed imaging and by X ray tomography (see chapter III.C) and shown to increase with compaction force. It is possible that the presence of major cracks in the tablet caused scattering of the THz beam and distortion of the data.

Comparison of DCL 11 and DCL 14

DCL11 and DCL 14 form tablets of equivalent hardness for given compaction conditions, as described in chapter IIA. However the dissolution times for DCL 14 tablets are much longer than those for DCL11 tablets (chapter IIB). One hypothesis to account for the difference in dissolution was different proportions of amorphous and α-monohydrate lactose in the two grades. If so, the TPS spectra ought to be different, as demonstrated by the absorption spectra for the different lactose hydrate forms (Figure 36). However, no such difference has been observed.
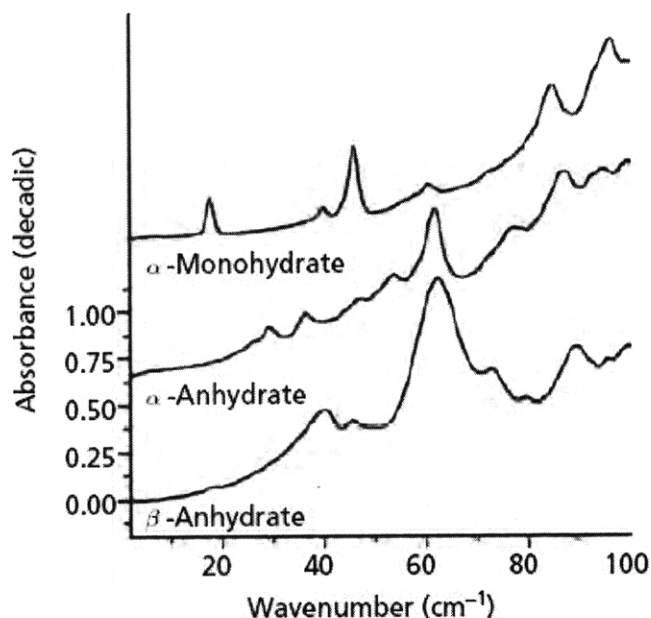
Figure 36: Terahertz spectra of different lactose hydrate forms. Spectra are vertically offset and normalized for clarity (Source: Zeitler et al 2007)

Physical significance of THz refractive index

When compaction force is increased, an increase in average refractive index is seen for MCC, DCL 11 and DCL 14 tablets. However, there is negligible change in the shape of the refractive-index versus wavenumber plot. Spectral changes are known to correspond to different crystal or hydrate forms in solids (Zeitler et al. 2007). However it is not yet known what physical differences in the solid structure give rise to a spectral translation. Further basic research into the THz spectrum is required for it to be a useful research tool. It is not yet possible, as it is, for example, in IR spectroscopy, to look at spectral features and directly connect them to physico-chemical characteristics of the sample. Some attempts have been made in this direction by using molecular dynamics models of single molecules and clusters to calculate vibrational modes in the solid state (Day et al, 2006, Allis et al 2006, Saito et al 2006 (a), (b)). However, much further research in this direction is required.

Conclusions

THz spectroscopy has potential as a tool to predict tablet hardness, or for quality control. However, its predictive capability for dissolution behavior is limited. For TPS to be a

useful research tool, further work is required to understand the physico-chemical basis for features and shifts in the spectra.

Acknowledgements

References

Allis D.G.; Prokhorova D.A.; Korter T.M. *J. Phys. Chem. A*, **2006**, *110*, 1951-1959

Day G.M.; Zeitler J.A.; Jones W.; Rades T.; Taday P.F. *J. Phys. Chem B.*, **2006**, *110*, 447-456

Ho L.; Zeitler J.A.; Rades T.; Gordon K.C.; Rantanen J.; Strachan C. *Pharm. Tech. Eur.*, http://www.ptemag.com/pharmtecheurope/ **November 2006**

Saito S.; Inverbaev T.M.; Mizuseki H.; Igarashi N.; Kawazoe Y. *J Appl. Physics Part I-Regular Papers Brief Commun. Rev Papers*, **2006a**, *45*, 4170-4175

Saito S.; Inverbaev T.M.; Mizuseki H.; Igarashi N.; Kawazoe Y. *Chem. Phys. Lett.* **2006b**, *423*, 439-444

Strachan C.J.; Rades T.; Newnham D.A.; Gordon K.C.; Pepper M.; Taday P.F. *Chem. Phys. Letters* **2004**,390 (1-3) pp20-24

Strachan C.J.; Taday P.F.; Newnham D.A.; Gordon K.C.; Zeitler J.A.; Pepper M.; Rades T. *J. Pharm. Sci.* **2005**, *94(4)*, 837-846

Taday P.; Bradley I.V.; Arnone D.D.; Pepper M. *J. Pharm. Sci.* **2003**, *92 (4)*, 831-838

TeraView www.teraview.co.uk, accessed April 5, **2007**

Upadhya P.C.; Nguyen K.L.; Shen Y.C.; Obradovic J.; Fukushige K.; Griffiths R.; Gladden L.; Davies A.G.; Linfield E.H. *Joint 29ᵗʰ Conference on Infrared and Millimeter Waves and 12ᵗʰ Int. Conf on Terahertz Electronics* **2004**, 429-430

Walther M.; Fischer B.M.; Jepsen P.U. *Chem. Phys.*, **2003**, *288 (2-3)*, 261-268

Zeitler J.A.; Taday P.F.; Newnham D.A.; Pepper M.; Gordon K.C.; Rades T. *J. Pharm. Pharmacol.* **2007**, *59*, 209-223

III.B: Microstructure Analysis using X ray microCT

Introduction

X ray tomography is a method that allows high-resolution 3D mapping of density variations in a sample. It is well suited for samples such as the tablet fragments investigated here, which consist of two phases, solid and gas, with distinctly different densities.

This technique has been used to study the structure and porosity of materials such as bone, soil, ceramics and pastes. The potential of this technique within the pharmaceutical industry is discussed by Hancock and Mullarney (2005). It is being used (in conjunction with other experimental and modeling methods) to study powder packing and particle movement during compaction by Xiaowei et al. (2006 (a), (b)) at the Pfizer Institute for Pharmaceutical Material Science, Cambridge, UK.

As with any tomographic technique, the sample is first scanned in multiple configurations and then undergoes several steps of data-processing to obtain the three-dimensional data. The steps are outlined below.

Scan

A SkyScan™ 1172 microCT instrument was used in this study. The X ray point source and detector are stationary and the sample is rotated to obtain multiple grayscale shadow images (e.g. Figure 38), similar to those obtained by standard medical X ray imaging.
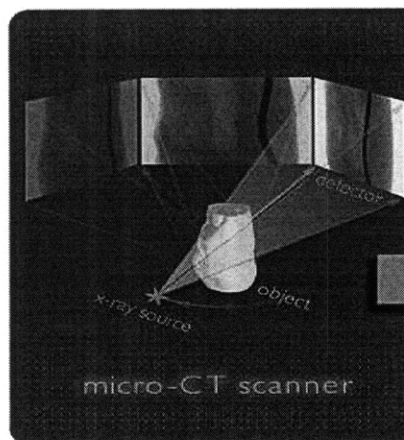
Figure 37: X ray micro CT scan configuration (source: Skyscan, 2007)
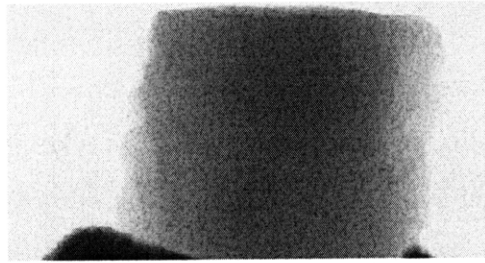
Figure 38: X ray shadow image of lactose tablet fragment

Reconstruction

A Fourier transform–based Feldkamp reconstruction algorithm is used to obtain cross section slices of the sample as grayscale images (Figure 39). These can be read sequentially or interpolated to create a 3D grayscale map of the internal structure. The main qualitative features of the structure are visible at this stage. However, to extract quantitative parameters to characterize the structure, two further steps are required: binarization and analysis.
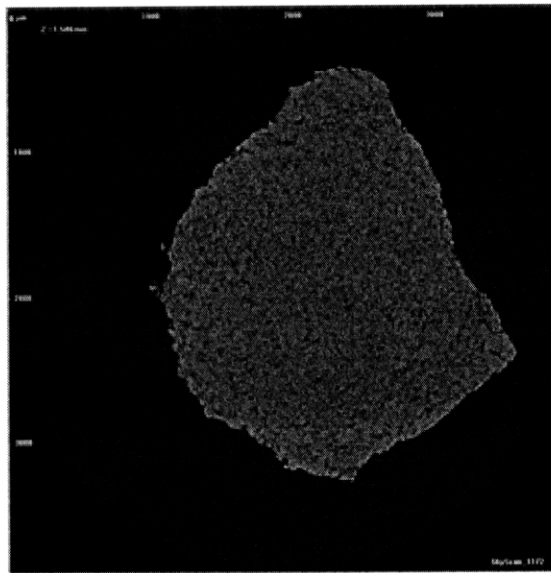
Figure 39: Example of reconstructed grayscale cross section of a fragment of lactose DCL 11 tablet at a depth of 1.586mm into the sample

Binarization

For the purposes of this research, the 3D grayscale internal map was converted into a binary map to mark the boundaries between the two phases; solid and pores. This was done using a global segmentation technique, as described by Pal and Pal (1993). Voxels with intensity less than a certain grayscale value are marked as empty space and those with higher intensity are marked as solid. The threshold intensity is determined for each

scan set to allow for drift and fluctuations of the X ray tube. An intensity histogram is calculated for the entire dataset (e.g. Figure 40). This forms a bimodal distribution with one low-intensity mode (solid pink line) corresponding to the voxels indicating empty space around the sample and in the pores, and another mode (dotted blue line) representing the intensity distribution of 'solid' voxels. As there is always an overlap between the two distributions, the valley where they intersect is selected as the threshold value.
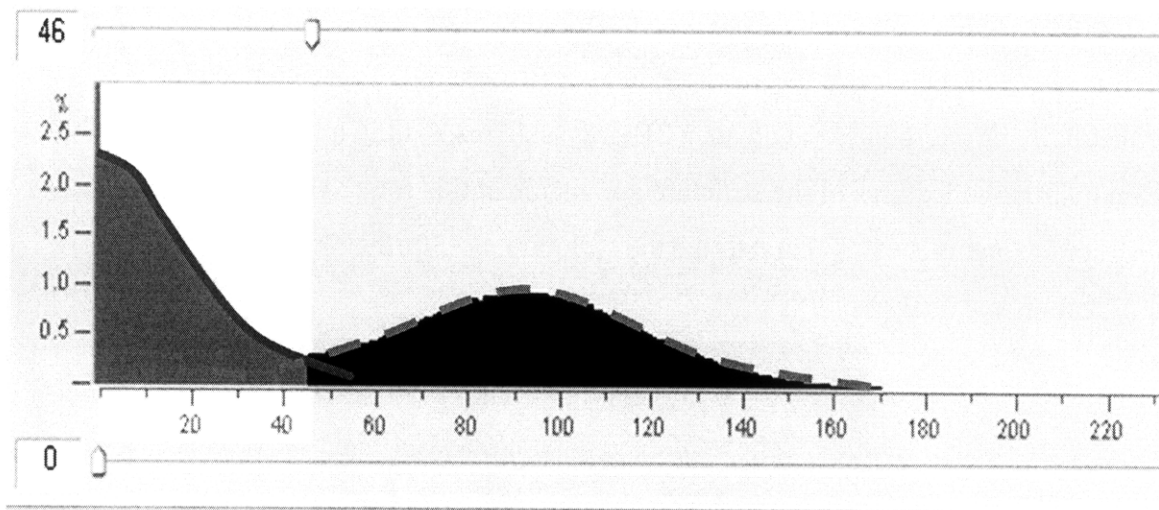
Figure 40: Intensity histogram for a set of reconstructed slices (global threshold: 46)

Analysis

The dataset of binary images can be analyzed as a set of 2D images or as a 3D structure by interpolating between the images. The average porosity can be calculated in 2D (pore area/total area of interest) or in 3D (pore volume/total volume of interest).

A relevant 2D parameter is the average cross section area of each pore. This is calculated for each cross section slice and averaged over the dataset. A highly interconnected structure with large pores will result in fewer, larger discrete pores in cross section than a homogenous structure with lower porosity (SkyScan, 2007b).

A relevant 3D parameter is the volume-weighted pore diameter (average and distribution). This parameter is known more generally in stereology (the field of estimating geometrical quantities of spatial objects from lower dimensional probes) as the structure thickness. A detailed discussion on the calculation of this parameter can be found in Hildebrand and Ruegsegger (1997). For our purposes it is sufficient to understand that the method works by fitting maximal spheres to each voxel marked as

pore volume (Figure 41). The diameter of this sphere is the pore diameter at that point. From these local pore diameters a volume-weighted mean diameter and a distribution are calculated.
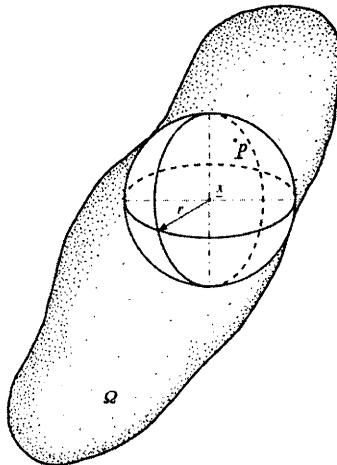
Figure 41: Pore diameter calculation for point x. The structural thickness is the volume average of the spherical diameter, $2r$.

Objectives

The aims of the following experiments were to:

o   Identify morphological features of tablet structure for different materials

o   Quantify pore structure parameters of tablets and

    o   investigate the effect of compaction parameters on tablet structure

    o   compare different grades of lactose

Method

MCC, DCL 11 and DCL 14 powders were sieved to obtain the sieve fraction 106-212 microns. The powders were stored over saturated magnesium nitrate solution (at 55% relative humidity) for a minimum of 10 hours before compaction.

Powder beds of depth 4mm were compacted at constant upper punch speed (0.5, 5 or 50 mm/min) and to a range of final compaction forces (5-75kN). This corresponded to 430±10 mg MCC and 350±10 mg lactose. Flat-faced punches were used with a 12.7mm diameter punch. An Instron 4260 mechanical tester was used to compact the tablets. Tablets were then stored at 55% relative humidity for a minimum of 72 hours before testing.

A SkyScan™ 1172 microCT machine (SkyScan N.V., Artselaar, Belgium) was used to scan tablet fragments of approximately 2 millimeters in diameter cut from the center of the tablet.

The reconstructed cross sections were created using NRecon software and binarization and analysis was conducted using CTAn software from SkyScan™.

The scanning and reconstruction parameters for the lactose tablets are shown in Table 10. A cylindrical region approximately 1mm^3 in volume (Figure 42) was selected for analysis of each sample. The global threshold method for image segmentation was used to convert the grayscale images into binary images. The effects of noise were minimized by removing clusters of connected 'pore' voxels less than 3 voxels in size.

Table 10: X ray microCT scanning and reconstruction parameters for tablet fragments

Scanning (SkyScan 1172)	
Beam voltage	40kV
Beam current	250 µA
Sample total rotation	180°
Rotation degree	0.1°
Exposure time	147 ms
Frame average	4
Random movement correction	10
Pixel linear dimension	1.9 µm
Camera make and model	Hamamatsu 10Mp camera
Camera resolution	2000 x 1048 pixels
Filter	No filter
Flat field	Gathered prior to each scan. Frame average for flat field = 100
Median filter	OFF
Reconstruction (NRecon v1.4.4)	
Image post alignment	Automatic (Range: -12 to 12 pixels)
Beam hardening correction factor	10
Ring artifact correction factor	10
Cross section intensity limits	0.001 – 0.15
Voxel dimension (isotropic cube)	1.9 µm
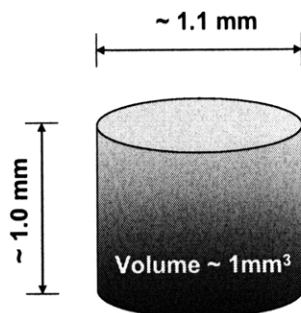
Figure 42: Cylindrical region selected for analysis

Results

Grayscale cross sections were used to compare the morphologies of tablets made from different materials. Quantitative analysis was used to investigate the effect of compaction parameters on DCL 11 and to compare between the structure of DCL 11 and DCL 14 tablets.

Morphological comparison between lactose and microcrystalline cellulose

A comparison of lactose DCL 11 and MCC compacted under similar conditions is presented in Figure 43 and Figure 44. The powder granules are clearly visible in the images of MCC tablets (Figure 43). The pores become smaller in size as extensive plastic deformation of the granules occurs when the tablet is compacted at higher speeds and forces. The porosity in the tablet is due entirely to these inter-granular spaces which are highly connected.

With the lactose (Figure 44) tablets there is no evidence of the initial granule shape or size. The pores are irregular in shape and scattered throughout the cross section. They decrease in size as compaction force and speed are increased, resulting in a homogeneous, monolithic structure.
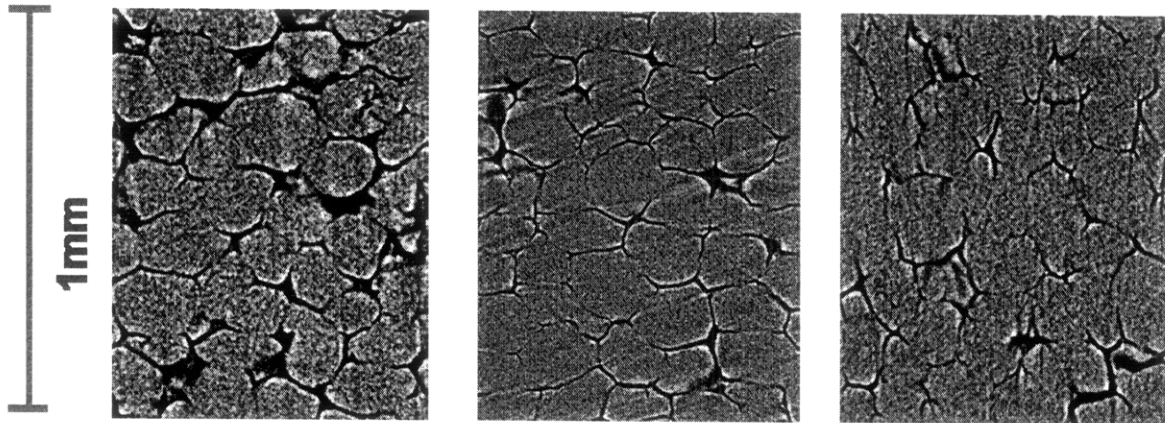
Figure 43: Grayscale cross section of MCC tablets (from left to right), (a) 0.5mm/min 19kN, (b) 5mm/min 40kN, (c) 50mm/min 72kN
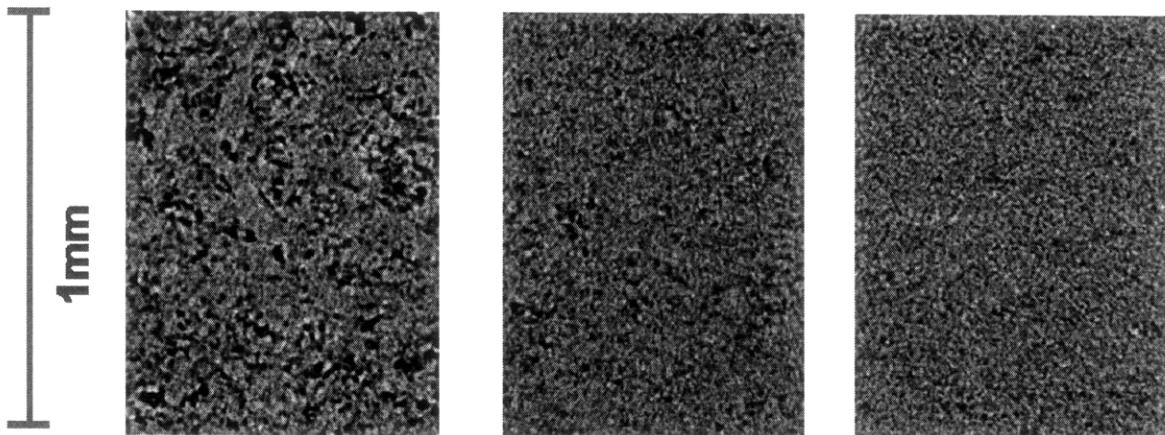
Figure 44: Grayscale cross section of DCL 11 tablets (from left to right), (a) 0.5mm/min 19kN, (b) 5mm/min 40kN, (c) 50mm/min 72kN

Effect of compaction parameters on lactose DCL 11

Lactose DCL 11 tablets compacted at 0.5, 5 and 50mm/min and to a range of forces were scanned and analyzed. An example of a binarized cross section through the region of interest is shown in Figure 45.
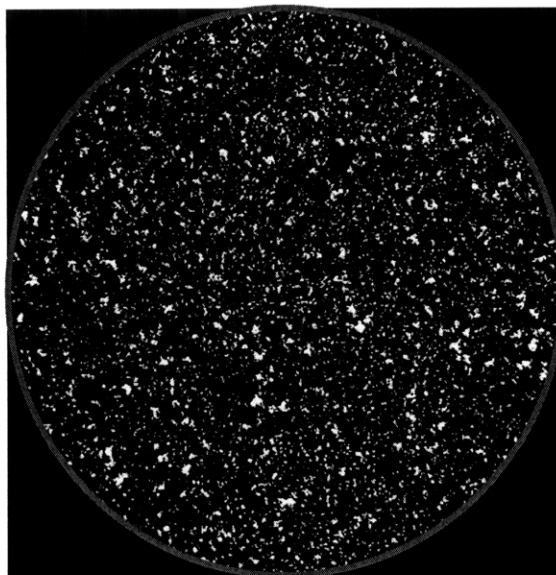
Figure 45: Example of binarized cross section of lactose DCL 11 tablet (white: pores, black: solid/area outside region of interest)

The average (3D) porosity, the average pore area (2D) and the volume weighted distribution and average pore diameter were calculated.
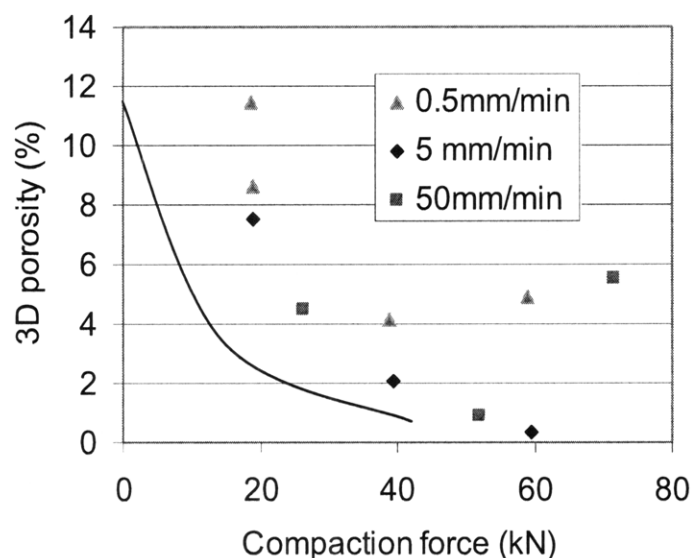
Figure 46: 3D porosity of lactose DCL 11 tablets compacted under different conditions

As seen in Figure 46, average porosity decreases with compaction force, as indicated by visual observation of the grayscale images (Figure 44). However two data points deviate from the trend at higher forces. There is no noticeable effect of speed. The minimum porosities are close to zero for the range of forces investigated and the selected scan settings. This could be due to a decrease in the number of pores, or a decrease in pore

size, or a combined effect of both. For example, if the pore size becomes smaller than the resolution of the scan (1.9 μm), then they will not be detected and porosity would fall to zero.
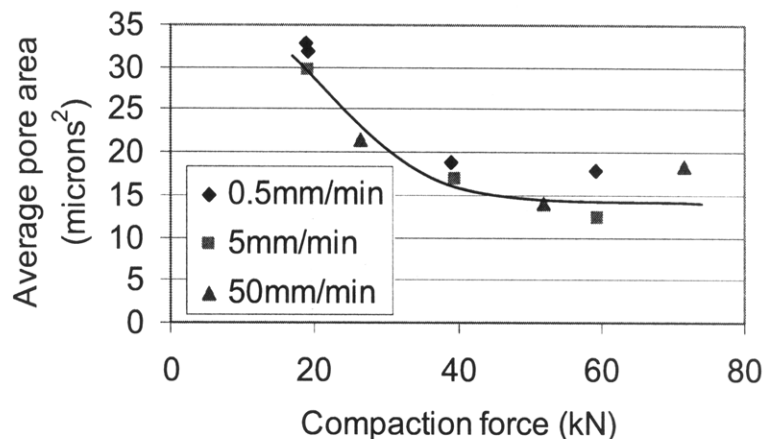
Figure 47: Average pore cross section area (2D analysis) of DCL 11 tablets decreases as compaction force increases

A clearer trend is observed if the average cross section of the pores is analyzed (Figure 47). The pore size decreases from approximately 32 microns^2 to 15 microns^2 between the force range of 20 to 40kN. At loads above 40kN, the average pore area appears to remain unchanged. An average pore area of 15 μm^2 indicates that the pore size is within the detection limit of the scan, therefore the decrease in porosity seen in Figure 46 must be due to a decrease in the number of pores, rather than the decrease in pore size. Again, there appears to be no effect of compaction speed.

The volume average pore diameter (a 3D parameter) shows the same trend as the average pore cross section area (a 2D parameter). It decreases by about 40% between the force range 20-40kN, after which there appears to be little decrease (Figure 48). This indicates that the decrease in pore size is a real phenomenon and can be detected independently of the characterization parameter selected.
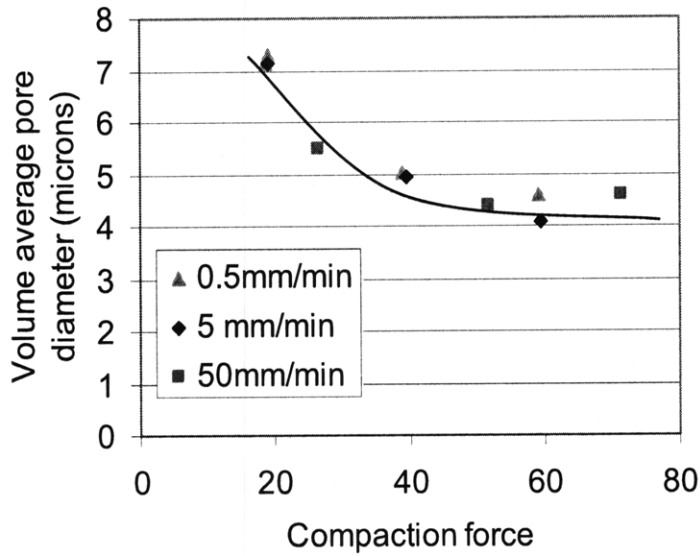
Figure 48: Volume average pore diameter of lactose DCL 11 decreases as compaction force increases
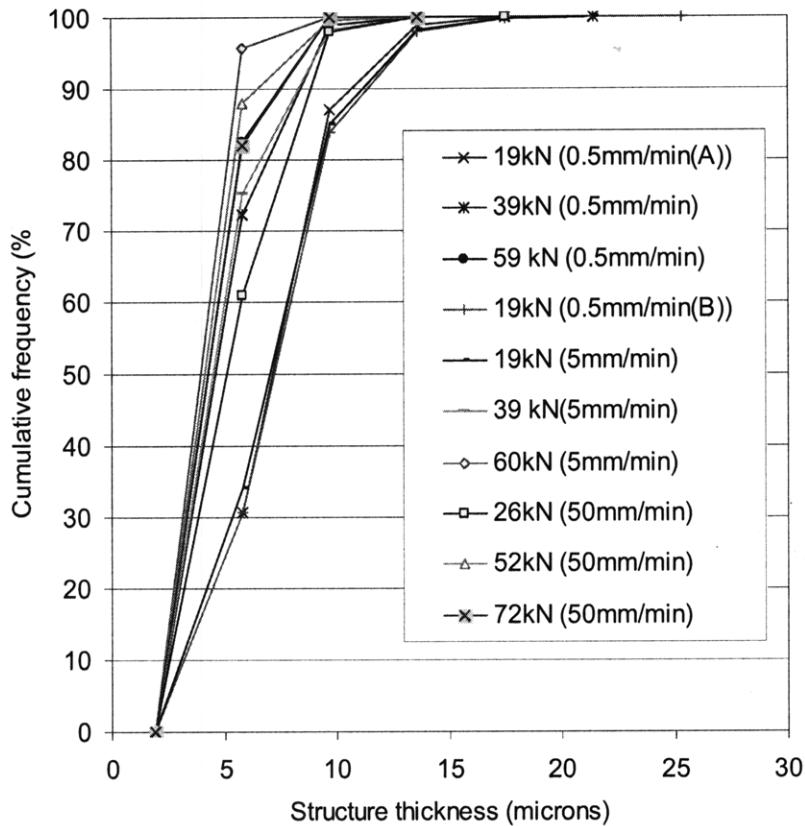
Figure 49: Effect of compaction conditions on volume weighted pore diameter distribution of DCL 11 tablets

The volume weighted distribution of pore diameter (Figure 49) shifts to smaller pore sizes as compaction force increases. The two exceptions to the trend (72kN, 50mm/min

and 59kN, 0.5mm/min) correspond to the two data points that deviate significantly from the trend in Figure 46.

<u>Comparison of lactose DCL 11 and DCL 14</u>

There are no morphological differences between DCL 11 and DCL 14 tablets compacted under the same conditions. Figure 50 contains binarized versions of cross sections through tablets compacted at 0.5mm/min to a range of forces. For both materials, we see no evidence of initial granule size or shape. Pores are scattered randomly across the cross section of the tablet. There is a decrease in pore size as compaction force is increased.

Table 11: Average porosity of DCL 11 and DCL 14 tablets compacted to the same conditions

	DCL 14	DCL 11
19 kN	7.4 %	11.4 %, 8.6%
39 kN	8.2 %	4.1 %
59 kN	3.8 %	4.2 %

The average (3D) porosity measurements are presented in Table 11. No clear trend is seen between compaction force and average porosity. This suggests that average porosity is not the correct parameter to characterize microstructural changes, as differences between tablets compacted to different forces are clearly visible in the cross section images (Figure 50).

	DCL 14	DCL 11
19kN		
39kN		
59kN		
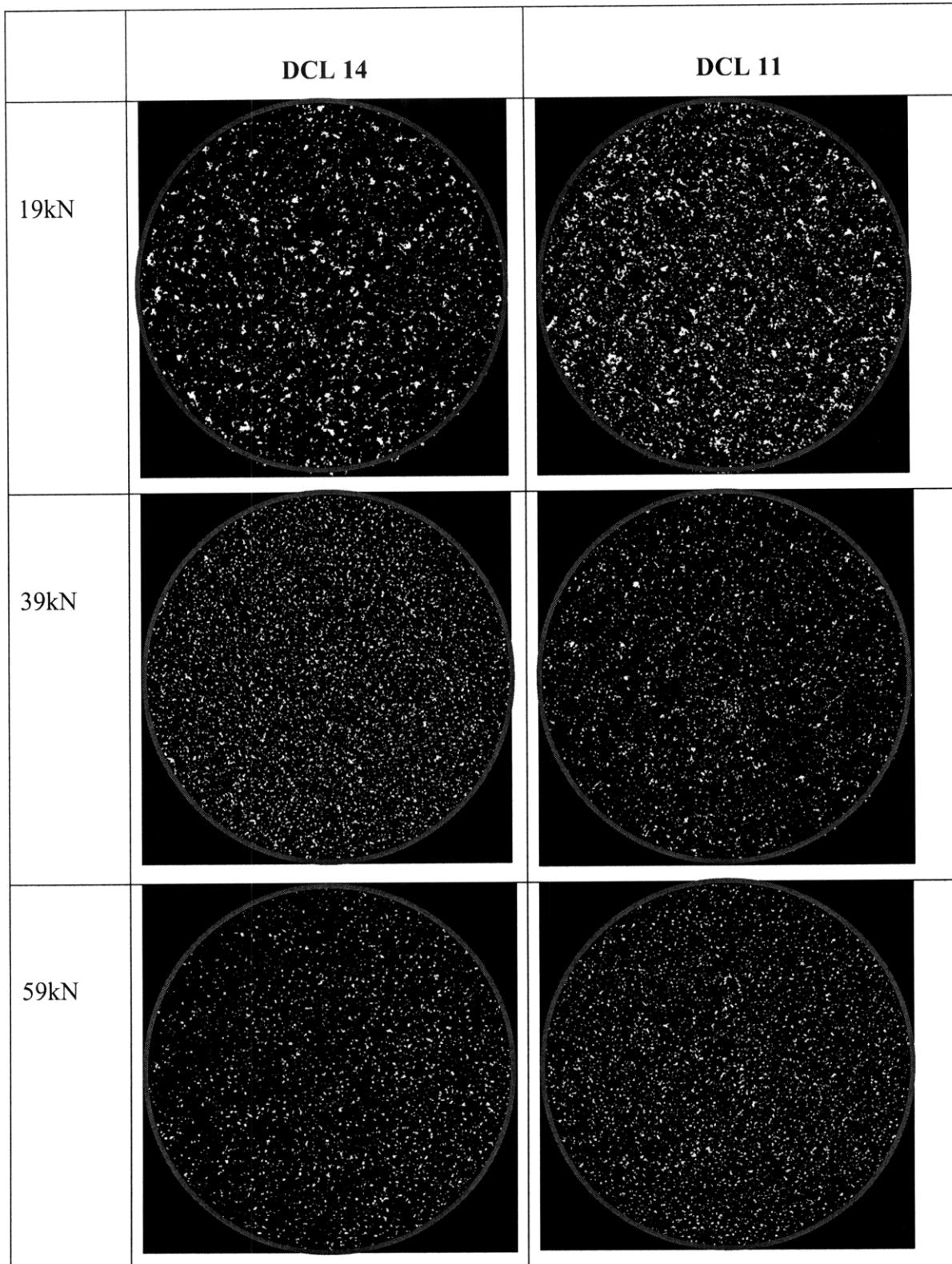
Figure 50: Cross sections of DCL 11 and DCL 14 tablets compacted to the same final force at a speed of 0.5mm/min. White: pores, Black: solid/area outside region of interest (diameter ~1mm).
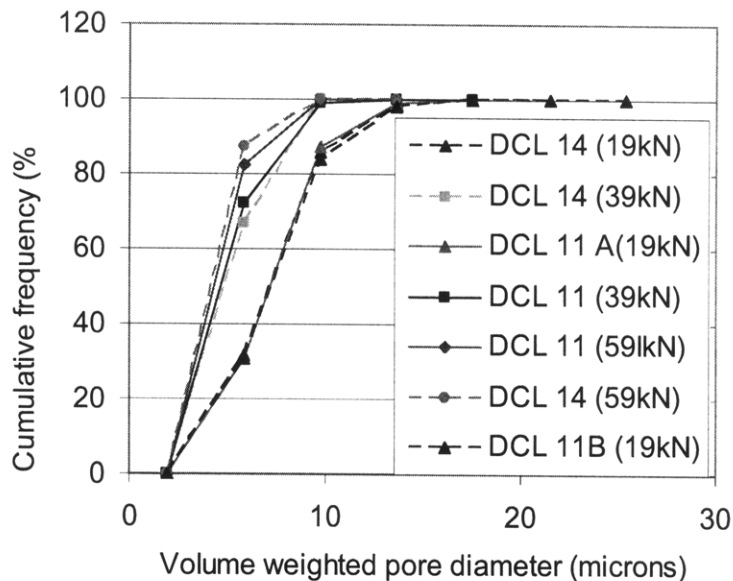
Figure 51: Comparison of volume-weighted pore diameter distributions of DCL 11 and DCL 14 tablets compacted to the same conditions

The volume-weighted pore size distributions are almost identical for DCL 11 and DCL 14 tablets compacted at the same conditions (Figure 51). It was possible to do only one repeat measurement (a second tablet of DCL 11 at 0.5mm/min to 19kN). This reproduced the previous result.

Discussion

X ray micro CT allows us to visualize the internal structure of compacted tablets. The qualitative features of the tablet morphology are clearly visible and elucidate the compaction mechanism of the materials; MCC granules consolidate by plastic deformation, whereas lactose DCL 11 and DCL 14 granules appear to undergo fracture or crushing.

However, if tablet structure is to be a product specification, quantitative characterization of the structure is necessary. The relevant parameters must be selected from a range of two and three-dimensional parameters commonly used for image analysis.

Average porosity was not found to correlate to compaction force, although a decreasing porosity could be observed visually from gray-scale cross-sections. There are several possible explanations.

Noise was filtered by removing isolated voxels, so it is unlikely to play a significant role in disguising trends in average porosity.

Absolute porosity measurements will be sensitive to resolution if the resolution is not much greater than the features of interest. At higher compaction forces, the size of pores becomes comparable to the size of a single voxel. Therefore the pore morphology cannot be fully captured and measurements become sensitive to resolution (compare Figure 52 (a), (b) and (c)) and also to relative location of the artifact to the voxel grid (compare Figure 52 (c) and (d)). However, the latter effect will likely get averaged out over all the pores in the sample, (there are tens of thousands of pores in each sample).

If the pores are smaller than the voxel size, they may not be detected and will not appear in the contribution to average porosity of the pore diameter distribution.
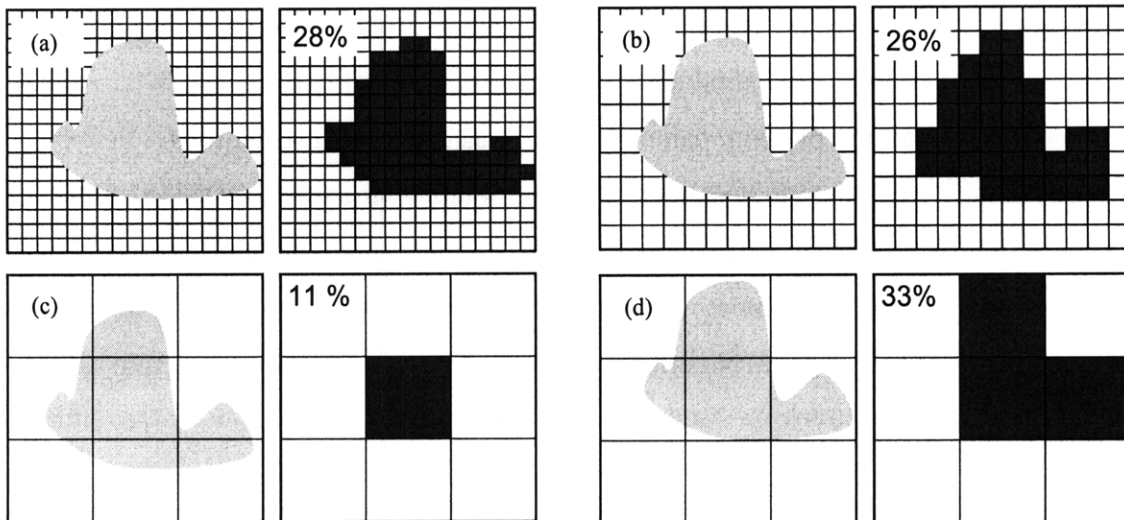
Figure 52: Effect of resolution and voxel positioning on porosity measurement. Left hand images represent real object, right hand images represent binary image. Grid size represents resolution.

The only way to circumvent this issue is to have a voxel size that is much smaller than the features of interest. However, higher-resolution imaging requires longer exposure times and more image-averaging to improve the signal to noise ratio. This results in larger datasets and hence longer reconstruction and analysis times. Therefore a compromise is always necessary between image quality and the dataset size and processing times.

The average pore area (a 2D parameter) and the structural thickness of the pores (volume-weighted pore diameter) were found to show clearer trends for DCL 11 and DCL 14 tablets compacted under a range of conditions. These can be reported as distributions or

average quantities. The visually observed decrease in pore size and pore size range can be captured by these parameters.

One limitation with the equipment was that the point source with fan beams allows for greater resolution imaging, by creating projections of the sample which can be moved back and forth. However, resolution is restricted by sample size. Therefore only a fragment of the tablets needed to be broken into fragments for analysis, so although it is a non-invasive technique, it was destructive and it was not possible to obtain spatially resolved data on porosity. For example, future research might consider whether the anisotropic compaction process causes axial variation in porosity.

Conclusions

X ray micro CT is a useful tool for qualitative and quantitative investigation of the microstructure of pharmaceutical tablets. It can be used to identify compaction mechanisms and measure porosity parameters, such as pore size distributions. Average porosity was found to be a poor indicator of tablet structure for DCL 11 and DCL 14 tablets. Pore size (measured by 2D pore area and volume-weighted pore diameter) decreased with increasing compaction force, but the range of measurement depends on scanning resolution. No effect of compaction speed on microstructure was observed.

Acknowledgements

References

Hancock B.C.; Mullarney M.P. *Pharm.Tech.* April **2005**, 92-100

Hildebrand T.; Ruegsegger P. *J. Microsc.* **1997**, *185*, 67-75

Pal N.R.; Pal S.K. *Pattern Recogn.* **1993**, *26(9)*, 1277-1294

SkyScan, www.skyscan.be, accessed June **2007**(a)

SkyScan, *Structural Parameters measured by the SkyScan™ CT-analyzer software*, SkyScan N.V., Artselaar, Belgium **2007b**

Xiaowei F.; Elliot J.A.; Bentham A.C.; Hancock B.C.; Cameron R.E. *Part. Part. Syst. Charact.* **2006a,** *23*, 229-236

Xiaowei F.; Dutt M.; Bentham A.C.; Hancock B.C.; Cameron R.E.; Elliot J.A. *Powder Tech.* **2006b,** *167*, 134-140

III.C: Tablet Defect Detection

Introduction

Internal defects can form in tablets during the compaction process. Two of the most common tablet defects are lamination and capping. Capping is the detachment of a convex portion of a (usually biconvex) tablet during ejection, usually from the top face of the tablet (Figure 53(a)). Lamination (Figure 53(b)) is defined varyingly as the splitting of a tablet into two or more laminar layers, parallel to the punch face, with or without detachment of fragments (Au et al, 2004). In each case, cracks are initiated at the perimeter of the tablet and propagate radially inwards. These problems are often encountered during scale up of tablet compaction, particularly as compaction (and de-compression) speeds are increased.

(a) Lamination   **(b) Capping**
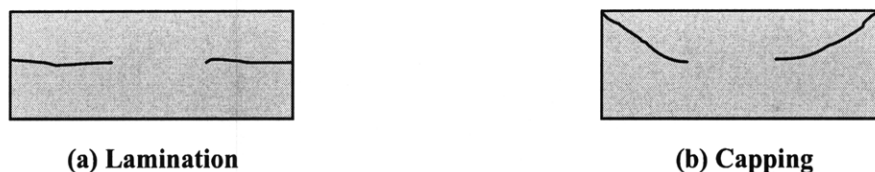
Figure 53: Common tablet defects (shown for cylindrical tablet geometry)

Two common explanations for these defects are (Kuppuswamy et al, 2001):

1) entrapment of air during the compaction

2) the build up of anisotropic stresses during uniaxial compaction, such that there is considerable residual radial stress, which is released during ejection, causing lateral cracking (Sugimori et al, 1989)

It has been observed that materials that consolidate by powder particle fracture have a greater tendency to capping and lamination than materials that undergo plastic deformation. This suggests that explanation (2) is the most likely cause of defects, as plastic materials will tend to reduce the tendency for cracking. Also, consolidation by fracture tends to cause greater stress anisotropy in the compact due to the presence of a compact zone propagating from the moving punch face.

Little effort has been made to characterize the capping and lamination patterns, beyond a qualitative description (capping: cracks propagate from top edge of tablet to bottom center, creating a biconvex cap (Wu et al, 2005), lamination: cracks parallel to punch

(Kuppuswamy et al, 2001). This is presumably because it is the presence or absence of defects that is the most important, in terms of quality control and process design. Even small cracks at the tablet edge will lead to chipping and wear and are therefore undesirable. Therefore most experimental work, such as that by Au et al (2004) present results in a binary format- the presence or absence of detectable defects.

Terahertz pulsed imaging is a nondestructive analysis tool which generates and detects ultra-short pulses of THz radiation (0.6-3.6THz, or 2-120cm^{-1}). The THz electric field-versus-time profile is obtained at a point on the sample. The time delay associated with receiving the reflected signal is used to measure film thicknesses, or the depth of embedded objects or defects. The intensity of the reflected signal will depend on the difference in refractive index between the two materials at the interface (Figure 54). A robotic arm can be used to move the sample in multiple axes for sampling and a 3D image of the sample can be constructed from this data (TeraView, 2007). Therefore, this technique can be used to measure film thicknesses, or detect embedded objects. It should therefore also detect cracks in tablets.

The technique operates much the same way as ultrasound or radar is used to locate embedded or distant objects, and the sample itself is unaffected by the measurement.
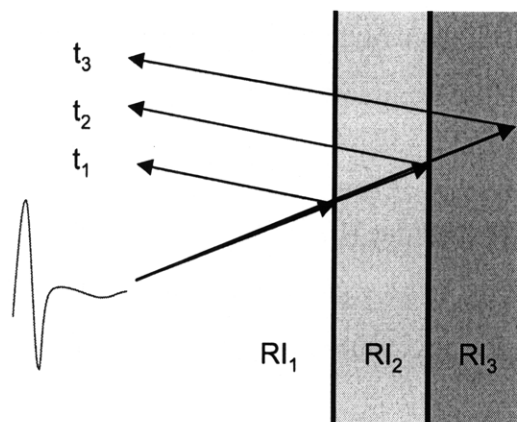
Figure 54: Principle of THz pulsed imaging. RI$_n$ indicates the refractive index of the different layers and t$_n$ indicates the signal reflection time from the corresponding interfaces.

Objectives

The objective of this study was to test whether THz pulsed imaging could detect internal tablet defects. The presence of defects was confirmed by X ray micro CT imaging.

Method

Sample preparation

MCC Celphere® and Pharmatose® DCL 11 powders were sieved to obtain the sieve fraction 106-212 microns. The powders were stored over saturated magnesium nitrate solution (at 55% relative humidity) for a minimum of 10 hours before compaction. Powder beds of depth 4mm were compacted at constant upper punch speed (0.5, 5 or 50 mm/min) and to a range of final compaction forces (5-75kN). This corresponded to 430 ± 10 mg MCC and 350 ± 10 mg lactose. Flat-faced punches were used with a 12.7mm diameter punch. An Instron 4260 mechanical tester was used to compact the tablets. Tablets were then stored at 55% relative humidity for a minimum of 72 hours before testing. Two sets of tablets were made under the same conditions: one for the THz and one for the Xray study.

THz Imaging

A TPI imaga 2000 machine (TeraView Ltd., Cambridge, UK) was used to scan the tablets in triplicate. A central area of diameter 10mm was scanned point-by-point with 0.2mm spacing. Images were taken from both tablet faces to ensure that the full depth of the tablet was probed. The tablets were scanned within 3 weeks of manufacture.
The intensity-time data was de-convoluted and a 3-D image of the tablet section was constructed using custom TPicsView software.

X ray microCT

A SkyScan™ 1172 microCT machine (SkyScan N.V., Artselaar, Belgium) was used to scan tablets. The reconstructed cross sections were created using NRecon software from SkyScan™. The scanning and reconstruction parameters are presented in Table 12.

Table 12: X ray microCT scanning and reconstruction parameters for whole tablets

Scanning (SkyScan 1172)	
Beam voltage	40kV
Beam current	250 µA
Sample total rotation	180°
Rotation degree	0.3°
Exposure time	1178 ms
Frame average	4
Random movement correction	20
Pixel linear dimension	3.54 µm
Camera make and model	Hamamatsu 10Mp camera
Camera resolution	2096 x 4000 pixels
Filter	0.5 mm Al
Flat field	Gathered prior to each scan. Frame average for flat field = 4
Median filter	ON
Reconstruction (NRecon v1.4.4)	
Image post alignment	Automatic
Beam hardening correction factor	0
Ring artifact correction factor	10
Cross section intensity limits	Automatic
Voxel dimension (isotropic cube)	3.54 µm

Results

No interfaces were observed in microcrystalline cellulose tablets (Figure 55) or in lactose tablets compacted to 20kN (Figure 56). The images in Table 13 show that lactose tablets compacted to 40kN have a narrow interface along the rim of some tablets. For higher forces, larger, crescent-shaped areas of interfaces were seen. The cracks appear to penetrate further into the tablet and become wider. The effect of speed is inconclusive. For example at 40kN, tablet compacted at 0.5mm/min appear more cracked than those at 5mm/min, however at 60kN, higher speed corresponds to more cracking.
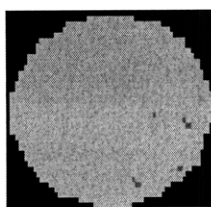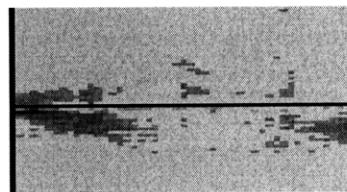
(a) Axial cross section   (b) Diametral cross section

Figure 55: TPI images of MCC tablet compacted to 72kN at 50mm/min

Table 13: TPI cross section images of DCL 11 tablets (scale indicates THz signal in a.u.) showing most extensive defects

Compaction conditions	Tablet A	Tablet B	Tablet C
20kN 5mm/min			
28kN 50 mm/min			
40kN 0.5mm/min			
40kN 5 mm/min			
52 kN 50mm/min			
60kN 0.5mm/min			
60kN 5mm/min			
72kN 50mm/min			
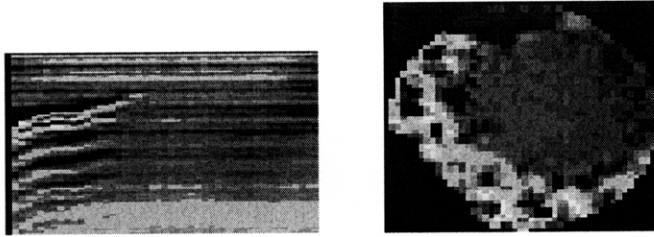
Figure 56: Diametral and axial cross sections of lactose DCL 11 tablet compacted to 60kN at 5mm/min (Tablet B)

X ray micro CT imaging also found no evidence of cracking of MCC tablets (Figure 57). An example of MCC tablet cross section is presented in Figure 57. DCL 11 tablets show evidence of cracking for all compaction conditions (Table 14). The cracks appear to propagate from the sides of the tablet towards the center and extent of cracking increases with increasing compaction force. The crescent feature observed with TPI is found her as well, but mostly for lower forces. At higher forces, the tablets appear to have more extensive cracking when imaged with X ray, rather than TPI.

The whole tablet is imaged with this technique, so a full diametral cross section can be seen (Figure 58). This shows that lamination is occurring. Cracks are propagating from the sides of the tablet inwards. The cracks appear to be closer to one tablet face than the other.
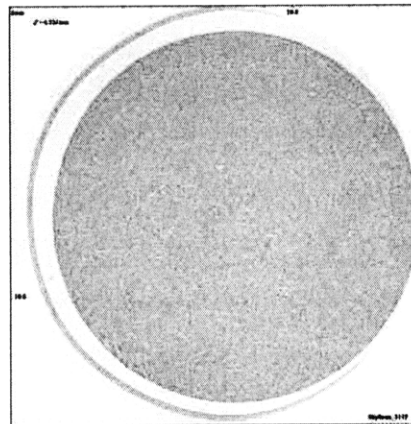
Figure 57: Cross section of MCC tablet compacted to 60kN at 5mm/min
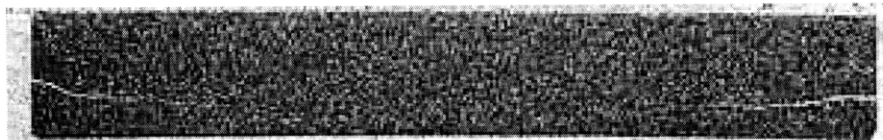
Figure 58: Diametral cross section of DCL 11 tablets

Table 14: X ray micro CT cross section images of DCL 11 tablets, showing most extensive defects

Compaction conditions	Tablet A	Tablet B	Tablet C
20 kN 0.5mm/min			
20kN 5mm/min			
28kN 50mm/min			
40kN 0.5mm/min			
40kN 5mm/min			
52kN 50mm/min			
60kN 0.5mm/min			
60kN 5mm/min			
72kN 50mm/min			

Discussion

No cracking was observed for MCC tablets with both imaging techniques. This is consistent with previous literature, which states that materials that deform plastically have a lower tendency to tablet defects than those that consolidate by fracture.

As the entire tablet was not scanned for the THz images (the outer rim was not scanned), it is not certain whether the cracks are initiated at the top edge towards the center of the tablet (capping) or along the cross section (lamination). However, from the X ray images we are able to see that in fact, the cracks are due to lamination and that the cracks do become wider and larger with increasing force.

Both sets of images indicate that the extent of cracking increases with increasing compaction force. There is no apparent trend with compaction speed. The observed 'crescent' fracture shape is likely due to poor alignment of the die, punches or the compaction machine, causing higher pressure on one side of the tablet than the other. More extensive cracking was observed in the X ray images than in the TPI images. This could have been due to differences in the imaging techniques, but it could also have been due to the different sample sets. Although all efforts were made to duplicate the tablet compaction conditions, it is possible that differences in environmental conditions during material storage or tablet compaction led to different fracture patterns.

It is not possible to extract data about the detection capability of TPI relative to Xray micro CT, as the sample sets for the two techniques were different. The purpose of the comparison presented here was to qualitatively observe the fracture patterns detected by the two techniques. A comparison of TPI and X ray micro CT is presented in chapter III.D.

Conclusions

Terahertz pulsed imaging can be used to detect internal cracks tablets. Fracture patterns were confirmed, by X ray micro CT images, to be due to tablet lamination. The extent of cracking was found to increase with increasing compaction force, but there was no apparent trend with compaction speed. TPI is a faster and less data-intensive method for detecting tablet defects than X ray micro CT, however, more studies are required to determine the resolution and limits of detection of the technique.

Acknowledgements

References

Au Y.H. J.; Eissa S.; Jones B.E. *Ultrasonics* **2004**, *42* , 149–153

Kuppuswamy R.; Anderson S.R.; Augsburger L.L.; Hoag, S.W. *AAPS Pharm. Sci.* **2001**, *3 (1)*

TeraView www.teraview.co.uk, accessed April 5, **2007**

Wu C.Y.; Ruddy O.M.; Bentham A.C.; Hancock B.C.; Best S.M.; Elliott J.A. *Powder Tech.* **2005**, *152*, 107-117

SkyScan www.skyscan.be, accessed April 5, **2007**

Sugimori K.; Mori S.; Kawashima Y. *Powder Technol.* **1989**. *58 (4), 259-264*

III.D: Comparison of Analytical Techniques

Various methods for probing the physical properties of the tablet core were presented in chapters III.A-III.C. Terahertz pulsed spectroscopy (III.A) and X ray micro CT (III.B) were used to analyze the microstructural characteristics of the tablet core, either directly (X ray) or through a correlation with tablet hardness (TPS). The first part of this chapter discusses how TPS compares to NIR spectroscopy; currently the only other non-destructive spectroscopic technique for assessing tablet hardness. The second part compares some of the practical issues of TPS and X ray micro CT, and the relative value of the generated data is discussed. It must be noted that some of the practical issues may be resolved by development of the technologies, as both THz and X ray microCT devices have become available as lab instruments fairly recently. Therefore the technology is still evolving at considerable speed.

In chapter III.C, a comparison was made between Terahertz pulsed imaging (TPI) and X ray micro CT in their ability to map tablet defects. A comparison of these imaging techniques and areas for future work are presented in the final part of this chapter.

Assessing microstructure: NIR diffuse reflectance spectroscopy and Terahertz pulsed transmission spectroscopy

Near Infra-Red (NIR) spectroscopy is gaining in popularity as a non-destructive analytical tool for the pharmaceutical industry. It is known to be sensitive to both the physical structure and the chemical composition of pharmaceutical solids. Much of the NIR literature in the pharmaceutical field discusses its capability to identify or quantitatively characterize the chemical composition of tablets or powders. It can also be used to produce spatially resolved maps of chemical components. Reviews of pharmaceutical applications for NIR have been published by Kirsch and Drennen (1995), Blanco et al (1998), Reich (2005). NIR in diffuse reflectance mode has been used to study tablet hardness (Morrisseau and Rhodes, 1997, Ebube et al 1999, Donoso et al, 2003, Cogdill et al, 2004, Blanco and Alcala, 2006). NIR spectroscopy can also be used in transmission mode to investigate hardness, but this technique has not been used extensively (Reich, 2000, 2005).

An overview of Terahertz pulsed spectroscopy (TPS) technology and its pharmaceutical applications has been presented in part III.A.

Both TPS and NIR methods have the advantage of being fast (a few seconds) and non-destructive. It is likely that there is no general correlation between spectroscopic measurement and tablet hardness for all materials, particularly as the relationship between spectroscopic data and physico-chemical properties is poorly understood for both methods. Therefore, both methods will require some sort of calibration for a new formulation (Morrisseau and Rhodes, 1997). However, there are some particular differences that indicate that TPS may have an advantage over NIR as a rapid, non-destructive analytical technique.

1. NIR diffuse reflectance spectroscopy only probes a short distance into the tablet whereas THz examines the entire thickness at one point. Therefore a greater volume of the tablet is sampled and the measurement reflects properties of the core. This issue could be resolved by using NIR in transmission mode (Reich, 2000, 2005).

2. NIR spectra show an increase in absorbance with increased tablet hardness. However, the spectral shift is baseline-dependent (Figure 59) hence the data is usually analyzed using multilinear and partial least squares regression on the second derivative of the absorption spectrum.

Multivariate data analysis may not be necessary for TPS data, as the shift in RI does not appear to depend on the wavelength, unlike NIR.

3. The measured reflected NIR signal is somewhat arbitrary and known to be affected by surface roughness (which causes diffusion), particle size and experimental configuration e.g. beam length. THz spectrometry is performed in transmission mode, so surface morphology has a less pronounced effect. Also, the measured quantity is the refractive index; an inherent property of the material, rather than a reflected beam spectrum which depends on the equipment configuration.

NTR Spectra of Theophylline Tablets at Seven Hardness Levels
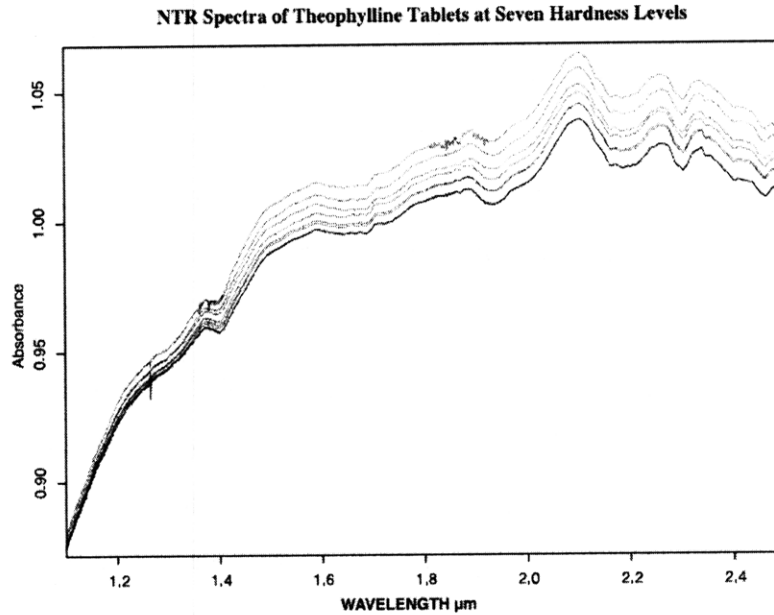
Figure 59: NIR spectra show a wavelength dependent shift with tablet hardness (Source: Donoso et al, 2003)

Assessing microstructure: X ray micro computed tomography (micro CT) and Terahertz pulsed transmission spectroscopy (TPS)

As described in chapter III.B, X ray micro CT can be used to obtained detailed, three-dimensional data about the structure of tablets. Both THz and X ray micro CT are relatively new, non-destructive techniques for probing the tablet core. Neither technique requires any sample preparation and can be performed with commercial, off-the-shelf instruments.

In order to obtain high-resolution images by microCT, it is not possible to scan a whole tablet due to equipment and data constraints. In effect, it becomes a destructive technique as a fragment of the tablet must be broken off for scanning. X ray data is able to give us much more insight into the physical structure of the tablet. Instruments are now available capable of resolutions on a sub-micron scale. However, this data comes at high costs in terms of time and computation. Scans can take between 40 mins to a couple of days and raw data sets for a single sample are typically on the order of 1-20GB. Furthermore, the data requires multiple steps of processing before it can be analyzed, which increases the computational and memory burden.

TPS scans, on the other hand, take a matter of seconds and the data is easily manipulated by a standard PC. It is possible to obtain 2-D spatial information by using robotics to

manipulate the sample and scan it at different points. Trends have been observed in the data, but it is, as yet, unclear what its physical significance is.

Although TPS may have a place as a development or quality control tool, the current level of understanding is insufficient to allow any insight into the tablet physics. Therefore, it is recommended that X ray microCT should be used for studies into the physical structure of tablets.

Detecting tablet defects: Terahertz pulsed imaging (TPI) and X ray micro CT

In order to consider whether TPI is a useful tool for defect detection, the purpose of detection must be determined. If the purpose is simply to determine the presence or absence of defects, the data from this experiment suggest that TPI is sufficient and has considerable time advantages over X ray micro CT. However, further studies are required to determine the maximum acceptable defect size and assess whether the accuracy and sensitivity of TPI is sufficient. The resolution of the TPI method is limited by the fact that scanning is performed in a point-by-point fashion, whereas for X ray micro CT resolution can be varied continuously, down to sub-micron levels.

The time required for data collection and processing varied significantly between TPI and X ray for whole tablet scans. A single tablet scan with the THz imager took approximately 25 minutes and de-convolution and reconstruction of the 3D image took a few seconds on a 2.66GHz processor speed PC.

A single tablet scan with the Xray microCT took approximately 90 minutes and the reconstruction took about 7 hours on the same PC. Lower scanning and computational times are possible, but this will likely require considerable trial and error and may compromise image quality.

Conclusions

While neither TPS nor NIR give detailed morphological information about the tablet microstructure, both spectroscopic signals indicate changing tablet hardness. TPS has some advantages over NIR in terms of the sampling and data analysis. Some of these advantages arise because TPS was carried out in transmission mode, rather than reflectance (the common mode for NIR).

As yet, the physical significance of shifts in TPS spectra is unknown. Therefore, although TPS offers several advantages in terms of time for data collection and processing, X ray micro CT is recommended for future studies of tablet microstructure.

TPI is a much faster and less data-intensive technique for tablet defect detection than X ray micro CT. However, further studies are required to do a quantitative assessment of the resolution and limits of detection of TPI systems.

References

Blanco M.; Coello J.; Itirriaga H.; Maspoch S.; De la Pezuela C. *Analyst* **1998**, *123*, 135R-150R

Blanco M.; Alcala M. *Anal. Chim. Acta* **2006**, *557*, 353-359

Clark F. *Vib. Spectrosc.* **2004**, *34*, 25-35

Cogdill R.P.; Anderson C.A.; Delgado M.; Chisholm R.; Bolton R.; Herkert T.; Afnan A.M.; Drennen J.K. *AAPS Pharm. Sci. Tech.* **2005**, *6(2)*, 38

Donoso M.; Kildsig D.O.; Ghalyn E.S.; *Pharm. Dev. Tech.* **2003**, *8 (4)*, 357-366

Ebube N.K.; Thosar S.S.; Roberts R.A.; Kemper M.S.; Rubinovitz R.; Martin D.L.; Reier G.E.; Wheatley T.A.; Shukla A.J. *Pharm. Dev. Tech.* **1999**, *4(1)*, 19-26

Kirsch J.D.; Drennen J.K., *Appl. Spectrosc. Rev.* **1995**, *38*, 139-174

Morrisseau K.M.; Rhodes C.T. *Pharm. Res.* **1997**, *14(1)*, 108-111

Reich G. *Proc. 3rd World Meeting APV/APGI, Berlin 3/6* **2000**, 105-6

Reich G. *Adv. Drug Deliver. Rev.* **2005**, *57*, 1109-1143

Part IV: Implications for Design

A systematic strategy for the design of pharmaceutical tablets is presented and the scope of the thesis within the design framework is highlighted (IV.A). Two aspects of design were considered for the tablet compaction step: the formulation and the process. The results of these investigations are presented in chapters IV.B and IV.C.

The single granule compression test can be used to measure the mechanical properties of commercial excipient powders (MCC Celphere®, Pharmatose DCL 11 and DCL 14). The granule failure mechanisms were consistent with features of the tablets, as observed by X ray micro CT, confirming the link between granule mechanical properties and tablet microstructure. However, quantitative differences in fracture parameters of DCL 11 and DCL 14 had no effect on tablet structure. The qualitative features of the X ray scans explained trends observed in tablet hardness and dissolution. Compaction force was found to affect tablet microstructure and hence hardness and dissolution. Hardness was found to be linked to structural parameters, but tablet structure alone was not sufficient to predict differences in dissolution between DCL 11 and 14. This suggests that additional characterization methods are necessary.

Further work is recommended to

1) Study a greater range of pharmaceutical materials

2) Further develop experimental techniques for application in pharmaceutical R&D

3) Build a process model for compaction that can be used for process and product design

4) Develop quality criteria for tablet performance

IV.A: Product and Process Design Overview

Design methodology

The chemical product design methodology, as outlined by Cussler and Moggridge (2001), starts with a problem statement based on customer needs. Ideas are generated to fulfill these needs and one of these ideas is selected for further development. Simultaneous product and process design is then carried out to design the manufacturing process. Heuristics-based approaches for pharmaceutical dosage forms are presented by Fung and Ng (2003) and Hardy and Cook (2003).

This thesis deals with the final step in this process. Tablets are an established form of drug delivery that fall in the category of 'structured chemical products': multi-component, multi-phase products, whose performance depends on both their chemical composition and their physical structure. Design approaches for such products were presented by Cussler and Moggridge (2001) and developed further by Hill (2004, 2005) and Gani et al. (2007).

One key difference between this approach and traditional chemical process design is that the chemical identity of the product is not known at the start of the design process. Instead there is a performance target for the final product, which is achieved by a combination of chemical composition and physical structure (Figure 60).

Raw material Inputs (Formula) ⟺ **Process** ⟺ **Structure** ⟺ **Performance**
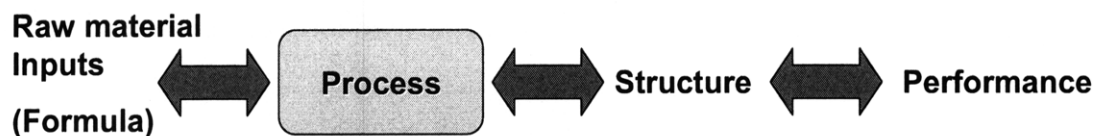
Figure 60: Design approach for structured products (adapted from Hill, 2005)

The process itself is often a key factor in achieving the desired performance, as structure is often dependent on processing history (Hill, 2005). Performance is usually assessed by the application process: quality indicators may be quantitative (dissolution time of a tablet) or subjective ('feel' of icecream in the mouth), therefore design is an iterative process.

Gani et al (2007) identify three classes of approaches to solve this design problem:

assessments of performance. Hardness is used as an indicator of the physical stability of the tablet core in coating, handling and transportation. The dissolution test is an in-vitro indicator for bioavailability, the primary performance indicator for pharmaceutical products. Therefore, although the tests are of importance from a regulatory and industrial perspective, developing predictive capability for hardness and dissolution was not a focus of research for this work.

Instead, the focus was on identifying techniques for characterizing the microstructure (length scale of 1-100microns), an area that has received little interest to date, and investigating how microstructure is affected by the formulation and the process. Correlative connections were made between microstructure and tablet performance.

Degrees of Freedom in Tablet Compaction Design

There are two main areas for design: the formulation and the process. For a structured product, the two are not independent, as the structure will be a result of both the chemical components and the history of their processing (Hill, 2005). In order to predict this combined effect, a process model is required that allows formulation and process parameters to be independent inputs and that gives the product structural parameters as outputs. The development of a process model for compaction was not part of this thesis, but is discussed in chapter IV.D.

<u>Formulation</u>

Tablet cores consist of a mixture of active ingredient (API) and excipients. In this study, only the effect of filler/binder excipients was investigated. These are usually bought from external vendors and come in powder form. Therefore, formulation parameters include not only chemical, but physical specifications of the materials.

The requirements for the filler/binder are:

- o It should be chemically compatible with the API e.g. chemically inert, moisture content etc.
- o The powder mixture should be stable and not segregate during pre-compaction processing
- o The powder mixture should create a physically stable tablet upon compaction

Only specifications relating to compactibility of the tablet are considered here.

1) Experiment-based trial and error: This approach is used when mathematical models for the properties are not available. The extent of experimentation limits the number of alternatives that can be investigated, so design is based on past knowledge and experience (this is common in the pharmaceutical industry today). Databases of materials may be used to generate candidates for experimentation. This is a highly labor- and material-intensive approach and may involve a lot of iteration in the design process.

2) Model-based search techniques: This approach requires validated mathematical models for estimation of the desired properties and to evaluate performance (Figure 61).

3) Hybrid experiment-model based techniques: If models are not available for all the desired properties or for performance evaluation, then mathematical models can be used to generate a small pool of candidates for further experimentation.

Therefore, for the design process to be less time and material-intensive, models are required to predict the product properties (e.g. the structure) and performance.
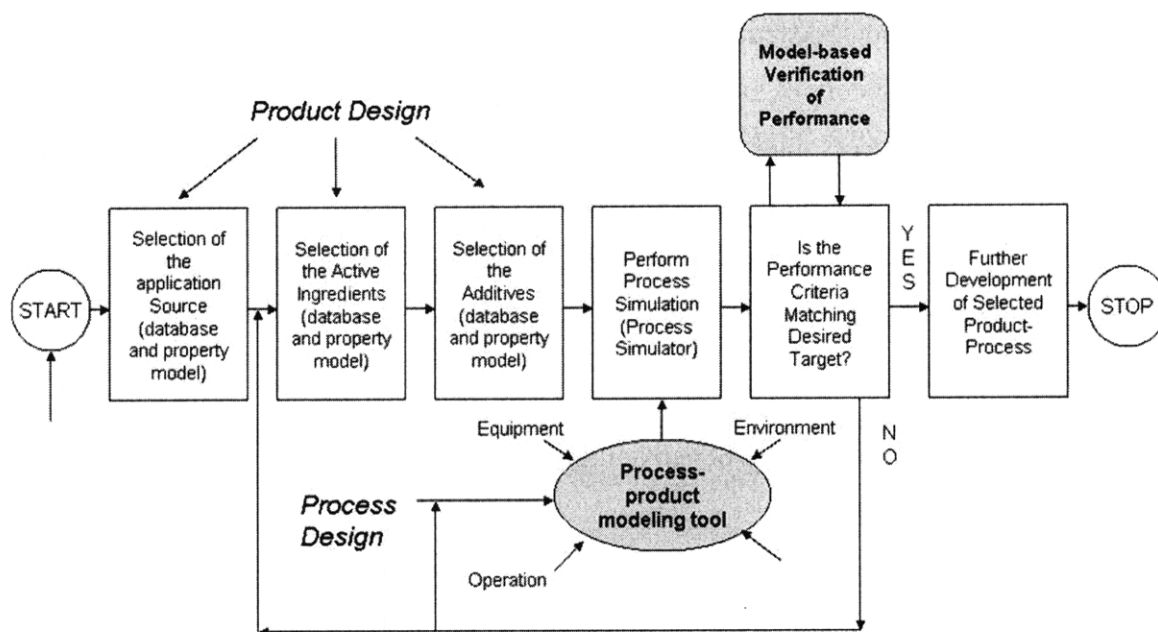
Figure 61: Model-based framework for systematic product-process design and development (Adapted from: Gani et al, 2007)

In this study, two common indicators of tablet performance were selected: mechanical strength (commonly termed 'hardness') and dissolution times, as measured by the USP tests. As discussed in Part II, there are no models to predict tablet performance in standard tests and there is insufficient understanding of which tablet properties contribute to hardness and dissolution. The tests themselves are used as quick laboratory

Currently, some of the specifications for excipient powders are:

- o Chemical composition
- o Polymorph (crystalline form) composition
- o Particle size (usually defined as a range)
- o Particle shape

These physico-chemical properties of the powder are not sufficient to predict the mechanical behavior of the powder bed during the compaction process. Therefore, the mechanical properties of powders were investigated and the results are linked to tablet structure and performance (chapter IV.B).

Process Flow Sheet Design

The manufacture of tablets from its raw material powders is most commonly performed as a wet-granulation process. This consists of multiple blending steps, as well as shear granulation, milling and fluid-bed drying. In this study, the compaction step itself is of interest, as it creates the tablet microstructure. Therefore a direct compression process was selected. This is the simplest and most cost-effective process at the manufacturing scale, so is desirable, but not often implemented. Most of the tablets in this study had only one component and could be compacted directly. For the dissolution studies, a blending step preceded compaction.

Tablet compaction is performed as a semi-continuous operation in the pharmaceutical industry. The powder hopper-filling is performed in batch mode, but the rotary press works in continuous mode. The operation is scaled by time, rather than volume, so the learnings of this work are applicable to a batch or a continuous system.

Unit Operation Design

Degrees of freedom in process design of a unit operation include:

- o Equipment geometry
- o Environmental conditions for materials and process
- o Operational parameters

In this study, the unit operation considered was the tablet compaction step. Equipment geometry was kept constant; flat punches were used to obtain cylindrical tablets. The die radius was kept constant at 12.7mm and a fixed volume of powder (4mm bed depth) was

used for all tablets. As the physical properties (size distribution, shape, density) are similar, it was assumed that their packing properties would be similar. Therefore a given volume would contain approximately the same number of granules.

The environmental conditions were controlled as far as possible, by storing the powders and tablets at 55% relative humidity during sample preparation and testing, and in air-tight containers during transportation. However, humidity was not controlled during powder storage. This may have resulted in changes over time.

Compaction cycles in commercial manufacturing equipment may be quite complex, due to the rotary press configuration and pre-compression steps (Fette, Natoli, MCC, 2007). For the purposes of this study, an Instron 4206 mechanical testing apparatus was used to create a simple compaction cycle. The powder bed was simply loaded at constant speed (varied between 0.5, 5 and 50mm/min), to a specified force, and unloaded at constant speed (kept constant at 0.5mm/min). Therefore, the only two operational parameters that were varied were the compaction speed and the final force of compaction (in the range of 5-75kN). The effects of these variables are discussed in chapter IV.C.

Acknowledgements

References

Cussler E.L.; Moggridge G.D. *Chemical Product Design*, Cambridge University Press, **2001**

Fette, *www.fette.com*, accessed **July 2007**, Fette GmbH

Fung K.Y.; Ng K.M *AIChE J.* **2003**, *49 (5),* 1193

Gani R.; Dam-Johansen K.; Ng K.M. in *Chemical Product Design: Toward a Perspective through Case Studies*, Elsevier, **2007**

Hardy I.J.; Cook W.G. *J. Pharm. Pharmacol.* **2003**, *55 (3)*

Hill M., *AIChE Journal*, **2004**, 50 (8)

Hill M., *Presentation at Process Systems and Engineering Consortium Meeting, Amherst, MA,* **October 14, 2005**

Natoli, *www.natoli.com,* accessed **July 2007**, Natoli Inc.

MCC, *www.mcc-online.com,* Metropolitan Computing Corporation, accessed **2007**

IV.B Formulation Design

Introduction

Three different excipient powders were investigated: microcrystalline cellulose (MCC) Celphere® CP102 and two grades of spray-dried lactose: Pharmatose® DCL 11 and DCL 14. MCC and lactose are two commonly used excipients for direct compression and the grades were selected for the similarity of their shape and size (see chapter I.A).

Part I describes physical and mechanical characterization of the powders. As described in chapter IV.A, mechanical characteristics of powders do not currently form part of the raw material specifications, yet are very important in tablet compaction. The aim was to test individual granules to:

- o Understand the mechanism of compaction for different materials and how it affects tablet structure and performance
- o Characterize the materials using parameters that are independent of compaction equipment
- o Obtain parameters that could be used as inputs for a compaction process model to predict microstructure (this is discussed in chapter IV.D)

Effect of granule mechanics on tablet structure

The single granule mechanical tests indicate that MCC granules are tough and ductile, whereas lactose granules fracture when loaded (chapter I.B). The microstructures of MCC and lactose tablets, as viewed by X ray micro CT (chapter III.B), are consistent with the single granule crushing results. MCC granules were found to be tough and yield, which is consistent with the plastic deformation observed in tablets (Figure 62). DCL 11 and 14 granules were both found to collapse when a load was applied. This is consistent with the observation that there is no evidence of granule shape or size in the monolithic structure of the compacted tablet (Figure 62).
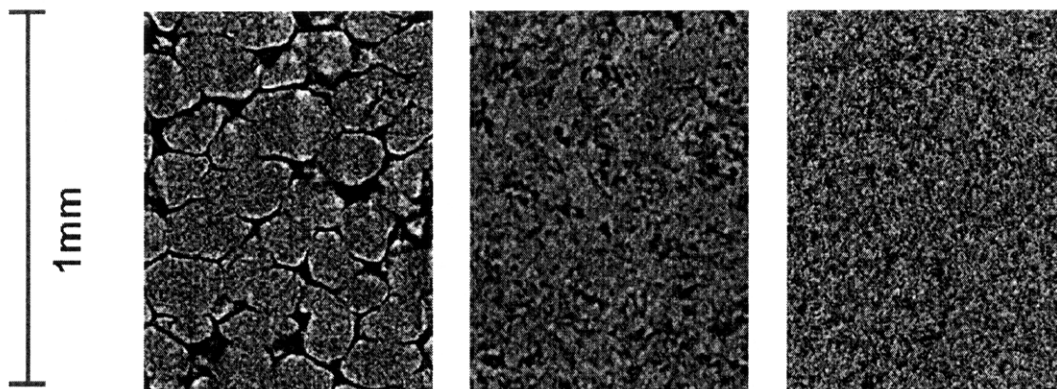
Figure 62: Tablets compacted to 19kN at 0.5mm/min (left to right) (a) MCC, (b) DCL 11, (c) DCL 14

The quantitative comparison between DCL 11 and DCL 14 showed that the difference in mechanical properties of the two grades of lactose is not reflected in the tablet structure. DCL 11 was found to consist of stronger granules than DCL 14 (Table 15), but the pore diameter distribution was the same for tablets made of the two materials (Figure 63). It is likely that the observed difference in mechanical properties (when tested to a few mN) was too small to be significant after compaction (to loads of several kN). Terahertz pulsed spectroscopy also shows no difference between compacts made of the two materials. This suggests that the composition of amorphous and α-monohydrate lactose is the same for both grades (see chapter III.A for details).

Table 15: Comparison of fracture toughness of DCL 11 and DCL 14 tested at 10mN/s

		DCL 11	DCL 14
Fracture load	Median (X_{50})	48.88 mN	18.71 mN
	Standard deviation $(X_{84}/X_{16})^{1/2}$	1.32	1.72
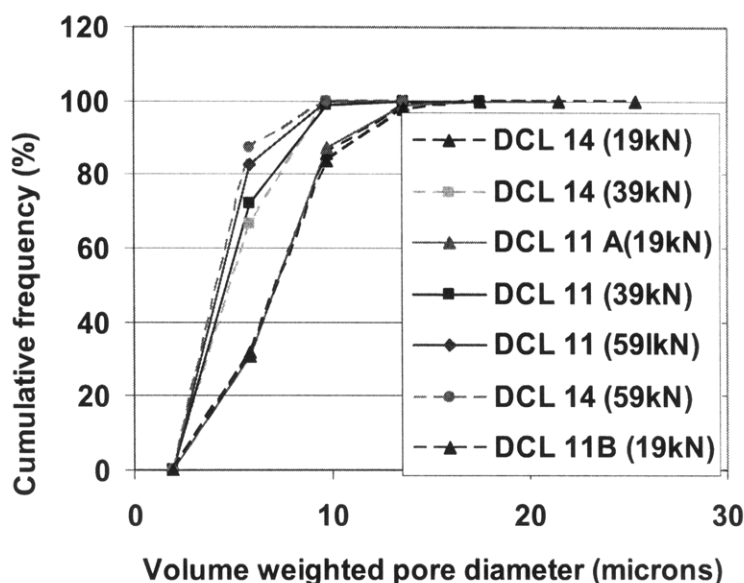
Figure 63: DCL 11 and DCL 14 tablets have same pore size distribution

Effect of tablet structure on performance

The single granule tests and the X ray images can be used to explain differences in hardness and dissolution between MCC and lactose tablets. DCL 11 was found to form stronger tablets than MCC (Figure 64). The fracture of DCL 11 granules will generate smaller particles which will allow for denser packing and hence greater bonding area and stronger tablets.
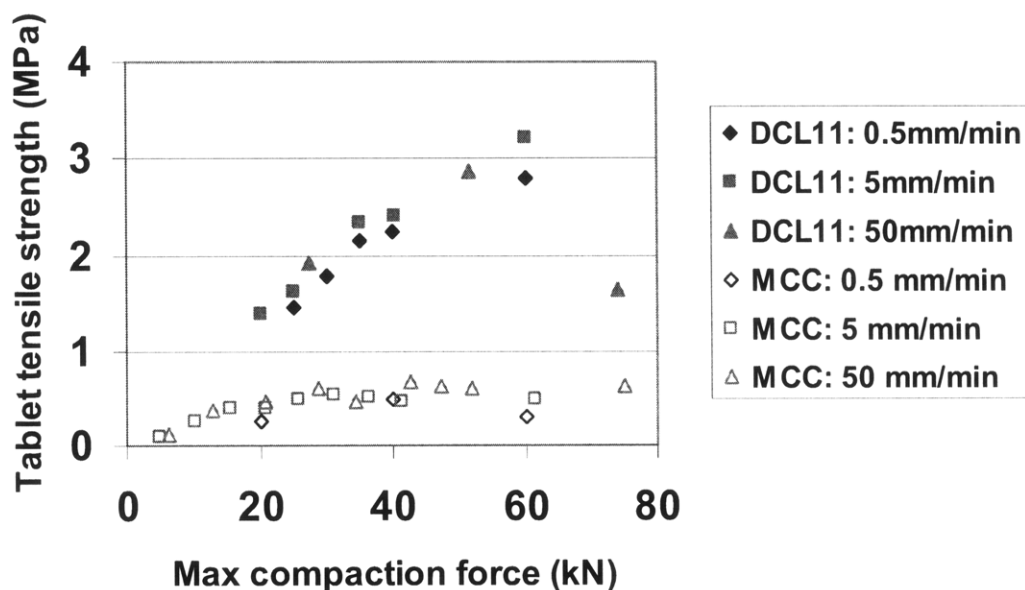
Figure 64: Tensile strength of MCC and DCL 11 tablets

The MCC powder bed contains larger pores between the granules which must be filled by plastic deformation and flow. The granule boundaries and inter-granular pores are likely to remain planes of weakness in the structure, and cracks will propagate along these planes, resulting in relatively weak tablets. As the inter-granular pores close up, there will be an increase in tablet strength, but this reaches a maximum value after which incremental decreases in porosity will have little effect.

Lactose DCL11 granules typically fail at loads less than 100mN. The loads applied to the powder bed are in the order of kiloNewtons. Therefore, it is likely that most granules are fractured near the start of the compaction process. However, results indicate that intact tablets are not formed at loads less than 20kN. It is possible that the extra surface area created by fracture of lactose granules is not sufficient to generate enough binding to form a coherent tablet at low forces. This suggests that another consolidation mechanism (e.g. melting, plastic deformation) generates stronger binding between the powder particles at forces of 20kN and greater. This would also explain why DCL11 and DCL14 form tablets of equal strength (Figure 65), although the granules have different resistances to fracture (Table 15).
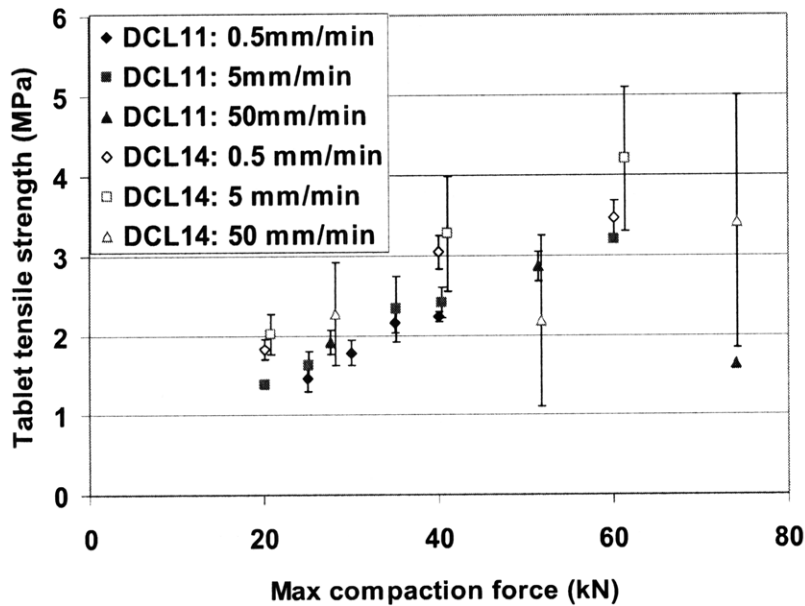
Figure 65: Lactose DCL11 and DCL 14 form tablets of equal strength

The X ray and TPS analysis showed DCL 11 and 14 to have the same structural characteristics, and tablet hardness is the same for the two materials. However, they were

found to differ in their dissolution behavior; DCL 14 tablets take up to four times as long to dissolve as DCL 11 tablets (Figure 66). Lactose tablets were found to be subject to lamination, which is believed to be the source of variation in the hardness and dissolution data. However, the difference in dissolution times is not believed to be due to lamination. If the tablets are cracked, they will break into fragments before dissolution. This would lead to discontinuities in the dissolution profile. However, all the individual dissolution profiles are smooth functions of time. The lactose tablets were observed to dissolve fully. Erosion of the lactose matrix is believed to be the rate-determining step in the dissolution process (see chapter II.B for details). The dissolution behavior of the two grades of lactose is believed to differ because of physico-chemical differences in the two materials. Although TPS found no difference, techniques such as X ray diffraction and DSC could be used to analyze the polymorphic composition of the two powders.
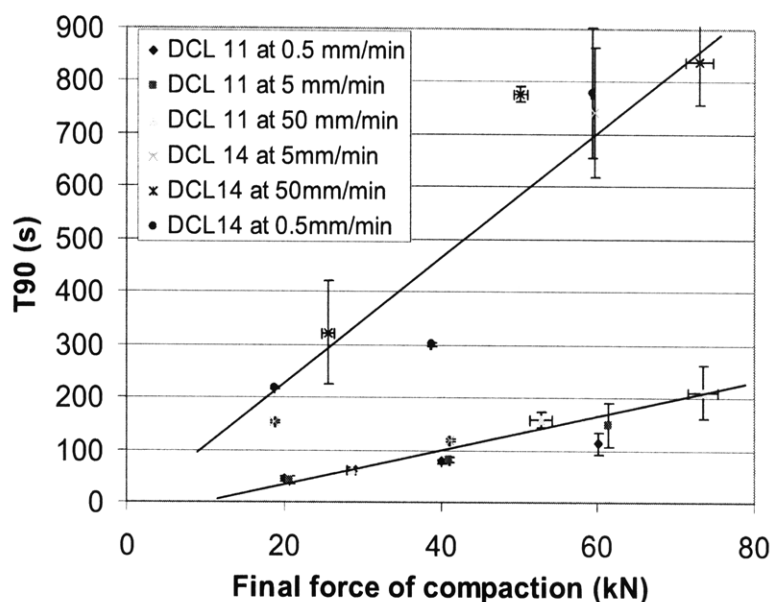
Figure 66: DCL14 tablets dissolve at slower rates than DCL 11 tablets

In contrast to the smooth dissolution profiles for lactose tablets, MCC tablets released their drug load in bursts. The X ray images show that MCC tablets have highly connected pores which would allow penetration of water throughout the tablet, causing it to disintegrate rapidly. MCC is insoluble in water, so drug release occurs by disintegration, not dissolution of the excipient matrix.

DCL 11 and 14 varied in their mechanical properties, but produced tablets with similar pore size distributions. Structural characterization techniques (X ray and TPS) did not

predict any difference between DCL 11 and DCL 14 grades, yet their dissolution behaviors vary. Therefore the combination of techniques was not sufficient to capture variation in performance, and other techniques are necessary. TPS has been shown to have some success as a tool for identifying polymorphs and different hydrate forms (III.A), but it is not yet an established method. Therefore, techniques such as X ray diffraction and differential scanning calorimetry are suggested to identify the crystal structure and composition of the powders. It is possible that the crystalline form is affected by the high loading during compaction.

Conclusions

The single granule compression test can be used to measure the mechanical properties of commercial excipient powders. The consolidation mechanisms seen in the single granule tests are consistent with the microstructure of the tablets, as observed by X ray micro CT. The structural features of the tablets provide an explanation for the trends seen in tablet hardness and allow us to postulate mechanisms of dissolution. However, tablet structure alone was not sufficient to predict the difference in dissolution rates between DCL 11 and DCL 14. Therefore a more extensive set of characterization methods are required to predict dissolution. X ray diffraction and DSC techniques are suggested.

IV.C Process Design

Parts II and III presented the effects of compaction speed and force on tablet performance and structure. Compaction force was found to be the dominant effect for the experimental space investigated. The experimental ranges of force and speed were determined by the range within which intact tablets could be formed.

Effect of compaction speed

No effect of speed was observed on tablet hardness, dissolution, TPS spectra, or pore size for any of the materials investigated, and the effect of speed on tablet lamination for lactose tablets was inconclusive.

The range of speed investigated was narrow (0.5-50mm/min), mainly due to equipment limitations. The maximum speed for the Instron 4206 is 50mm/min, whereas rotary presses have ranges of 400- 2400 mm/sec (MCC, 2007). To achieve these speeds, a full-scale rotary press or a compaction simulator is needed (e.g. MCC, ESH, 2007).

The other factor that may limit the speed range is tablet lamination. This will depend on the compaction force and the tablet geometry selected. Lamination and capping are known to increase during scale-up, when de-compression speeds are increased (Wu, 2006), so this may be another limit on the range of speed. For this study, a cylindrical geometry was selected, as analytical equations could be used to calculate tensile strength and models for disintegration. However, it has been observed that punch geometry affects the shape and extent of capping and lamination (Wu, 2006). Therefore, one way of increasing the speed range, without creating tablet defects, would be to modify the geometry.

As well as experimental considerations, limitations of the process model may determine the compaction speed range for future work. For example, DEM models of powder compaction (see chapter IV.D) often assume pseudostatic loading, where the rate of punch movement is slow relative to the rate of particle re-arrangement (e.g. Hassanpour et al, 2003, Sheng et al, 2004). For experimental validation of these models, compaction must be performed at strain rates much lower than that of commercial equipment.

Effect of compaction force

For MCC tablets, the effect of force and speed was not assessed separately for tablet structure (results from chapter III.B are reproduced below). However, it was observed that the structure changed significantly within the range studied: there was plastic deformation of the granules, resulting in increasing consolidation as force and speed are increased (Figure 67). As consolidation occurs by plastic deformation and flow, it is likely that, as porosity decreases, increasing force leads to progressively less consolidation.
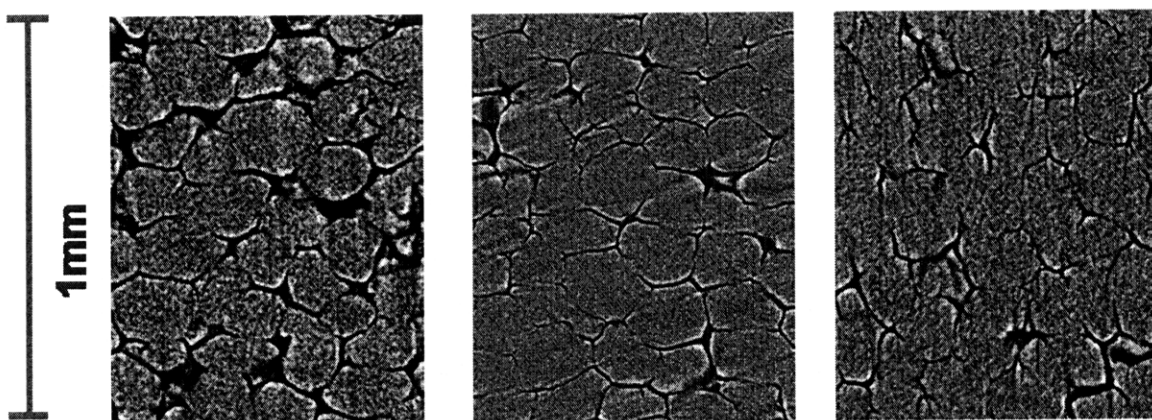
Figure 67: Grayscale cross-section of MCC tablets (from left to right), (a) 0.5mm/min 19kN, (b) 5mm/min 40kN, (c) 50mm/min 72kN

In the X ray images we see clear structural differences between tablets compacted at 19, 40 and 72kN, but when tablet hardness was measured (II.A), no significant changes were observed within the same force range (Figure 68). Similarly, there was no detectable difference in dissolution times (II.B), as all tablets disintegrated within 100s. The 'bursting' mechanism observed during dissolution suggests that there was penetration of water into the highly connected pores (Figure 67) which caused the rapid disintegration. This highly-connected pore network would also lead to planes of weakness, along which cracks could propagate during hardness testing. The X ray images indicate that even though these pores become narrower, the networks are still extensive. This is the likely cause for the limited strength of MCC tablets.
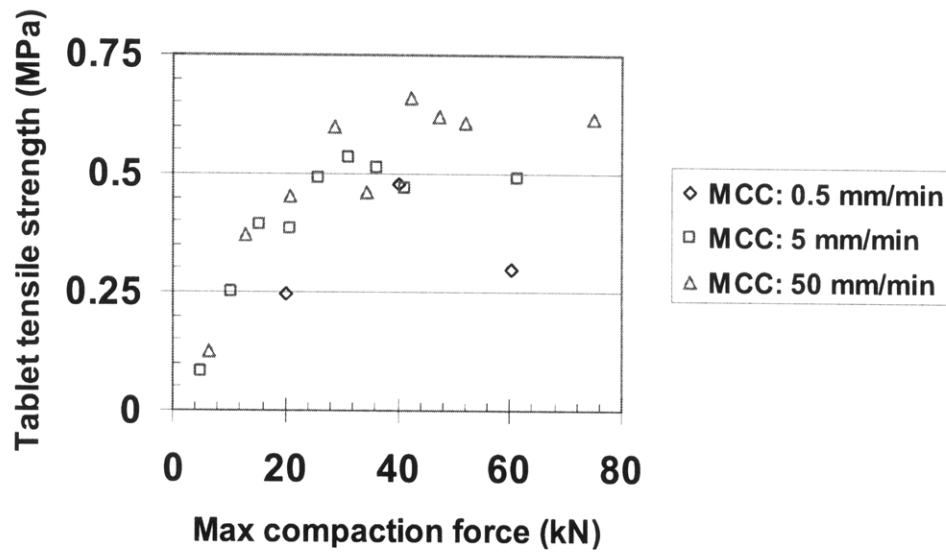
Figure 68: Tensile strength of MCC tablets compacted under different conditions

These findings suggest that it is not just the porosity or pore diameter that affect tablet hardness and dissolution, but the morphology of the pore network itself. The X ray images are therefore a valuable tool in understanding tablet mechanical characteristics. For lactose tablets, a clear trend with force was observed in both structure and performance for DCL 11 and DCL 14. As compaction forces are increased, pore size decreases (Figure 69) and correspondingly the THz refractive index (see chapter III.A), the tablet hardness and dissolution times increase.
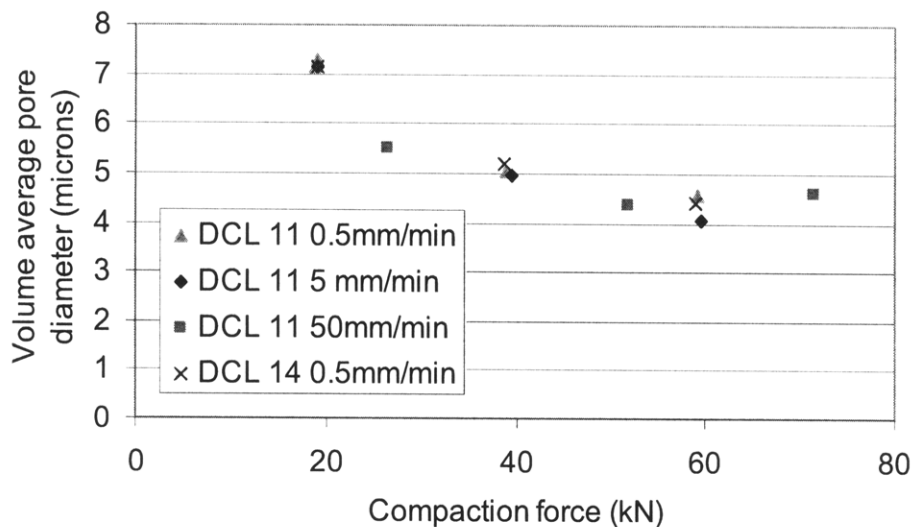
Figure 69: DCL 11 and DCL 14 tablet pore size decreases with increasing compaction force
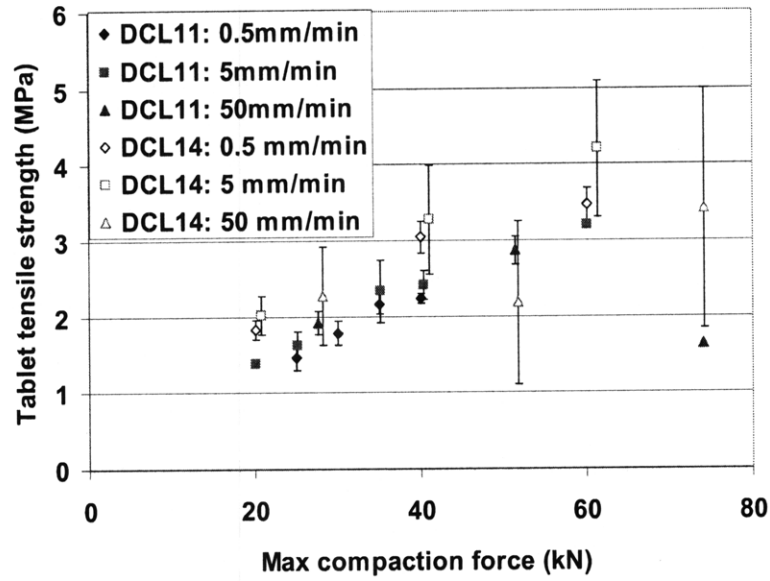
Figure 70: Lactose DCL11 and DCL 14 tablets show increasing strength with increasing compaction force

DCL 11 and DCL 14 were found to show similar pore sizes when compacted to the same force (Figure 69). This is reflected in tablet hardness, as both materials form tablets of similar hardness for a given force (Figure 70, II.A). However, Figure 28 demonstrates that, although varying compaction force can be used to manipulate structure, knowing the effect on structure is not sufficient to predict the effect on dissolution. Information on the physico-chemical properties of the tablet matrix is also needed.
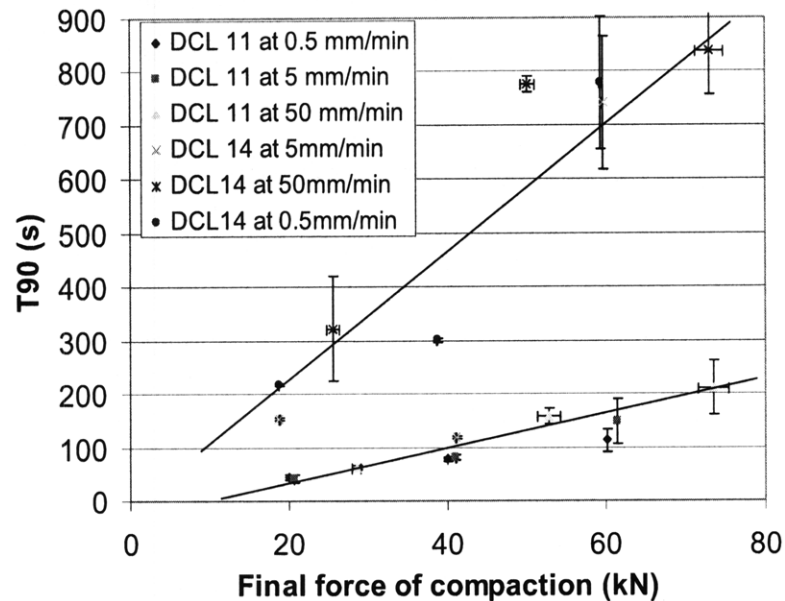
Figure 71: Dissolution times for lactose DCL11 and DCL 14 tablets increase with compaction force at different rates

Tablet lamination was also found to increase with compaction force (III.C), therefore the formation of defects will form an upper limit to the force range that can be used for a given tablet composition, geometry and mass.

Conclusions

Compaction force can be used to manipulate tablet structure. X ray microCT is a useful tool to assess these structural changes. Depending on the microstructure morphology and the chemical properties of the binder, modifying the geometry of the structure may or may not be an effective tuning tool for tablet hardness and dissolution. The range of force that can be used for tuning depends on the tablet composition, geometry and mass, and is limited at the lower end by the compactibility of the material and at the upper limit by the formation of tablet defects, such as lamination.

References

ESH Powder Compaction Simulator, Huxley Bertram Engineering Ltd., *www.powdercompaction.com*, accessed **2007**

Hassanpour A.; Ghadiri M.; Bentham A.C.; Papadopoulos D.G. *Adv. Powder Technol.* **2003**, *14 (4)*, 427-434

MCC, *www.mcc-online.com*, Metropolitan Computing Corporation, accessed **2007**

Sheng Y.; Lawrence C.J.; Briscoe B.J.; Thornton C. *Eng. Computation* **2004**, *21*, 304-317

Wu C-Y. *'Capping Mechanisms during Pharmaceutical Powder Compaction'* Proceedings of the Fifth World Congress on Particle Technology, Orlando, **April 2006**

IV.D Recommendations for Future Work

Four major areas for further work are identified: expanding the range of materials studied, developing the experimental techniques described in this thesis, process modeling of tablet compaction and clarification and development of tablet performance criteria.

Investigation of Pharmaceutical Materials

Only two types of binders were investigated in this study: microcrystalline cellulose and spray-dried lactose. Many other direct compression filler/binders are available and investigation should be extended to materials that deform by a range of mechanisms. Only single component tablets were considered here, but studies have shown that excipients can be mixed to obtain further tunability (Allard et al, 2006, Cotton et al, 2007).

The effect of APIs (active pharmaceutical ingredients) was not considered, as it was assumed that excipient properties would dominate the tablet microstructure for low-dosage tablets. However, there are many formulations where APIs (either a single API, or a mixture) make up a significant volume of the tablet. APIs are often in crystalline form so methods other than single granule compression may be needed to characterize their mechanical properties, such as nanoindentation (chapter I.B).

Other constituents of commercial tablet formulations include excipients to act as lubricants, disintegrants etc. These materials will likely have different mechanical properties which may affect the tablet microstructure and will affect hardness and the mechanics of dissolution.

Development of Characterization Techniques

Several of the experimental techniques used in this thesis have had limited application in the pharmaceutical sector. Therefore, further research is recommended to investe the potential and limitations of these techniques.

Granule mechanical properties

A modified nanoindenter apparatus was found to be a useful means of measuring the mechanical properties of spherical excipient granules. However, the load and displacement range of this apparatus was found to be insufficient to test tough granules such as MCC. Instruments with a wider load and displacement range are required, such as a MTS indenter with high load cell, or an Instron testing machine, for some materials. The major limitations of the nanoindenter technique are:

i) Long times required for testing

ii) Data on the size, shape and number of daughter particles cannot be captured after the test

A limited data set (25-30 granules per loading condition) was collected due to the long times associated with indenter calibration, maneuvering and tip-cleaning. More data would be desirable for more statistically reliable values of the granule stiffness and strength.

Thornton et al (2004) demonstrated that impact testing and compression testing of granules results in similar fracture patterns. The two tests could be used in parallel, as suggested by Couroyer et al. (2000): compression testing to get quantitative data about fracture mode and impact testing to get quantitative data on the particle size distribution of the resulting fragments.

Only spherical, excipient powder materials have been considered in this study. To understand the mechanical behavior of realistic multi-component blends, it is necessary to characterize API crystals and irregular excipients. This will require a combination of powder particle compression with different testing techniques, such as nanoindentation.

X ray micro CT

X ray micro CT was found to be a valuable tool to analyze the microstructure of tablets, both qualitatively and quantitatively. However, further investigation is required on quantitative parameters to describe the relevant microstructural characteristics. The 2D pore area and volume-averaged pore diameter were used to characterize pore size, but other significant features may include pore connectivity and length. The reported pores sizes are averaged over the whole volume tested, but it is possible that there is spatial variation in the tablet, particularly along the axis of compaction.

Terahertz technologies

This study showed the Terahertz pulsed spectroscopy can be used to obtain the refractive index of tablet materials and that this correlates with tablet hardness for DCL 11 (chapter III.A). However, it is not yet known exactly what physical changes in the structure correspond to changes in refractive index. X ray micro CT has shown that decreasing pore size in lactose tablets corresponds to increasing hardness and hence correlates with refractive index in the THz range. However, further studies are required to understand the physical significance of the TPS spectrum.

TPS did not indicate any difference in the polymorphic composition of tablets of DCL 11 and DCL 14. Other techniques for characterizing the crystal structure in tablets should be investigated and the effects on dissolution studied. Some techniques that have been used to study the crystal structure of lactose are thermogravimetric analysis (Buckton et al,2002), solution calorimetry (Harjunen et al, 2004), Raman spectroscopy (Katainen et al., 2005) X ray diffraction (Jouppila et al, 1998) and differential scanning calorimetry (Gabbott et al, 2003). However, these techniques require the sample to be in solution or in powder form. TPS is worth further investigation for its potential to non-destructively analyze the polymorphic composition in commercial tablets. However, to date, studies have made use of binders that are not common in the pharmaceutical setting, such as polyethylene or polytetrafluoroethane (Upadhya et al, 2004, Taday et al, 2003).

TPI was found to be a useful tool for rapid detection of tablet defects such as lamination. However, the study presented here is not sufficient to determine the technique's limits of detection. Further work is required to determine the maximum permissible size of defects and investigate the technique's capabilities of differentiating faulty and good tablets.

Process Model of Tablet Compaction

For systematic design, a process model is required of the tablet compaction process. In the ideal case, the model would have the material properties, the tooling geometry and the operating parameters as independent inputs and the tablet microstructure as an output.

An overview of methods for modeling powder compaction is presented below. Empirical models to predict porosity, such as the Heckel (1961) and the Kawakita-Ludde (1970) equations have been excluded, as they are one-dimensional models that rely on

experimentally derived parameters that are specific to the materials and equipment used in the experiment. The powder bed can be modeled as a continuum (FEM models), or a representative volume element can be considered and the mechanical response of the element assumed to represent the average for the entire bed (micromechanical models), or the individual powder granules can be modeled explicitly (DEM models).

Finite element models

The powder bed can be modeled as a continuum with FEM models. Much work has been done using finite element modeling to analyze powder compaction using a single-phase constitutive equation (usually the Drucker-Prager cap constitutive model, e.g. Wu et al., 2005). This can be used to analyze stress states for different equipment geometries or materials. However, these models depend on an accurate constitutive equation and do not give insight into the granule-scale mechanisms of compaction. It is possible to include some information and spatial resolution of porosity by having two-phase constitutive equations or using multiscale modeling (Wang and Karabin, 1990, Biner and Spitzig, 1990, Lukowski et al, 1992, Justino et al, 2000, Lee et al, 2004).

Micromechanical models

Geometric models of a representative volume element can be used to model the porosity evolution of a powder bed. A model is developed for single particle deformation and average stress on a particle during compaction. Arzt (1982) and Lum et al. (1998) presented models for 2D spherical monodisperse systems. Lum et al used experimentally derived material parameters to test the model for polymeric pharmaceutical materials.
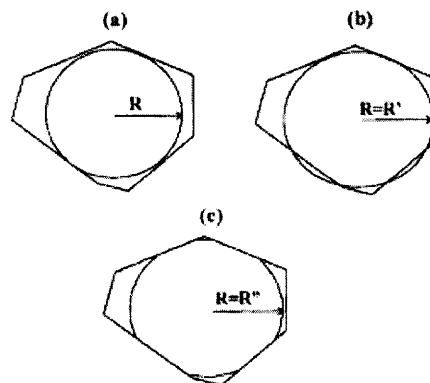
Figure 72: Particle geometry is considered as a Voronoi cell (a), densification is modeled by concentric growth (b) and redistribution of the excess volume (c) (Source: Lum et al, 1998)

The main limitation of these models is that they do not incorporate any particle rearrangement during compaction and can be used only for viscoelastic or plastic deformation. Only the average porosity of the powder bed can be calculated and spatial variation or wall effects cannot be included.

Gardiner and Torsedillas (2006) have used micromechanical models to incorporate3D polydisperse assemblies, incorporating contact anisotropy, particle rotation and sliding Their models can be used to study void evolution and shear bands (Torsedillas and Walsh, 2002).

This approach has the advantage of being computationally tractable, but has limitations when it comes to modeling a uniaxial compaction process where there is considerable particle rearrangement and wall effects are significant.

Discrete element models of compaction

Discrete element modeling accounts for the heterogeneous nature of granular material in processes including compaction. The method considers each granule as a discrete particle and Newton's equations of motion are solved explicitly for each particle at each time step. The complexity and computational requirements of the DEM model depend on the model for the particle interactions with other particles or any bounding surfaces, the number of particles in the system and the geometry of the system.

The advantage of DEM modeling is that it enables us to investigate the effect of individual particle properties on the macroscopic processing behavior and thus opens up the possibility for both process and particle optimization. Particles are usually modeled as rods (in 2D) or spheres (in 3D) as this simplifies algorithms to determine inter-particle contact, although algorithms have also been developed for contact of non-spherical particles (Yang et al, 2002). Structural information of the powder bed can be obtained and it is temporally and spatially resolved.

DEM can be used to model consolidation by plastic deformation or by fracture.

Two approaches have been taken for modeling plastic deformation of particles; either the contact damping and deformation is modeled, or the entire particle is modeled as a continuum in a combined discrete/finite element method to incorporate volumetric deformation.

The particle contact can be modeled to incorporate cohesion, friction and deformation of the particle. A model of elastic-plastic contacts has been presented by Li et al. (2002), based on the Hertzian theory for perfectly elastic spheres. In these models, the 'deformation' of the particles is incorporated by allowing the spheres to overlap and by considering the deformed particles as truncated spheres with volume reduction. The contact force-displacement model can be obtained by single granule compression testing (chapter I.B) and inter-granule friction and cohesion can be measured by atomic force microscopy (Domike, 2003, Ngai, 2005, Pu, 2007). A 3D model incorporating cohesion, friction and elastic-plastic deformation was implemented by Sheng et al., (2004) and the effect of friction and yield stress on a unit cell with a periodic boundary condition was investigated.

Another approach that has been taken to model plastic deformation is to treat the particle as a continuum using combined DEM / FEM approach (Komodromos and Williams, 2002). This method gives more insight into the mechanisms of volumetric particle deformation, but is considerably more computationally intensive. Gethin et al (2003) developed a code with both brittle and ductile failure criteria for a confined 2D system. The number of particles was limited to sixteen due to computational intensity.

Models have been developed for binary composite materials where the two components have greatly different properties by assuming one component to be hard and rigid and the other to be perfectly plastic. This has been used with a contact (truncated Hertzian) model by Martin and Bouvard (2003) and with a combined DEM / FEM model by Gethin et al. (2003). It has been shown that this combination of materials leads to the plastic material extruding around harder materials (Figure 73).
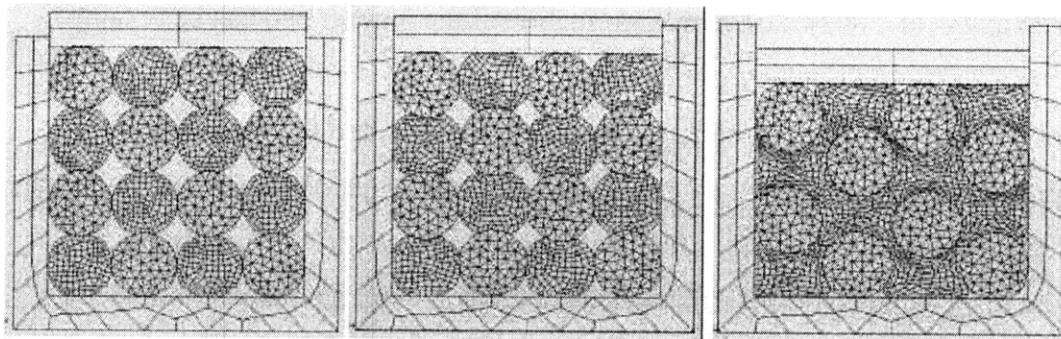
Figure 73: DEM/FEM model of compaction for a binary mixture with equal components of soft ductile particles and hard, brittle particles. (Source: Gethin et al., 2003)

This would be a suitable approach for binary formulations, as most API's are crystalline and hard, and several binder excipients exhibit plastic deformation. ESEM pictures of a caffeine-MCC tablet (Figure 74) show a largely undamaged caffeine particle in a MCC matrix, which supports this theory.

MCC matrix

Embedded
caffeine particle
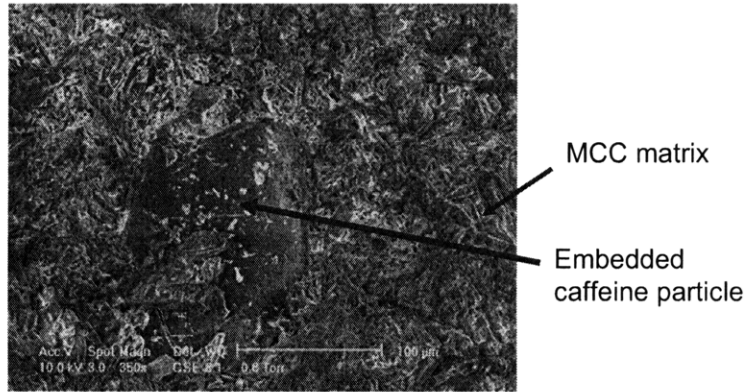
Figure 74: ESEM picture of fractured tablet of caffeine and micro-crystalline cellulose

Brittle fracture of granules can be addressed in a contact model by incorporating a threshold stress after which particles are considered to be broken. Hassanpour et al, (2003) used the experimentally-obtained fracture toughness as the criteria for brittle fracture. However, due to the complexity of incorporating non-spherical broken pieces, these were not included in the model and once particles were broken, they were simply removed from the assembly to allow for the decrease in contacts and stress transmission. It is possible to include some fraction of the particle volume by using geometric filling of the 'broken' particle space, but this increases the computation requirement as the number of particles increases rapidly as compaction proceeds.

Alternatively, DEM can be used to incorporate the heterogeneous nature of agglomerates, such as spray-dried lactose, by explicitly including the primary particles that make up the granule (as described in chapter I.B). Simulations of single-granule compression show consistency with experimental results. An assembly of agglomerates can be generated and subjected to compaction (Figure 75). Mass is conserved in these simulations, as the primary particles only deform locally. However, it is not possible to obtain the intra-granular parameters (size and binding strength of the primary particles) experimentally due to the small scale (few microns) of the primary particles. The total number of primary particles in these simulations gets large when only a few granules are considered,

therefore there are computational limits on the size of the assembly and it is not yet possible to simulate at the process scale (Martin and Bouvard, 2006).
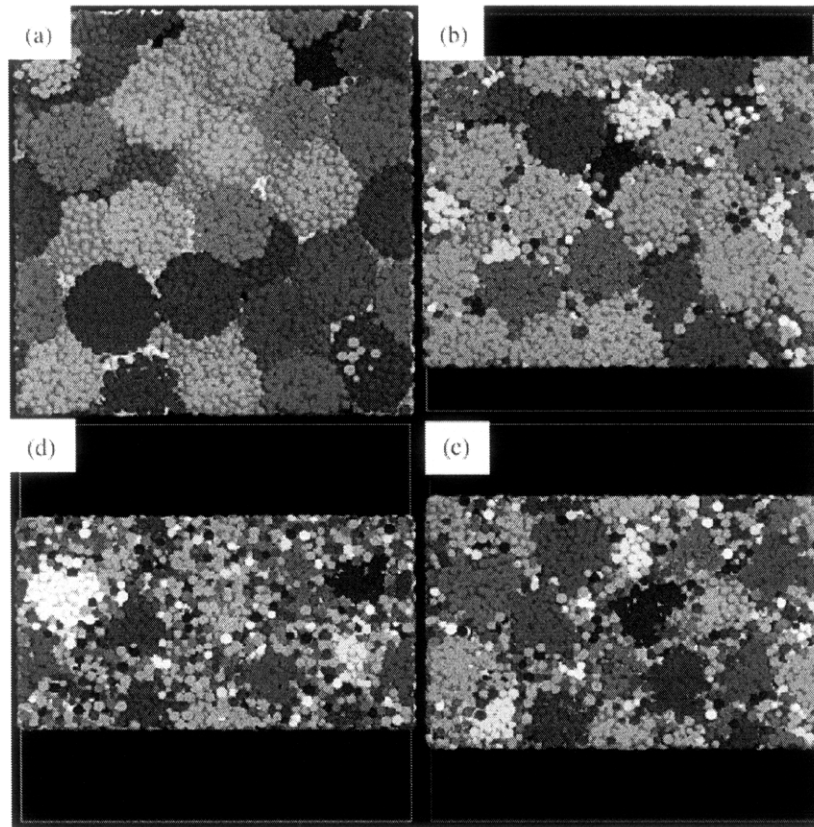
Figure 75: Slice of 3D packing evolution during uniaxial compaction of 100 breakable aggregates (indicated by different colors) Source: Martin and Bouvard, 2006

Smoothed Particle Hydrodynamics

Another potential method for modeling of powder compaction is smoothed particle hydrodynamics. In SPH, the fluid or solid is discretized and the properties of each element are attributed to their centres (to create 'particles'). An interpolation kernel is used to smooth values held by the particles, giving smooth continuous interpolated fields (eg. of density or pressure). These fields are used in the solution of the governing equations (Cleary et al, 2007).

This method has been used for modeling of solids processing, such as fine powder flow (Sugino and Yuu, 2002), and solid fragmentation (Libersky et al., 1997; Parshikov et al., 2000; Rabczuk and Eibl, 2003). Although this method can be used to generate density, pressure and velocity fields, its effectiveness at predicting microstructural characteristics of a compacted powder bed is unclear.

Evaluating and Modeling Tablet Performance

As discussed in chapter II.A and II.B, the tablet properties affecting tablet hardness and dissolution are not well understood. The testing conditions and equipment are standardized, but do not enhance understanding of the physics. In the case of hardness, the strength of the material can only be calculated analytically for cylindrical tablets, whereas most tablets are biconvex. Also, the strength calculation assumes that the material is homogeneous, whereas several studies have shown that it is, in fact, the heterogeneity (porosity or pore structure) of the material that determines resistance to crack propagation. In the case of dissolution, the geometry of the tablet and the complex hydrodynamics of the testing apparatus do not allow for a simple model of dissolution. In order to build predictive models of tablet performance, it is vital to understand the physics of the performance assessment and how the properties of the tablet (chemical and microstructural) affect the test. Therefore, further experiments should investigate non-standard testing configurations to assess the mechanical and dissolution characteristics of tablets.

Nanoindentation is a possible method for quantifying mechanical properties of the compact. Mohammed et al. (2005) studied the response of tablets made from various pharmaceutical materials, but did not investigate the effect of compaction force. Solution sampling was used to monitor the progression of dissolution in our experiments, but this is labor-intensive, prone to error and limits the sampling rate. Other ways to monitor dissolution are an automated HPLC, or an in-situ FTIR system (van der Weerd et al. 2004). The hydrodynamics of the system should be designed to allow for analytical solution and geometric factors should be minimized, for example, by sealing faces of the tablet, so that medium penetration and drug diffusion occurs through a single face.

For a soluble matrix, both disintegration and dissolution studies are necessary. In addition, the evolution of the tablet structure can be inspected by X ray CT or MRI at different steps during dissolution (Karakasota et al, 2006). This will provide insight into the mechanism of dissolution and hence how it is affected by initial tablet structure.

Concluding Remarks

This study has identified a framework for rational design of pharmaceutical tablets and identified some of the tools that can be used for future research. The research presented here indicates that a more systematic design paradigm is a feasible, if long-term, goal. Much further work is required in the areas of pharmaceutical materials, analytical technology and process modeling. In particular, modeling of the tablet compaction process and the tablet applications process (e.g. dissolution behavior) is necessary to reduce the time and materials required for design.

The FDA's Process Analytical Technology (FDA, 2004) and international harmonization (ICH, 2007) initiatives are generating much interest in the analytics sector and increasing attention is being paid to developing applications for the pharmaceutical industry. The pharmaceutical industry is also becoming more receptive to new technologies in development and manufacturing as a result of changing business and regulatory environments. It is anticipated that pharmaceutical product and process development will be a fertile area of future research.

References

Allard C.; Kessler M.; Nees S. *Tunable Formulation of Pharmaceutical Tablets* 10.26 Class Project, MIT, **2006**

Arzt E. *Acta Metall.* **1982**, *30*, 1883-1890

Biner, S.B.; Spitzig, W.A. *Acta Metall. Mater.* 1990, 38(4), 603-610

Buckton G.; Chidavaenzi O.; Koosha F. *AAPS Pharm.Sci.Tech.* **2002**, *3(4)*

Cleary P.W.; Prakash M.; Ha J.; Stokes N.; Scott C. *Prog. Comput. Fluid Dy.* **2007**, *7(2-4)*, 70-90

Cotton J.; Machado M.; Roy-Mayhew J. *Tunable Formulation of Pharmaceutical Tablets* 10.26 Class Project, MIT, **2007**

Couroyer C.; Ghadiri M.; Laval P.; Brunard N.; Kolenda F. *R. I. Fr. Petrol* **2000**, *55 (1)*, 67-85

Domike R.R. *Pharmaceutical Powders in Experiment and Simulation* PhD Thesis, MIT **2003**

FDA, Guidance for Industry: PAT- A Framework for Innovative Pharmaceutical Development, Manufacturing, and Quality Assurance, US Food and Drug Administration, **2004**

Gabbott P.; Clarke P.; Mann T.; Royall P.; Shergill S. *A High-Sensitivity, High-Speed DSC Technique: Measurement of Amorphous Lactose, Technical Note*, Perkin Elmer Inc. www.perkinelmer.com , **2003**

Gardiner B.S.; Torsedillas A. *Powder Technol.* **2006**, *161*, 110-121

Gethin D.T.; Lewis R.W.; Ransing R.S. *Modelling Simul. Mater. Sci. Eng.* **2003**, *11*, 101-114

Hassanpour A.; Ghadiri M.; Bentham A.C.; Papadopoulos D.G. *Adv. Powder Technol* **2003**, *14(4)*, 427-434

Harjunen P.; Lehto V.; Koivisto M.; Levonen E.l Paronen P.; Jarvinen K. *Drug Dev. Ind. Pharm.* **2004**, *30(8)*, 809-815

Heckel R.W. *Trans Metal Soc*, AIME, **1961**, *221*, 671

ICH, International Conference on Harmonisation of Technical Requirements for Registration of Pharmaceuticals for Human Use, *www.ich.org*, accessed 2007

Jouppila K.; Kansikas J.; Roos Y.H.; *Biotechnol. Prog.* **1998**, *14*, 347-350

Justino, J.G; Alves, M.K.; Klein, A.N.; Al-Qureshi, H.A. *J. Mater. Process. Tech.* **2006**, *179(1-3)*, 44-49

Karakasota E.; Jenneson P.M.; Sear R.P.; McDonald P.J. *Phys Rev E* **2006**, *(74)*, 011504

Katainen E.; Niemela P.; Harjunen P.; Suhonen J.; Jarvinen K., *Talanta*, **2005**, *68(1)*, 1-5

Kawakita K.; Ludde K.H. *Powder Technol.* **1970**, *4*, 61

Komodromos P.I.; Williams J.R. *Geotechnical Special Publications* **2002**, *17*, 138 – 144

Lee, P.D.; Chirazi, A.; Atwood, R.C.; Wang, W. *Mat. Sci. Eng. A*, **2004**, *365(1-2)*, 57-65

Li L.Y., Wu C.Y., Thornton C. *P. I. Mech. Eng. Sci. C* **2002**, *216(4)*, 421-431

Libersky, L. D.; Randles, P. W.; Carney, T. C.; Dickinson, D. L. *Int. J. Impact Eng.* **1997**, *20*, 525-532

Lukowski, J.; Grosman, F.; Misiolek, W.Z. *Adv Powder Metall.* **1992**, *2*, 301-311

Lum S.K.; Hoag S.W.; Duncan-Hewitt W.C. J. Pharm. Sci. 1998, 87(8), 909-916

Martin C.L.; Bouvard D. *Acta Materialia,* **2003**, *51*, 373-386

Martin C.L.; Bouvard M. *J. Am. Ceram. Soc.* **2006**, *89(11)*, 3379-3387

Monaghan J.J. Annu. Rev. Astron. Astrophys. **1992**, 30, 543-74

Ngai S.S.H. *Multiscale Analysis and Simulation of Powder Blending in Pharmaceutical Manufacturing,* PhD Thesis, MIT **2005**

Parshikov, A. N.; Medin, S. A.; Loukashenko, I. I.; Milekhin, V. A., *Int. J. Impact Eng.* **200**0, *24*, 779-796.

Pu Y. *Theoretical and Experimental Investigation of Particle Interactions in Pharmaceutical Blending* PhD Thesis, MIT **2007**

Rabczuk, T.; Eibl, J. *Int. J. Numer. Methods Engng* **2003**, *56*, 1421-1444.

Sheng Y.; Lawrence C.J.; Briscoe B.J.; Thornton C. *Eng. Computation* **2004**, *21*, 304-317

Sugino, T.; Yuu, S. *Chem. Eng. Sci.* **2002**, *57*, 227-237.

Taday P.; Bradley I.V.; Arnone D.D.; Pepper M. *J. Pharm. Sci.* **2003**, *92 (4),* 831-838

Thornton C., Ciomocos M.T., Adams M.J., *Powder Technol.* **2004 (a)**, 140, 258– 267

Torsedillas A.; Walsh D.C.S. *Powder Technol.* **2002,** *124,* 106-111

Upadhya P.C.; Nguyen K.L.; Shen Y.C.; Obradovic J.; Fukushige K.; Griffiths R.; Gladden L.; Davies A.G.; Linfield E.H. *Joint 29th Conference on Infrared and Millimeter Waves and 12th Int. Conf on Terahertz Electronics* **2004**, 429-430

Van der Weerd J.; Chan K.L.A.; Kazarian S.G.; *Vib. Spectrosc.* **2004**, *35(1-2),* 9-13

Wang, P.T.; Karabin, M.E. *ASME PED, Microstructural Evolution in Metal Processing,* **1990**, *46,* 47-58

Wu C.Y.; Ruddy O.M.; Bentham A.C.; Hancock B.C.; Best S.M.; Elliott J.A. *Powder Tech.* **2005**, *152,* 107-117

Yang X.S.; Lewis R.W.; Gethin D.T.; Ransing R.S.; Rowe R.C. *Geotechnical Special Publications,* **2002**, *17,* 74-78

Part V: Patent Expiry of Statin Products - A Study of Market Dynamics

This project investigates the interactions between innovators and generics manufacturers in the US market for statin drug products. In particular it looks at the market dynamics during the period when branded products lose their patent-protected status and generic products emerge.

Statins comprise the largest segment of prescription drug sales by revenues and are typical of the 'blockbuster' model employed in major multinational pharmaceutical firms. In fact, statin products comprise of a significant percentage of revenue for several of these firms. This project is particularly timely, as the branded product family is at a midpoint in its lifecycle. Earlier products have gone off-patent and seen generic substitution. Generics manufacturers are being more aggressive about attacking the remaining market through intellectual property challenges, and the manufacturers of the remaining on-patent products are being forced to be more creative in their strategies to maximize profits from existing products.

This work follows that of Ngai (Ngai, 2005), who explored value creation strategies during the early phases of the statin family lifecycle. That model captured the dynamics of the entire statin market when the only players are the innovators. This work presents the argument that statins have moved up the 'technology S curve', and the market is currently in a mature phase, where the goal of value capture dominates value creation. Rather than a market view, we look at the actions taken at a firm level, based on historical studies of the six statin products currently in the market. A model has been created to explore the major value-capture strategies employed at a firm level around the period of patent expiry. The major leverage points for both branded and generic manufacturers during this period are price and intellectual property. For branded product manufacturers, investing in marketing and R&D for new indications and formulations is an effective means of maintaining or gaining market share.

Part V.A of this report presents a history of the statin's trajectory along the technology S curve. Part V.B looks at the structural and regulatory aspects of the market that influence what strategies can be employed. Part V.C explores specific strategies that are employed

in the period surrounding patent expiry, through the lens of a systems dynamics model applied to case studies of the six statin products. Part V.D considers the future direction for the market and presents recommendations for a continuation of this work.

V.A Statin Products: the Perspective of Technology Market Dynamics

The literature on the dynamics of innovative industries characterizes the evolution of a technology by the 'technology S curve' (Foster 1986; Utterback, 1994; Weil and Utterback, 2005). This framework is used here to analyze the statin market. The four stages in a technology's lifetime are: ferment, take-off, maturity and discontinuity. The curve maps product performance as a function of time, although some argue that effort or investment may be more accurately used as the independent variable (Foster R., 1986).
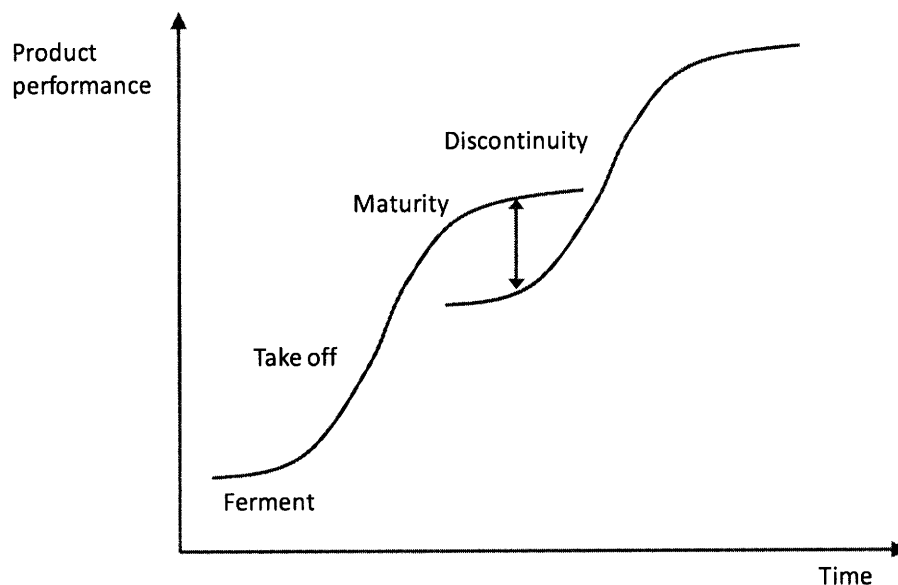
Figure 76: The technology 'S' curve

The fermentation phase is characterized by intense activity and a multitude of ideas being explored, but with very slow growth in performance improvement. At some point, a superior or dominant design emerges, followed by rapid take-off in the industry. Performance improves by leaps and bounds, as R&D investment is focused on optimizing functionality of the dominant design and reducing costs. This corresponds to an uptake in demand, and commercial success encourages many firms to enter the market with 'me too' products. Over time, R&D investment focused on these incremental improvements generates diminishing returns. Commoditization occurs as competition becomes increasingly intense in an established market where products are undifferentiated. Firms

increasingly compete on price and focus on low-cost production as a source of competitive advantage. Innovation now comes from process improvement, rather than product improvement (Abernathy and Utterback, 1978). Eventually, value may get destroyed in a 'race to the bottom' within the industry. A new technology may emerge and completely erode the market for the established players, creating a discontinuity. The purpose of this section is to track the statin family of products as it has moved along this curve, and demonstrate that the dynamics in this market are consistent with what has been observed in many other technology markets.

What are Statins?

Statins are a family of small-molecule drugs used to reduce blood cholesterol levels, particularly low-density lipoproteins that are believed to be responsible for atheroschlerosis (Pfizer, 2007), or the build-up of plaque on coronary arteries. They work by inhibiting the enzyme HMG-CoA reductase that is required for cholesterol biosynthesis (Manzoni and Rollini, 2002). High cholesterol levels are believed to be a cause of heart disease and stroke, the first and third leading causes of death in the US (CDC, 2009).

These drugs come in tablet form and are administered orally. They are prescribed as prophylaxis or chronic therapy of patients at risk of primary or secondary heart disease, i.e. those who may be at risk of a heart attack or stroke, but are asymptomatic and have no history of cardiovascular problems, as well as patients who have already had heart attacks/ heart surgery.
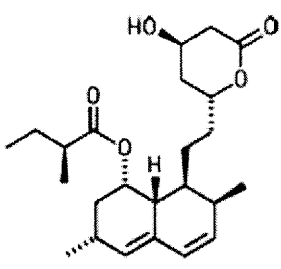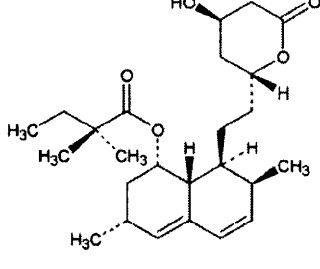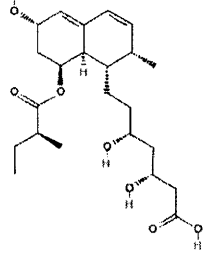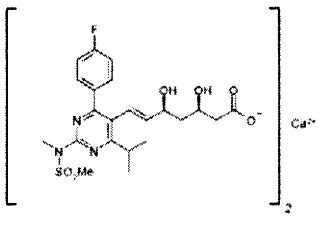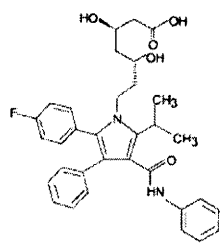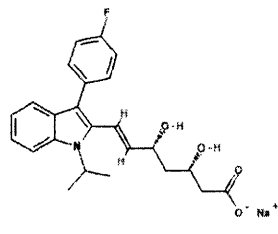
Ferment and Emergence of a Dominant Design

Statins were first discovered at Sankyo Pharmaceuticals in Japan in 1971 by a research scientist, Akira Endo. Roy Vagelos, ex-CEO of Merck and head of research at the time, describes the sense of competition within the industry to find a molecule that inhibited the HMG-CoA reductase enzyme pathway, the uncertainty surrounding whether this was going to be an effective mechanism, and the relative ineffectiveness of existing therapies at the time (Vagelos and Galambos, 2006). Although Sankyo did develop the first drug, mevastatin, they never commercialized it. Instead they worked with Merck to co-develop

lovastatin, the first commercial product. This product set the standard for the dominant technology: all subsequent statin products work via the same metabolic pathway. Chemical entities are based on similar structures (Table 16), although two generations are clearly evident.

Table 16: Chemical structure of active ingredients of the statin family

Top: Natural statins share a polyketide portion and a hydroxy-hexahydro naphthalene ring structure. They vary in their side chains.		
Lovastatin (C&EN, 2005)	**Simvastatin (Merck Sharpe and Dohme, 2007)**	**Pravastatin (NCBI, 2007)**
Bottom: Synthetic statins have a very different structure to natural statins		
Rosuvastatin calcium (Astra Zeneca, 2007)	**Atorvastatin (Manzoni and Rollini, 2002)**	**Fluvastatin (NCBI, 2007)**

Take-off

Take-off in the statin market is described by Ngai's model (Ngai, 2005). It was characterized by growing sales, and the entry of multiple players in the branded market, with incremental improvements in product performance. It created what is still the largest segment of the pharmaceutical market, and some of the most profitable products in the industry.

Ngai's model captures the increasing R&D investment that led to a proliferation of statin products in the market between 1987 and 2003. Six statin active ingredients are currently approved by the FDA: Lovastatin (launched by Merck in 1987), Pravastatin (BMS, 1991), Simvastatin (Merck SP, 1991), Fluvastatin (Novartis, 1993), Atorvastatin (Pfizer,

1997) and Rosuvastatin (Astra Zeneca, 2003) (FDA Orange Book, 2009). Cerivastatin (Baycol, LipoBay, Bayer AG) is a synthetic statin that was withdrawn from the market in 2001 due to serious side effects.

These products have had huge commercial success. They form the largest therapeutic segment by dollar sales in the US (Table 17). Lipitor® alone is the highest grossing drug in the US. The data in Table 18 indicates that for firms with statin products still under patent protection, they form a substantial portion of US and world revenues.

Table 17: US Sales (Source: IMS Health, 2007)

US Sales ($bn)	2003	2004	2005	2006	2007	2008
Total pharma	219.6	239.9	253.9	276.1	286.5	
Lipid regulators (statins)	15.4	18.1	19.8	21.7	18.4	
Lipitor	6.8	7.8	8.4	8.7	8.1	

Table 18: US and worldwide statin sales for firms with products under patent protection. Sources: Annual reports to shareholders

2008	US			Worldwide		
	Statin sales ($M)	Total pharm. sales ($M)	%	Statin sales ($M)	Total pharm. sales ($M)	%
Pfizer (Lipitor only)	6,300	18,851	33.4%	12,401	44,174	28.1%
Astra Zeneca (Crestor)	1,678	13,510	12.4%	3,597	31,601	11.4%
Novartis (Lescol)	154	8,616	1.8%	645	26,331	2.4%

Mature Market

As the statin market has matured, innovation has shifted to include process innovation, an increase in the number of products has led to debate on substitutability and the entry of generic products has led to price competition, reducing the dollar value of the overall market. Current efforts by branded manufacturers are focused on differentiation to delay the scenario where products are completely commoditized.

Statins are small molecule products that can be classed by their method of manufacturing into two generations: the earlier products are naturally-occurring, or derivatives of natural products, and the later products are synthetic.

Lovastatin and pravastatin, the first two commercial products, are naturally present as microbial secondary metabolites. Simvastatin is a semi-synthetic derivative of lovastatin. The natural statins can be produced by fermentation and biomodification techniques, using strains such as *Aspergillus terreus* or filamentous fungi such as *Penicillium*. An

example of natural statin manufacture is Biocon's solid matrix fermentation technology to produce lovastatin (NCBI, 2007).

The later products- fluvastatin, rosuvastatin and atorvastatin- are completely synthetically derived (Robison et al, 1994; NCBI, 2007; Astra Zeneca, 2000). Atorvastatin and fluvastatin are synthetic derivatives of mevalonate and pyridine respectively (Manzoni and Rollini, 2002).

The patents on natural statins (lovastatin, pravastatin and simvastatin) have expired and generics manufacturers have entered the market aggressively. There are currently between nine and twelve generics companies competing in the market for each product (Figure 77, Table 19). The synthetic statins are still under patent protection, although as they near expiry, they are being subject to patent challenges from generic companies. However, the entry of generics has created a scenario that encourages substitutability between products. Prescribers and health care providers now have a range of choice of both branded and generic statins. There has been considerable discussion on the relative effectiveness of statin products, and generics firms capturing market share not only from the same branded statin product, but from other statin products that are still on patent.

	1987	1988	1989	1990	1991	1992	1993	1994	1995	1996	1997	1998	1999	2000	2001	2002	2003	2004	2005	2006	2007	2008	2009	2010	2011	2012	2013	2014	2015
Lovastatin (reformulated)															1	2	2	2	2	2	2	2							
Lovastatin (generics)															6	7	7	7	7	8	9	9							
Pravastatin (reformulated)																		1	1	1	1	1	1						
Pravastatin (generics)																				8	9	12							
Simvastatin (reformulated)																	1	1	1	1	1	1							
Simvastatin (other reform.)																					1								
Simvastatin (generics)																				8	8	10							
Fluvastatin (reformulated)															1	1	1	1	1	1	1	1	1						
Atorvastatin (reformulated)																		1	1	1	1	1							
Rosuvastatin																													

Legend:
- Branded product lifetime between FDA approval and patent expiry
- Reformulated product released by patent holder e.g. extended release, combination therapy
- Reformulated products released by other manufacturers
- Number of generic product manufacturers
- Expected patent life

Figure 77: Lifecycles of statin products to date (Data from: FDA Orange Book, 2009; Smith 2006; Herper, 2006)

The result of generic substitution has been a decrease in the dollar amount of statin sales between 2006 and 2007, while total prescribed volumes have been increasing (Figure 78), particularly following patent expiry of Zocor® (S&P, 2008). There is also increasing advocation for lower prices. Consumers' Union and Consumer Reports Best Buy Drugs, cite research claiming that up to US$8.2bn of savings could be made in 2007 alone by prescribing generic statin drugs rather than branded alternatives (BMI, 2009).

Table 19: Branded and generic stating products approved by the FDA (Source: FDA Orange Book, 2009)

Active ingredient	Doses	Proprietary name	Applicant
Lovastatin	10,20,40,60 mg	Mevacor	Merck
		Advicor	Abbott
		Altoprev	Andrx Labs LLC
		Lovastatin	Actavis Elizabeth, Apotex Inc., Carlsbad, Genpharm, Mutual Pharm, Mylan, Sandoz, Teva
Pravastatin	10,20,40,80 mg	Pravachol, Pravigard Pac	Bristol Myers Squibb
		Pravastatin	Apotex, Cobalt, Dr Reddy's Labs Inc, Genpharm, Glenmark, LEK pharma DD, Pliva Hrvatska DOO, Ranbaxy, Teva, Watson Labs, Zydus
Simvastatin	5,10,20,40,80mg	Zocor, Vytorin,	Merck
		Simcor	Abbott
		Simvastatin	Accord Healthcare, Aurobindo Pharma, Cobalt, Dr Reddy's Labs Inc, Ivax Pharma, Lupin, Perrigo R&D, Ranbaxy, Sandoz, Zydus Pharma
Rosuvastatin	5,10,20,40mg	Crestor	Astra Zeneca
Fluvastatin	20,40,80mg	Lescol	Novartis
Atorvastatin	10,20,40,80 mg	Lipitor, Caduet	Pfizer

As competition in the market has intensified, firms have been increasingly trying to differentiate their products. This has led to a wider range of dosages, extended release formulations and combination therapies (two or more drugs co-packaged or in one tablet).
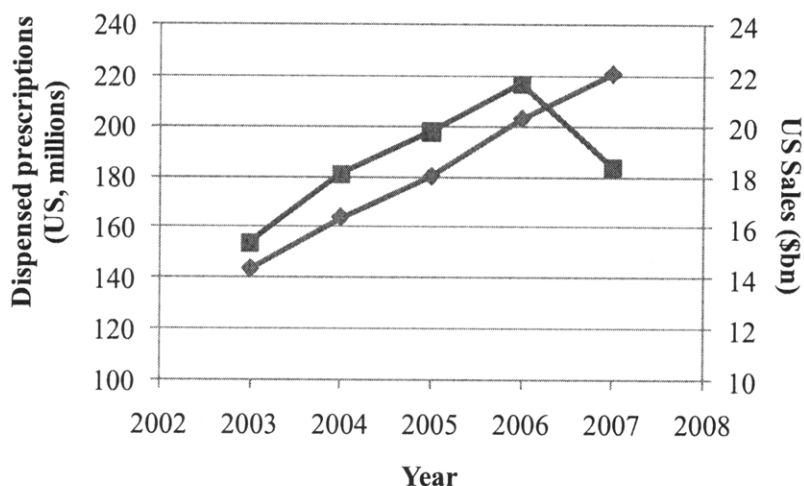
Figure 78: Growth in dispensed prescriptions versus sales for the lipid regulator market in the US (Source: 2007 Top-line industry data, IMS Health, 2007)

Lovastatin was available only in 10, 20 and 40mg dosages. Merck initially got approval for 5,10, 20 and 40mg dosages of simvastatin in 1991, and then introduced 80mg dosage in 1998. Lescol XL®, the extended release formulation of fluvastatin was the first extended release statin product. It was launched in 2000, seven years after the launch of Lescol® (FDA Orange Book, 2009). It has since been followed by Altoprev® and Simcor®. Some examples of combination therapies are Caduet (atorvastatin with amlodipine besylate, Pfizer), Praviguard (pravistatin with aspirin, Merck-Schering Plough), Vytorin® (simvastatin with ezetemide, Merck and SP) and Advicor (lovastatin with niacin, Abbott).

Future Prospects

The US statin market is set to grow in volume. There is an increasing demand for prescription drugs overall, due to an ageing population in the US. Statins are particularly likely to see growth as they are often prescribed both for prophylactic and therapeutic use. There is evidence to suggest that statins may also be effective against Alzheimer's disease, multiple schlerosis (C&EN, 2005) and several cancers, including breast, colon and esophageal cancer (FT, 2005). However, manufacturers have not shown interest in pursuing new indications, largely due to the long timelines for clinical trials in cancer that

would extend beyond the patent lifetimes, and the risks of opening themselves up to the liabilities of stricter safety requirements for cancer drugs (WSJ, 2005).

Currently the focus is still on incremental innovation, with the goal of differentiating between the current products. There is growing belief that it is possible to control cholesterol, not only by lowering low density lipoproteins, but increasing high density lipoproteins. AstraZeneca's product Crestor®, claims to do both and has been seeing growth in market share (Astra Zeneca, 2007, 2009). Pfizer had committed to spend $800M on development of torcetrapib, a product to increase HDL levels, with a plan of creating a combination therapy to tie-in patients to Lipitor®. Development of the drug was cancelled following higher-than-expected mortalities in clinical trials (WSJ, 2006a). Pfizer has since announced that it will be exiting research for cardiovascular therapies. As yet, there are no signs of new technologies emerging for either cholesterol control, or to seriously reduce the chances of cardiac events.

Implications for strategy

Statins are a mature technology, as characterized by the presence of multiple, similar products and the growing price competition. Generics are rapidly capturing value created by the innovators. Although the branded product manufacturers are continuing to attempt value-creating strategies, such as investing in product improvements, it is becoming increasingly important for them to switch to value capturing strategies to sustain their revenues for as long as possible. This analysis focuses on strategies to maximize value capture during the current phase, as opposed to the value-creation strategies explored by Ngai.

Teece (1986) suggests that value capture strategies depend on regimes of appropriability and access to the necessary complementary assets. Part V.B explores the role of regulation and intellectual property law in determining what strategies firms can take to develop or sustain uniqueness of their products, and how different complementary assets affect commercial success of the innovator and the generics firms. These structural dynamics affect the entire market, yet the strategies that will benefit an individual firm depend also on its timing and competitive position in the market relative to other products (e.g. whether it is an early versus late entrant). This is most clearly seen in pricing and branding strategies, discussed in the context of particular case studies in Part V.C.

V.B. Regulatory and Structural Features Influencing Strategic Decision Making

Teece (1986) argues that capturing value from innovation requires an understanding of the regimes of appropriability, the structure of the value chain, and complementary assets. Each of these is explored with respect to the statin market. Many of the standard models for technology industries are distorted in this case due to heavy regulation and a complicated industry structure, where it is unclear who the actual customer is.

Appropriation of technology can be ensured through three means: intellectual property, secrecy and speed. Secrecy is not a viable option in the pharmaceutical industry, due to documentation requirements for health and safety. Innovator firms rely on speed of R&D to demonstrate uniqueness and on formal intellectual property, in the form of patents, to sustain it. For the generic entrants in the market, speed is also important if they take an aggressive IP strategy of challenging the innovator's patents. The FDA approval process acts to sequence entry into the innovator market (Ngai, 2005) and determines the entry of generics players once patents expire.

Statins are currently sold only by prescription in the USA (FDA Orange Book, 2009), although companies are applying for OTC status for low dose statins (USA Today, 2007). This means that statin sales depend on the prescribing habits of physicians, and the coverage provided by healthcare insurance schemes. The sales, distribution and reimbursement systems are complicated and involve many parties, each with different incentives. Understanding where the pricing power lies in these systems is important for maximizing the value captured in a rapidly-changing environment, particularly for generics firms when they consider their entry strategy.

Complementary assets are those which allow the firm to sell a non-unique product at a reasonable return. For the period covered by this project, the relevant assets are the brand of the innovator products, and manufacturing facilities, supply chains and regulatory and IP expertise of the generics firms. The degree to which these assets can be used to sustain an advantage depends on how tightly held they are. We find that each of these assets is tightly held by the respective firms.

The role of intellectual property rights and regulatory procedures in generic entry

The primary federal agency responsible for implementing food and drug safety laws in the US is the Food and Drug Administration. Their policies, combined with the patent protection granted by the US Patent Office play a key factor in determining the windows of high profitability in the drug industry.

Patent term extensions for innovators (Grabowski and Vernon, 2000)

When developing and launching a new drug, firms will apply for patents on the product, its use, and the process. These include patents on the active ingredient, its crystalline polymorphs, the formulation and the manufacturing process. A US patent has a life of 20 years. As product patents are issued early in the development process, this usually translates into seven to sixteen years of market monopoly, in which to recoup their investment and realize returns. Part of the Hatch Waxman amendments (1984) to the Food, Drug and Cosmetics Act (officially known as the Drug Price Competition and Patent Term Restoration Act, 1984) created provisions to extend patent life to compensate for time lost during regulatory approval and clinical trials. This is capped at 5 years, and constrains maximum effective patent life (i.e. the period during which the product is under patent and in the market) to fourteen years.

Other relevant legislation is the FDA modernization act of 1997 which allows six-month extension of market exclusivity for drugs that have been shown to deliver health benefits in children (FDA, 1997). This creates an incentive to invest in post-launch trials for pediatric use, e.g. Merck used this strategy to get an extension for Zocor®. These clinical trials are expensive, but the return can be highly lucrative, although there is evidence that returns can vary widely. A study on the economic returns of pediatric clinical trials for antihypertensive drugs found that average costs for these trials was $2.7 - $14.7 mn but the extensions on patent life generated returns on cost anywhere in the range of 4 to 64.7 (average 17). (Baker-Smith et al, 2008).

Generic approval and 180 day exclusivity (CDER 1998, 2009)

To enter the US market, generic products must be approved by the Food and Drug Administration and be listed in the 'Orange Book' public database. The Hatch Waxman

amendments also established the abbreviated new drug application (ANDA) process, which requires demonstration of bioequivalence, but does not require costly clinical trials. The intention behind this legislation was to allow consumers to benefit from the entry of lower cost generic products, while maintaining incentives for innovators to continue to invest in new drug development.

The timing of ANDA approval depends partially on the patent expiry timeline of the innovator drug. An ANDA application must provide certification of each patent listed in the innovator drug's NDA and state one of the following:

I.   that the required patent information relating to such patent has not been filed;

II.   that such patent has expired;

III.   that the patent will expire on a particular date; or

IV.   that such patent is invalid or will not be infringed by the drug, for which approval is being sought.

Certification under paragraphs I or II permits the ANDA to be approved immediately, and certification under paragraph III indicates that the ANDA may be approved on the patent expiration date. There is no period of exclusivity for the generics manufacturer in these cases.

An ANDA citing paragraph IV certification requires the generics company to give notice to the original manufacturer of the patent challenge, and explain the basis for the challenge. In this case, the dispute must be settled by the courts.

If the generics manufacturer intends to market their product before this patent has expired, they can be sued for patent infringements. If the patent owner files a patent infringement suit against the ANDA applicant within 45 days of receiving the patent challenge notice, the FDA cannot give final approval to the ANDA for at least 30 months from the date of the notice (unless the court reaches a decision earlier in the patent infringement case or orders a different duration of the stay).

In the case that the generic firm is first to successfully challenge a patent under paragraph IV, they are granted an incentive of 180 days of market exclusivity as the only competitor to the branded product. The FDA cannot approve ANDAs from other applicants until this 180 day period is ended. However, this period can be deemed by the courts to start on the earlier of:

1. The day the generics firm begins commercial marketing of the product

2. The date of a court decision finding the patent invalid, unenforceable or not infringed

Therefore the generics firm may not be able to take full advantage of their period of exclusivity, unless they are ready to market their drug on the day of the court ruling. This requires an irreversible investment in manufacturing and distribution capacity in anticipation of approval.

This legislation creates different paths that a generics manufacturer can take to enter the market. One option is to follow a purely low-cost, high volume strategy, relying on efficient manufacturing and economies of scale (see the following section). They minimize their R&D and marketing costs, enter the market when patents expire and try to capture a share of the competitive market by competing on price. If price competition is triggered, firms with the lowest costs will win in this scenario.

Alternatively they can invest in R&D to develop their own patentable manufacturing processes, or formulations to circumvent the patents held by the innovator. The returns on this investment will be rewarded if the patent challenge is successful, and they are able to create a short-term duopoly market where they need only a small price difference to capture significant market share. Eventually other players will enter and erode away any price advantage associated with early entry, so investment must be in line with the returns they can expect in the six month period. The internal capabilities that will be built up in taking this route can create an advantage to the firm when they consider entering other product markets with the same strategy. However, it does increase upfront costs. It seems, therefore, that a generics firm must choose to be committed to an aggressive IP strategy or not. An example of a firm pursuing the latter strategy is Dr Reddy's laboratories, who have established an R&D center in the US to do process development (Reddy, 2009) and be aggressive on ANDA filings, while relying on global manufacturing to keep costs low.

For manufacturers of branded products, this legislation creates incentives for them to continue to invest in defensive IP after the launch of a product to delay a successful challenge. It also increases their expected legal costs of defending the patent life of their

product. This may result in lower profitability or higher prices during the monopoly regime.

<u>Authorized generics</u>

Authorized generics are products licensed by the branded manufacturer to a third party, who then markets them. (Business Week, 2008). This allows them to pursue a market segmentation strategy, where they continue to market the branded product at high profit margins, as well as entering the generics market at a lower price point in a profit-sharing model with their licensee. Within the statin products, Pravachol® was marketed as an authorized generic by Bristol Myers Squibb, and Zocor® was licensed by Merck to Dr Reddy's (FDA 2009a).

This strategy can soften the blow to innovators by allowing them to share some of the generic revenue. Offering to authorize generics to the most aggressive ANDA filers may also be an effective way to reduce direct competition and possibly sustain their patent protection. It also reduces the incentive for other generics firms to pursue a para IV strategy, as 180 day exclusivity period is now shared between three, not two, manufacturers. For the licensee, this model allows them to participate in a triopolistic market without investing in the R&D and legal fees associated with a paragraph IV filing. They can also benefit from the brand value of the innovator's product, and may gain a market share advantage that carries them through the period when more competitors enter.

An example of this is in 2006, Dr Reddy's entered into an agreement with Merck in January to act as an authorized generics distributor for Zocor®, provided another firm gets the180 day exclusivity period. Ivax (FDA 2009b) got the 180 day exclusivity for generic simvastatin, starting in June. At the same time, under the terms of the agreement, Dr Reddy's procured product from Merck at a specified rate and sold it to their customers, sharing profits with Merck. When the 180 day exclusivity period expired in December 2006, Dr Reddy's maintained a 24% market share of simvastatin (Reddy, 2007).

Authorized generics have been opposed by some generics manufacturers. Mylan (FDA, 2004a), Teva (FDA, 2004b), Apotex (Apotex Corp, 2004) and Andrx (FDA, 2004c) have all communicated their desire for authorized generics not to be allowed during the 180

days' exclusivity period granted to the first-to-file applicant. The FDA refused to change the current policy, citing that their interest and jurisdiction is not in business interests, but in public safety. They claim that increased competition leads to better prices for consumers, although they recognize that the presence of authorized generics reduces the incentive for generics manufacturers to pursue a paragraph IV strategy (FDA, 2004d).

Market power in the value chain

Once a firm is authorized by the FDA to market its products, it relies on a complicated network of wholesalers, pharmacies, physicians, insurers and pharmacy benefit managers to get its products to patients, and to receive payment in return. The interactions between these parties are presented in Figure 79. The distribution of goods happens via a wholesaler or distributor from the manufacturer to the pharmacies, and then to patients. However, pharmacy benefit managers play a major role when it comes to negotiating prices, both the price that the manufacturer will receive, and the price to the end consumer, the patient. Physicians, who are not represented on this diagram, also play a critical role in creating and influencing demand. Understanding the positions and interests of these players in the market is essential in developing an effective value capture strategy. It must be noted that by "generic drug manufacturer" we refer to the firm that is responsible for marketing the packaged product, not manufacturers of intermediates and active ingredients. Although sourcing and contractual agreements are important strategic variables (Teece, 1986), there is very little data available in the public domain about such contracts and these firms are therefore excluded for simplicity.

There are currently no explicit price controls on pharmaceuticals in the USA, and manufacturers are free to set prices. However, prices are controlled by negotiations between the different parties in the healthcare system, including insurers, benefit managers and government programs such as Medicare and Medicaid (BMI, 2009). Due to the complicated reimbursement structure, different parties see different prices.
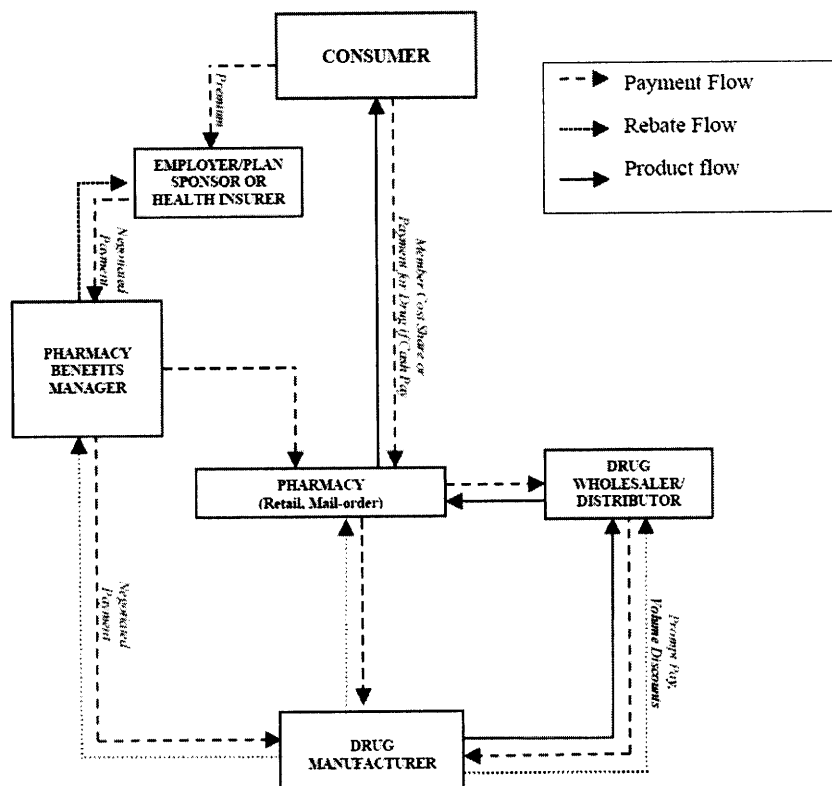
Figure 79: Flow of physical goods and financial transactions in the pharmaceutical supply chain
(Source: Kaiser, 2005)

Wholesale drug distributors

Wholesalers and distributors are a key player as they handle nearly 80% of the volume of drugs in the US market (Booz Allen, 2007). There has been a wave of consolidation in the US drug distribution industry, resulting in an effective triopoly between McKeeson, Cardinal Health and AmeriSourceBergen. This would suggest that they have considerable market power, but these firms operate at very low profit margins – in the range of 1.7 - 5.0% (BMI, 2008).

In the commercial, rather than the clinical, supply chain, availability of the drug is of utmost priority. Distributors traditionally made margins on 'buy and hold' strategies to benefit from price fluctuations and inflation, but have since switched to a 'fee for service' model whereby manufacturers pay them a fee for distributing their products (Singh 2005). The distributors do not have much power when it comes to branded products and do not get significant discounts on the average wholesale list prices (AWP) of branded products, unlike government organizations, hospital chains and other institutional buyers

(S&P 2008, Kaiser 2005). Some manufacturers have been pursuing a strategy of building in-house distribution capabilities, although this is not necessarily cost effective (Booz Allen, 2007).

By contrast, distributors have significantly more negotiation power with generics firms, who seek to secure low-cost access to the market. The economies of scale offered by the distributor, their brand power and ability to drive volume makes it vital for a generics firm to build a good relationship with a distributor. This is particularly true when they need to rapidly introduce a product into the US market or if the generics firm is a relatively new entrant to the US market. From the distributors' point of view, generics dampen total sales figures, but they are generally more profitable (AmerisourceBergen, 2007), so they will secure supplies from multiple manufacturers, as ensuring low-cost supplies is vital for their success.

Pharmacies and retailers

Pharmacies are the final point in the goods supply chain where the product reaches the end consumer, the patient. They also generate the prescription claims data that pharmacy benefit managers (PBMs), insurers, employers and government organizations rely on. It is up to them to implement PBM policies, such as mandatory generic substitution for a prescription.

A large chunk of this market is dominated by chain stores (who filled 52% of all prescriptions and accounted for 36% of sales in 2004, according to IMS Health (2005)). CVS/Caremark claims to be the largest purchaser of generic drugs in the USA. They believe that although selling more generics depresses their revenues, they are more profitable than branded drugs (CVS, 2007). Large pharmacies have pricing power for branded products, and typically negotiate directly with manufacturers for discounts and rebates. This can lower prices below the wholesalers cost, in which case, the wholesaler will 'charge back' the extra cost to the manufacturer (Kaiser, 2005).

Other pharmacy segments are: independent pharmacies, specialty pharmacies, mail order, and long-term care, and other non-specialist retailers. Independent pharmacies must pay higher prices than the large chains to buy directly from wholesalers, or they may come to some pooled purchasing agreement to get better prices (Kaiser, 2005). Most small pharmacies will stock only one generic for each product, and will choose primarily on

price and conditional on availability from their wholesalers, although they typically have two or three suppliers and may switch suppliers based on price, supply availability or customer demand (Skendarian, 2009).

Large retailers are taking advantage of the price sensitivity of uninsured customers to increase their sales of low-cost generics (BMI, 2009). E.g. Wal-Mart introduced 90 day course of /generic drug prescriptions for US$10, a move that was followed by Target, K-Mart and others. This includes some dosages of lovastatin and simvastatin. (Target, 2009).

Pharmacies and retailers have power in determining the market share of the individual generics manufacturers , as they are the major retailers of generics products, with each retailer typically stocking products from only one or two manufacturers. Hence they can exert pricing pressure on the generics segment, via the distributors.

Pharmacy benefit managers

Pharmacy benefit managers have considerable negotiating power with manufacturers of branded drugs because of their ability to keep a product in their formularies, and hence under insurance coverage. This makes it considerably cheaper for patients, and doctors are much more likely to prescribe it if they know that their patients have coverage. Their negotiating power is determined by how much market share their formulary can generate. The evidence suggests that price is the major factor influencing a PBM's coverage of a particular product.

One example of a PBM's ability to shift between products is Express Scripts Inc's shift to emphasizing Zocor® as the preferred statin, six months before it went off patent. This gave rise to 2.4% increase in new prescriptions of Zocor®. 2/3 of these patients previously took Lipitor® then switched to Zocor®, and eventually onto generic simvastatin, once it became available (WSJ, 2006b).

Another example of this is Lescol's entry strategy which focused on a low price (30 - 60% below the competition), while emphasizing equal efficacy to the competitors. This strategy rapidly got the product onto 600 formularies (Liebman, 2001).

<u>Physicians</u>

Physicians are not directly linked into the chain of product supply or payment in the US, but play a very influential role in determining demand by writing prescriptions and advising their patients. By law, pharmacies are required to fill a prescription with a generic product (generic substitution), unless the physician has indicated otherwise. Promotion to physicians through detailing, advertising and research publications has been vital to creating a market for the statin products (see following section and Part V.C).

The role of complementary assets in generating returns

Historically, the major pharmaceutical firms have relied on their monopoly and the brand power of their company and products to realize high returns. For example, when it comes to products, 'Lipitor', 'Prozac' and 'Claritin' are household names. They rely on this brand value to maximize returns during the patent-protected period. In comparison, generics firms have positioned themselves as low-cost manufacturers through their global supply chains and in-house manufacturing in low-cost regions such as India and Eastern Europe. An important complementary asset required for them to market their products in the US is expertise in regulatory affairs and intellectual property legal processes.

<u>Brand-building by innovators</u>

Spending on promotion for branded products is a substantial portion of costs for innovator firms. A PhRMA study found that total PhRMA member promotional spending in 2006 was $12bn, of which $4.8bn was DTC and $7.2bn was on office promotion, hospital promotion and journal advertising (PhRMA, 2008) – this is in comparison to an R&D spend of $58.8bn for the same period. Pharmaceutical firms build the brand of their products through promotional activities directed at two major groups: physicians and patients.

Promotion to physicians includes journal advertising, office and hospital promotion (detailing to physicians by sales representatives) and giving free samples. These tactics have been used successfully to educate physicians and grow the total market for statin products. As more products have entered the statin market, firms are conducting post-launch clinical trials with the intention of demonstrating clinical superiority of a given

product over its competitors. The results of these studies are published in medical journals and are intended to influence the perceptions of the medical community. DTC (direct-to-consumer) advertising is targeted towards existing or potential patients, much of it taking the form of television advertising. It is used mainly as a tool to gain market share from the competition, rather than as a means to get pricing power. A Federal Trade commission study found that DTC advertising had little, if any effect on prescription drug prices. A 2002 study from Harvard on the effect of DTC advertising on demand for pharmaceuticals revealed that DTC advertising may increase demand for a particular brand drug, but only if it has a favorable status on the insurer's formulary (Wosinska, 2002).

Firms generally hold these assets tightly. Promotion efforts are led by large in-house teams, which allows the firms to build up internal expertise and the teams build relationships with doctors. However, co-promotion of products with a partner has also been used very effectively by Merck/Smith-Kline Beecham with Zocor® and by Parke-Davis/Pfizer with Lipitor®.

Are generic brands a potential strategy within a competitive market?

Although makers of the innovator products rely heavily on promotion and brand management to develop a market and capture market share, there has been relatively little investment in promotion by the generics manufacturers. There is some brand sensitivity amongst patients and the smaller, independent pharmacies will respond to the brand preferences of customers (Skendarian, 2009). There are also indicators that brand may be increasingly important as a differentiator in the generics market: For example, Actavis has started marketing their products, as well as those from recent acquisitions, under a single 'Actavis' brand. Similarly, Teva pursues a brand-building strategy for the wholesale market, by advertising in trade journals and exhibitions (Teva, 2008). As competition in the generics market increases, it is likely that the generics firms increase their spending on promotion as a means to capture market share, even though this creates upward pressures on costs.

Maintaining a low-cost supply chain for the US generics market

Generics manufacturers derive their competitive advantage from being able to offer the same product as the innovator at a lower price. Part of their cost advantage arises from the fact that they have not faced the upfront R&D and marketing costs required to develop the product and create a market. However, to gain reasonable returns, the must also have tight control over a low-cost manufacturing base, as ANDA approval requires manufacturing facilities to be in place at the time of the application (Scott Morton, 1998). Non-US companies who are based in low-cost regions have an advantage in this market. Many are fully integrated manufacturers of their products (see Appendix 1), who own and operate their own FDA-approved facilities. They rely on acquisitions of US firms to gain a local foothold to enter the US market. They rely on their relationships with distributors to sustain a low-cost distribution strategy, although several firms are increasingly building up their US sales and marketing capabilities (Teva, 2008, Reddy, 2008).

Once generic entry has occurred and competition shifts to price, the innovator is only in a position to participate in this market if they too have a low-cost manufacturing base. If they are able to signal this to generics manufacturers, they may, in fact, be able to deter some generic entry. Therefore, in a situation like today, where successful drugs do face aggressive generic entry, innovators should consider a low-cost manufacturing strategy to be a critical component of the lifetime profitability of the drug.

Although maintaining low manufacturing and distribution costs is a necessary long-term strategy for the generics players, it is unlikely to be a dynamic strategy for a firm in the period around patent expiry of a specific product. Competitive tactics seem to focus more on price than on costs, although there is also little cost data available to validate this. We will therefore not consider manufacturing costs further in this analysis.

Tightly held IP and regulatory expertise is an essential asset for a generics firm taking an aggressive strategy based on paragraph IV ANDA applications

The six-month exclusivity clause offers a period for extraordinary returns to generics manufacturers. As a result paragraph IV filings have become increasingly frequent. However it requires significant upfront investment in R&D as well as regulatory and legal filings. For example, Dr Reddy's has invested in a dedicated R&D center in the US.

These investments will create economies of learning for a firm taking this strategy, as much of this expertise is transferable across products. Therefore as firms accumulate expertise in process innovation, drug delivery technology, regulatory filings and IP law, their R&D investments will become more productive, giving them an advantage relative to their competitors. These learning effects occur over a period of time, and will create early-mover advantages for firms who have led this trend.

Conclusions

This analysis demonstrates that FDA regulations determine the timelines for uniqueness of a given statin product, and also create sequencing effects in market entry. Much of the pricing power is held by the pharmacy benefit managers, although access to the supply chain is likely to be a differentiating factor for success of a generics product. Overall, access to complementary assets: low-cost manufacturing base, a low-cost supply chain, strong brand, expertise in IP/regulatory procedures and the ability to innovate on process/ drug delivery technology are critical to be a successful player in this market. Complementary assets are particularly important for generics players, but innovators must consider the need for these assets in evaluating their competitive position and the lifetime profitability of their products.

Given the regulation and structure of the pharmaceutical industry, the most significant value-capture strategies available for the innovators in the period immediately surrounding patent expiry are:

1. Competitive pricing
2. Promotion as a means to increase the size of the market, and gain market share from competitors
3. Investment in R&D and IP to extend patent life and deter patent challenges

For the generics firms, the major opportunities to capture value can be created by

1. Competitive pricing
2. Investment in R&D and IP to take a strategy based on challenging patents on the basis of process innovation

These dynamics are incorporated into the system dynamics model described in part V.C.

V.C Modeling Statin Market Dynamics during Patent Expiry

A systems dynamics model was used to capture the interactions between the innovator and generic entrants for a single statin product. This model differs from that of Ngai (2005) because it explores decisions and actions at the firm level, rather than behavior of the entire market. The scope includes the effects of pricing and promotion on market share (and hence revenues), and begins to explore the dynamics of IP investment.

The model was used to simulate the markets for each of the statin products, based on the data in Appendix 2. The model was tested in the context of the first three products that have already lost patent protection. The model was then used to predict market reactions to potential strategies for the manufacturers of the three statin products that have not yet faced generic entry.

Why System Dynamics?

The period considered in this work represents the transition from an established monopoly, into a threatened monopoly, followed by a duo/triopoly, and then a competitive market. A dynamic model is particularly appropriate for this situation because of the multiple transitions and because the legislation sequences market entry of the generics firm, allowing participants to anticipate, observe and react to market movements. There are also different time horizons involved. Some changes, such as pricing, can be made relatively fast and result in rapid changes in the market whereas a marketing campaign will be associated with slower shifts.

Model Structure

The model simulates a time period of 400 weeks: approximately five years prior to expiry and three years after. Full documentation of the model is provided in Appendix 3, but the main features are outlined here.

The impact of 'perceived' product value index (PVI) on market share

The model assigns a market share based on the relative price of the product to the average statin price and the relative perceived PVI of the product. The concept of a perceived PVI is an extension of the concept of an 'intrinsic' product value index defined by Ngai

(2005). In the value creation model, cumulative R&D spend leads to products with greater PVI value, where PVI is an arbitrary index with higher values indicating greater therapeutic benefits and lower side effects. For FDA approval, a product must demonstrate a PVI benefit relative to other products above a certain threshold. However, this becomes more difficult to do the more products there are on the market.

The case studies (Appendix 2) highlight the importance of both promotion and price in determining the market share that a product is able to capture. For example, Lescol® was not able to capture the most market share, despite a low price and an intrinsic PVI equal to the market average. Conversely, Zocor® was able to charge high prices due to its strong brand. Therefore we define:

Perceived PVI = Intrinsic PVI + Premium generated by promotion

This definition allows us to capture the effect of promotion to boost market share. Figure 80 shows a schematic of intrinsic versus perceived PVI. The intrinsic PVI curve is based on results from Ngai's model. The PVI premium from promotion is initially small, as sales and marketing efforts are needed to create the market for the new products. However, as the technology starts gaining momentum in the market, there is greater scope to use promotion to differentiate a specific statin product versus the competition. As more products enter the market, this becomes more difficult. Unwise or excess promotion spend could even lead to a negative return on investment if, for example, post-launch clinical trials give unfavorable results (see Appendix 2 for examples). This scenario is represented in the lower of the two perceived PVI curves.
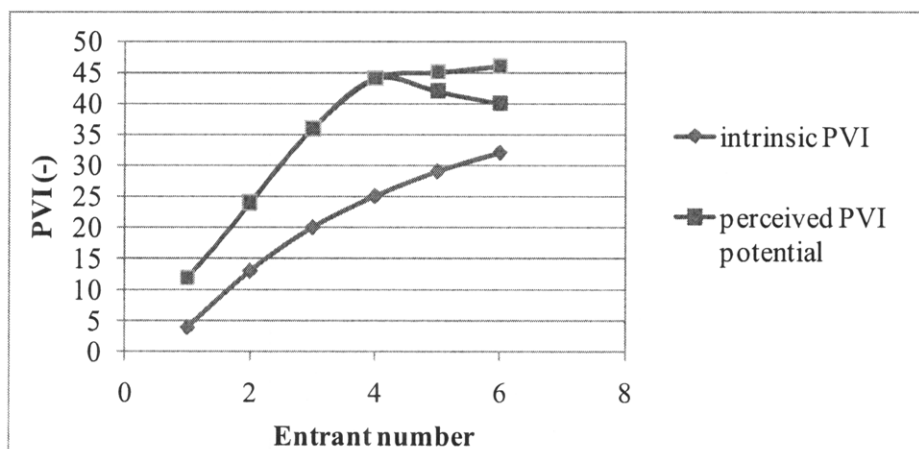
Figure 80: Intrinsic versus perceived product value index (PVI)

The weighting on perceived PVI is non-linear. The model assumes that differences in perceived PVI become more significant when price differences are small. When price differences become very large, they over-ride the marginal product benefits due to the tipping effects created by pharmacy benefit managers as they channel demand through the use of formularies.

Market share allocation

The market share algorithm described above is used to predict market share of the following categories:

1. The branded product
2. The generic product (market share is set to zero prior to patent expiry)
3. Other branded products
4. Other generic products

These market share values are normalized so that total market share is equal to one.

Promotion spend positive feedback

Firms are assumed to chase a target market share that is always above their current market share, allowing for lags in observation and decision-making times. In this way we can explicitly model the management decision-making and the aggressiveness of a management team. Based on the discrepancy between the observed and target market share, an investment is made in promotion, as a fraction of current revenues. This creates a positive feedback loop where products that are successful and have a significant market share have more revenue to invest in promotion and are able to create a higher perceived PVI. Conversely, if a product loses market share rapidly, it becomes extremely difficult to recapture this market share, because of the reduced revenues available for promotional spend.

IP investment 'race'

Generic entry via a paragraph IV ANDA filing becomes more attractive for products with higher revenues. We assume that all statin products have revenues high enough to attract strong generic competition. Therefore, the incumbent must invest in defensive IP to protect their patent life and maintain a high barrier to entry. The generics firms will also

start to invest in IP to erode the barriers to entry, mount a patent challenge and shorten the monopoly period.

The difference between these two parties arises from the productivity of their R&D spend. The incumbent already has in-house expertise on the product and process, so will have higher initial productivity than the generics firm that must first reverse-engineer the product and process from publicly available data. The effectiveness of the generics R&D spend will depend also on longer term dynamics, such as the overall strategy that the firm pursues, as outlined in part V.B. Both the innovator and the generics firm see diminishing returns on R&D spend after a certain point. Therefore the timing and the rate of investment is critical in determining whether the generics firms are able to overcome barriers to entry at any point and reduce the patent protected lifetime.

The model aggregates investment in process and delivery technology R&D with the costs of legal and regulatory proceedings.

Model Calibration

Data from several sources was used in setting the parameters for this model, and in producing the case study simulations. Average wholesale prices (AWP) were obtained from the Red Book™ publication by Thomson Reuters. These are self-reported, published prices that manufacturers charge distributors, and are used as an indicator of relative pricing. They were averaged across dosages to get an average price per mg. Market share data was obtained from analyst reports, mostly the dataset presented in Figure 81and Figure 82. The parameters for promotion spend were estimates based on anecdotes in PhRMA publications, media publications and trade journals. No data was available for IP investment or productivity.
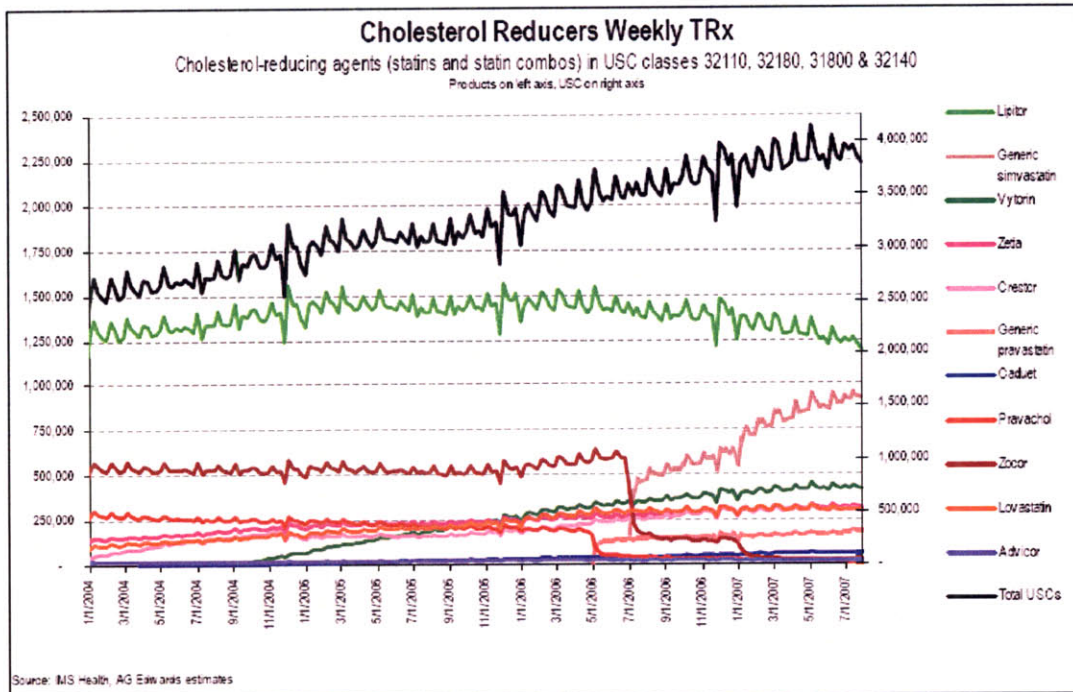
Figure 81: Number of statin prescriptions January 2004- July 2007 (Source: Tooley and Steadman, 2007)
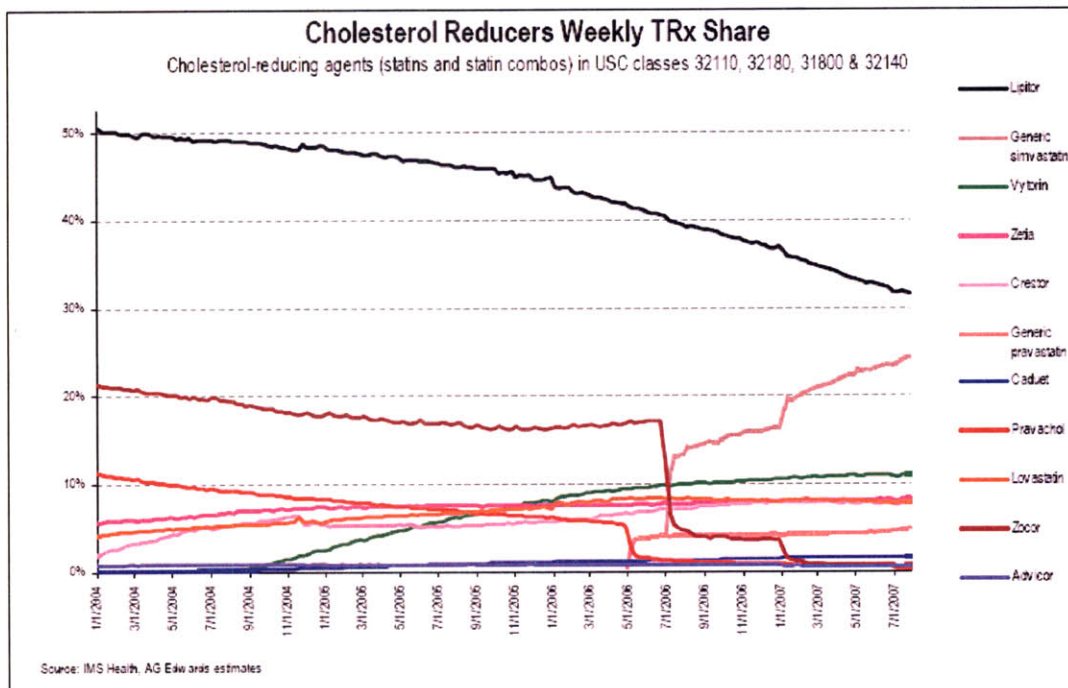
Figure 82: Market share of statins prescriptions January 2004- July 2007 (Source:Tooley and Steadman, 2007)

Case Study Simulation Results and Discussion

Anecdotal case studies of each of the statin products are in Appendix 2. Based on this data, the model was used to simulate the market dynamics for each product in the period surrounding patent expiry. Case studies focused on the price/ perceived PVI trade-offs for different products. We find that sequenced entry of products during the take-off phase of the market results in firms facing very different issues at patent expiry, depending on whether they were early, mid-stage or late entrants.

Mevacor® (lovastatin)

Market share for Mevacor® is about 17% five years prior to patent expiry. This is because it has low PVI relative to the other products in the market and the lower price is not sufficient to overcome this disadvantage. All the other products in the market are branded products, with large promotional campaigns, and there is little price competition as no generics have entered this market. Therefore PVI sensitivity is high (Figure 83). Promotional spend for Mevacor® has been used mostly for creating a market for statins, rather than differentiating lovastatin against other statins.

weight on PVI : Test lovastatin 4
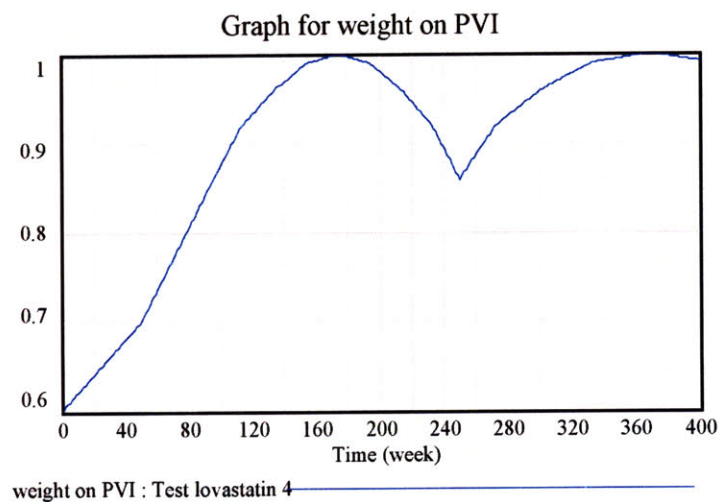
Figure 83: Weight on PVI for lovastatin

Market Share B : Test lovastatin 4
"Market share, G" : Test lovastatin 4
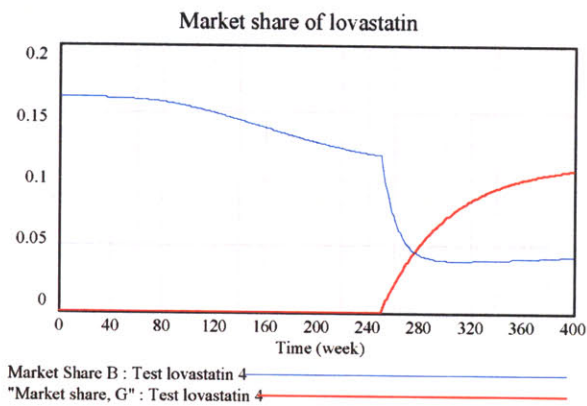
Figure 84: Mevacor® (B) and generic lovastatin (G) market share

"Revenues, B" : Test lovastatin 4
Revenues G : Test lovastatin 4
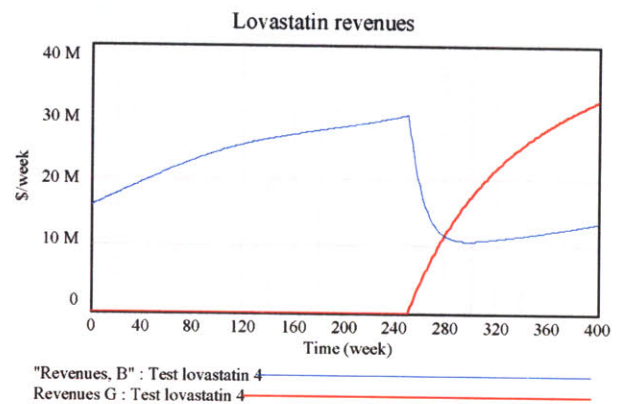
Figure 85: Revenues for Mevacor® (B) and generic lovastatin (G)

Options for maximizing returns on this product are limited at this stage. Price increases in the run- up to patent expiry leads to decreased market share for Mevacor® (Figure 84), but does create an increase in revenues (Figure 85). This seems a reasonable strategy to maximize returns, as does dropping price after patent expiry. This results in the slight upswing in market share and revenues for the branded product after patent expiry. These results suggest that the first entrant in the market must realize their returns earlier in the product's lifecycle, as they are at a significant disadvantage once several other players have entered. Me-too products have higher PVI and can take advantage of the sales and marketing efforts that the first mover must make to create a market for the new technology. If the PVI disadvantage is not very large, they could focus on other aspects of adding value to the customer, such as combination therapies and novel drug delivery technologies. However, if there are fundamental differences in therapeutic benefits, this will be difficult. Alternatively, they could use their expertise in this product to create a follow-on product, as Merck did with Zocor®. The final alternative is to drop prices dramatically, but this will accelerate the onset of price competition, which could erode profitability of follow-on products. For example, in this case, if Merck had dropped the prices of Mevacor®, they would have reduced the profitability of their follow-on statin product, Zocor®.

Pravachol® (pravastatin)

The Pravachol® case illustrates the trade-off that a firm must make between spending on promotion to boost market share and increasing prices to maximize revenue. We see the

initial effect of promotion, eventually being over-ridden by price increases that lead to loss of volume (Figure 86).
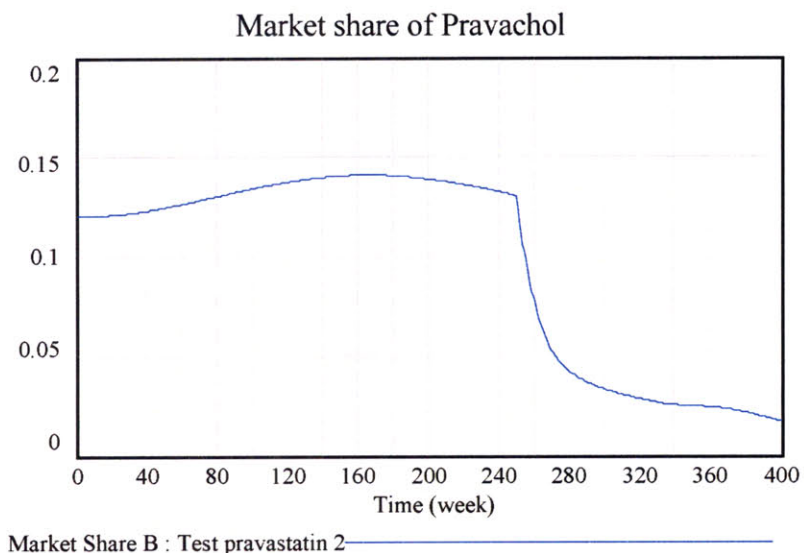
Figure 86: Market share of Pravachol®
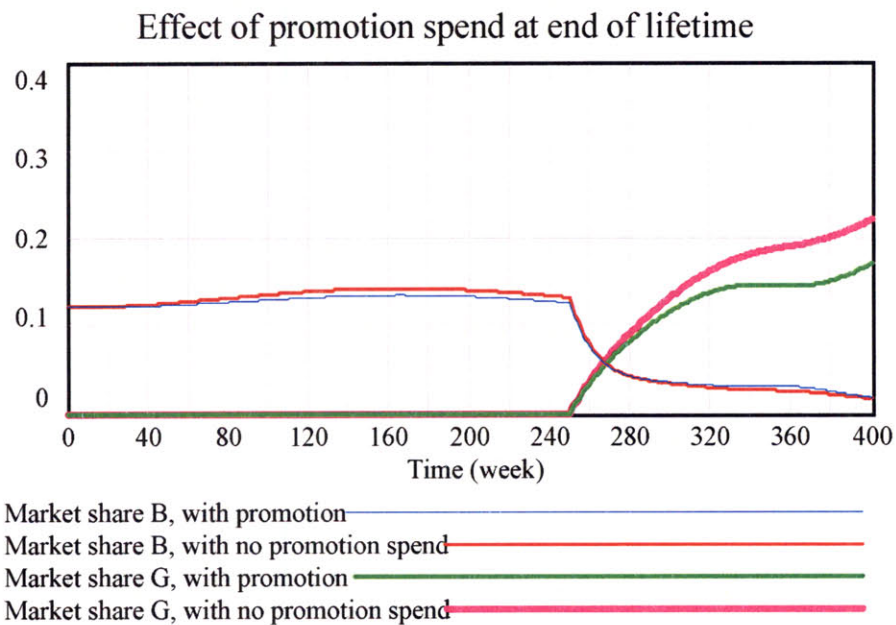
Figure 87: Effect of promotion spend on market share of Pravachol® and generic pravastatin

Effect of promotional spend on revenues
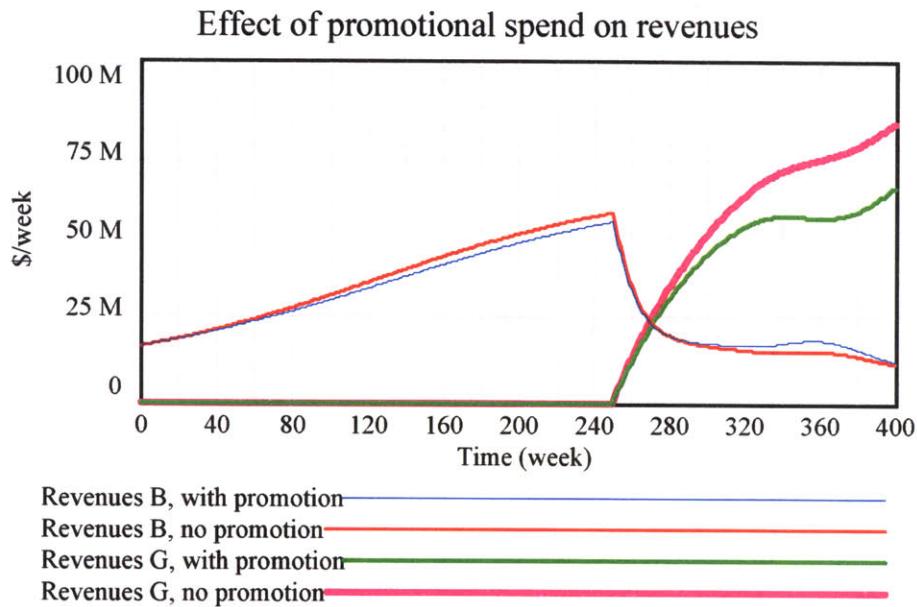
Figure 88: Effect of promotion spend on revenues of Pravachol® and generic pravastatin

The model suggests that the generics firms capture the majority of the benefits of the PVI boost generated by promotional spending close to patent expiry (Figure 87 and Figure 88). Therefore cutting promotion spending early and increasing prices are a better option for the branded manufacturer. At this stage of the market, only one product has generic equivalents, therefore there is strong competition on branding amongst the innovators, which will likely encourage the early players to continue to spend on promotion beyond the point where it is productive. This is to the advantage of the generics manufacturers of early products who can capture the benefits of the marketing with a price discount.

In the case of Pravachol®, the data indicates that the generics did not in fact capture more market share than the pre-patent expiry share of the branded product. The discrepancy between the model and the historic data is likely due to the "Prove-It" study that led to negative publicity for Pravachol® and probably also impacted the market share of the generics.

Zocor® (simvastatin)

Zocor® is the most expensive statin and was the most recent product to see generic entry. It required an intensive promotion spend to boost the perceived PVI high enough to justify its high price. Since patent expiry, generic simvastatin has not only taken away

market share from the branded product, it has also eaten into the market share for Lipitor® (Figure 81and Figure 82). Using the published prices in the model does not give this result (Figure 90), but testing the sensitivity of generic price discount indicates that there is greater substitutability for Zocor® (Figure 90) versus Pravachol® (Figure 89), i.e. generic simvastatin is able to take market share away from other statin products. The extent to which it is able to do so depends on the price of the generics. The discrepancy between the model and the actual market share data is likely due to the difference between published and negotiated price, as well as the effect of lower co-pays on generic simvastatin versus branded Lipitor®.

This result indicates that there is growing price sensitivity in the market and this stage can be described as the true onset of commoditization. Generics firms in this phase of market entry do not face a cap on volume, simply based on generic substitution. Instead they face a trade-off between pricing and volume. As competition within the generics market increases, the size (volume) of the simvastatin market will grow.
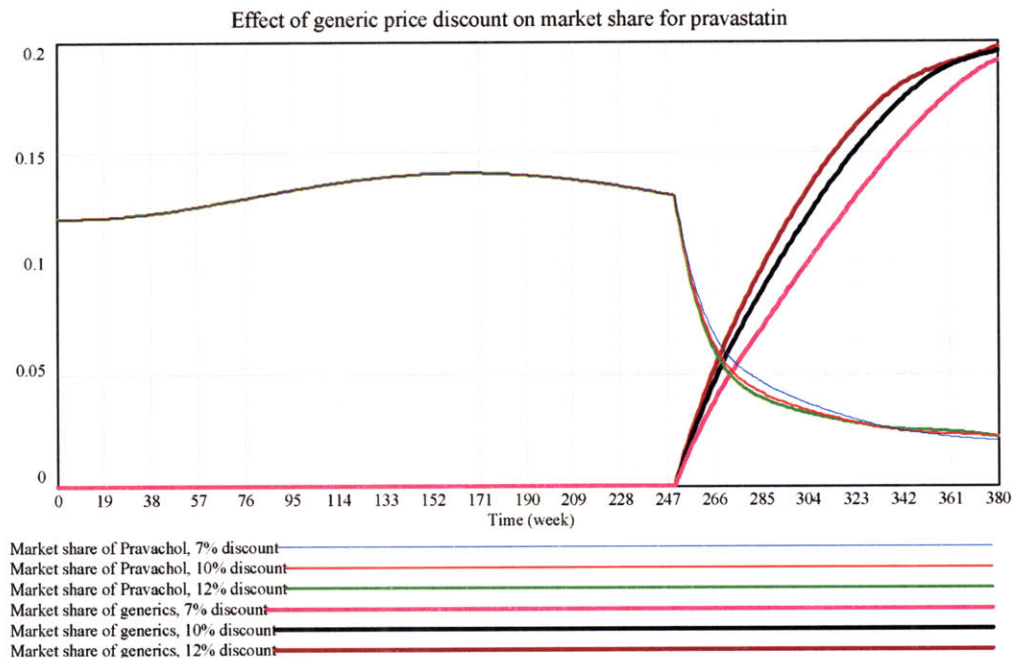
Figure 89: Effect of the generic entry price on market share of pravastatin

Effect of generics price discount on market share for simvastatin

Market share generic simvastatin, 7% generic price discount	——
Market share generic simvastatin, 10% generic price discount	——
Market share generic simvastatin, 12% generic price discount	——
Market share Zocor, 7% generic price discount	——
Market share Zocor, 10% generic price discount	——
Market share Zocor, 12% generic price discount	——
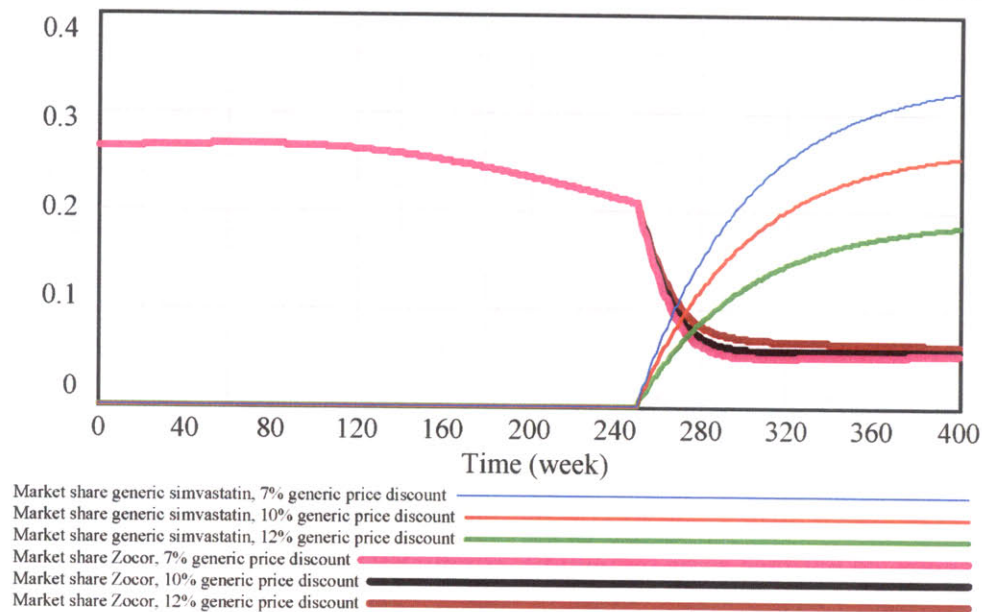
Figure 90: Effect of the generic entry price on market share of simvastatin

Lescol® (fluvastatin)

Lescol® was priced at the low end of the market and there was relatively low investment in promotion. Assuming that the model is calibrated correctly, based on the results for the other case studies, Lescol® ought to have a much larger market share based on its low price and relatively high PVI (Figure 91).

The fact that its market share is significantly lower than the predicted value suggests that branding efforts are still necessary to pursue a low-cost high-volume strategy as an innovator company. This reinforces that generics firms rely on the branded manufacturer to do a minimum level of sales and marketing to create a market for that product.

Effect of removing PVI contribution on Lescol market share

Relative perceived PVI = 0 ———
Relative perceived PVI >0 ———
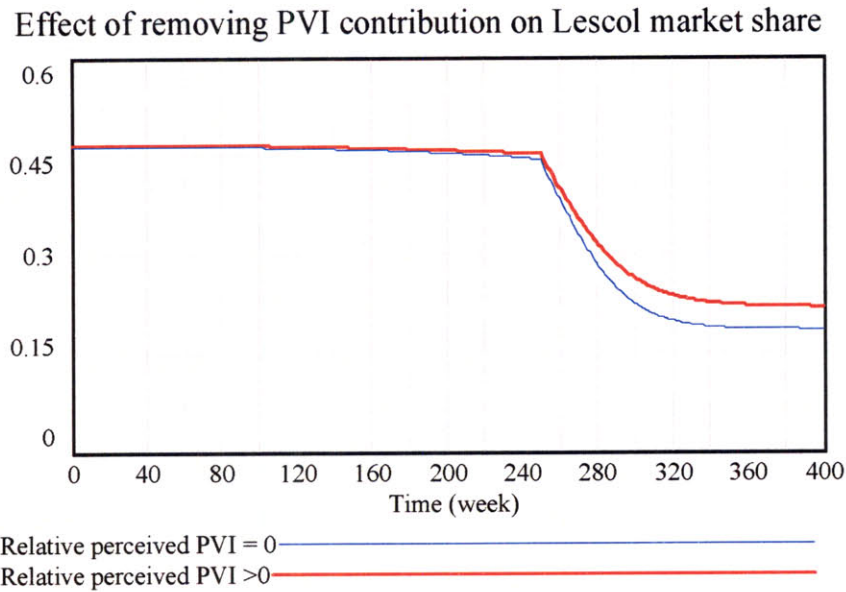
Figure 91: Predicted market share for Lescol®

Lipitor® (atorvastatin)

The entry of generic atorvastatin has been a much anticipated event, and will occur in November 2011. Lipitor's success has been driven by its high perceived PVI, which has allowed it to capture market share as high as 50 - 60%. However, with growing price competition, market share has been declining. In response, Pfizer has been increasing the price of Lipitor® and has cut promotion spending. With three statins already off-patent, and simvastatin considered a potential substitute, competition has clearly shifted from PVI to price (Figure 92).

Weight on PVI
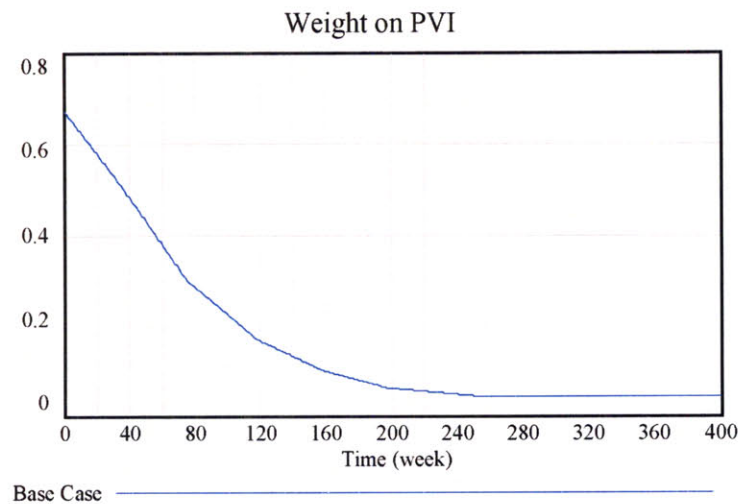
Base Case ————

Figure 92: Weight on PVI for Lipitor®

The model was used to simulate the results of (i) a base case scenario of continuing price rises at the current rate, (ii) freezing prices at their current level and (iii) reducing prices. The effects on market share and revenues are shown in Figure 93 and Figure 94. Continuing price hikes result in the 'cliff' profile seen for earlier products. Freezing prices at their current levels may be an effective strategy for Lipitor®, as it would reduce the margins at which Ranbaxy can enter the market. It would also allow theoretically allow Lipitor® to compete after patent expiry. However, the model does not incorporate state laws requiring pharmacists to substitute a generic product for all prescriptions, unless stated otherwise. These laws will cause the market to tip in favor of generics firms.
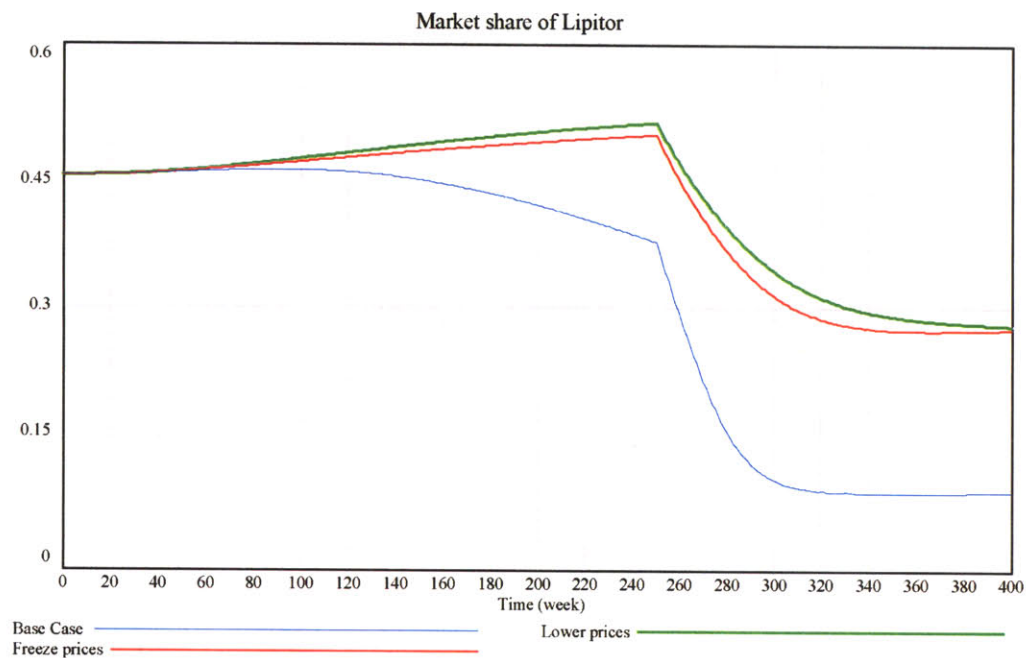
Figure 93: Pricing scenario analysis for Lipitor® market share
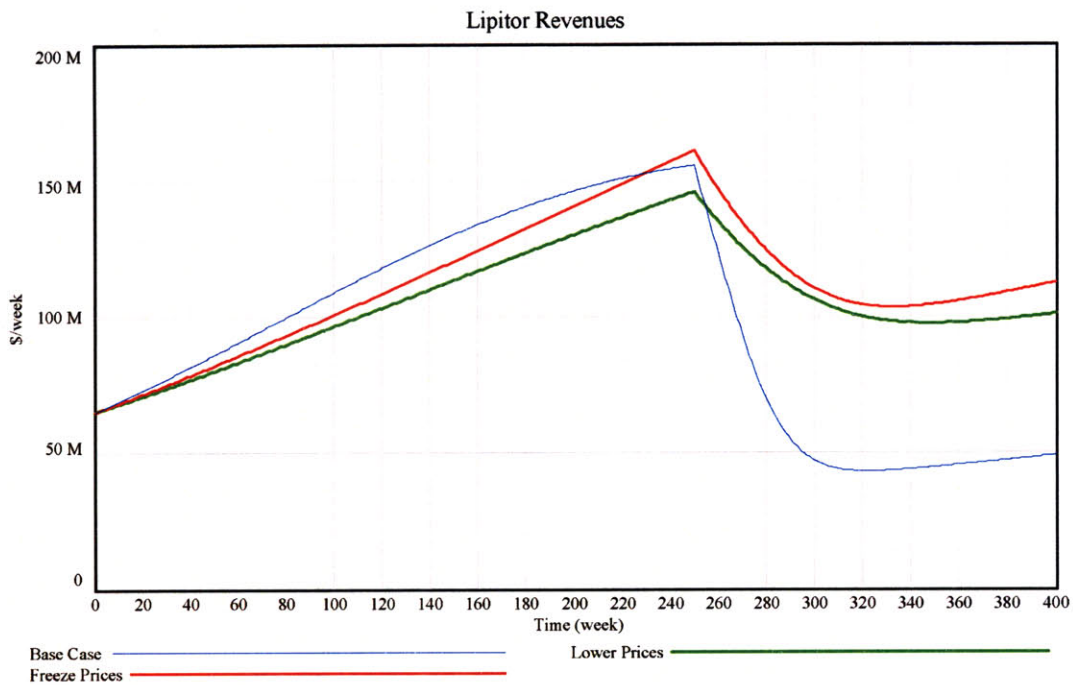
Figure 94: Pricing scenario analysis for Lipitor® revenues

Crestor® (rosuvastatin)

Crestor® will be the last statin product to face patent expiry. As such, it will be competing against the generic versions of all its predecessors. Competition will clearly be driven by price, and it is possible that some generics firms may exit the market or pull out of certain products in the US if they are unable to operate profitably. In order to get FDA approval, Crestor® clearly had to demonstrate some PVI advantage, but in order to capture market share, it must be in a price range that allows for market sensitivity to that PVI difference. Astra Zeneca appears to be following this strategy, pricing at the low end of the market. The base case simulation suggests that they may be able to get into the virtuous promotion cycle if they can profitably set prices very close to the market average, by having low average costs. This is one way to bring competition away from price and back to perceived PVI (weight on PVI is 0.67). PVI can then be influenced through promotion. Astra Zeneca will be able to utilize its strong sales and marketing organization to compete against the generics firms, who do not have the same capabilities.
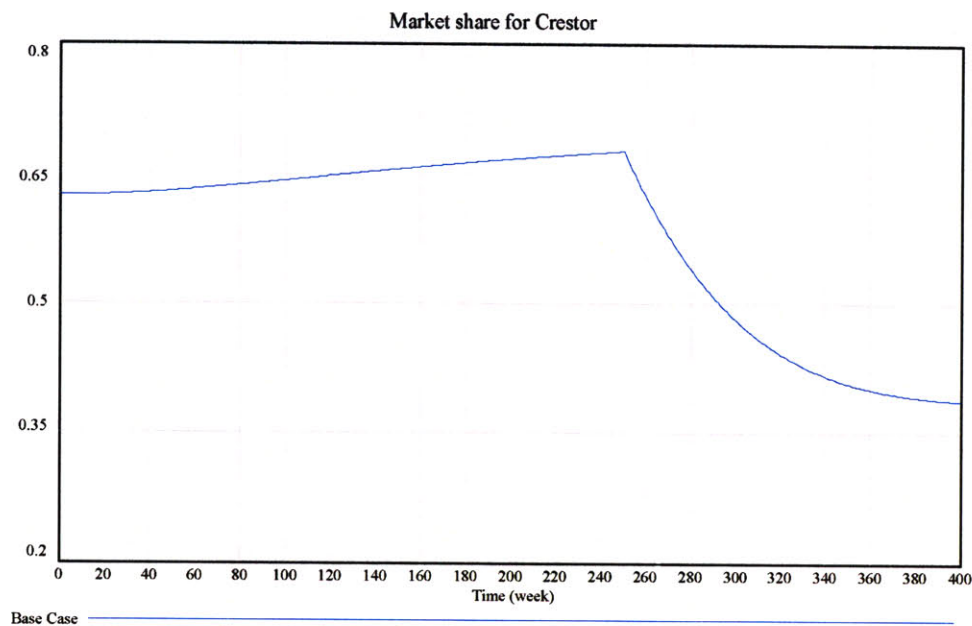
Figure 95: Base case market share for Crestor®

The Significance of Sequenced Patent Expiry on Strategic Decisions

The model simulates the market dynamics of the branded and generic products in the period surrounding patent expiry. It is able to capture the effects of different market conditions that firms face at patent expiry, based on whether they were early, mid-stage, or late entrants to the statin market. This determines whether competition is largely on brand and perceived product value index (PVI), or on price (and eventually on low production and distribution costs).

Early entrants face patent expiry during a period where competition is largely on perceived PVI, and their low relative PVI puts them at a disadvantage to compete in the market. Their profit maximizing strategy during this period is to maximize revenues by increasing prices. Promotional spending very close to patent expiry may translate into more benefit for the generics entrant than the innovator. The early entrants may be well-positioned to create follow-on products within the same market, as Merck did with Zocor®.

Mid-stage entrants see the transition from competition on perceived PVI to price, and the onset of commoditization is clearly seen at this stage. Prior to patent expiry, these products can capture market share through heavy promotion to emphasize their PVI

differences. This allows them to charge high prices and realize large profits as they get into a virtuous cycle. There are incentives to invest in lavish promotion campaigns while revenues are strong, but these can breed skepticism or generate backlash amongst the medical and payer communities and bring an end to the virtuous cycle. As more of the earlier products lose patent protection, competition shifts to price. There is increased substitutability between products during this period, as a result of the diminishing returns on R&D seen in Ngai's model.

Late stage entrants must compete in a market dominated by price competition. By the time they approach the end of their patent life, not only have all the earlier products seen generic entry, there has been considerable competition within the generic sub-markets, leading to price erosion. In order to be a player in the market, they must price at, or just slightly above the average price. This may enable them to get into a virtuous cycle and use their sales, marketing and brand management capabilities to differentiate their product. If there is intense price competition, all product prices will converge and a small PVI advantage may be enough to steadily gain market share. However, this strategy is only profitable until severe price competition in a crowded market drives margins to zero.

Intellectual Property Investments

A portion of the model incorporates spending on defensive IP by the innovator firms as well as anticipatory investment in R&D by the generics firms. Creating this model highlighted some key issues that require further data on investment decisions to explore this phenomenon further. First of all, the branded manufacturers face a positive feedback loop, whereby the more successful their product, the more they need, and are willing, to invest in defensive IP to prolong their monopoly. This results in higher barriers to entry that will extend patent lifetime, and allow them to spend more on defensive IP. These investments have a much longer time horizon than promotional spend, due to the timelines for research and development.

There are longer time horizons involved in the evolution of productivity of the generics firms (as mentioned in part V.B). Sequencing of patent expiry could also play a part here, with learning from the IP generated by earlier statin products leading to investment rates being a function of entry position.

V.D: Conclusions and Further Work

The market for statins has evolved in a way that is largely consistent with the theory on technology market dynamics. Pharmaceutical markets differ from the standard models due to the presence of heavy regulation that restricts and sequences the entry of firms. A complex supply chain and reimbursement structure means that pricing can affect market dynamics in a highly non-linear manner. Complementary assets are vital in determining a firm's ability to execute an effective strategy during this period. The relative importance of the type of assets differs between innovators and generics manufacturers.

A system dynamics model has been created that simulates the competition between the branded and generic versions of a single statin product during the period surrounding patent expiry. Case studies of each of the statin products indicate that competition shifts from brand and perceived product value index (PVI) to price as the market evolves. Therefore firms must compete differently depending on whether they were early, mid-stage or late entrants into the market. Positive feedback loops can create incentives for over-investment in promotion and R&D, particularly for the mid-stage entrants. Late stage entrants must price at par with generics in order to have effective promotion and gain market share.

This model considers all generic players to be equal, and considers the generics response of multiple firms in aggregate. However, there is considerable heterogeneity between generic firms and generic entry is sequenced, each phase requiring different capabilities and entry strategies. System dynamics would be an appropriate tool to explore these sequencing effects and further work should focus on the effects of heterogeneity and competition on the evolution of the generics market.

Firms that pursue an aggressive patent challenge strategy compete to be early entrants and capture a brief period of market protection. A firm's ability to successfully challenge patents will evolve over time as it builds up capabilities in R&D, international patent law and regulatory procedures.

The number of firms that enter after the 180 day exclusivity period is likely a function of the pre-patent expiry revenues, and the decision to enter the market will be based on their experience in manufacturing/sourcing certain compounds and formulations (Scott-

Morton, 1998). In addition, their ability to capture market share in a competitive market will depend on their supply chain capabilities and relationships, and ability to differentiate themself through a brand.

There are also late entrants who apply for ANDAs after the patents have expired, and whose profitability is less than assured in a crowded market. Some assessment of likely profitability is required to justify investing in the manufacturing capacity required to file an ANDA.

Although annual reports give some indication of each firm's strategy, as outlined in the appendix, much of this information is not available in the public domain, so I recommend an interview-based approach to data collection for the next portion of the work stream.

Acknowledgements

V.E Appendices and Bibliography

Appendix 1: Profiles of Firms in the US Generic Statins Market

Actavis Elizabeth LLC

The Actavis group is headquartered in Iceland. They have grown through aggressive acquisition, particularly in India, China, and Eastern Europe, and have a global network of R&D, manufacturing and sales and marketing facilities. The firm was taken privatize in 2007 and is currently owned by the group's chairman, Thor Bjorgolfsson. Their strategy focuses on low-cost operations, and being fast to market through investment in regulatory and development expertise (Actavis, 2009).

In the USA, they operate five manufacturing sites, with solid-dosage manufacturing concentrated in New Jersey. They completed two major acquisitions (Amide and Alpharma) in 2005 to enter the US market and create the 8th largest US generics firm. Following these acquisitions, they launched a marketing campaign to consolidate under the Actavis brand (Actavis, 2005). Out of the statin products they market only lovastatin in the US, now sold under their own brand.

Apotex

Apotex is a Canadian firm focused on the generics market. They are vertically integrated and make their own API and formulations, as well as doing their own marketing and distribution (Apotex, 2009).

Dr Reddy's Laboratories Ltd.

Dr Reddy's is a vertically-integrated pharmaceutical firm based in Hyderabad, India. It is a public company, cross listed on the NYSE.

The firm has had FDA approval to market generic statins in the US since 2006. They currently market simvastatin and pravastatin in the US under their own name. They had 15% of the current simvastatin market in the US in June 2008 (Reddy, 2009). Their strategy is to be aggressive in ANDA filings (particularly under para IV), and have an experienced North American team in sales, marketing, regulatory, sales operation and supply chain (Reddy, 2008).

Lupin Pharmaceuticals Inc.

Lupin Pharmaceuticals Inc. is a US subsidiary of Lupin Ltd, an Indian pharmaceuticals manufacturer. They entered the US market in 2003 (Lupin, 2009).

Mylan Laboratories

Mylan is a US pharmaceuticals firm that started as a distributor and has moved into generics and branded products. They have operations in 140 countries, having grown through acquisitions, including Merck KGaA's generics business, a controlling stake in Matrix Laboratories, Hyderabad, and UDL, the largest unit-dosage packaged product company in the US. (Mylan, 2009)

RanbaxyLaboratories Ltd.

Ranbaxy is a publicly listed company based in India. They have an aggressive strategy of filing ANDAs under paragraph IV, and have first-to-file rights for both pravastatin and simvastatin (80mg). They have also been contesting Lipitor® patents worldwide, and have come to an agreement with Pfizer that allows them to launch atorvastatin in the US market from November 2011 (FT, 2008a). They received first to file on 80mg pravastatin in 2007, and captured 30% of prescription market share during the 180 day exclusivity period (Ranbaxy, 2007).

Ranbaxy Pharmaceuticals Inc. is a wholly owned US subsidiary that was established in 1994, and operates in the generic, branded and OTC space. They are aiming for growth through organic means, in-licensing and acquisition. Their product strategy focuses on aggressive IP challenges, ANDA submissions and developing 'niche' products (Ranbaxy, 2009).

Sandoz

Sandoz is the generics division of Novartis AG and is headquartered in Germany. They have manufacturing sites in Latin America, Europe (Poland, Slovenia, Austria, Turkey and Germany), India and the North America (Novartis, 2009). Their strategy is to focus on higher-value generics that are difficult to make and have limited competition (Novartis, 2007). They entered the statin market through the acquisition of Geneva pharmaceuticals in 2003, and filed ANDA applications for simvastatin.

Teva Pharmaceutical Industries Ltd.

Teva is a global generics firm incorporated in Israel and operating in the US through a subsidiary, Teva Pharmaceuticals USA Inc., who market 320 generic products in more than 1,000 dosages. They are the leading manufacturer of generics in the US. They focus on first-to–market strategies, including through paragraph IV filings, broadening their product portfolio, vertical integration in production, as well as investing in R&D capabilities, and increasing market share through acquisitions and collaborations. In 2008, Teva grew their US market share through the acquisition of Barr pharmaceuticals in 2008 (Teva, 2008) and Ivax corporation in 2006.

Watson Pharmaceuticals Inc.

Watson is a US-based pharmaceuticals firm with operations in North America and Asia. Developing and marketing generics now makes up 60% of their revenues. Their plans for the future include being more aggressive with para IV filings. They focus their generics R&D on drug delivery systems in order to differentiate themselves in the generics market. They use a manufacturing site in Goa, India for products that can benefit from low-costs and high volumes. They have forward-integrated, creating Anda, a pharmaceutical distribution division. They see this as a way to develop 'stickier' relationships with pharmacies, and ensure good penetration of their products (Watson, 2008).

Zydus Pharmaceuticals (USA) Inc.

 Zydus is a generics-focused subsidiary of Zydus Cadila, a vertically integrated Indian pharmaceutical firm with a global presence. They have expressed an interest in pursuing difficult-to-make formulations, and have built up expertise in formulation and drug delivery methods. Zydus has 70 R&D personnel dedicated to the US market.
Their strategy focuses on supply chain excellence with low costs as well as US marketing partnerships with Covidien and other parties. They have their own product distribution system and source bulk chemicals and APIs from their manufacturing sites in India, which are operated by the parent company. Their goal is to move to developing their own products by 2015 (Zydus, 2009).

Appendix 2: Case Studies of Statin Products

Mevacor® (lovastatin)

Mevacor® was the first statin product to go off patent in December 2001 (FDA Orange Book, 2007). By the time it reached the end of its patent life, Mevacor® was priced below the average for the market. Merck-SP raised the prices of the branded product in anticipation of patent expiry, and kept prices constant for six years following expiry (Figure 96). Price now appear to be converging to generics prices, which have remained constant since 2001 when they entered the market at a 10% discount to the branded product price. Interestingly, the extended release version, Advicor, has seen rapid price increases.
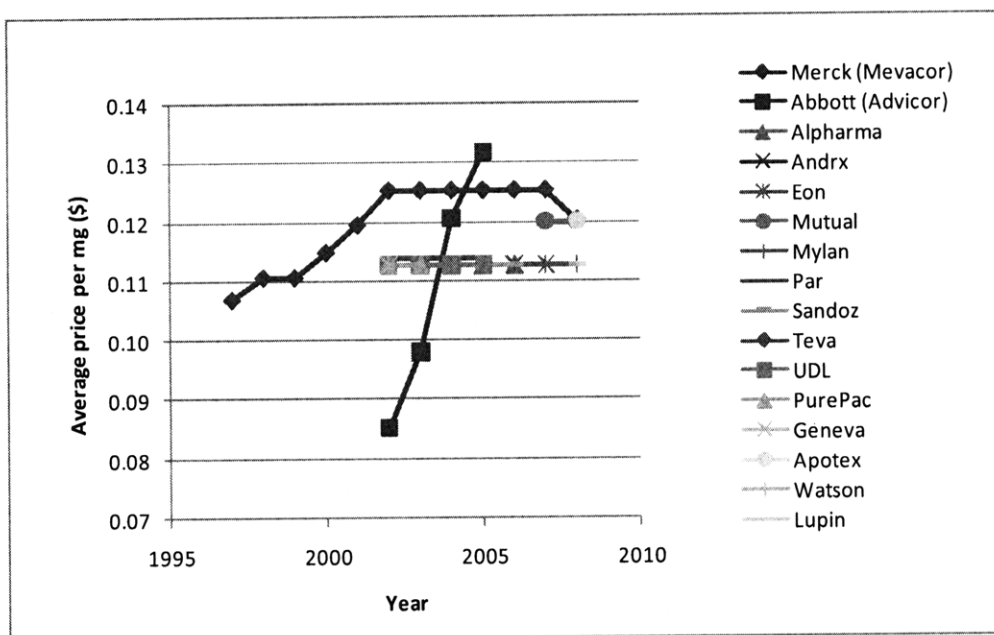
Figure 96: Lovastatin average wholesale prices (own analysis, based on data from Red Book™)

As the first statin product, a considerable part of promotion focused on educating physicians and patients of the new technology. By the time that Mevacor® was facing generic entry, Merck-SP had a new statin product (Zocor®, simvastatin) in the market. Therefore, they were shifting promotional spend from Mevacor® to Zocor® (Liebman, 2001). Data from analysts reports suggests that lovastatin had a market volume share of approximately 5% in early 2004, that was rising slowly, with approximately 8% of the statin market in 2007 (see Figure 82).

Pravachol ® (pravastatin)

Pravachol® was the second statin product to face generic entry in 2006. Teva won 180 day exclusivity for the 10, 20 and 40 mg dosages starting in April 2006 and Ranbaxy had exclusivity for the 80mg starting in April 2007 (FDA, 2009b). BMS raised prices aggressively in the run-up to expiry and has continued to increase prices on the branded product (Figure 97). Generics entered the market at a 12% price discount to the branded product and have so far seen no price erosion. Pravachol® saw a decline in its market share from about 12% in early 2004 to 5% just before generic entry.

BMS invested heavily in promotion, spending $210 million in 1997, and $200 million in 2000 (Liebman, 2001). In 2004, they published the results of a four-year study (sponsored by BMS) comparing the efficacy of Pravachol® and Lipitor®. BMS had believed that the study would demonstrate equivalence, however the study showed that Lipitor® led to a lower rate of mortality of 2.2% versus 3.2% for Pravachol® (WSJ, 2004).
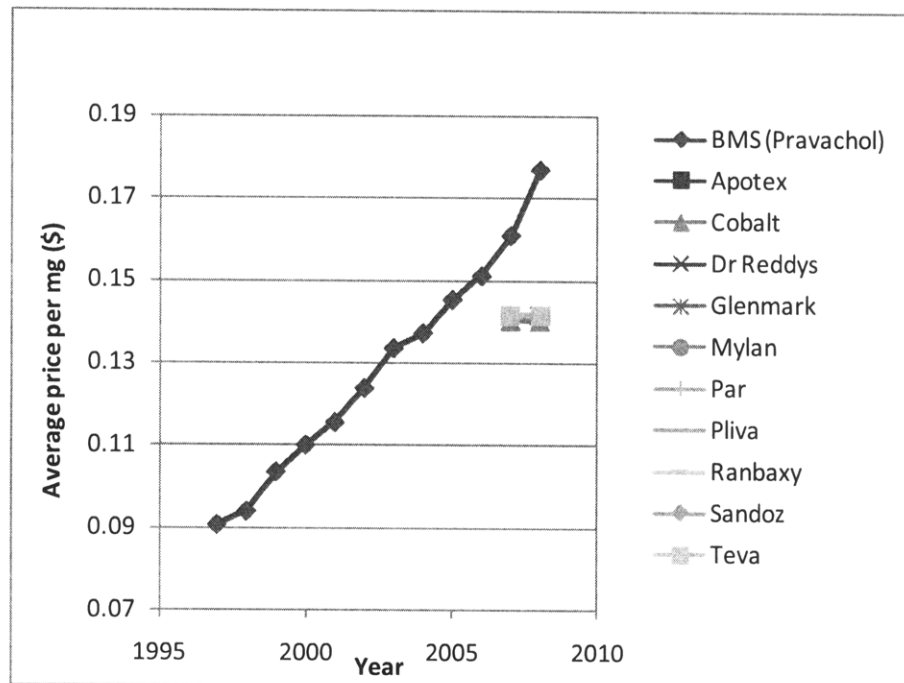
Figure 97: Pravastatin average wholesale prices (own analysis, based on data from Red Book™)

Zocor® (simvastatin)

Zocor® lost patent protection just three months after Pravachol®, in June 2006. Ivax pharmaceuticals won 180 days of market exclusivity for the 5, 10, 20, 40mg dosages and Ranbaxy won exclusivity for the 80mg dosage (FDA, 2009b).
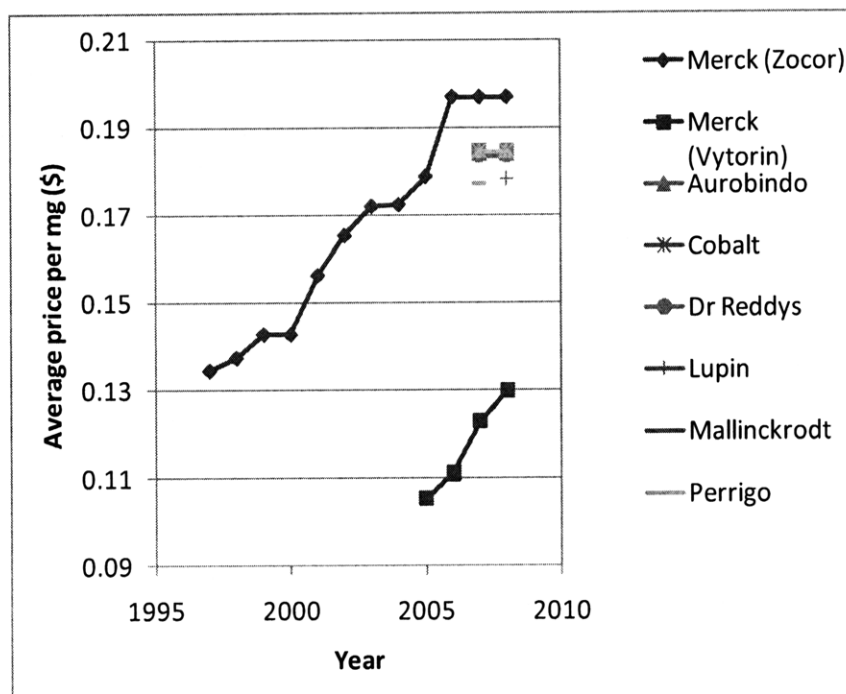
Figure 98: Simvastatin average wholesale prices (own analysis, based on data from Red Book™)

Zocor® is the most expensive statin per mg, based on the published prices. Merck-SP raised prices prior to expiry and has kept them constant since then. The generics firms entered the market at a 7% discount to the branded price, and most have stuck to the same price, although a couple of firms appear to be trying to undercut the market (Figure 98). In 1997, Zocor® led the statin category in promotion spend, with $265 spent dominantly on samples. In 2000, annual spend was still high, but second to Lipitor®, at $180 million. By 2006, Merck- SP was also marketing a combination therapy, Vytorin®. As patent expiry for Zocor® approached, marketing efforts were focused on shifting patients from Zocor® to Vytorin®. However, these efforts were impacted by the release of the 'Enhance' study in 2008 that reported that Vytorin® delivered no benefit over Zocor® on important dimensions (The Economist, 2008). Merck and Schering Plough received considerable bad press for this result, particularly as the study had been completed in 2006 and release of the results had been delayed for two years.

Since Zocor® has gone off patent, the market share of generic simvastatin has risen above the Zocor® market share (Zocor® market share in 2004 was 22%, generic simvastatin market share in mid 2007 was 25%). This has been primarily at the cost of Lipitor® market share (Figure 82).

Lescol® (fluvastatin)
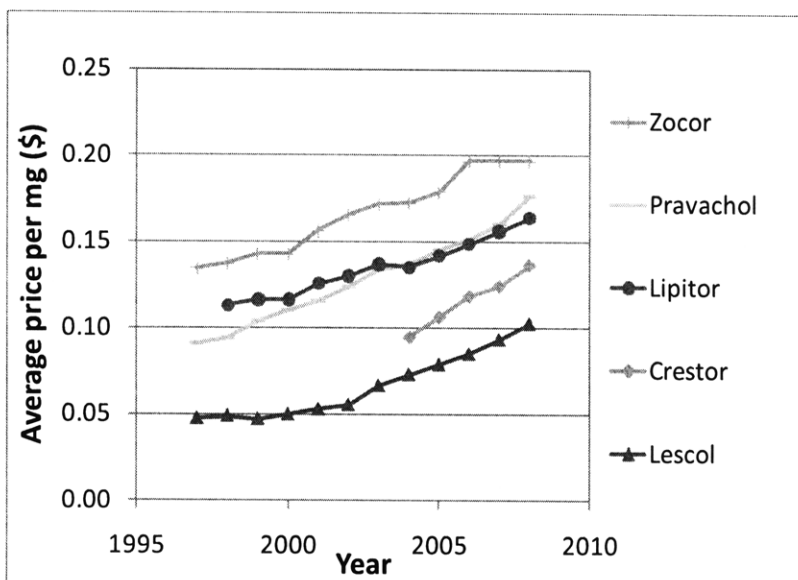
Figure 99: Average wholesale prices of branded single-active ingredient statin products 1997-2008 (own analysis based on data from Red Book™)

Lesco®l is the lowest priced product out of the statin products (Figure 99). It is manufactured by Novartis, and patent expiry is anticipated in 2012. Novartis consistently spends less than its competition in promoting Lescol®, In addition to having no direct-to-consumer advertising, and relatively low levels of detailing, they also attempt to sell on the price discount, rather than by differentiating on therapeutic benefits (Liebman, 2001). No data was available on Lescol® market share, but given that US sales in 2008 were $154 M (Table 18) versus $1,678 M for Crestor® and $6,300 M for Lipitor®, we can assume it is small, even after accounting for the lower price.

Lipitor® (atorvastatin)

Lipitor® is the most well-known of the statin products and has had up to 50 - 60% market share at its peak in 2000-2003. This was despite the fact that it was the fifth product to enter the statins market. Currently, it is losing market share, largely to generic simvastatin, although it still had about 33% of the market in mid 2007. Pfizer had a large

branding campaign for Lipitor®, spending $285 million on promotion in 2000 (Liebman, 2001).

Lipitor® has been generally perceived to be superior to other statins. Initially it was sold on its ability to reduce cholesterol levels more aggressively than other products, but further studies have demonstrated its success in lower cardiac events and mortality.

Lipitor® has faced the most aggressive and public IP challenges from a variety of firms. In June 2008 Ranbaxy won a court ruling allowing it to market generic atorvastatin in the US from November 2011 (FT, 2008a). However, they were fielding challenges as early as 2003.

In terms of pricing, Pfizer has been a price-leader, partly as a result of its large market share. Lipitor® has been consistently priced slightly above the weighted market average.

Crestor® (rosuvastatin)

Astra Zeneca bought Crestor® to be the sixth entrant in the statin market. It has been priced at the low end of the market (Figure 99) and has been consistently gaining market share, despite being a late entrant. However, the trajectory in Figure 82 suggests that it is unlikely to gain more than 10-15% market share. Astra Zeneca have invested in the 'Jupiter' trial which demonstrated that Crestor® reduced the likelihood of severe heart attacks, but did not attempt to do a head-to-head comparison with other products (FT, 2008b). The patents on Crestor® are anticipated to expire in 2015 (Figure 77).

Appendix 3: Model documentation

The model (Statin Patent Expiry.mdl) consists of three views. View one (Figure 100) contains the market share allocation for the branded product manufacturer, and the promotion feedback loop. View 2 (Figure 101) consists of the market allocation for other players in the market. View 3 (Figure 102) is the generics firms' perspective and includes the IP investment model.
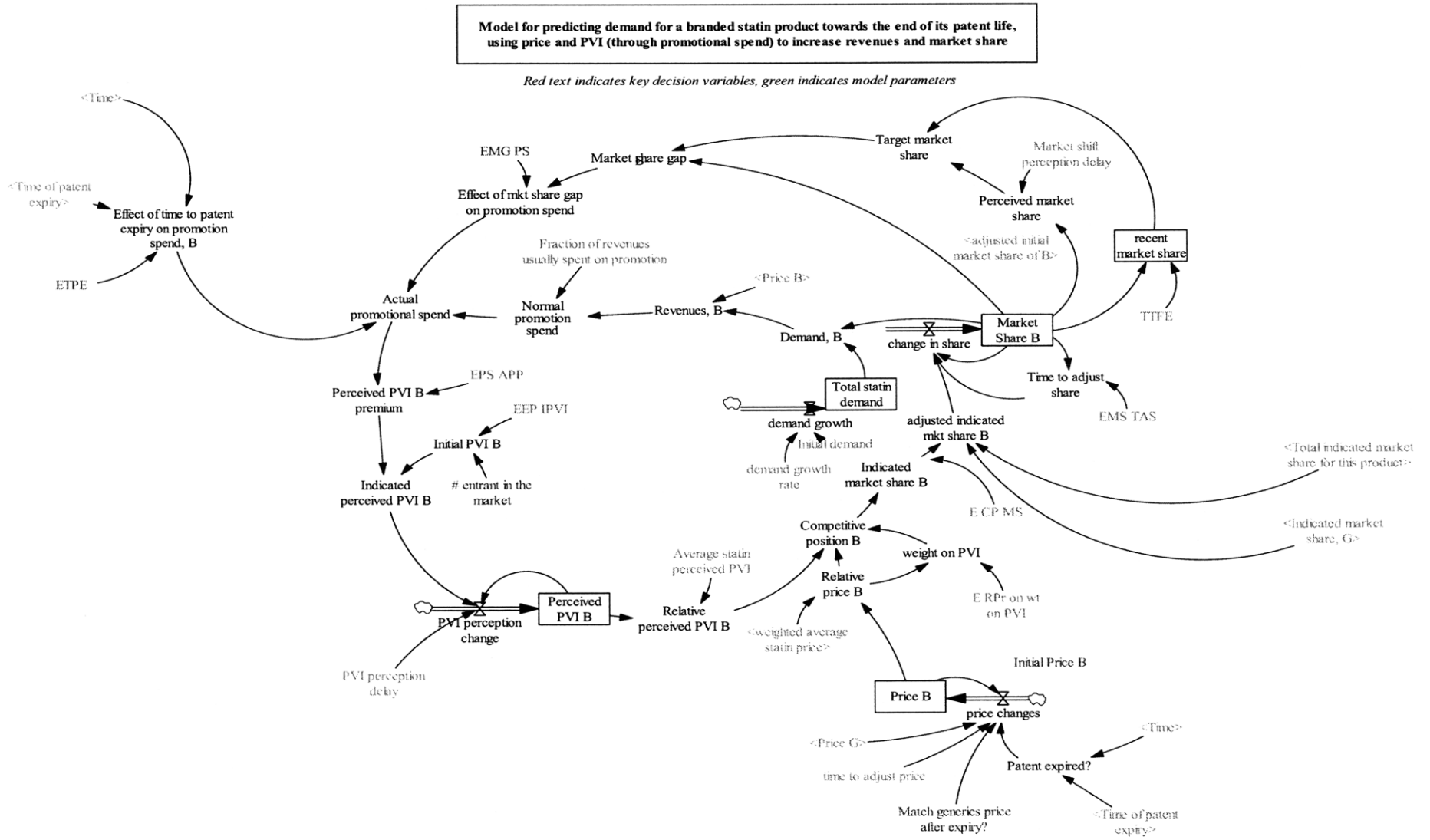
Figure 100: Model View 1: Market share for the branded product and the effects of promotional spend
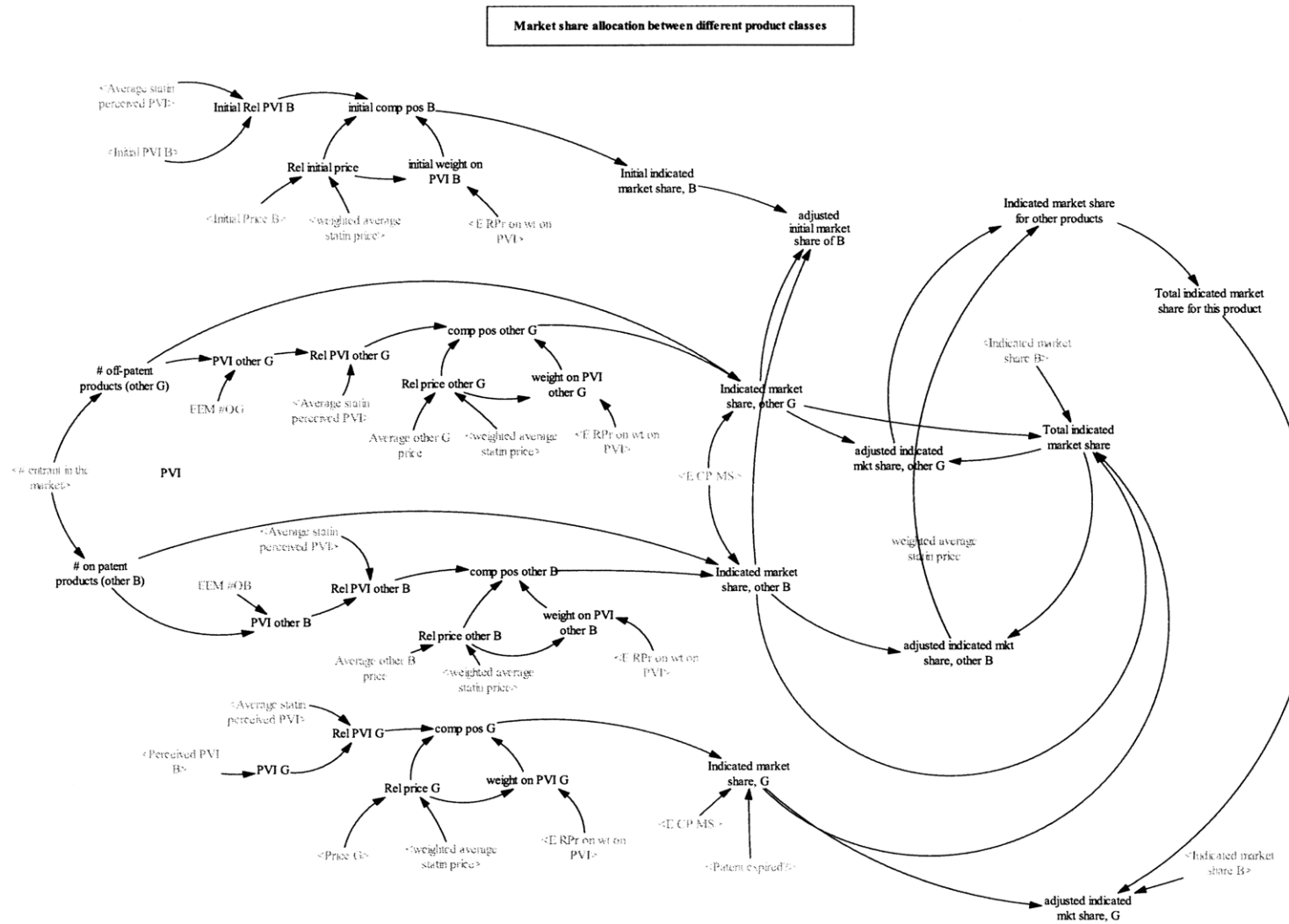
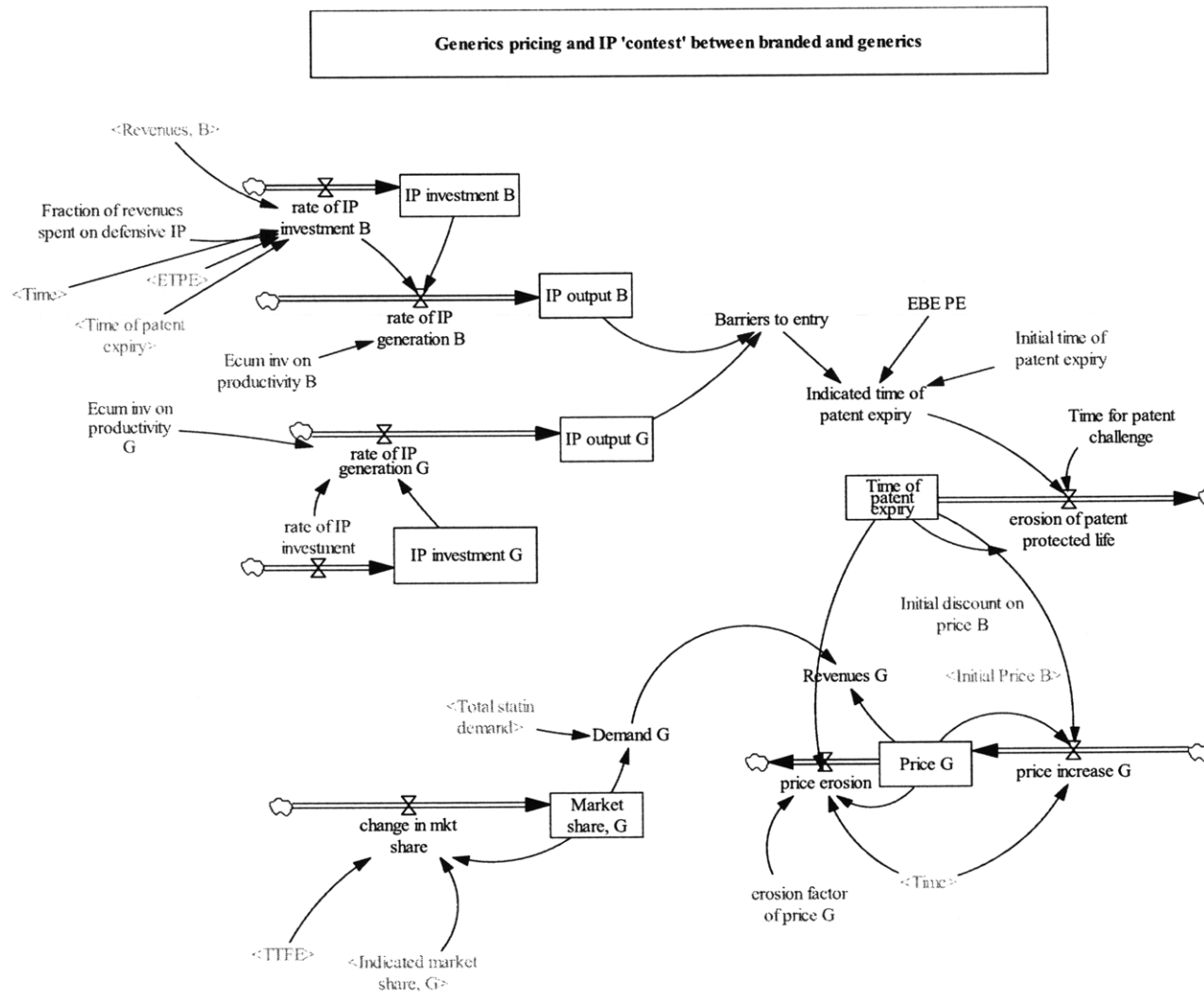**Figure 101: Model View 2: Market share allocation**

Figure 102: Model View 3: Market share of generics and IP investments by the branded and generics manufacturers

The model equations are documented below, with inputs for the Crestor® base case simulation.

"Indicated market share, other B"=   IF THEN ELSE("# on patent products (other B)"=0, 0 , E CP MS(comp pos other B))   ~   ~ |
"Indicated market share, other G"=IF THEN ELSE(("# off-patent products (other G)"=0),0,E CP MS(comp pos other G)) ~   ~ |
Indicated perceived PVI B=Initial PVI B+Perceived PVI B premium   ~   ~|
Actual promotional spend=   Effect of mkt share gap on promotion spend*Normal promotion spend*"Effect of time to patent expiry on promotion spend, B"   ~$/week ~|
Indicated time of patent expiry= Initial time of patent expiry+(EBE PE(Barriers to entry)) ~
        ~|
price changes= IF THEN ELSE("Patent expired?",IF THEN ELSE("Match generics price after expiry?", ((\Price G-Price B)/time to adjust price), 0),Price B*-0)   ~ $/mg/week ~|
Indicated market share for other products= SMOOTH("adjusted indicated mkt share, other B"+"adjusted indicated mkt share, other G", 200)   ~   ~ |
Total indicated market share for this product=1-Indicated market share for other products ~|
adjusted indicated mkt share B= Indicated market share B*Total indicated market share for this product/(Indicated market share B+"Indicated market share, G") ~ ~ |
"adjusted indicated mkt share, G"=   "Indicated market share, G"*Total indicated market share for this product/(Indicated market share B\ +"Indicated market share, G")~ ~ |
erosion factor of price G=   0   ~   ~ |
erosion of patent protected life= MIN(0,-(Time of patent expiry-Indicated time of patent expiry)/Time for patent challenge)   ~   ~ |
Time for patent challenge=   50   ~   week ~ |
EBE PE([(-25,-60)-(25,60)],(-25,-52),(-10,-52),(-7,-45),(-5,-40),(-4,-35),(-3,-30),(-2,-20),(-1,-8),(0,0),(1,8),(2,20),(3,30),(4,35),(5,40),(7,45),(10,52),(25,52))   ~   ~|
"Indicated market share, G"=   "Patent expired?"*E CP MS(comp pos G)   ~   ~|
Normal promotion spend=   Fraction of revenues usually spent on promotion*"Revenues, B"
        ~ $/week ~ |
price erosion= IF THEN ELSE(Time>(Time of patent expiry+26), Price G*erosion factor of price G, 0)   ~   ~ |
"Effect of time to patent expiry on promotion spend, B"= ETPE(Time of patent expiry-Time)
        ~   ~   ~   :SUPPLEMENTARY |
rate of IP investment B=   ("Revenues, B"/1e+006)*Fraction of revenues spent on defensive IP*ETPE(Time of patent expiry\   -Time) ~ $/week ~ $ in millions |
Time of patent expiry= INTEG (erosion of patent protected life, Initial time of patent expiry)
        ~   ~ |
ETPE([(-400,0)-(400,1)],(-400,0),(0,0),(28.1346,0.0131579),(50,0.05),(70,0.2),(100,0.5),(\
        120,0.8),(140,0.95),(162.691,0.991228),(400,1)) ~   ~ |
Barriers to entry=IP output B-IP output G   ~   ~ |
Effect of mkt share gap on promotion spend= EMG PS(Market share gap B)   ~   ~
        |
E CP MS([(-1,0)-(1,1)],(-1,0.001),(-0.9,0.005),(-0.761468,0.0175439),(-0.522936,0.0482456),(-0.425076,0.0745614),(-0.33945,0.100877),(-0.25,0.140351),(-0.217125,0.162281),(-0.168196,0.192982),(-0.119266,0.22807),(-0.058104,0.27193),(-0.00917431,0.307018),(0.1,0.4),(0.2,0.5),(0.5,0.63),(0.7,0.69),(0.8,0.72),(0.9,0.74),(1,0.75))
        ~   ~   Effect of competitive position (range approx -1:1) on market share.
                Current market share for older products (low PVI and low price) is about \

2-3%, average products are in the range 10-20% and lipitor is in the \
50-60% range |
comp: b, other b, g, other g   ~   index   ~ |
PVI[b]=   2 ~~|
PVI[other b]=   3 ~~|
PVI[g]=   1.5 ~~|
PVI[other g]= 1.25   ~   ~   ~   :SUPPLEMENTARY |
Ecum inv on productivity B([(0,0), (600,1)], (0,0.2), (12,0.18), (25,0.16), (50,0.13), (75,0.1),
(100,0.08), (125,0.06), (150,0.04), (175,0.03),(200,0.02),(225,0.01),(250,0.01), (500,0.005))
        ~   patents/$ ~ $ in millions |
IP investment B= INTEG (rate of IP investment B, 0)   ~ $ ~ |
IP investment G= INTEG (rate of IP investment,   0)   ~ $ ~|
IP output B= INTEG (rate of IP generation B,0) ~   patents ~ |
IP output G= INTEG (rate of IP generation G,   0)   ~   patents ~ |
Price G= INTEG (price increase G-price erosion, Initial Price B*(1-Initial discount on price
B))~$/mg~|
price increase G=IF THEN ELSE((Time<(Time of patent expiry)), Price G*0, 0) ~
        $/(mg*week)~|
"Patent expired?"=IF THEN ELSE(Time of patent expiry<=Time , 1 , 0) ~   ~|
rate of IP generation G=Ecum inv on productivity G(IP investment G)*rate of IP investment
        ~   patents/week~ |
Ecum inv on productivity G([[(0,0)(200,0.8)],(0,0),(10,0.09),(20,0.18),(25,0.195),(30,0.2),
(35,0.195),(40,0.19),(50,0.165),(60,0.13),(70,0.1),(80,0.07),(90,0.045),(100,0.03),
(120,0.017),(150,0.01),(200,0.005))
        ~   patents/$
        ~   Effect of total investment in IP on productivity. Assume that at low levels of
investment, learning is slow, but increases with investment. At some point, increased investment
is not productive|
Initial discount on price B=   0.1*(1.001)^250   ~   ~ |
Initial time of patent expiry=   250 ~   week   ~ |
rate of IP generation B= Ecum inv on productivity B(IP investment B)*rate of IP investment B ~
        patents/week ~ |
rate of IP investment=   0.5 ~ $/week ~   in millions|
Fraction of revenues spent on defensive IP= 0.04~   ~ |
"Market share, G"= INTEG (change in mkt share,   0)   ~   ~ |
change in mkt share=   ("Indicated market share, G"-"Market share, G")/TTFE   ~~|
Demand G=   "Market share, G"*Total statin demand ~   mg/week   ~|
Revenues G=   Price G*Demand G   ~ $/week ~   ~ :SUPPLEMENTARY |
time to adjust price= 300 ~   week ~ Takes about 5-7 years to adjust price |
Price B= INTEG (price changes, Initial Price B) ~ $/mg   ~ |
Market Share B= INTEG (change in share, adjusted initial market share of B)   ~ ~|
"adjusted indicated mkt share, other B"= "Indicated market share, other B"/Total indicated market
share   ~   ~ |
"adjusted indicated mkt share, other G"="Indicated market share, other G"/Total indicated market
share   ~   ~|
weighted average statin price=0.15   ~   ~ |
Rel price G=   (Price G-weighted average statin price)/weighted average statin price ~ |
change in share=(adjusted indicated mkt share B-Market Share B)/Time to adjust share
        ~1/week   ~|

Total indicated market share=MAX((Indicated market share B+"Indicated market share, other B"+"Indicated market share, other G"), (+"Indicated market share, other B"+"Indicated market share, other G"+"Indicated market share, G"\)) ~ ~|

Relative price B=(Price B-weighted average statin price)/weighted average statin price ~ ~ |

"Match generics price after expiry?"= 0 ~ ~ 1: want to eventually match generics price. 0: want to maintain price |

Perceived market share= DELAY FIXED (Market Share B, Market shift perception delay, adjusted initial market share of B) ~ ~ |

"Initial indicated market share, B"= E CP MS(initial comp pos B) ~ ~ |

Indicated market share B= E CP MS(Competitive position B) ~ ~ |

Rel price other G=(Average other G price-weighted average statin price)/weighted average statin price ~ ~ |

Rel initial price= (Initial Price B-weighted average statin price)/weighted average statin price ~~|

Rel price other B=(Average other B price-weighted average statin price)/weighted average statin price ~ ~ |

adjusted initial market share of B="Initial indicated market share, B"/("Indicated market share, other B"+"Indicated market share, other G"+"Initial indicated market share, B") ~ ~ |

"# off-patent products (other G)"= "# entrant in the market"-1 ~ ~ |

"# on patent products (other B)"= 6-"# entrant in the market" ~ ~ |

"EEM #OG"([(0,0)-(10,40)],(0,0),(1,8),(2,17),(3,24),(4,27),(5,28),(6,29))
~ ~ Effect of # entrant on the average PVI of generic products in the market|

Rel PVI G= (PVI G-Average statin perceived PVI)/Average statin perceived PVI ~ ~ |

Average other B price= 0.15 ~ $/mg ~ |

Average other G price= 0.14 ~ $/mg ~ |

initial weight on PVI B= E RPr on wt on PVI(Rel initial price) ~ ~ |

weight on PVI other G= E RPr on wt on PVI(Rel price other G) ~ ~ |

comp pos G=weight on PVI G*Rel PVI G-((1-weight on PVI G)*Rel price G) ~ ~ |

comp pos other B=(weight on PVI other B*Rel PVI other B)-((1-weight on PVI other B)*Rel price other B\) ~ ~ |

comp pos other G=(weight on PVI other G*Rel PVI other G)-((1-weight on PVI other G)*Rel price other G\ ) ~ ~ |

PVI other G = "EEM #OG"("# off-patent products (other G)") ~ ~ |

Initial Rel PVI B=(Initial PVI B-Average statin perceived PVI)/Average statin perceived PVI~~|

Rel PVI other G=(PVI other G-Average statin perceived PVI)/Average statin perceived PVI ~ ~|

weight on PVI G= E RPr on wt on PVI(Rel price G) ~ ~ |

weight on PVI other B= E RPr on wt on PVI(Rel price other B) ~ ~ |

"EEM #OB"([(0,0)-(10,50)],(1,33),(2,37.2),(3,41),(4,42),(5,41),(6,40)) ~ ~ |

Rel PVI other B= (PVI other B-Average statin perceived PVI)/Average statin perceived PVI ~ ~|

initial comp pos B=initial weight on PVI B*Initial Rel PVI B-(1-initial weight on PVI B)*(Rel initial price~~|

PVI other B= "EEM #OB"("# on patent products (other B)") ~ ~ |

PVI G=Perceived PVI B ~ ~ |

"Revenues, B"="Demand, B"*Price B ~ $/week~ |

"# entrant in the market"= 6 ~ ~|

EEP IPVI([(0,0)-(10,60)],(1,12),(2,24),(3,36),(4,32),(5,42),(6,38))   ~~Effect of entry
position on intrinsic PVI (Source: Ngai, 2005). Diminishing returns of R&D lead to smaller
increments in PVI of new products|
Average statin perceived PVI= 32   ~   ~ |
Initial Price B= 0.14   ~   ~ |
Initial PVI B=   EEP IPVI("# entrant in the market")~   ~ |
Market share gap B= MAX(0, (Target market share-Market Share B)/Target market share)~
        ~|
recent market share= SMOOTH(Market Share B, TTFE) ~   ~|
Target market share= MAX(recent market share, Perceived market share + (Perceived market
share-recent market share\   ))   ~   ~ |
TTFE= 52~   week   ~   Time to form expectations- assume annually|
Relative perceived PVI B= (Perceived PVI B-Average statin perceived PVI)/Average statin
perceived PVI~ ~ |
Perceived PVI B premium= EPS APP(Actual promotional spend) ~ ~~   :SUPPLEMENTARY |
EMG PS([(0,0)-(1,2)],(0,1),(0.01,1),(0.02,1),(0.025,1),(0.03,1),(0.04,1),(0.05,1),(0.1,1),(\
        0.15,1.1),(0.2,1.35),(0.25,1.4),(0.3,1.25),(0.4,0.9),(0.5,0.6),(0.8,0.15),(1,0)) ~   ~|
Perceived PVI B= INTEG (PVI perception change,   Initial PVI B) ~ ~ |
EPS APP([(0,0),(2e+007,40)],(0,0),(500000,1),(1e+006,1.5),(1.5e+006,2.5),
(2e+006,3.75),(2.5e+006,5),(3e+006,7.5),(3.5e+006,11.5),(4e+006,14.5),
(4.5e+006,17),(5e+006,19),(6e+006,21),(7e+006,23),(8e+006,23.75),(9e+006,24.5),
(1e+007,25),(1.2e+007,25),(2e+007,25)) ~ ~|
PVI perception change=MAX(0,(Indicated perceived PVI B-Perceived PVI B)/PVI perception
delay) ~1/week ~|
PVI perception delay= 12   ~   week ~ |
Market shift perception delay= 4   ~   week
~   Low perception delay- newspapers were printing details of drops in new prescriptions
within two-three weeks after Zocor went off patent |
"Demand, B"= Market Share B*Total statin demand ~mg/week ~ |
Fraction of revenues usually spent on promotion=   0.06   ~   ~   Includes phase
IV clinical trials (13.4% of R&D spend), detailing, journal advertising and hopsital promotioin.
Excludes retail value of free   samples. Annual R&D spend is 17.4% of sales, or $56M total ,
vs $12bn promotion. i.e. = (.174*0.134)+(12/56)*.174 = 0.06 (source: PhRMA industry profile,
2009) |
Time to adjust share= EMS TAS(Market Share B) ~ week ~ |
EMS TAS([(0,0)-(1,80)],(0,10),(0.01,10),(0.02,10),(0.05,10),(0.1,12),(0.15,15),(0.2,18),
(0.3,26),(0.4,37),(0.5,45),(0.6,50),(0.7,55),(0.8,59),(0.9,59.5),(1,60)) ~   ~ |
Initial demand= 1.5e+006*20*30 ~   mg/week
~   1.5 million prescriptions per week in Jan 2004. Assume each prescription is for 20mg, 30
days|
weight on PVI=E RPr on wt on PVI(Relative price B)   ~   ~|
Competitive position B= (weight on PVI*Relative perceived PVI B)-((1-weight on
PVI)*Relative price B) ~   ~ |
E RPr on wt on PVI([(-1,0)-(1,1)],(-1,0),(-0.7,0.005),(-0.5,0.03),(-0.4,0.035),(-0.3,0.06),(-
0.25,0.1),(-0.2,0.17),(-0.15,0.3),(-0.1,0.53),(-0.06,0.7),(-0.04,0.85),(-0.03,0.92),(-0.02,0.96),(-
0.01,0.99),(0,1),(0.01,0.99),(0.02,0.96),(0.03,0.92),(0.04,0.85),(0.06,0.7),
(0.1,0.53),(0.15,0.3),(0.2,0.17),(0.25,0.1),(0.3,0.06),(0.4,0.035),(0.5,0.03),(0.7,0.005), (1,0)) ~
        ~   Effect of relative price on weight on PVI |
demand growth= demand growth rate*Initial demand   ~   mg/week/week ~|
demand growth rate=0.005 ~ ~|
Total statin demand= INTEG (demand growth, Initial demand) ~ mg/week~|

Bibliography

Abernathy W.J. ; Utterback J.M. *Technol. Rev.* **1978** *80(7)* 40-47

Actavis *Annual Report to Shareholders* **2005**

Actavis *www.actavis.com, accessed March 14,* **2009**

AmerisourceBergen *Annual report to shareholders* **2007**

Apotex Corp. *'Comment of Apotex Corp. in Support of Citizen Petition Docket No. 2004P-0075/CP1'* Submitted to Division of Dockets Management, Janet Woodcock, Gary Buehler and Daniel Troy, FDA, March 24, **2004**

Apotex Inc. *www.apotex.com, accessed May* **2009**

Astra Zeneca *www.crestor.com, accessed April 25,* **2007**

Astra Zeneca *'Astra Zeneca's new statin shows potential to improve treatment for the world's leading cause of death'* Press Release, June 29, **2000**

Astra Zeneca International *Annual report to shareholders* **2008**

Baker-Smith C.M.; Benjamin D.K.; Grabowski H.G.; Reid E.D.; Mangum B.; Goldsmith J.V.; Murphy M.D.; Edwards R.; Eisenstein E.L.; Sun J.; Califf R.M.; Li J.S. *Am. Heart. J.* **2008** *156(4),* 628-688

Booz Allen and Hamilton *'The role of distributors in the US healthcare industry: a study prepared for the center for healthcare supply chain research'* **2007**

BMI *'Industry Trend Analysis- Slim profit margins for drug distributors'*, Business Monitor International, July 10, **2008**

BMI *'United States Pharmaceuticals & Healthcare Report Q1 2009'* Business Monitor International, **2009**

Bristol Myers Squibb *www.bms.com, accessed on April 25,* **2007**

BusinessWeek *'Big Pharma's Patent Headache'* Feb 26, **2008**

Chemical and Engineering News, *'Lovastatin'* **2005** *83(25)*

Center for Disease Prevention and Control, *www.cdc.gov, accessed April 11,* **2009**

CDER *'Guidance for Industry: 180 days of Generic Drug Exclusivity Under the Hatch-Waxman Amendments to the Federal Food, Drug, and Cosmetic Act'*, Center for Food and Drug Evaluation and Research, US Food and Drug Administration, June **1998**

CDER (Center for Food and Drug Evaluation and Research), US Food and Drug Administration *www.fda.gov/cder, accessed March 13,* **2009**

CVS/Caremark *Annual report to shareholders* **2007**

Drug Price Competition and Patent Term Restoration Act, (Public Law 98-417) U.S.C. **1984**

FDA Act, *Food and Drug Administration Improvement Act of 1997,* Section 111, 105th Congress USA, **1997**

FDA *'Mylan Pharmaceuticals Inc/Prohibit the marketing and distribution of Authorized Generics until the expiration of the first generic applicant's exclusivity period'* Citizen Petition Docket No. 2004P-0075 February 18, **2004a**

FDA *'Teva Pharmaceuticals USA, Inc./ Prevent Pfizer Inc. from marketing a generic version of Accupril until after the expiration of Teva's 180-day exclusivity period'* Citizen Petition Docket No. 2004P-0261 June 10, **2004b**

FDA *'Andrx Pharamceuticals, Inc./Re-evaluate FDA's policy concerning the marketing of "Authorizied generic" versions of brand name prescription drugs'* Citizen Petition Docket No. 2004P-0563 December 27, **2004c**

FDA *'FDA supports broader access to lower priced drugs'* FDA Talk Paper, July 2, **2004d**

FDA *'Listing of Authorized Generics'* *www.fda.gov, accessed March 16,* **2009a**

FDA *'FDA Generic Drug approvals'* *www.fda.gov, accessed March 16,* **2009b**

FDA Orange Book, *Food and Drug Administration, Electronic Orange Book Database, http://www.fda.gov/cder/ob/default.htm, accessed on April 13,* **2009**

Foster R. *'The S-curve: A new forecasting tool'* Chapter 4 in *'Innovation: The attacker's advantage'* Simon and Schuster, New York (NY) **1986** 88-111

FT *'Statins 'reduce risk of colon cancer',* Financial Times, May 27, **2005**

FT *'Pfizer agrees Lipitor sales deal',* Financial Times, June 19, **2008a**

FT *'Astra set to receive boost in drug sales',* Financial Times, November 10, **2008b**

Grabowski H.G.; Vernon J.M. *Int. J. Technol. Manag.* **2000** *19(1/2)* 98–120

Herper M. *'Storm warnings; who will come out ahead?'* Forbes, June 6, **2006**

IMS Health *National Prescription Audit™Plus* January **2005**

IMS Health *'2007 Top-line US Industry data'* *www.imshealth.com, accessed April 12*, **2009**

Kaiser *'Follow the Pill: Understanding the U.S. Pharmaceutical Supply Chain'* Prepared for The Kaiser Family Foundation by The Health Strategies Consultancy LLC, March **2005**

Liebman M. *Med. Mark. Med.* November **2001** 86 - 92

Lupin Pharmaceuticals Inc. *www.lupinpharmaceuticals.com, accessed May* **2009**

Manzoni M.; Rollini M. *Appl. Microbiol. Biotechnol.* **2002**, *58*, 555-564

Merck Sharpe and Dohme *www.vytorin.com, accessed April 25*, **2007**

Mylan Inc. *www.mylan.com, accessed May* **2009**

NCBI (National Center for Biotechnology Information) *http://pubchem.ncbi.nlm.nih.gov, accessed April 25*, **2007**

Ngai S.S.H. *'Business dynamics of patent expiry and commoditization in the pharmaceutical industry: A case study on the US statins market'*, Chapter 15, PhD Thesis, MIT, **2005**

Novartis AG, *Annual report to shareholders* **2007**

Novartis AG *Annual report to shareholders* **2008**

Novartis AG *'Sandoz at a glance'*, *www.novartis.com* **2009**

PhRMA *'The truth about pharmaceutical marketing and promotion'*, Pharmaceutical Research and Manufacturers of America, July **2008**

Pfizer Inc. *Annual report to shareholders* **2008**

Pfizer *www.lipitor.com, accessed on April 25*, **2007**

Ranbaxy *Annual report to shareholders* **2007**

Ranbaxy *www.ranbaxy.com, accessed March 14*, **2009**

Red Book™ Annual Publication by Thomson Reuters Healthcare

Reddy *Annual Report to shareholders* Dr Reddy's Laboratories **2007**

Reddy *Dr Reddy's Product Guide 2008, North America, www.drreddys.com,* **2008**

Reddy *www.drreddys.com, accessed March 14*, **2009**

Robison R.L.; Suter W.; Cox R.H. *Toxicol. Sci.* **1994** *23 (1)* 9-20

Scott-Morton F. *'Entry Decisions in the Generic Pharmaceutical Industry'* NBER working paper, October **1998**

Singh M. *'The Pharmaceutical Supply Chain: a Diagnosis of the State-of-the-art'* MEng thesis, Engineering Systems Division, MIT **2005**

Skendarian, *Conversations with Skendarian apothecary,* Cambridge, MA, March **2009**

S&P (Standard and Poor's) *'Industry Surveys: Healthcare and pharmaceuticals'* November 27, **2008**

Smith A. *'Pfizer may lose billions in sales of Lipitor'* CNN News, August 2, **2006**

Target Corp. *www.target.com, accessed March 25,* **2009**

Teece D.J. *Res. Pol.* **1986** *15* 285-305

Teva Pharmaceutical Industries Ltd. *Annual report to shareholders* **2008**

The Economist *'Shock to the system – Pharmaceuticals'* February 2, **2008**

Tooley J.F.; Steadman D.D. *Weekly Prescription Trends,* A.G. Edwards, August 8, **2007**

USA Today *'Cholesterol buster Mevacor again seeks OTC approval'* December 9, **2007**

Utterback J.M. *'Mastering the Dynamics of Innovation'* Harvard University Press, Boston MA, **1994**

Vagelos R.; Galambos J. *'The moral corporation – Merck experiences'* Cambridge University Press, NY, **2006**

Watson, *www.watson.com, accessed May* **2008**

Weil H.B.; Utterback J.M. *'The dynamics of innovative industries'* International conference on system dynamics, Boston, **2005**

Wosinska M. *'Just What the Patient Ordered? Direct-to-Consumer Advertising and the Demand for Pharmaceutical Products'* HBS Marketing Research Paper No. 02-04, October **2002**

WSJ *'Blood Feud: For BMS, Challenging Pfizer was a big mistake',* The Wall Street Journal, March 9, **2004**

WSJ *'Do statins help prevent cancer? Few tests slated.'* The Wall Street Journal, May 20, **2005**

WSJ, *'Pipeline problem: Demise of a blockbuster drug complicates Pfizer's revamp'* The Wall Street Journal, December 4, **2006a**

WSJ *'The week ahead'* The Wall Street Journal, April 15, **2006b**

Zydus *www.zydususa.com, accessed April 23,* **2009**

Conclusions

o   A systematic design methodology for design of pharmaceutical tablets is presented. Models to predict tablet microstructure and performance are required.

o   Nanoindentation and X ray micro CT can be used to measure mechanical properties of powders and structural parameters of the tablet. This can be a basis for future compaction modeling work.

o   Tablet microstructure can be modified by a combination of formulation and process variables. Microstructure influences tablet hardness and dissolution behavior.

o   The standard testing configurations for measurement of tablet performance (hardness and dissolution) are not well-suited for developing process models.

o   Terahertz pulsed spectroscopy is sensitive to microstructural changes and THz imaging can be used to detect internal defects.

o   The market for statins has evolved in a way that is largely consistent with the theory on technology market dynamics.

o   Case studies of each of the statin products show that there are strong sequencing effects and competition shifts from brand and perceived product value index (PVI) to price as the market evolves.

Abbreviations

AFM	Atomic Force Microscopy
ANDA	Abbreviated New Drug Application
API	Active Pharmaceutical Ingredient (also called Drug Substance)
DEM	Discrete Element Modeling
CAMP	Consortium for the Advancement of the Manufacturing of Pharmaceuticals
CFD	Computational Fluid Dynamics
CT	Computed Tomography
ESEM	Environmental Scanning Electron Microscope
FDA	US Food and Drug Administration
FEM	Finite Element Modeling
IP	Intellectual Property
MCC	Microcrystalline Cellulose
PBM	Pharmacy Benefit Manager
PVI	Product Value Index
TPI	Terahertz Pulsed Imaging
TPS	Terahertz Pulsed Spectroscopy
USP	United States Pharmacopeia